UNIVERSITY OF CAPE TOWN
IYUNIVESITHI YASEKAPA • UNIVERSITEIT VAN KAAPSTAD

Clogging in Permeable Interlocking Concrete Pavement (PICP)

Prepared by:
Motlatsi Monyake

Supervised by:
Professor Neil Armitage (PrEng)

Department of Civil Engineering
University of Cape Town, Private Bag X3, Rondebosch 7701

September 2023

Dissertation submitted in partial fulfilment of the requirements for the degree of Master of Science in Engineering in Civil Engineering (MSc(Eng))

Plagiarism Declaration

1. I know that plagiarism is wrong. Plagiarism is to use another's work and to pretend that it is one's own.
2. I have used the Harvard Convention for citation and referencing. Each significant contribution to and quotation in this report from the work or works of other people has been attributed and has been cited and referenced.
3. This report is my own work.
4. I have not allowed and will not allow anyone to copy my work with the intension of passing it as his or her own work.

I know the meaning of plagiarism and declare that all the work in the document, save for that which is properly acknowledged, is my own. This thesis has been submitted to the Turnitin module and I confirm that my supervisor has seen my report and any concerns revealed by such have been resolved with my supervisor.

Student name	Motlatsi Monyake
Student number	MNYMOT004
Signed	Signed by candidate
Date	28th September 2023

Acknowledgments

I would like to acknowledge the following people and/ or organisations:

1. The Water Research Commission of South Africa (WRC) and UCT International and Refugee Scholarship for their financial support of this study.
2. My supervisor, Professor Neil Armitage, for his guidance, mentoring and ready availability to assist me throughout my research. Most importantly, I would like to really appreciate Prof. for accepting me as one of his Masters students and entrusting me to work on the WRC C2021/2022-00436 project: '*Guidelines for the design, construction and maintenance of Permeable Interlocking Concrete Pavements (PICP) for South Africa*'. It was humbling how Prof always availed himself to kindly assist me in any challenges I was faced with.
3. The WRC Reference Group for their warm and positive feedback:

Dr Shafick Adams	Water Research Commission (Chair)
Prof Matthys Dippenaar	University of Pretoria
Mr Justin Kretzmar	Technicrete
Mr Kwazikwakhe Majola	Department of Water and Sanitation
Ms Nathalie Smal	City of Ekurhuleni: Roads and Stormwater Department
Mr David Still	Partners in Development (Pty) Ltd

4. The PICP Working Group for sharing their wealth of knowledge with me. The group comprised of:

a) Representatives from academia, local authorities, suppliers, and consultants:

Mr Johan Barnard	Newton Landscape Architects c.c.
Mr Paul Baxter	Geotextiles Africa – Fibertex
Mr David Beer	Concrete Manufactures Association
Mr Benjamin Biggs	JG Afrika
Mr Chris Brooker	cba Specialist Engineers
Prof Kirsty Carden	University of Cape Town Future Water Institute
Prof Sue Charlesworth	Coventry University, UK
Mr Henry Cockcroft	Concrete Manufacturers Association
Mr Peter Davies	Peter Davies and Associates
Prof Anne Fitchett	University of Witwatersrand
Mr Vivian Hill	De Villiers Sheard Consulting Engineers

Mr Eugene Hlongwane	City of Cape Town Stormwater
Mr Justin Kretzmar	Technicrete
Ms Sjanel Martin	City of Cape Town Stormwater
Mr Andre Nel	Johannesburg Roads Agency
Ms Elgin Rust	Terraforce CC
Mr Munier Salie	De Villiers Sheard Consulting Engineers
Ms Nathalie Smal	City of Ekurhuleni: Roads and Stormwater Department
Mr Deon Stipp	Kaytech Engineered Fabrics
Dr Charles Teta	University of Cape Town Future Water Institute
Mr Geoff Tooley	eThekwini Municipality: Catchment Management
Mr Riaan van Biljon	Concrete Manufacturer
Mr Deon van Vuuren	Ubuntu Concrete Works
Mr Gert van Wyk	Bosun Group
Mr Hadley Warren	Bosun Group
Prof Ryan Winston	Ohio State University, USA
Mr Peter Wium	Peter Wium Consulting Engineers

b) The undergraduate and postgraduate students from the University of Cape Town (UCT) and the University of Witwatersrand (Wits) who participated in this research:

Mr Joshua Barnes	BSc (Eng)	UCT Civil Engineering
Mr Joshua Blackshaw	BSc (Eng)	UCT Civil Engineering
Mr Kyle Bowman	BSc (Eng)	UCT Civil Engineering
Mr Luke Brown	MSc (Eng)	UCT Civil Engineering
Ms Arushka Chetty	BSc (Eng)	Wits Civil Engineering
Mr Talha Chothia	BSc (Eng)	Wits Civil Engineering
Mr Mohammed Desai	BSc (Eng)	Wits Civil Engineering
Mr Husain Essop	BSc (Eng)	Wits Civil Engineering
Mr Mohammed Khan	BSc (Eng)	Wits Civil Engineering
Mr Zandisiwe Khumalo	BSc (Eng)	Wits Civil Engineering
Mr Mahlewuli Khosa	BSc(Eng)	Wits Civil Engineering
Mr Abdul Mahomed	BSc (Eng)	Wits Civil Engineering
Ms Azraa Mahomed	BSc (Eng)	Wits Civil Engineering

Ms Rasa Maistry	BSc (Eng)	Wits Civil Engineering
Ms Melody Masuku	MSc (Eng)	Wits Civil Engineering
Mr Qama Matolengwe	BSc (Eng)	UCT Civil Engineering
Mr Abdul Mayimele	BSc (Eng)	Wits Civil Engineering
Mr Thobani Mqadi	BSc (Eng)	UCT Civil Engineering
Mr James Morrit-Smith	BSc (Eng)	UCT Civil Engineering
Mr Shadrack Mothadi	BSc (Eng)	Wits Civil Engineering
Mr Tlhologelo Mphela	BSc (Eng)	UCT Civil Engineering
Ms Nolulama Msomi	BSc (Eng)	Wits Civil Engineering
Ms Kiasha Naidoo	BSc (Eng)	Wits Civil Engineering
Mr Lutho Ncayo	BSc (Eng)	UCT Civil Engineering
Mr Moyahabo Phaladi	BSc (Eng)	Wits Civil Engineering
Mr Thando Peyi	BSc (Eng)	UCT Civil Engineering
Mr Chuene Seduma	BSc (Eng)	Wits Civil Engineering
Ms Zulieka Silinda	BSc (Eng)	Wits Civil Engineering
Mr Hikmet Soyertas	BSc (Eng)	Wits Civil Engineering
Ms Kamogelo Tleane	BSc (Eng)	Wits Civil Engineering

5. The UCT Urban Water Services research group for their constructive suggestions during the research progress meetings. Anabel, my research friend and pillar of strength, for her encouragement and patience.
6. Dr Carden and Dr Okedi for sharing their knowledge and kind support they offered.
7. The UCT civil engineering technical and laboratory staff for their technical support and guidance during the laboratory experiments: Mr Nooredien Hassen, Mr Elvino Witbooi, Mr Christopher Ceasar, Mr Charles May, Mr Masimthembe Swayiza, Mr Leonard Adams and Mr Angus Rule.
8. The AspireYouth Group for assisting with the maintenance trials.
9. My family, more specially my sister: Ausi Refiloe and Ausi Ntséliseng, and friends for their emotional, spiritual, kindness, encouragement and endless love throughout my academic journey.
10. To the love of my life, Lieketseng, thank you for always encouraging me, patience and freely sharing ideas that most times helped me with my research.
11. To God who has been with me ever since I embarked on this research journey.

Abstract

Imperviousness caused by urbanisation leads to increased runoff volumes, flow rates, and contaminant loads. These may be mitigated by measures such as Sustainable Drainage Systems (SuDS) that seek to mimic the natural hydrology of a site. Permeable Pavement Systems (PPS) are a popular SuDS source control measure, with Permeable Interlocking Concrete Pavements (PICP) being the most common. PICP comprise specially designed concrete pavers, *inter alia*, with grooved and dentated sides forming 'joints' to allow runoff to percolate into the underlying single-sized basecourse layers and potentially the subgrade. A geotextile may be fitted between the bedding and base layers and/or base layer and subgrade. However, many PICP installations in South Africa have prematurely failed through clogging. While some failures can be attributed to poor design, construction and site management, there is ongoing debate regarding the principal failure mechanisms, particularly in connection with the inclusion of a geotextile under the bedding layer.

Field investigations were thus conducted at eleven sites in Cape Town and Gauteng to provide evidence-based data related to clogging. Additionally, accelerated laboratory tests that focused on the role that different pavers and upper geotextiles played in the clogging process were conducted at the University of Cape Town (UCT). The investigations identified four types of clogging mechanisms: i) Type I is when sediment fills up the top 30 mm of the joints, ii) Type II is when the sediment deposits on the bedding immediately below the joints, iii) Type III is when the sediment mixes with the bedding and clogs the geotextile, iv) Type IV is clogging of the underlying layers.

The field observations indicated that rapid failure of PICP correlates with: high sediment loading from adjacent areas for example as a consequence of being linked to excessively large impervious surfaces, leaf and pollen drop from overhanging vegetation, abrupt braking at highly trafficked areas – in particular at intersections often widening joints, and lack of maintenance. The non-woven heat-bonded upper geotextiles that have been specially selected in the past owing to their ability to promote nutrient removal in PICP were found to be susceptible to puncturing in areas with considerable turning traffic. Maintenance trials demonstrated that air blowers could remove Type I clogging, but probably at the cost of accelerating Type II clogging. The presence of a geotextile was seldom a cause of clogging except in limited, specific circumstances. Accelerated laboratory tests showed that the smaller the paver joint opening ratio, the faster the joint was clogged by non-cohesive soils.

Table of Contents

List of Figures

List of Tables

List of Equations

Glossary of terms

Aggregate: Angular crushed quarry stone for grit, bedding, base, and subbase materials.

Basecourse: The aggregate layer of the pavement section below the bedding layer but above the subbase and subgrade.

Bedding: The aggregate layer supporting the pavers. Usually 7.1 mm roadstone.

Best Management Practices (BMPs): Devices, practices or methods for removing, reducing or retarding runoff flows or preventing contaminants from reaching receiving waters.

Clogging: Reduction in the surface infiltration capacity of permeable pavements as a result of sediment acculation.

Conventional Stormwater: In the South African context, this refers to drainage systems consisting of concrete pipes and canals designed to rapidly transport stormwater to the nearest convenient receiving water.

Geogrid: Pavement biaxial or triaxial plastic reinforcement that distributes traffic load uniformly onto the underlying layers.

Geomembrane: A liner that prevents the movement of water into the subgrade.

Geosynthetic: Synthetic products used to stabilise terrain or pavement layers.

Geotextile: A planar, permeable, polymeric (synthetic or natural) textile material, which may be nonwoven, knitted or woven, used in contact with soil/rock and/or any other geotechnical material in civil engineering applications. They are used to separate different material layers, and can also contribute to the reinforcement of the system and potentially the treatment of stormwater.

Gritstone: The rounded 5 mm Grade 1 roadstone used in the paver joints.

Nutrients are chemicals in urban runoff that cause eutrophication, mainly nitrogen and phosphorus.

Nutrient Load: The quantity or concentration of nutrients entering a water body or ecosystem.

Open-graded aggregate reservior: Angular aggregates material free of fines that highly permeable and thus can store water.

Single sized aggregate: Aggregate that predominately passes one sieve but is retained on the one immediately smaller.

Subbase: The lowest part of a pavement section, usually characterised by the largest aggregate.

Subgrade: The founding soil on which the pavement structure is constructed.

Sustainable Drainage Systems (SuDS): are techniques used to manage runoff quality and quantity while also enhancing the biodiversity and amenity of a development. Also called Low-Impact Development (LID – USA), Water Sensitive Urban Design (WSUD – Australia), Nature-based Solutions (NbS) etc.

SuDS treatment train refers to a sequence of stormwater management practices that work together to improve the water quality and reduce runoff discharge.

Permeable Interlocking Concrete Pavement (PICP): A specific type of permeable pavement comprising block pavers designed with stone-filled slots – termed 'joints' that allow rainwater to pass through to single-sized base courses.

Permeable Pavements (PPs): A pervious pavement allows infiltration to take place.

Washed aggregates: Aggregates free of 0.075 mm or lower sized material (sieve No. 200). This is can be achieved by passing running water through aggregates at the quarry or on site.

Water Quality Volume (WQV): The volume of runoff that is treated to reduce the runoff pollutants.

Water Sensitive Design (WSD): Design that considers the whole water cycle.

Acronyms

ASTM	American Standard Testing Method
BMP	Best Management Practices
CIRIA	Construction Industry Research and Information Association
CoCT	City of Cape Town
DRIT	Double Ring Infiltrometer Test
FSIT	Full Scale Infiltration Test
LID	Low Impact Development
Mod-ASTM	Modified American Standard Testing Method
Mod-SWIFT	Modified Stormwater Infiltration Field Test
MUSIC	Model for Stormwater Improvement Conceptualisation
PCSWMM	Personal Computer Stormwater Management Model
PICP	Permeable Interlocking Concrete Pavement
SDG	Sustainable Development Goals
SIT	Simple Infiltration Test
SRIT	Single Ring Infiltrometer Test
SuDS	Sustainable Drainage Systems
SWIFT	Stormwater Infiltration Field Test
SWMM	Stormwater Management Model
WQV	Water Quality Volume
WSD	Water Sensitive Design

1. Introduction

1.1 Background of the study

Rapid urbanisation since the beginning of industrialisation has resulted in substantial increases in the proportion of impervious land cover (Xian *et al*., 2021). This, in turn, has increased urban stormwater runoff flow rates and volumes whilst simultaneously reduced groundwater recharge and water quality (Hein, 2018b; Simpson *et al*., 2021). Most stormwater systems in South Africa (SA) were designed to rapidly convey runoff to the nearest surface water bodies through concrete channels and pipes, sometimes referred to as hard engineering (CSIR, 2019). This approach is increasingly degrading the state of the water bodies by erosion of natural channels and pollution of downstream receiving waters, whilst increasing the risk of downstream property damage (CSIR, 2019; van Vuuren *et al*., 2022).

Since 1990, there has been a shift towards the use of Sustainable Drainage Systems (SuDS) (Roesner *et al*., 2001; CSIR, 2019; Smith, 2019) in a bid to combat the damage caused by conventional stormwater management techniques. This approach is also being adopted in SA (Armitage *et al*., 2013). SuDS are stormwater management practices that attempt to mimic natural processes in the management of runoff quality and quantity while also seeking to enhance the biodiversity and amenity of infrastructural development (Marchioni & Becciu, 2015).

Permeable Pavement Systems (PPS) are SuDS source control options that manage onsite runoff. They are designed and constructed with permeable surfaces laid on top of open-graded or single-sized aggregate sublayers that infiltrate and temporarily store the water before releasing it for groundwater recharge and/or attenuated downstream flow peaks. They can even be potentially used for rainwater harvesting. The most common PPS in SA is Permeable Interlocking Concrete Pavement (PICP). PICP consists of specially designed concrete block pavers placed on the single-sized base layers. Specially designed grooves create gaps between the pavers, termed ‘joints’, that allow surface water to pass through the surface. Specially selected coarse sand in the 2-5 mm range, termed ‘gritstone’, is placed between the paving blocks to hold back sediment (ASCE, 2018). Geotextiles may be placed between the bedding layer and the top-most base layer, and between the bottom and sides of the lowest base layer and the in-situ material to separate the layers and/or improve the runoff water quality. Stormwater is temporarily stored in the base layers where it may undergo some improvement in water quality as a consequence of sedimentation and bacteriological activity (Sehgal *et al*., 2018). Ultimately, the stormwater infiltrates into the subgrade and/or is removed by sub-surface drains (Woods Ballard *et al*., 2015; ASCE, 2018).

One of the first PICP installations in SA was in 2007 at The Reeds complex in Johannesburg (CMA, 2020). Since then, PICP has been installed in numerous places – mainly parking areas and driveways – in Cape Town, Ekurhuleni, Johannesburg, Midrand, and Pietermaritzburg using various different designs and following a miscellany of international guidelines and standards. The guidelines include those used in the United States of America (USA), United Kingdom (UK) and Australia – although others are available. At the time of the

study, two standards were available: those published by the American Society of Civil Engineers (ASCE 68-19) and the British Standards Institution (BS 7533-13:2009).

1.2 Problem Statement

Infiltration tests conducted between 2017 and 2019 on various PICP sites in Cape Town and Johannesburg by University of Cape Town (UCT) civil engineering researchers indicated that many PICP sites were clogged or nearly clogged resulting in premature failure of the surface. In some places, the pavers had been dislodged. In many sites, there was clear evidence of poor design, poor construction and/or lack of maintenance. Other factors that appeared to be contributing to PICP failure included:

- Loose fine soils from surrounding areas transported by wind or runoff onto the PICP surfaces.
- High run-on of sediment-laden stormwater onto the PICP from adjacent impermeable surfaces causing unacceptably high quantities of fine material to be deposited on its surface.
- Poor construction practices leading to premature failure such as the use of inappropriate filling material such as sand, dirty aggregates, or the lack of suitable edge restraints.
- Little or no maintenance that might have slowed the inevitable clogging of the PICP. In many instances, there was little evidence of the gritstone between the pavers thus allowing the accumulation of fine sediment material in the lower parts of the openings between the pavers.
- Rutting or differential settlement of the PICP structure owing to the settling of the underlying base layers as a result of poor compaction.
- Unsuitable environmental conditions such as proximity to vegetation with high leaf or pollen drops or unacceptable sediment exposure.

Clogging usually comes about as a consequence of the build-up of fine material between the joints of the pavers and within the pavement sublayers. Severe clogging inhibits runoff surface infiltration (Støvring *et al*., 2018). While the source of this fine material is usually from local environmental conditions, laboratory tests have shown that considerable quantities are also introduced through the use of unwashed aggregates (Biggs, 2016). Concerns have also been raised about the potential blockage of any geofabric placed between the bedding and base-course layers due to the migration of fine material from the bedding aggregate or surface. Typical practice in the UK is to install geotextiles to improve the quality of runoff (Charlesworth *et al*., 2017). Further, geotextile protects the underlying pavement layers from possible migration of fine material from the surface (DEWHA, 2010). Conversely, various USA guidelines and ASCE/T&DI/ICPI 68-19 (ASCE, 2018 – the US standard for Permeable Interlocking Concrete Pavement) state that the inclusion of a geotextile is at the discretion of

the design engineer with warning that it may increase the risk of premature PICP clogging through the trapping of fine material on its surface (Hein & Smith, 2016).

The SA construction industry currently adapts various international guidelines and standards for the design, construction and maintenance of PICP. However, this has resulted in inconsistent PICP practices across the country as different designers have taken different approaches. It appears highly likely that PICP is failing because of the lack of understanding by local designers as to the chief mechanisms involved in PICP clogging and how these can be mitigated (Mullaney & Lucke, 2014; Biggs, 2016).

1.3 Aim of the Research

The aim of this study was to provide evidence-based data of PICP clogging mechanisms and ways of mitigating them.

1.4 Objectives of the Research

The study objectives were to:

- Determine the hydraulic performance of existing PICP sites in SA (largely restricted to Cape Town and Johannesburg) and attempt to link this to the materials, method of construction, and maintenance practices – if any.
- Perform diagnostic investigations on failing PICP sites in a bid to understand failure mechanisms.
- Investigate the most appropriate maintenance equipment and techniques for SA conditions.
- Investigate the behaviour of the different types of geotextiles typically used in PICP in the laboratory and compare with a graded filter substitute.
- Assist in the development of guidelines for the design, construction and maintenance of PICP in SA.

1.5 Method

The study had three main components:

i) Literature review of the design, construction, and maintenance of PICP through the consideration of journals, case studies, conference papers, books, websites, student dissertations, seminars, standards and guidelines.

ii) Collection of data from fieldwork and laboratory investigations including the input from students working on projects related to the study from both UCT and the University of the Witwatersrand (Wits).

iii) Input from a specially created PICP Working Group comprising experts from academia (inclusive of the USA and UK), local authorities, consultants, and suppliers.

1.6 Report Layout

The report consists of the following chapters:

- **Chapter 1** is the introduction of the study. The study background, problem statement, research aims, and objectives are discussed. The study method is briefly outlined.
- **Chapter 2** covers the literature review of the design, construction, and maintenance of PICP. Research illustrating the different designs, environmental factors that affect the design and construction of PICP, and potential maintenance techniques are presented.
- **Chapter 3** presents the method followed for the collection of data for the study.
- **Chapter 4** describes the field investigations that were carried out in Cape Town and Gauteng. These included infiltration tests, maintenance trials, and diagnostic investigations.
- **Chapter 5** describes the outcome of accelerated laboratory tests that took place in the UCT hydraulics laboratory. These includes investigations into the performance of different geotextiles as well as the impact of different paver opening areas.
- **Chapter 6** presents the conclusions and recommendations for future research.

2. The Literature Review

2.1 Overview

Infrastructural developments such as commercial centres, most roads, and residential complexes increase the proportion of impermeable surfaces resulting in an increase in runoff quantity, flowrate, and downstream contamination (CSRMB, 2009; CSIR, 2019). Consequently, these degrade surface water bodies (Tirpak *et al*., 2021). To counteract this, Sustainable Drainage Systems (SuDS) have been developed that attempt to mimic the natural hydrology (National Research Council, 2009; Armitage *et al*., 2014; Liu & Armitage, 2020). In this chapter, some background to stormwater management and the SuDS alternative will be provided. One SuDS option, namely Permeable Interlocking Concrete Pavement (PICP) will be discussed in detail.

2.2 Stormwater management on pavements

The management of stormwater runoff in South Africa (SA) has traditionally involved the implementation of concrete pipe and lined channel drainage systems which convey stormwater runoff to the nearest water body as quickly as possible (CSIR, 2019). These drainage systems are usually linked to pavements through a curb and channel system designed to minimise the inconvenience resulting from minor flows. Without some form of intervention, urbanisation leads to an increase in surface run-off and a decrease in interflow and baseflow to streams, evapotranspiration, and groundwater replenishment. Typically, the only attempt to attenuate the peak flow to something approximating the pre-development values has been via detention ponds (CSIR, 2019). Detention ponds, however, require space for implementation.

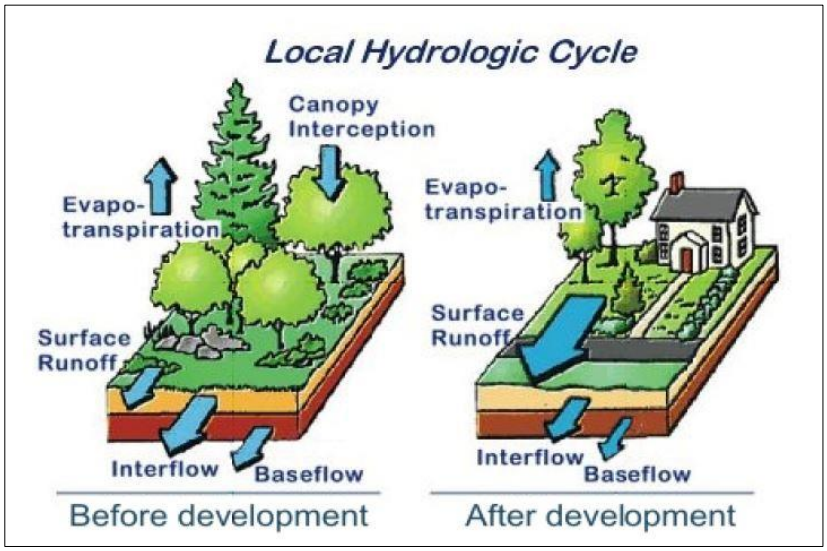

Figure 2-1: Impact of development on the natural hydrology of a site
(National Research Council, 2009)

Figures 2-1 and 2-2 show the general impact of development on the natural hydrology of an area. Meantime, there is increasing demand for access to water that needs to be brought into the urban environment over ever greater distances and higher costs. A more sustainable way of managing urban water is therefore required. This may be achieved through Water Sensitive Design (WSD) that strives to restore the pre-development hydrological conditions and encourage water reuse. The stormwater component of WSD is known as Sustainable Drainage Systems (SuDS) in SA and the United Kingdom (UK), Low Impact Development (LID) in the United States of America (USA), and Water Sensitive Urban Design (WSUD) in Australia.

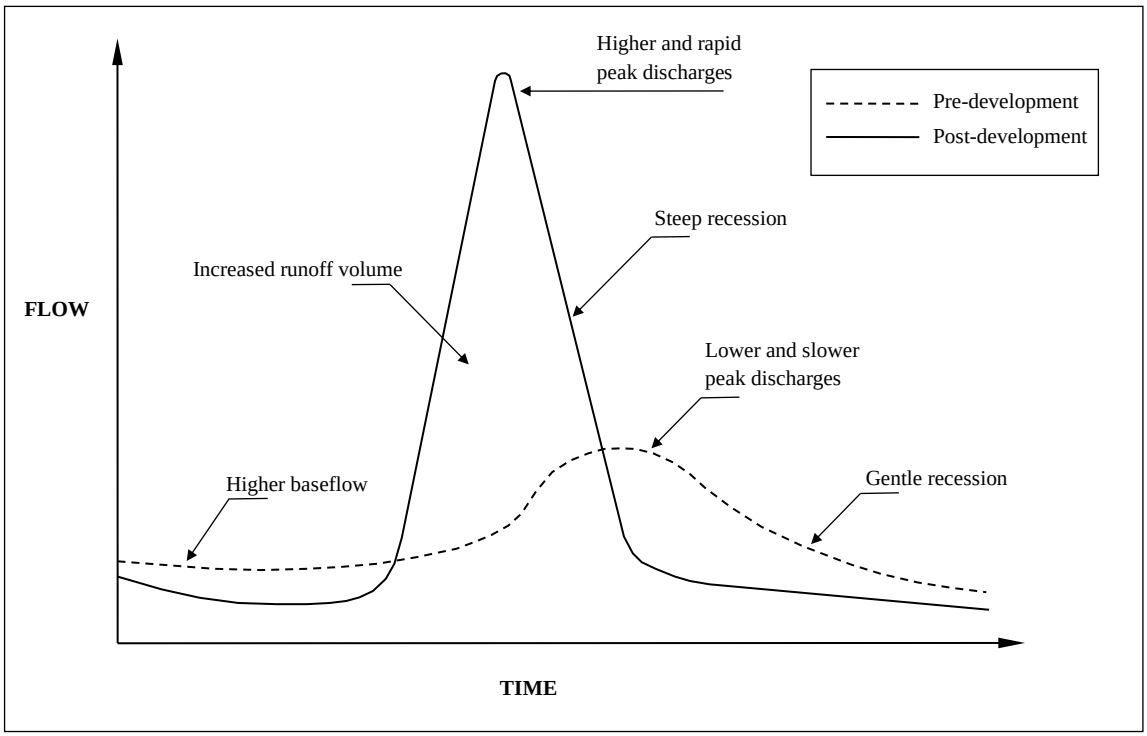

Figure 2-2: Pre-development versus post-development hydrology
(Armitage *et al*, 2013)

2.3 Sustainable Drainage Systems (SuDS)

SuDS considers stormwater as a sustainable and valuable resource. Well-managed stormwater can also contribute to the provision of amenity value for humans and preservation of biodiversity for all other life forms (Figure 2-3). Table 2-1 shows typical pollutants usually found in runoff. SuDS options can be installed in a series to manage and pre-treat stormwater runoff before disposal into the receiving waters. A SuDS treatment train is a combination of different SuDS alternatives implemented in sequence (Armitage *et al*., 2013; Woods Ballard *et al*., 2015).

SuDS are applicable in brownfield, greenfield environments, and retrofitted conventional stormwater systems (CSRMB, 2009). Brownfield sites are those that were previously developed,

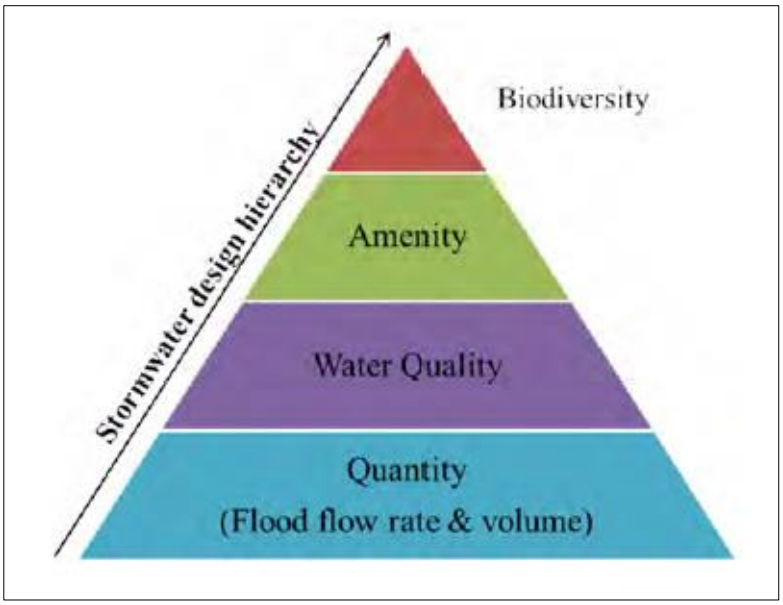

Figure 2-3: Stormwater design hierarchy (Armitage *et al*., 2013)

Table 2-1: Typical stormwater pollutants (Adapted from Armitage *et al.*, 2013)

Pollutant Group	Pollutants	Source	Impacts
Nutrients	Nitrogen and Phosphorus	Fertilisers	Excessive nutrients result in eutrophication. They are commonly associated with algal plumes and reduced clarity resulting in decreased biodiversity.
		Animal waste	
		Organic matter	
		Septic tanks	
Sediment	Suspended and settable solids	Erosion of landscaping	Increased turbidity, sedimentation, and smothering of aquatic plant and animal life.
		Erosion of construction sites	
Organic material	Plant litter	Landscaping	Increased nutrients and sediment.
Pathogens	Bacteria, viruses, and protozoa	Failing sewer / sewage systems	Public health risk. Contaminated recreational area. Threat to downstream irrigation water and edible crops. Decreased economic value of natural recreational areas.
		Animal waste	
Hydrocarbons	Oils, greases, and others	Motor vehicle emissions and wear	
		Industrial processes and waste	
Metals	Lead, copper, zinc and others	Motor vehicle wear	
		Industrial leaks	
		Galvanised construction materials	
Toxic chemicals	Pesticides and herbicides	Agriculture	
		Landscaping	
Solids	Debris and rubbish	Littering	Threat to wildlife. Aesthetic appeal decreased.
		Dumping	

while greenfield sites consist of previously undisturbed portions of the environment. Permeable Pavements (PPs) offer a solution directed at 'softening' the impact of roads and parking areas. They promote infiltration, attenuation, and gross pollutant removal of stormwater runoff through the pavement sublayers (Armitage *et al*., 2013; CSIR, 2019).

2.4 Permeable Pavement Systems (PPS)

Permeable Pavement Systems (PPS) are surfaces that promote the infiltration of surface stormwater runoff into its sublayers for groundwater recharge, attenuation, water harvesting and its pre-treatment by the removal of nutrients and gross pollutants (Hein & Smith, 2016; Liu & Armitage, 2020).

Various types of PP systems are available, including: Porous Asphalt (PA), Porous Concrete (PC), Porous Pavers (PP), pavers with gaps deliberately worked into the laying pattern, and Permeable Interlocking Concrete Pavement (PICP). Figure 2-4 illustrates some different types of PPS. The most suitable spaces in the urban fabric for PP systems include, but are not limited to, parking areas, driveways, lightly trafficked areas, and sidewalks (Armitage *et al*., 2013; Hein, 2018a).

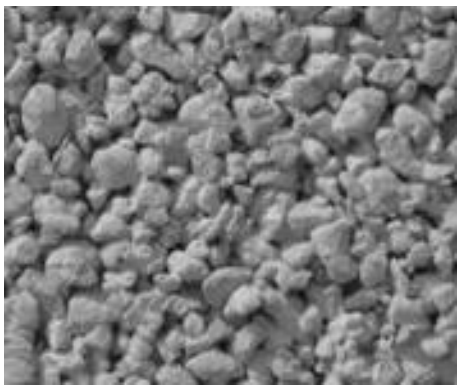

(a) PC (Bean *et al*., 2007)

(b) PICP (Lucke & Beecham, 2011)

(c) PA (Mullaney & Lucke, 2014)

(d) PICP (CSIR, 2019)

Figure 2-4: Examples of PPS types

2.5 Permeable Interlocking Concrete Pavement (PICP)

Permeable Interlocking Concrete Pavement (PICP) comprises of modular paving blocks that have vertical grooves down their sides to create highly permeable 'joints' laid on open-graded or single-sized aggregate sublayers (Figure 2-5.). The grooves are filled with 2-5 mm gritstone to ensure high rates of runoff infiltration while trapping most sediments (Beecham *et al.*, 2010; Armitage *et al*., 2013). A geotextile is sometimes fitted between the bedding layer and the base layer, and between the subbase and subgrade, to prevent the migration of different sized aggregate, improve the infiltrated runoff water quality, and protect the subgrade (CMAA, 2010).

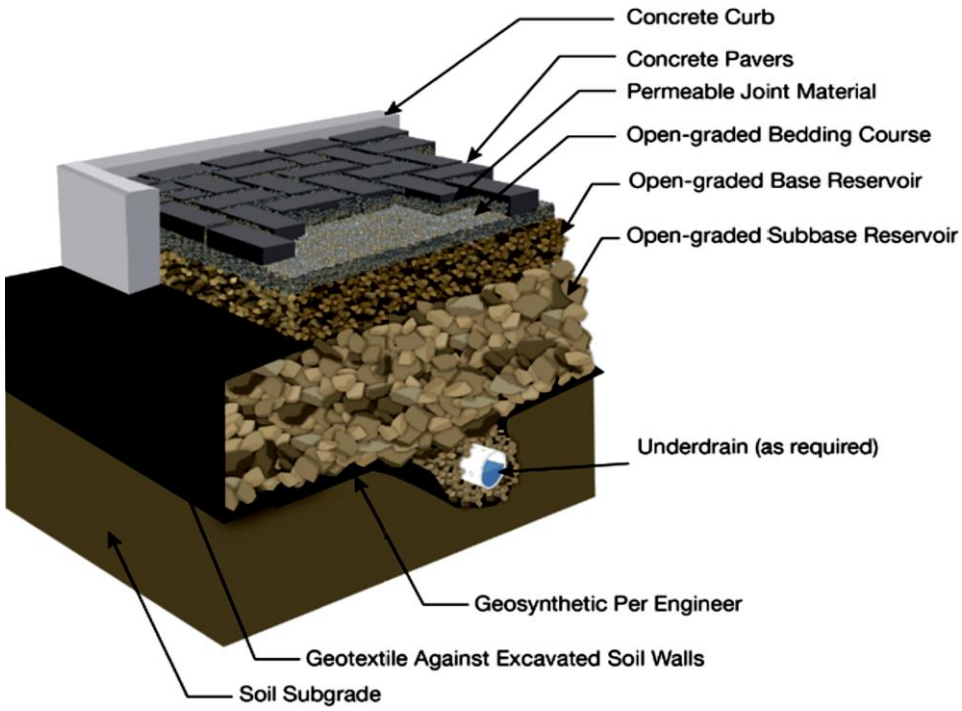

Figure 2-5: Typical PICP section (Smith, 2019)

2.5.1 Benefits of PICP

A well designed, constructed and maintained PICP can (Hein, 2018b; Sanicola *et al*., 2018):

- Reduce runoff flow rate and volume
- Improve runoff quality
- Recharge groundwater
- Provide harvested rainwater for further re-use
- Enhance amenity and biodiversity
- Reduce the urban heat island

2.5.2 The impact of PICP on runoff quality

A multitude of gross pollutants, nutrients, and other sundry contaminants find their way into the stormwater runoff, especially during the so-called 'first flush' of rainfall following a dry period (Section 2.3) (CSIR, 2019; Liu & Armitage, 2020). PICP filters out the gross pollutants and lowers the nutrient load in the stormwater thus improving its quality (Lucke & Beecham, 2011; Liu & Armitage, 2020).

It is essential to wash the aggregates before they are laid in PICP to avoid introducing sediment and its attached contaminants, such as nutrients and heavy metals, to the underlying pavement layer (Liu & Armitage, 2020). The sediments also pose a potential clogging threat to any geotextiles present which can, in turn, impede the infiltration capacity of PICP. On the other hand, Liu & Armitage (2020) found that the use of geotextiles within the PICP removes a significant quantity of fine material content from stormwater runoff versus a no geotextile design.

2.5.3 The impact of PICP on stormwater flood control

Impervious surfaces increase the flow rate and volume of runoff (Figure 2-6). Managing stormwater at its source reduces the potential volume that can cause inundation downstream and the possible erosion of the natural water channels (Armitage *et al*., 2013; CSIR, 2019). PICP reduces the volume of the stormwater runoff generated within a development by infiltrating and attenuating some of the stormwater runoff through temporary storage in the aggregate base layers (Beecham *et al*., 2010; Woods Ballard *et al*., 2015).

Figure 2-6: Flooding caused by a storm in an urban development
(Poon, 2018)

2.5.4 PICP's impact on Biodiversity and Amenity

Biodiversity is the variety of life while amenity is the pleasantness or attractiveness of a development (Armitage *et al*., 2013, 2014). A shortcoming of the PICP system is that it does not account for direct biodiversity but it can contribute to downstream or secondary biodiversity (Woods Ballard *et al*., 2015) by controlling the flow and quality of the stormwater. PICP may provide for some visual 'amenity' due to the availability of different paver colours, appealing shapes and hard durable quality.

2.5.5 PICP impact on urban heat island

Although evapotranspiration is reduced with the installation of PICP, the urban heat island is also reduced relative to conventional pavements (Cheng *et al*., 2019; Manteghi & Mostofa, 2020). PICP absorbs heat during a warm day, but it tends to release it more slowly than conventional pavers because of the evaporation of infiltrated runoff within the pavement structure. Moreover, the pavers can be manufactured in various colours, such as light-coloured pavers that have a high surface reflective index (SRI) relative to dark conventional pavements.

2.6 PICP Design

2.6.1 PICP system components description

Key components for PICP include the: subgrade, underdrain, observation wells, geosynthetics, the open-graded or single-sized aggregate reservoir, filter layers, edge restraints, pavers, and joint material. Typically, the structural design life of PICP is 20 years, however, the various PICP components have different service life (Swan & Smith, 2009)

2.6.1.1 Subgrade

The subgrade is the foundation soil on which the pavement structure is constructed (ASCE, 2018). The properties of the subgrade are therefore significant in determining the type of PICP cross-section. Subgrades are classified according to two design criteria: California Bearing Ratio (CBR) and permeability. CBR is referred to as the measure of a soil's capacity to safely carry traffic, while permeability is the ability of the subgrade to infiltrate runoff (Bruinsma *et al*., 2017). In cases where the subgrade CBR is less than 5%, ground improvement techniques and/or a capping layer are recommended (Interpave, 2018). A capping is a granular layer laid on top of a subgrade to improve the pavement foundation (BSI, 2009). CBR values are determined in accordance with ASTM D1883 *Standard Test Method for CBR (California Bearing Ratio) of Laboratory Compacted Soils*. Low CBR values require thick PICP layers to support vehicular traffic loads, and *vice versa*. Woods-Ballard *et al*. (2015) and ASCE (2018) state that CBR is inversely proportional to the moisture content and modulus of elasticity of soil. It is thus essential

to know the moisture content of a PICP subgrade as it impacts the potential infiltration into the insitu soil and the traffic carrying capacity.

Three types of PICP systems may be defined based on the permeability of the subgrade, the proximity of the water table, and the potential for pollution: i) Full infiltration, ii) Partial infiltration and iii) No infiltration (Table 2-2). In Table 2-2, a 'Yes' indicates that the PICP cross-section can be considered, while a 'No' suggests that it should not be considered. Further, any type of PICP can be used as a component for a SuDS treatment train to treat and manage runoff.

Table 2-2: PICP cross-section selection criteria (After Woods-Ballard *et al*., 2015)

Ground characteristics		**Full infiltration system**	**Partial infiltration system**	**No infiltration system**
Subgrade permeability, *k* (mm/hr)	3.6×10^{0} to 3.6×10^{3}	Yes	Yes	Yes
	3.6×10^{-2} to 3.6×10^{0}	No	Yes	Yes
	3.6×10^{-4} to 3.6×10^{-2}	No	No	Yes
Water table within 1000 mm of the formation level		No	No	Yes
High pollutants content present in stormwater		No	No	Yes
Infiltration water not recommended due to undesirable ground features e.g. mining activity, karst conditions, risk to slope instability etc		No	No	Yes

A full infiltration PICP system is recommended when there is no evidence of potential groundwater contamination and the subgrade permeability is greater than 3.6 mm/hr, that is, sandy soils. The runoff that infiltrates the pavement structure will also percolate into the subgrade to recharge the groundwater (Figure 2-7).

The pavement consists of pavers, joint material, washed unbound aggregates, optional upper and lower geotextiles, and edge restraints. When it rains, runoff percolates into the pavement through the paver joints, into the aggregate storage, and ultimately the subgrade.

Figure 2-8 illustrates the partial infiltration PICP system. This type of PICP cross-section is selected when the subgrade infiltration capacity is limited (Table 2-2). When it rains, runoff percolates into the pavement through the paver joints, into the aggregate storage, and partially into the subgrade. An underdrain is laid either on the subgrade or in the subbase to drain the excess runoff from the aggregate stone storage. The underdrain may be connected to a conventional stormwater line or discharged into other road site SuDS options such as a swale (Armitage *et al*., 2013).

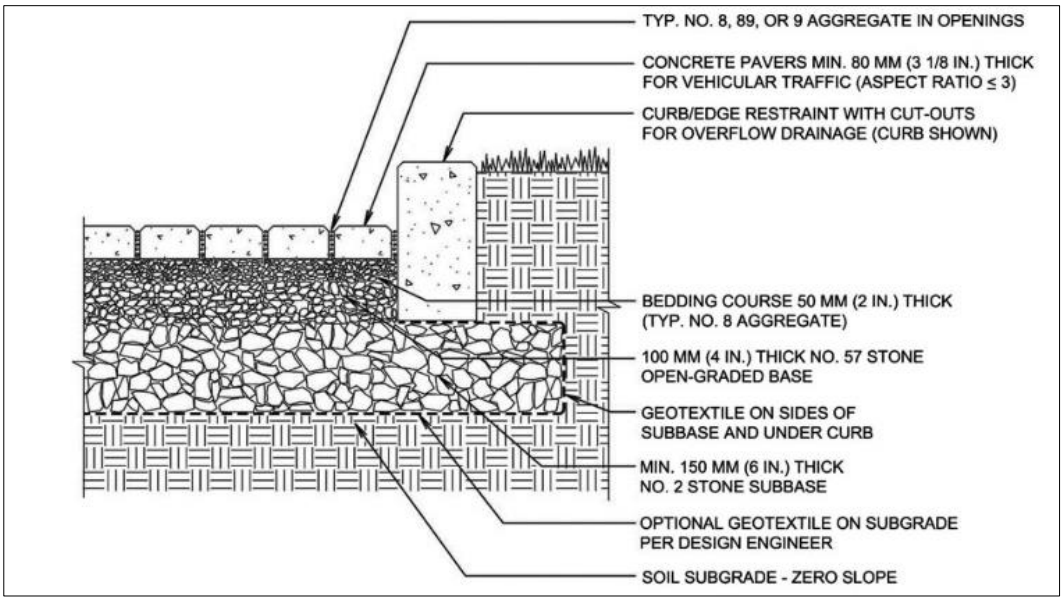

Figure 2-7: Typical full infiltration system design (ASCE, 2018)

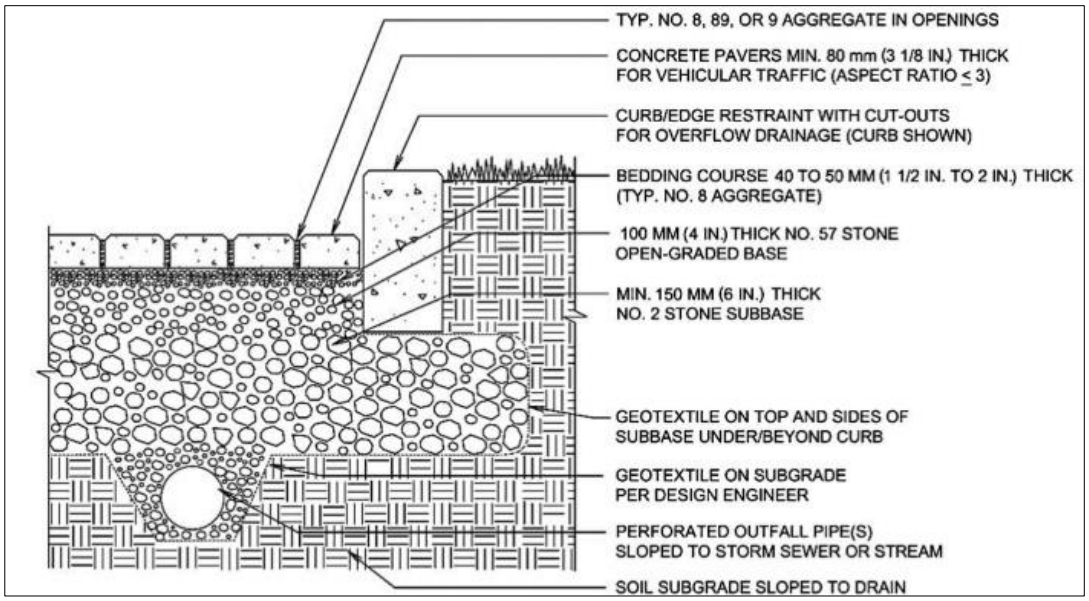

Figure 2-8: Typical Partial infiltration system design (ASCE, 2018)

A no-infiltration PICP system design is shown in Figure 2-9. This system is used when the ground conditions are not suitable for stormwater ingress. The reasons may include *inter alia*: a water table is within 1 m of the pavement formation, the rainwater is to be harvested for further reuse, the pavement is situated on expansive or contaminated underlying soils, where the runoff is highly polluted, or when the pavement is installed within 3 m of a building wall (ASCE, 2018). Some of the criteria for this type of pavement cross-section are shown in Table 2-2.

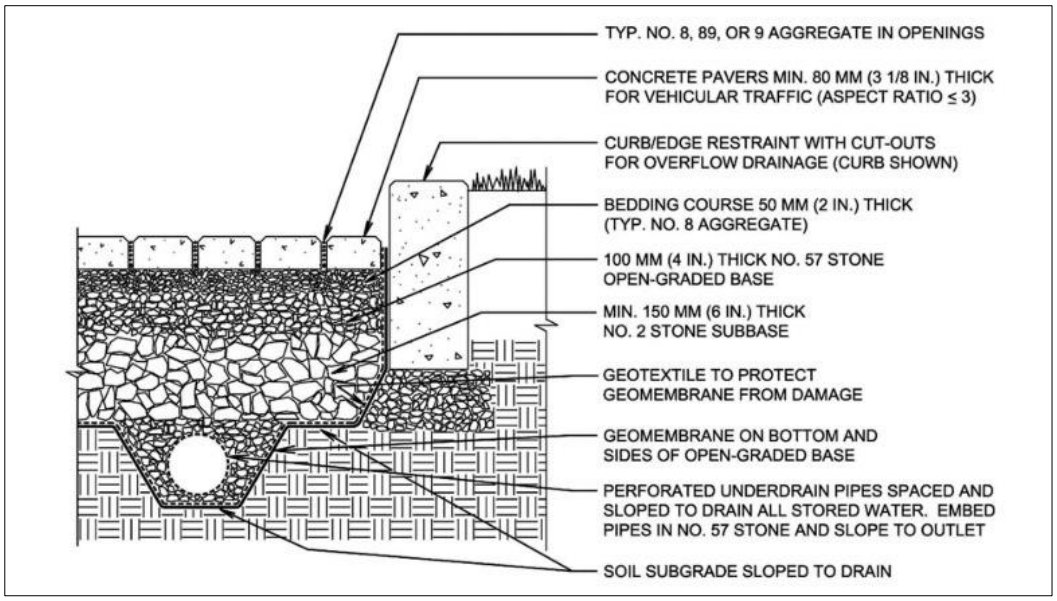

Figure 2-9: Typical no-infiltration system design (ASCE, 2018)

During a rainfall event, runoff infiltrates through the paver joints and into the aggregate's storage for attenuation. It is then channelled to a conventional stormwater system and/or SuDS option by an underdrain. An impermeable geomembrane is installed between the lowest aggregate layer and the subgrade to prevent infiltration into the ground and/or backflow from the groundwater. The geomembrane is also extended up the sides of the pavement sublayers. A geotextile is normally placed on the geomembrane to protect it from being damaged by the subbase aggregate (Charlesworth & Booth, 2017). This system effectively acts as a detention pond.

2.6.1.2 Sloping sites

At times, it might be necessary to install PICP on sloped sites. Ideally, the PICP should be laid as flat as possible to maximise the available storage in the stone reservoir created by the single-sized aggregates, maximise the infiltration into the subgrade, and restrict lateral flow within the pavement structures (BSI 2009; WDNR, 2021), however, slopes less than 2% can usually be tolerated (Bruinsma *et al*., 2017; NCDEQ, 2020). Once the surface slope of the PICP exceeds 5% there is a risk of water from running along the surface (ASCE, 2018). One way of reducing the effective slope is to lay the PICP in a series of level terraces with ramps linking them (NCDEQ, 2020). Alternatively, the PICP should be compartmentalised to maximise storage. Figure 2-10 presents the various options.

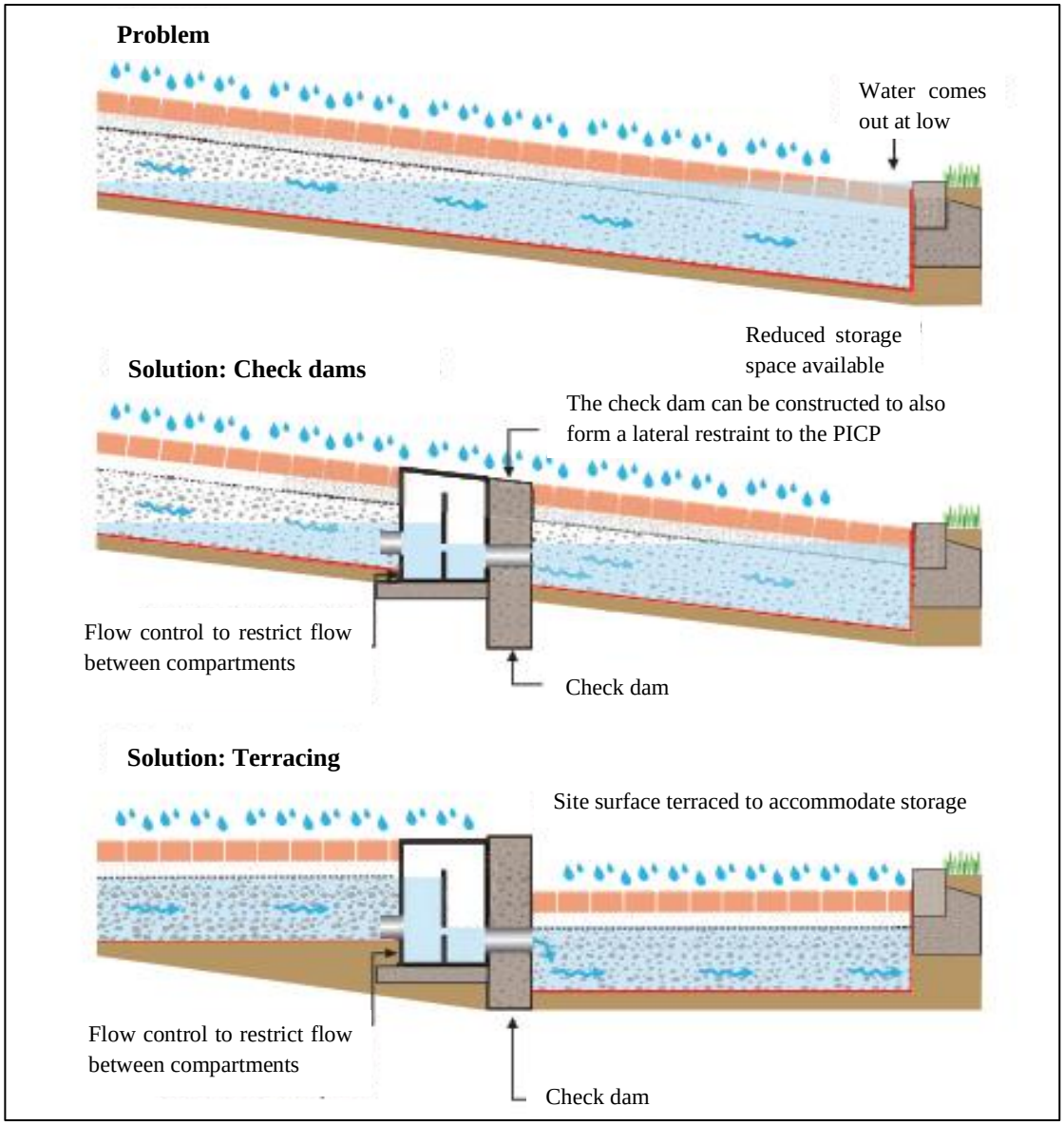

Figure 2-10: Managing runoff on a sloped subgrade
(After Interpave, 2018)

2.6.1.3 Geosynthetics

Geosynthetics come in main three types: geotextiles, geogrids, and geomembranes.

A geotextile is a permeable monofilament woven or non-woven, needle-punched and possibly heat-bonded fabric that can be used either horizontally or vertically in PICP to separate pavement layers (Interpave, 2018). It prevents the migration of fine material into the basecourse or subgrade when laid between the bedding layer and the base layer and/or the subbase and subgrade respectively (ASCE, 2018; NCDEQ, 2020). It may improve water quality through retention of moisture in the bedding layer and thus provide a medium for bacterial growth to

enhance the infiltrated runoff quality (Charlesworth *et al*., 2017). On the other hand, geotextiles can clog depending on various design and environmental factors that result in excessive sediment loads (Woods Ballard *et al*., 2015; CSIR, 2019). Geotextiles may break due to impact loading caused by traffic on the PICP (Bezuijen & Izadi, 2022).

It is possible to leave the geotextiles out but then it is important to ensure: i) no significant migration between the bedding and base layers that could impact the integrity of the system, and ii) no penetration of the subgrade by the subbase aggregate. These can result in reduced infiltration rates over time due to a reduction in porosity.

Geogrids are plastic reinforcements used to stabilize weak soils' subgrades, e.g., a CBR of less than 2% (Smith, 2019).

Geomembranes are impermeable liners that are installed between the lower stone aggregate sublayers and the subgrade, particularly for no-infiltration PICP systems.

2.6.1.4 Underdrains

Underdrains are perforated pipes, typically 110 mm uPVC (unplasticized Polyvinyl Chloride), that are installed in the subbase on top of the subgrade to drain runoff collected in the subbase, preferably within 72 hours of a rainfall event (ASCE, 2018; WDNR, 2021). The runoff may be channelled into other SuDS options or conventional stormwater systems. Sediment accumulation in underdrains can be removed at low points through the use of specially installed access/ observation wells (BSI, 2009; ASCE, 2018). In most cases, underdrains will not be required as the runoff will percolate into the subgrade.

2.6.1.5 Observation wells

Observation wells are typically 100 to 150 mm perforated vertical pipes that extend from the pavement surface through the subbase or base aggregate layer to the top of the subgrade (Figure 2-11). They are installed to monitor the permeability of the subgrade and/ or the depth of water in the pavement structure (ASCE, 2018; WDNR, 2021). In addition, observation wells can assist in determining whether the stone layers are clogged or not. PICP systems laid on flat or on less than 2% slopes should ideally have at least one observation well installed for every 4000 m^2 of permeable pavement (NCDEQ, 2020; WDNR, 2021). On sloped sites, it is advisable to have at least one observation well for each terraced PICP section (NCDEQ, 2020). The top of the observation well must be capped to avoid damage to the vertical pipe or entrance of sediment that may block it.

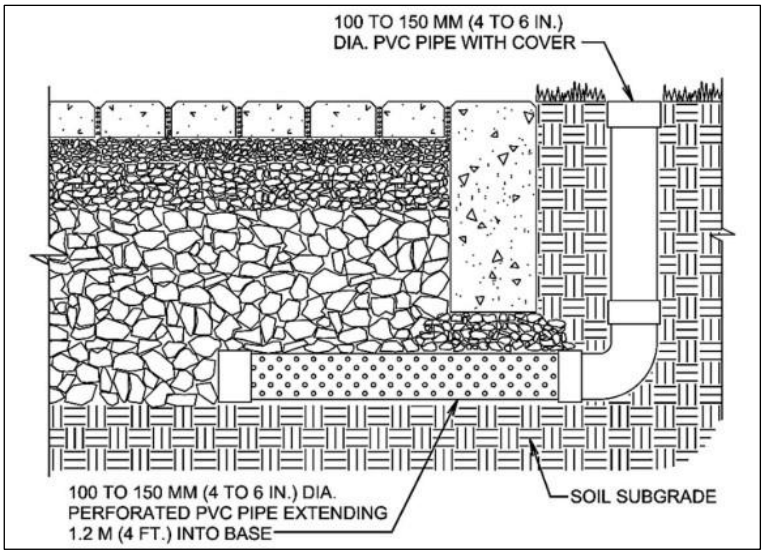

Figure 2-11: Typical observation well (ASCE, 2018)

2.6.1.6 Open-graded aggregate reservoir

The subbase and base layers comprise carefully selected crushed rock (granite, basalt, gabbro), and angular washed aggregates (BSI, 2009). The angular shape of the aggregates assists with 'lock-up' of the aggregates enhancing structural support and minimising segregation. As with conventional pavements, the aggregates need to resist traffic load. In addition, the aggregates should have a void ratio of at least 30% to 40% to provide storage volume for later infiltration into the underlying subgrade, attenuated runoff and/or reuse (Giroud, 2010; Smith, 2012). Thus, the material should have little to no fines. If the aggregates are unwashed, the fine material that may be attached to their surfaces may be washed down onto the subgrade ultimately clogging it.

The thickness of the base layer is typically 100 mm depending on the structural loading (Table 2-3). Pavement carrying vehicular traffic will usually require an additional subbase thick enough to carry the load. The base layers also need to fulfil hydraulic functions such as: adequate porosity, attenuation, temporary storage for later reuse. A typical specification is BSI (2009) *Standard Publication Pavements constructed with clay, natural stone or concrete pavers Part 13: Guide for the design of permeable pavements constructed with paving blocks and flags, natural stone slabs*. It is essential to assess the strength and durability of the open-graded aggregates for both wet and dry conditions.

Various methods may be considered to enhance the structural support and porosity of the base and subbase and thus reduce the required depth of the sublayers. Options include the use of (BSI, 2009; Woods-Ballard, 2015):

i) Hydraulically bound course grade aggregate (HBCGA) – Stabilised aggregates to improve the pavement's structural capacity (BS EN 14227-1: 2013).

ii) Geo-cellular box systems – Plastic cellular units that have a high porosity (>90%), and can replace the subbase (Interpave, 2018).

Table 2-3: Open-graded material requirements

Properties	Source	Base layer	Subbase
Depth	UNI-GROUP (2008); CMAA (2010); Hein & Smith (2016); ASCE (2018)	A minimum of 100 mm. It may be increased in pedestrian and residential driveways.	150 mm minimum
Aggregate distribution	UNI-GROUP (2008)	ASTM No.57 (25 to 4.75 mm)	ASTM No. 2 (63 to 37.5 mm)
	BSI (2009)	20 to 4 mm	20 to 4 mm
	CMAA (2010)	31.5 to 4.74 mm	63 to 4.75 mm
	Hein & Smith (2016)	ASTM No.57 (25 to 4.75 mm)	ASTM No. 2 (63 to 37.5 mm) or ASTM No. 3 (50 to 25 mm) or ASTM No. 4 (37.5 to 19 mm)
	ASCE (2018)	ASTM No.57 (25 to 4.75mm)	ASTM No. 2 (63 to 37.5 mm)

iii) Dense bitumen macadam (DBM) – A protective layer laid above a subbase (BS 7533-1:2001).

2.6.1.7 Filter (choke) layer

Uniformly distributed aggregates are prone to aggregate migration, that is the smaller-sized upper layers can migrate into the lower layers thus compromising the hydraulic and structural adequacy of the pavement (CMAA, 2010). To prevent this, washed natural stone aggregate filters may be specified by the designers to replace polymer-based geotextiles provided there is availability of the required aggregate material. Typical aggregate distribution of this filter – alternatively called a ‘choke’ or 'choker' layer – would be expected to comply with BSI 7533-13:2009 and ASCE 68-18.

2.6.1.8 Bedding layer and grit material

The bedding layer for the pavers typically comprises a 50 mm single-sized washed stone laid over the open-graded aggregates layer or a geotextile if in use (ASCE, 2018). This layer is not usually considered for the computation of water storage, however it must have a substantial infiltration capacity. Hein & Smith (2016) and ASCE (2018) advise that the aggregate grading is typically ASTM No. 8 (9.5 to 2.36 mm). On the other hand, BSI (2009) and CMAA (2010) suggest a bedding layer aggregate grading of 10 to 2 mm and 4.75 to 1.18 mm (ASTM No. 9)

respectively. It is critical that the bedding material does not generate fines under dynamic vehicle loading and have an angular shape to promote lock-up.

Gritstone is filled between the paving blocks. Its purpose is to filter most of the sediment from runoff while still having a significant infiltration capacity and provide increased friction between pavers (Hein, 2018a). Sometimes the same material is used for the bedding layer (CMAA, 2010). This eliminates any potential for aggregate migration. The choice of gritstone must be closely linked to the size of paver openings. It must easily fill the openings while still not being susceptible to migration into the bedding layer. The use of sand for bedding and infill must be avoided as it will lead to almost immediate clogging and thus failure of the system.

2.6.1.9 Pavers

The PICP surface layer is constructed from various types of concrete pavers that come in various shapes, colours, depths, and joint widths (Figure 2-12). Depending on the purpose of the pavement, the paver depths may be either 60, 80 or 100 mm for pedestrian walks, vehicular or industrial driveways respectively (CMAA, 2010; Knapton *et al*., 2012). As with conventional pavers, PICP pavers must be structurally sound against the dynamic traffic loading and interlock. They would typically conform to ASTM C936/ C936M *Standard Specification for Solid Concrete Interlocking Paving Units* or SANS 1200 MJ: *Segmented paving*.

The openings between the pavers – called joints in most specifications although this is something of a misnomer as there is no connection between the individual blocks – can comprise as much as 15% of the surface area with extremely high initial infiltration rates (7000 to 20,000 mm/hr) (Bruinsma *et al.*, 2017; ASCE, 2018). BIA (2012) recommends a joint width of 1.6 to 4.8 mm. This is to promote universal access such as avoiding having wheelchairs stuck between the pavers.

The paver aspect ratio (length to thickness ratio) needs to be less than or equal to three for vehicular paving purposes (Interpave, 2018). Standard PICP vehicular pavers are 200 mm long and 100 mm wide (ASCE, 2018). There are cases where vehicular and industrial pavers that are 60 mm and 80 mm thick respectively have been installed and are working perfectly well (McQueen *et al.*, 2003), however, these depths do not conform to the required vehicle pavers' aspect ratio.

It is recommended that pavers are laid at either 45˚ or 90˚ to the pavement edges in a herringbone laying pattern which is considered to have the best load transmission and interlock relative to other laying patterns such as parquet and stretcher bonds (CMAA, 2010; ASCE, 2018) (Figures 2-12 and 2-13). CMAA (2014) suggest that dentated geometry pavers have a better interlock than rectangular shaped pavers and better resist longitudinal and transverse movements due to vehicular dynamic movements through transference of traffic load between adjacent pavers. For example, pavers with nibs, for instance e.g., the Priora ® block, have the potential to restrict vertical, horizontal and rotational movements due to increased block-to-block contact by as much as 40% over a standard PICP block (Marshalls, 2013).

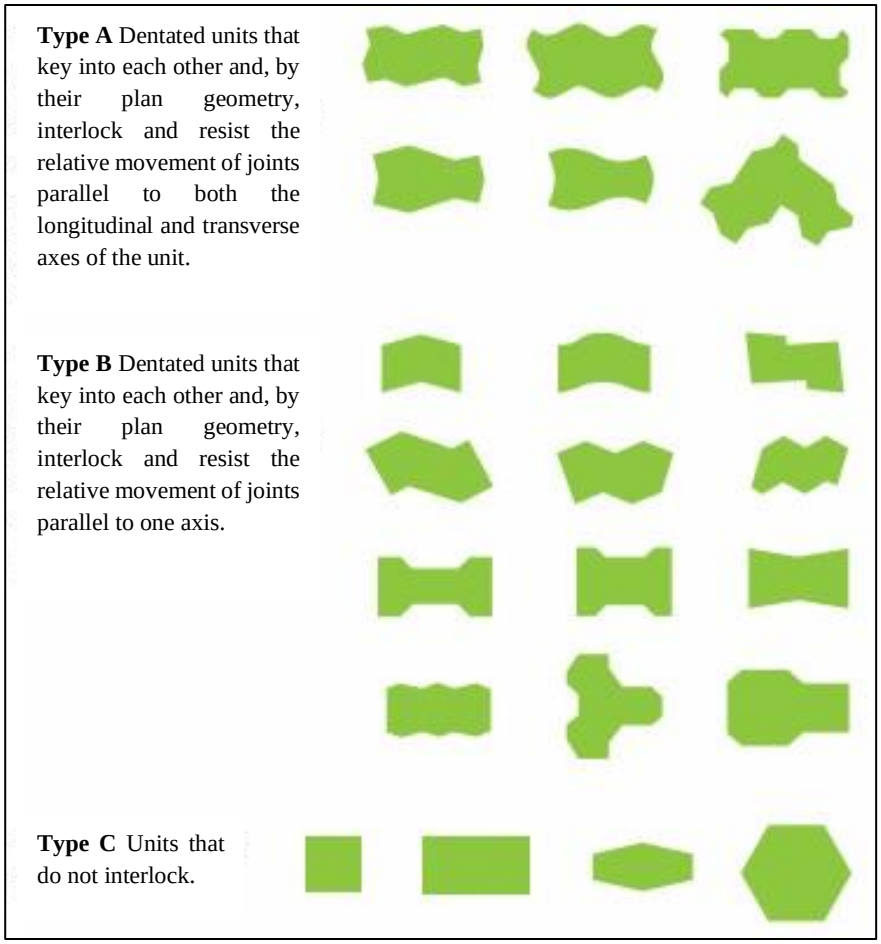

Figure 2-12: Some paver shapes (After CMAA, 2014)

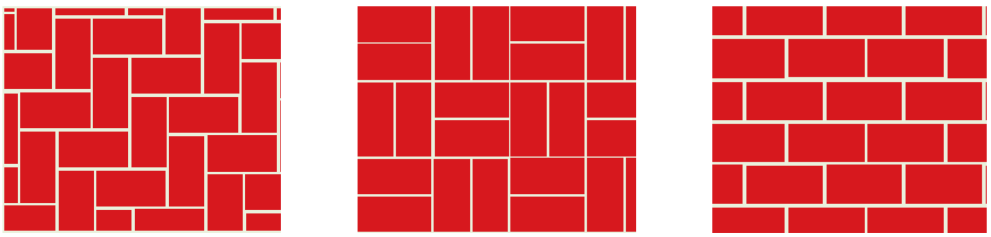

(a) Herringbone **(b) Parquet** **(c) Stretcher bond**

Figure 2-13: Typical paver laying patterns (CMAA, 2010)

2.6.1.10 Edge restraints

Edge restraints are essential components in PICP as they prevent lateral movement thus increasing the pavers' interlock and pavement structural adequacy. Typically, they are 150 mm × 225 mm (or 300 mm) concrete kerbs (ASCE, 2018). If there is a danger of movement between the PICP and adjacent layers they may need to extend much deeper. Lack of edge restraints support frequently leads to movement of the pavers opening up the joints and exposing

the underlying layers to wide range of contaminants such as sediment and organic matter that ultimately reduce the infiltration capacity of the system (Hein, 2018a). Edge restraints also help to detain runoff within the PICP layers.

2.6.1.11 Proximity to structures

PICP can be installed adjacent to conventional pavements and structures such as buildings, however protection of the substructures (pavement layers and building foundations) within 3 m of the PICP from runoff is essential. A typical detail would include the installation of an impermeable liner together with an underdrain next to the substructure (Figure 2-14) (Hein & Smith, 2016). In addition, the PICP surface should slope away from a structure. When PICP is installed adjacent to a conventional pavement, an edge restraint to separate the two is required (ASCE, 2018).

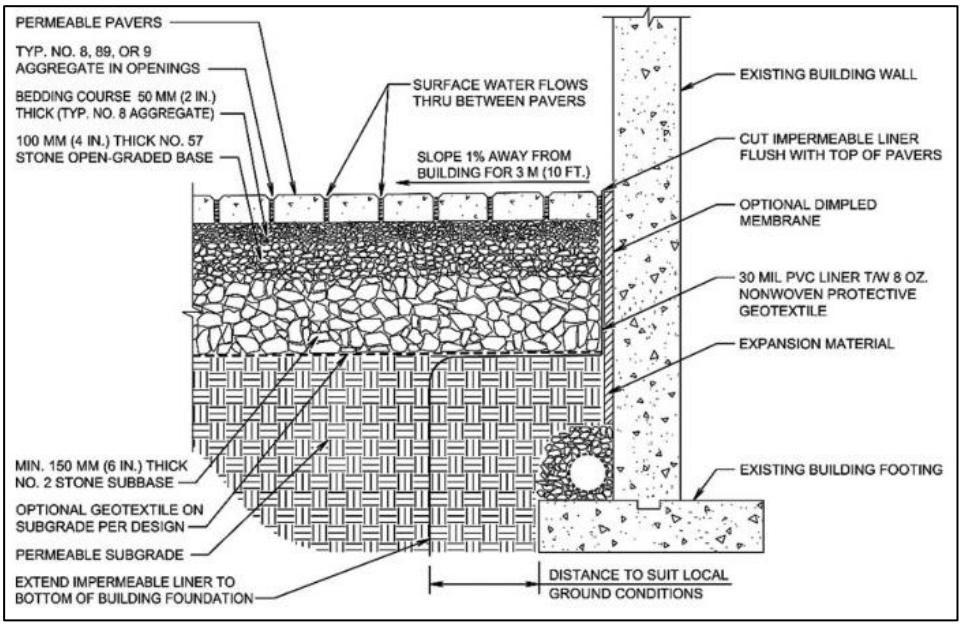

Figure 2-14: PICP installation near a building (ASCE, 2018)

2.6.2 Water Quality Volume (WQV)

There are two main components to PICP system design: structural and hydraulic (Beecham *et al*., 2010; CSIR, 2019). The structural design of PICP is typically in accordance with AASHTO (1993) for flexible pavements (Swan & Smith, 2009). The hydraulic design is usually determined by the Water Quality Volume (WQV) of a minor rainfall storm event (Armitage *et al*., 2013). The WQV is the targeted water volume to be treated by a SuDS option before it overflows into another stormwater management facility or component. The PICP base layers comprise single-sized aggregates with high porosities that act as a stone water tank for the WQV. Since the water

stored within the PICP layers is effectively at rest with a horizontal surface, maximum storage will be achieved when the PICP is laid with a flat surface (Interpave, 2018). Should there be a need to lay PICP on a slope, it should preferably be laid in a series of level terraces. Alternatively, internal check-dams situated at regular intervals parallel to the contours can be used to maximise the internal storage (NCDEQ, 2020), as described in Section 2.6.1.2.

2.6.3 The use of geotextiles and geomembranes in PICP

Geotextiles are used to separate different sublayers – most commonly between the bedding layer and the top-most base course. They can be woven or non-woven, heat-sealed or non-heat-sealed, depending on the intended use. Geotextiles or impermeable geomembranes are also sometimes used at the bottom of the PICP system to prevent the underlying soil from mixing with the coarse aggregate or when the designer wants to prevent infiltration of stormwater into the sub-grade (BSI, 2009; Hein & Smith, 2016). Apart from separating the different aggregates, the placing of geotextiles beneath the bedding layer potentially creates a suitable environment for water quality bacterial growth that can assist in the removal of various pollutants (Newman *et al*., 2002; Charlesworth *et al*., 2017; Liu & Armitage, 2020). It is however believed that the migration of fines from the surface onto the geotextile might result in premature clogging of the PICP (Armitage *et al*., 2013; Woods Ballard *et al*., 2015) although, according to some researchers, there is little evidence of the long-term clogging of geotextiles (ASCE, 2018). They may also create a 'slip zone' underneath the pavers that might cause premature failure (García-Casuso *et al*., 2020; Bezuijen & Izadi, 2022), particularly on the intersection approaches where vehicles brake and start to move abruptly (DPLG, 2010). The use of geotextiles in the UK is mandatory for the Aquapave ® system design because it is believed that geotextiles improve the effluent water quality (Woods Ballard *et al*., 2015). Consistent with the Aquapave ® design, Marshalls (2022) indicates that an MT120 ® geotextile can be installed to enhance the water quality of runoff and separate layers. In the USA and Australia, geotextiles are used at the discretion of the design engineer (CMAA, 2010; Hein & Smith, 2016), however, BES (2020) does not recommend it all.

2.6.4 The impact of run-on factor (RoF)

The PICP structure sometimes manages runoff from adjacent impervious surfaces and roof downpipes. The Run-on factor (RoF) is the ratio of the impermeable area that is serviced by the PICP to the permeable area of the PICP (Danz *et al*., 2020). Figure 2-15 shows a RoF = 2. A RoF of 0 implies that the PICP only handles direct rainfall, while a RoF of 1 implies that it also serves an equally-sized impermeable area. The RoF has implications for: i) the maximum hydraulic loading of the PICP, ii) the size of the WQV, and iii) the rate of clogging – particularly since run-on from adjacent impermeable areas is often a major sediment source. BSI (2009) suggests that the maximum RoF should not exceed 2. The Australian researchers Lucke & Beecham (2011a) suggest a maximum RoF of 3. WDNR (2021) however considers that a RoF of up to 5 can be

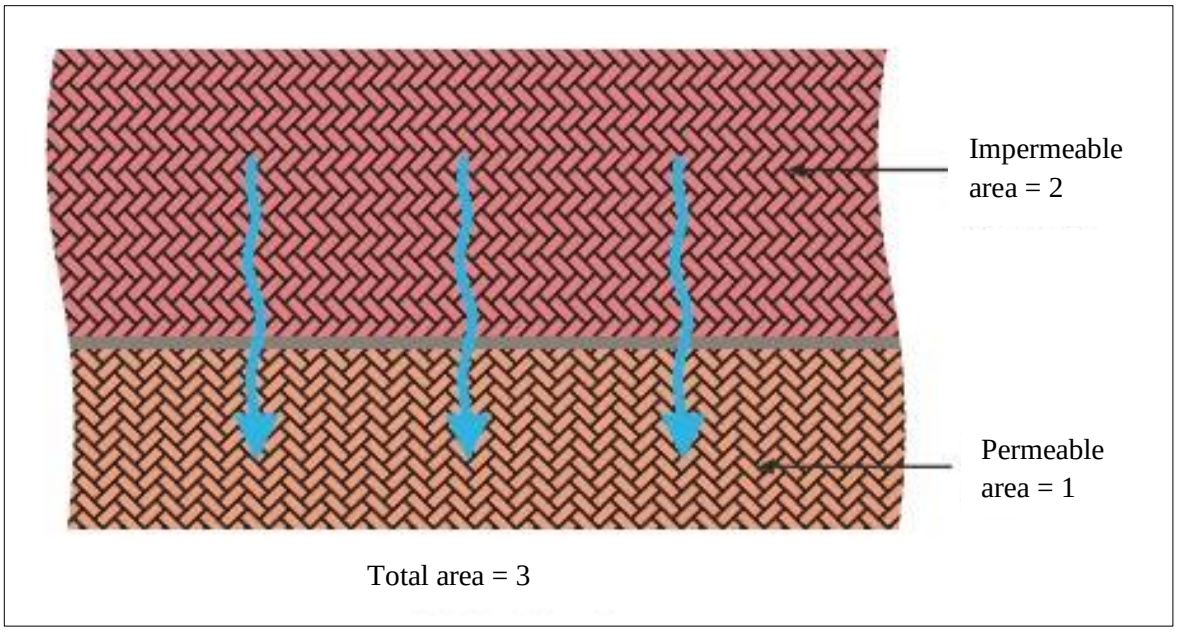

Figure 2-15: Ratio of impermeable to permeable area (Interpave, 2018)

accommodated provided the impervious surface is a relatively clean surface parking lot, rooftop, sidewalk, or residential driveway. The higher the RoF, the faster the clogging of the PICP surface thus the RoF should be kept low, e.g., not more than 2 (NCDEQ, 2020; WDNR, 2021).

2.6.5 Hydraulic failure in PICP

There are two main types of hydraulic failure in PICP: i) inadequate infiltration, and ii) inadequate storage e.g., for WQV.

It is hard to define infiltration failure in PICP – in part because of the difficulty of precisely measuring the inflow rate as the test water tends to flow sideways between the pavers rather than through their gaps and into the aggregate (Razzaghmanesh & Beecham, 2018). Freshly-laid PICP may have infiltration rates well in excess of 10,000 mm/hr (ASCE, 2018). Even poorly maintained or unmaintained PICP may still exhibit substantial infiltration rates (Beecham *et al*., 2009). However, there comes a point where stormwater cannot be effectively absorbed by the PICP in which case it has failed for practical purposes (Boogaard & Lucke, 2019; Drake *et al*., 2020). A common definition of infiltration failure is a measured infiltration capacity of less than 250 mm/hr (Sehgal *et al*., 2018). A more practical definition would be to say that PICP has failed when ponding on the surface is observed. Often, localised ponding is evident, indicating partial failure of the site (Interpave, 2018; WDNR, 2021).

Storage failure is usually linked to inadequate provision for WQV, although naturally, storm volumes greater than the WQV will also lead to hydraulic failure. As previously mentioned, the WQV is determined from the maximum level surface of the contained water.

2.6.6 Structural and hydraulic design flowcharts

Several design flowcharts are available to guide designers (Figures 2-16 to 2-18).

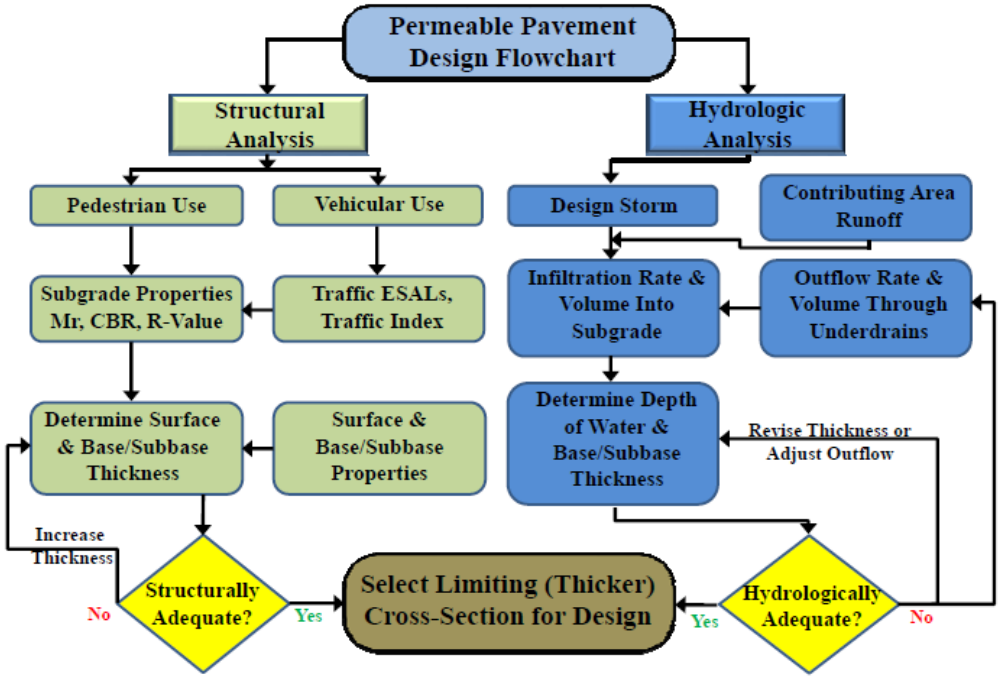

Figure 2-16: ASCE Permeable pavement design flow chart (Hein & Smith, 2016)

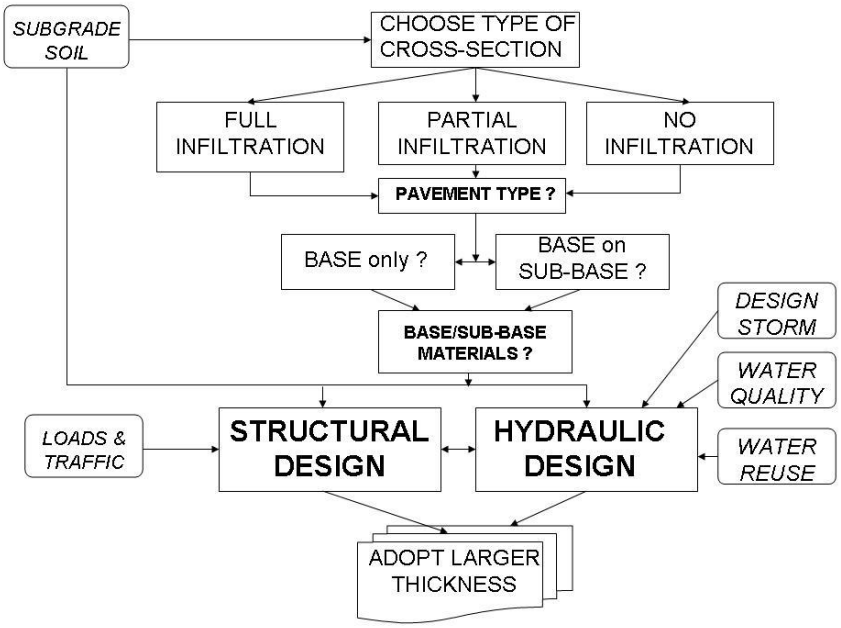

Figure 2-17: Methodology for designing a permeable pavement (Beecham *et al.*, 2010)

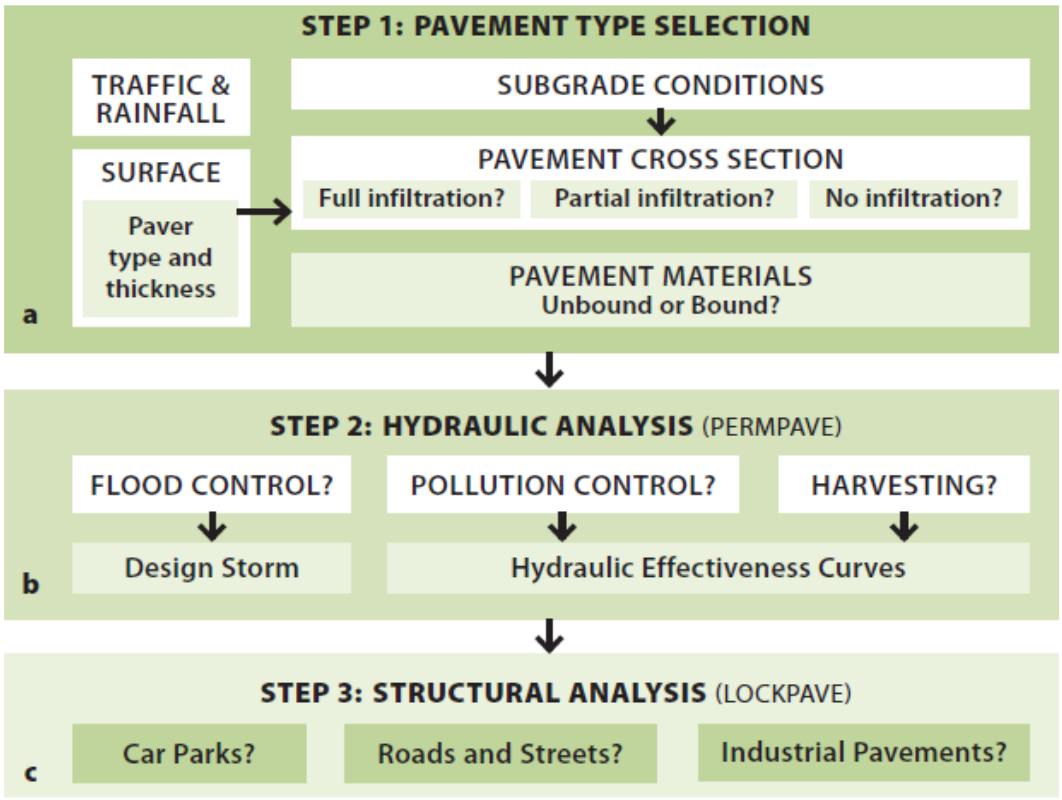

Figure 2-18: Design criteria for a PICP system based on Australian guidelines (CMAA, 2010)

All three flowcharts highlight key structural and hydrological design elements for PICP, but they vary slightly in the detail. None of the flowcharts mention anything about the use of geotextiles in the design. Indeed, very little detail is given in any of them. There is no mention of environmental, construction or maintenance issues.

2.6.7 Modelling tools

PICP can be a significant expense item and there is thus a need to ensure that they are correctly designed and assessed. It is thus unsurprising that software is available (BSI, 2009; Rosa *et al*., 2015; Xian *et al*., 2021). Modelling helps in determining and implementing cost-effective and optimised designs.

Two types of PICP models are available: i) general models that offer limited PICP functionality, and ii) models specifically written for the design of PICP.

i) General models that offer PICP functionality include: US EPA Stormwater Management Model (SWMM) and its variants, e.g., PCSWMM; MicroDrainage for SuDS (MDSuDS); and the Model for Urban Stormwater Improvement Conceptualization (MUSIC). SWMM is a hydrologic modelling tool developed in the USA and capable of simulating both single or long-term rainfall events and the associated runoff so as to replicate the quality and quantity of runoff generated from an urban environment (Azawi & Sachit, 2018; UWM, 2021). MDSuDS is UK-developed software that models various SuDS options for stormwater quantity and quality (Lashford *et al*., 2017; Innovyze, 2022). MUSIC is a stormwater assessment tool developed in Australia in 2001 to model the water quality and quantity of an urban environment while accounting for the water quality standards (Wong *et al*., 2002; Imteaz *et al*., 2013). It is capable of operating in catchment areas between 0.01 km^2 and 100 km^2 using time intervals ranging from 6 min – 24 hr (UWM, 2021).

ii) Specific models include Permeable Design Pro (PDP) and Designpave. PDP is software that was initially developed in the USA by the Interlocking Concrete Pavement Institute (ICPI) in 2010 to design the structural and hydrological components of PICP (ASCE, 2018). Similarly, Designpave, an Australian developed software – which incorporates two earlier software programs, Permpave and Lockpave – also accounts for the design of both the structural and hydrologic analysis of PICP (CMAA, 2022). Permpave assesses the potential for stormwater harvesting, fit-for-purpose reuse, and groundwater recharge (Beecham *et al*., 2010).

2.7 PICP construction

This section outlines the three-phased construction procedure of PICP – pre-construction, construction, and post-construction (i.e., just before the pavement can be opened for traffic). Table 2-4 presents a typical pre-construction checklist.

2.7.1 Preconstruction meeting

The construction of PICP needs care from the construction team and the end-user engagement before any work can take place. It is crucial that all stakeholders do a site walkover to inspect that the proposed site plan correlates with the actual site features. Some of the aspects that are usually discussed at a preconstruction meeting include (ASCE, 2018):

- The construction sequence.
- Availability and need of access routes to the site.
- Material storage, testing and laboratory requirements (on-site or off-site).
- Clear site demarcation to ensure that the PICP is not affected by adjacent activities.
- Subgrade and pavement layers compaction requirements.
- Sediment and erosion control (Stormwater Pollutants Prevention Plan).
- Temporary construction routes to support the construction traffic.

Table 2-4: PICP construction checklist
(After Woods Ballard *et al*., 2015; Hein & Smith, 2016; ASCE, 2018)

Item	Description
Preconstruction meeting	Discuss the construction requirements such as the sequence of work and sediment control. All the stakeholders must attend. Stakeholders include client's representative(s), site engineer, contractor, sub-contractor, landscape architects, architects, manufacturers.
Sediment control barriers	Installation of sediment control barriers.
Suitable PICP site conditions	Ensure a clear demarcation of PICP sections with site conditions appropriate to the construction of PICP.
Subgrade preparation	Excavate box cuts, test subgrade for CBR and infiltration capacity, and protect from sediment.
Lay lower geosynthetic (if any)	Ensure geosynthetic is laid such that it is not damaged.
Underdrains and observation wells laying	All elevations should be as per the design drawings and ensure the drains are not damaged.
Lay subbase	All elevations are as per the design drawings and the layer is protected from sediment, construction traffic and runoff.
Edge restraints	Installed at the permeable-impermeable surface interface and conforming to drawings.
Lay base	All elevations are as per the design drawings and the layer is protected from sediment, construction traffic and runoff.
Lay filter (choke) layer (no geotextile system)	Ensure that the filter layer is laid to level and compacted as required by the design.

Lay pavers	Adequate laying pattern and shape of pavers per design. Pavers are laid such that they interlock. The design slope is ≤5%.
Insert grit	Sweep in the grit to the paver joint brim and compact the surface.
Final inspection	Ensure no damaged pavers and edge restraints. The surface infiltration capacity must be 2500 mm/hr or more. A 250 mm/hr infiltration rate indicates that the surface is practically clogged, hence maintenance is required.

2.7.2 Material storage

The material should be stored on a hard surface or geosynthetic material free from significant sediment exposure (Hein & Schaus, 2013). It is essential that any fine material attached to the aggregates are washed off (CSIR, 2019). This could be achieved in one of the following ways: i) at the quarry site by running water (BoDean, 2022), or ii) by sprinkling with a water hose on a tipper truck as they come into the site at a designated wash station or away from PICP site. Unwashed aggregates tend to be washed by infiltrated water ultimately clogging the subgrade (ASCE, 2018). Ideally, the aggregates should not be stored for a long time as they are likely to accumulate dust and segregate. Alternatively, washed aggregate must be laid as it arrives from the quarry.

2.7.3 Sediment control

PICP is vulnerable to clogging with fine sediment. Sediment also impacts water quality control. It is thus essential to minimise exposure to sources of fine sediment, particularly during construction. Some of the measures that may be considered include, *inter alia*, sediment traps (Figure 2-19) or sediment mattresses for areas sloping towards the PICP site (NCDEQ, 2020).

Special care is required to install these measures as inappropriate installations could lead to catastrophic pavement sediment exposure. Figure 2-20 shows a sediment trap geotextile that has been incorrectly installed with a gap underneath that will allow sediment to flow onto the pavement.

Figure 2-19: Sediment trap (Industrial Fabrics, 2022)

Figure 2-20: Inadequate sediment trap installation (St John Source, 2022)

2.7.4 Stormwater and traffic management

Runoff carries many pollutants and consequently any runoff that may be generated during the construction of the PICP must be routed around the pavement e.g., via constructed swales (Hein & Smith, 2016). In the case of a small site, the pavement structure may be used to support the construction traffic, but it needs protection from the traffic load and sediment exposure (CMAA, 2010).

2.7.5 Preparation of the subgrade

The subgrade must satisfy the PICP hydraulic and structural design requirements, that is, have sufficient infiltration capacity (for full and partial infiltration designs) and carry the specified traffic. Typically, box cuts are excavated to lay the open-graded aggregate reservoir (OGAR) (NCDEQ, 2020). To achieve these, the California Bearing Ratio (CBR) specified in accordance with the ASTM D1883 *Standard test method for CBR of laboratory compacted soils* and the infiltration rate in accordance with ASTM C1781 *Standard test method for surface infiltration rate of permeable unit pavement system* or equivalent alternatives are conducted. If the subgrade CBR is less than 3%, then either soil stabilisation techniques or capping is applied to enhance the structural stability (BSI, 2009). NCDEQ (2020) advises that subgrade compaction should be avoided if possible since it reduces the infiltration capacity even though the CBR of the subgrade would be improved. As with conventional pavement construction, soft spots should be removed and replaced by either rock-fill material or suitable surrounding-like material to boost the infiltration capacity of the subgrade (NCDEQ, 2020).

The subgrade may be scarified, ripped or trenched to improve the infiltration rate. The ripped or trenched subgrade is then filled with free-flowing material. It is recommended that a geotextile or subbase is laid within 72 hours of the subgrade preparation to avoid sediment accumulation on the subgrade surface (NCDEQ, 2020).

2.7.6 Geosynthetics

Some of the PICP system's designs consider the use of either a geotextile or geomembrane within the pavement structure. These are typically laid in accordance with AASHTO M-288-15: *Standard specification for geotextile for highway applications* (2015). Woods Ballard *et al*. (2015) emphasize that geosynthetics should be laid with no folds, free of greases and breakages. For geosynthetic installations that require special considerations, for instance, on sloped sites, a specialist or a geosynthetic manufacturer needs to be consulted (Interpave, 2018). Many manufacturers recommend a welded geomembrane or 300 mm stitched geotextile overlap (NCDEQ,2020).

2.7.7 Underdrains and observation wells

Underdrains may be laid embedded in a base layer to avoid damage due to the pavement sublayer compaction and are connected to a SuDS or conventional stormwater outlet (Hein & Schaus, 2013).

2.7.8 Underground utility services

The underground utilities (e.g., telecommunication cables, water mains etc) may pass through the PICP site. Hein & Smith (2016) advise that the services may need to be relocated or protected from damage in high-density polyethylene (HDPE) casings or similar. Where possible, underground utilities should be preferentially laid under conventional pavements to minimise opening up PICP during utility maintenance.

2.7.9 Subbase placement

Clean specified open-graded aggregate reservoir (OGAR) aggregates may be laid in 100 – 150 mm layers using a tracked spreader (Woods Ballard *et al*., 2015). Hein & Smith (2016) recommends that a dead weight compactor may be preferred over a vibratory compactor to minimise the potential breakage of aggregates, subgrade compaction and damage of the lower geosynthetic (if any). In the case where the subbase is being used as a construction route, two options are suggested: laying a Dense Bitumen Macadam (DBM), or laying a sacrificial 50 mm base layer on a geotextile (Interpave, 2018). This is to protect the subbase from sediment exposure and potential rutting as the construction vehicles traverse the layer. 75 mm diameter orthogonal grid cores (filled with free-flowing base material) may be drilled into the DBM to allow for infiltration into the subbase layer (Woods Ballard *et al*., 2015). With the latter alternative, the sacrificial geotextile is removed and discarded once it is no longer needed. The stone may be washed and reused for the pavement base.

2.7.10 Edge restraints

Edge restraints are laid on top of the subbase to contain and ensure that the base aggregates lock up (NCDEQ, 2020). It is essential that the edge restraints are laid to conform with the site layout drawings.

2.7.11 Base placement

Usually the laying procedure followed for the subbase is also used for the basecourse (NCDEQ, 2020). However, if the pavement layer is to be used to carry the construction traffic, then an Asphalt Cement (AC) layer may be laid. Interpave (2018) recommends that the AC must be cleaned before it can be laid to remove any sediment or mud. A 100 mm filter (no geotextile

design) or geotextile layer may be laid above the base layer as per the design requirements (NCDEQ, 2020). The AC is generally laid in accordance with BS 594987 +A1:2017 – *Asphalt & other paved areas*. Upon completion of the AC layer, 75 mm diameter cores are orthogonally drilled 750 mm apart to allow for infiltration into the underlying pavement sublayer (Woods Ballard *et al*., 2015).

2.7.12 Upper geotextile

The procedure for laying the upper geotextile, between the base and bedding layer is similar to that described in Section 2.7.6. Occasionally bedding blinding is used to flatten the top of the base – to eliminate geotextile voids and avoid the angular base aggregates from puncturing the geotextile (Interpave, 2018). The blinding may reduce the infiltration capacity of the base layer, however an undamaged geotextile has the potential to trap sediment and improve water quality, thus protecting the underlying layers during the PICP service life. The period between bedding and geotextile laying should be minimised to reduce sediment exposure.

2.7.13 Bedding layer, pavers and gritstone

An uncompacted 50 ± 20 mm bedding layer is spread on top of the geotextile or base layer to provide support for the pavers (NCDEQ, 2020). The pavers are then laid on the bedding surface in such a way that they interlock with each other, thus reducing the risk of widened joints that make it easier for fines to migrate into the pavement system (Figure 2-21) (Marshalls, 2022). Clean gritstone is swept over the top of the paver joints and vibrated using a plate compactor. Once the surplus grit has been removed, more gritstone is added until it is flush with the surface of the pavement (Interpave, 2018).

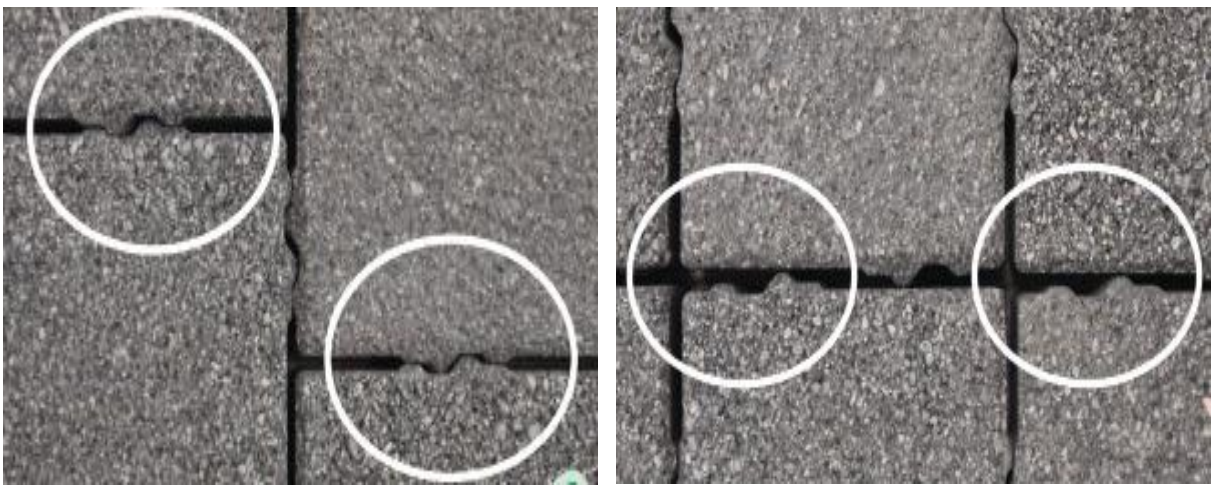

(a) Appropriate **(b) Inappropriate**

Figure 2-21: Paver installation interlock (Marshalls, 2022)

If the PICP is constructed in the early stages of the development and is required to access other parts of the site, it must be protected from sediment that may propagate into the system. A temporary sacrificial geotextile and 50 mm bedding layer may be laid to protect the pavement from fine material exposure. When the construction is completed, the adjacent soil must be stabilised and the site cleared (ASCE, 2018), after which the sacrificial layer is removed and the pavement restored using a vacuum sweeper to pick up any remaining sediment (Hein & Smith, 2016).

2.7.14 Post-construction

Upon completion of the construction, the infiltration rate should be determined to ensure that it is at least 2500 mm/hr (Hein & Smith, 2016). If not, the PICP surface will need remedial maintenance such as vacuuming to restore its infiltration. The site should be inspected within the first three to six months of operation to assess the pavement performance (ICPI, 2013).

2.8 PICP Maintenance

PICP maintenance may be categorised into two main types: routine and restorative. Routine maintenance is carried out at regular intervals to ensure the PICP system is performing as per the design – typically around twice a year (Woods Ballard *et al*., 2015). Structural maintenance is prompted by evidence of structural defects (Table 2-5) and is one form of routine maintenance. This could result in e.g., replacing broken pavers, refilling paver joints with gritstone, repairing damaged edge restraints (Figure 2-22), and removing any vegetation growth on the PICP surface (Hein, 2018a). The hydraulic performance of PICP is generally checked using surface infiltration tests or evidence of rainwater ponding. Restorative maintenance attempts to restore the PICP system to an acceptable operational state – typically annually upon completion of the pavement installation (Smith, 2017).

Table 2-5. PICP hydraulic and structural defects (Smith, 2017; Hein, 2018a)

Hydraulic defects	Structural defects
• Blocked surfaces & joints • Blocked sublayers • Blocked geotextile • Damaged geotextile	• Depression • Rutting • Faulting • Damaged pavers • Edge restraint damage • Excessive joint width • Joint filler loss • Horizontal creep • Additional minor distresses

(a) Rutting **(b) Widened joints** **(c) Damaged edge restraint**

Figure 2-22: Typical structural defects (Hein, 2018a)

Maintenance requirements are site-specific, Beecham *et al*. (2009) found sites that had not been exposed to any form of maintenance yet they still recorded significant infiltration rates 10 years after their installation. Maintenance can, however, significantly prolong the service life of PICP (Hein, 2018a).

2.9 Methods for determining the surface infiltration capacity of PICP

The hydraulic performance of PICP installation is generally measured using surface infiltration tests. A commonly used standard infiltration test procedure is the Single Ring Infiltrometer (SRIT) (ASTM C1781-2017) (Lucke *et al*., 2015; ASCE, 2018). Other tests include the: the Double Ring Infiltrometer (DRIT) (ASTM D3385-2009) (Nichols *et al*., 2014); the Stormwater Infiltration Field Test (SWIFT); the Simple Infiltrometer Test (SIT); and the Full-Scale Infiltration Test (FSIT) (Lucke *et al*., 2015; Marchioni & Becciu, 2015; Veldkamp *et al*., 2022). The tests are all presented in Figures 2-23 and 2-24. The four most common methods are summarised in Table 2-6. More detailed information follows.

Figure 2-23: Typical FSIT (Boogaard & Lucke, 2019)

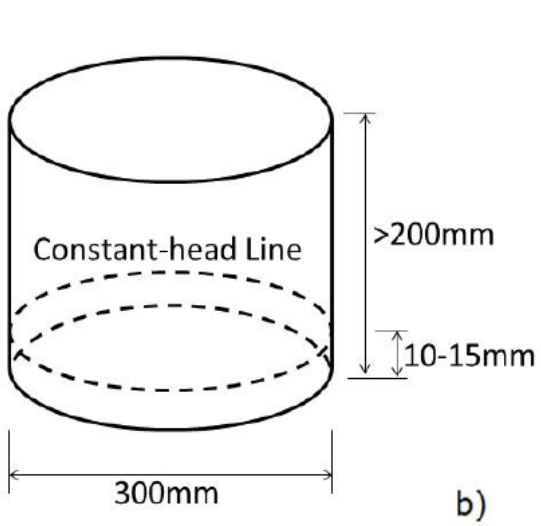

(a) SRIT (Lucke *et al*., 2015)

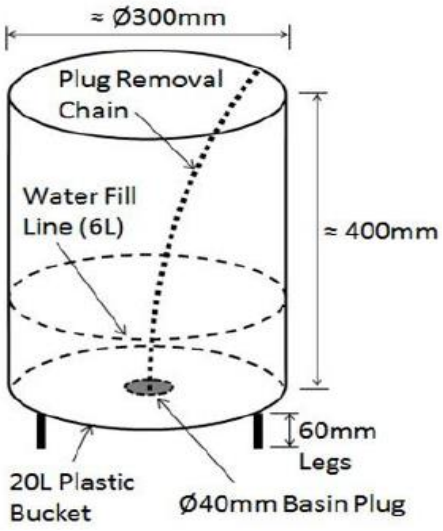

(b) SWIFT (Lucke *et al*., 2015)

(c) DRIT (Nichols *et al*., 2014)

(d) SIT (Winston, *et al*., 2016)

Figure 2-24: Different infiltration tests

Table 2-6: Infiltration tests' apparatus summary description

(Winston *et al*., 2016; Sanicola *et al*., 2018)

SRIT/ ASTM C1781	SWIFT	DRIT	SIT
The SRIT apparatus consists of a 300 mm diameter, 200 mm minimum height ring that forms a watertight seal with the PICP surface to prevent any lateral flow.	The SWIFT apparatus consists of a 20-litre bucket filled with 6 litres of water and fitted with a watertight 40 mm plug at the base. The bucket rests on 60 mm legs.	The DRIT apparatus consists of inner and outer diameter rings of 300 mm and 600 mm respectively. The rings' diameters are a minimum of 200 mm high.	The SIT apparatus is a square frame of 1 m x 1 m.

2.9.1 The SRIT / ASTM C1781 infiltration test method

The SRIT / ASTM C1781 infiltration test method is probably the most widely reported method for determining PICP surface infiltration. It is conducted as follows (Lucke *et al*., 2015, after ASTM C1781M-14a):

i) The surface to be tested should first be pre-wetted. This consists of pouring 3.6 litres of water into the ring.

ii) 18 litres of test water is poured into the ring while maintaining the head between 10 and 15 mm. The time taken to fully infiltrate the surface to the nearest 1.0 s is recorded.

iii) The infiltration rate is determined using Equation 2-1.

Equation 2-1 is used to determine the infiltration capacity of a PICP section for SRIT.

$$I = \frac{kM}{D^2 T} \qquad (2\text{-}1)$$

Where:

I	=	Infiltration rate (mm/hr)
M	=	Mass of infiltrated water (kg)
D	=	Inner ring diameter (mm)
T	=	Time required for water to infiltrate the pavement surface (s) and,
k	=	Constant value (4.58×10^9 in SI units).

2.9.2 The SWIFT method

The SWIFT test has the advantage of speed and low water use. It relies on counting the number of fully wetted bricks so it is important that the surface is initially dry. The SWIFT method involves the following steps (Lucke *et al*., 2015):

i) A 20 litre bucket with 40 mm hole in the bottom is placed 60 mm over the paver surface to be tested such that the drainage hole is located directly above the centre of one of the pavers.

ii) A plug fitted with a pull string is inserted into the drain hole to provide a reasonably watertight seal and six litres of water is poured into the bucket.

iii) The plug is removed using the pull string and the water is allowed to flow out of the bucket and onto the paving surface.

iv) The bucket is removed.

v) All fully wetted bricks are counted (A photograph may be taken for later analysis);

vi) The infiltration rate is estimated using the curve in Figure 2-25. The pavement blockage and maintenance requirements are determined in Table 2-7.

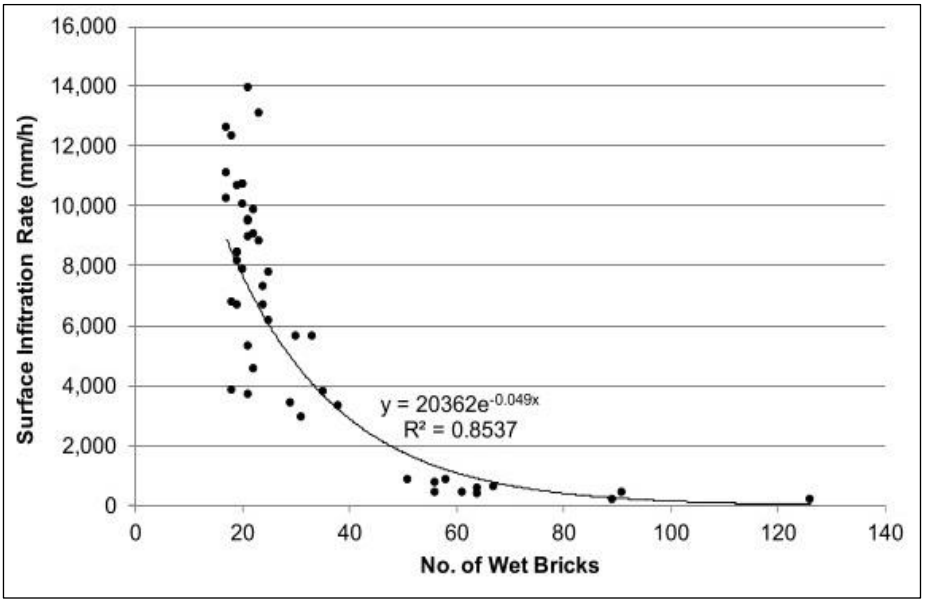

Figure 2-25: Wetted bricks vs Surface infiltration rate (Lucke *et al*., 2015)

Table 2-7: Suggested maintenance requirements for the SWIFT method
(Lucke *et al*., 2015)

Number of fully wetted bricks	Blockage category	Maintenance requirements
≤ 29	Unblocked	No maintenance for the foreseeable future
29 – 133	Medium Blocked	Plan for maintenance within 1 – 3 years
> 133	Fully Blocked	Immediate maintenance required

2.9.3 The DRIT method

The DRIT is conducted in accordance with ASTM D3385 *Standard Test Method for Infiltration Rate of Soils in Field using Double-ring Infiltrometer* (2009).

2.9.4 The SIT method

The SIT method is conducted by pouring 20 litres of water within the test apparatus in a falling head test and determining the time it takes for all the water to disappear (Winston *et al*., 2016).

2.9.5 The FSIT method

The FSIT is conducted by inundating a PICP surface with water (Boogaard & Lucke, 2019). The boundary of the permeable area is barricaded with sandbags and roadway kerbs to dam the water on the pavement surface (Veldkamp *et al*., 2022). FSIT is a more accurate infiltration test procedure than the other mentioned tests because it largely eliminates leakage at the edges and it is not a spot test (i.e., it measures infiltration for the whole PICP), however it requires a large volume of test water. The larger the test area, the higher the volume of the test water, hence, it is suitable for small-sized pavements.

2.10 Hydraulic surface maintenance techniques for PICP

PICP hydraulic maintenance largely revolves around the recovery of infiltration rates of stormwater runoff into the PICP system that has been lost due to clogging. This is measured by one of the PICP surface infiltration test methods described in Section 2.9.

The infiltration capacity of a PICP structure is reduced over time through surface clogging of the system by the build-up of windblown sediment or debris from the PICP surrounds (Sehgal *et al*., 2018; Tirpak *et al*., 2021) or transportation by runoff to cause hydraulic clogging (Drake *et al*., 2010; Nichols *et al*., 2015). The fine material gets trapped in the gaps between the PICP block pavers (Nichols *et al*., 2014), ideally within the gritstone, although there may be propagation into the system due to traffic movement vibration and runoff as it infiltrates the PICP (Armitage *et al*., 2013; Hein, 2018a). Rain also transport the material into the system. Eventually, it gets trapped on the geotextile if one is fitted, or propagates further down into the PICP reducing the runoff storage volume of the PICP (Lucke & Beecham, 2011)

In cold climatic regions where there is a need to infiltrate and melt snow; de-icing agents such as salt and sand accelerate the clogging of the PICP system increasing the required frequency and intensity of maintenance of the pavement structure (Drake *et al*., 2010).

Stormwater runoff carries many different types of sediment such as: flakes off vehicle tyres, plastics, loose fine material, tree leaves and cigarette butts, and these may get trapped between the joints. The material tends to build up on the PICP from the edges – that generally receives the heaviest sediment loading – towards the central part in the form of a clogging front between the relatively blocked zone and the relatively unblocked zone (Figure 2-26). For practical reasons, a measured infiltration capacity of less than 250 mm/hr is usually considered to be effectively blocked with a need for restorative maintenance (ASCE, 2018; Tirpak *et al*., 2021). The infiltration capacity of the restored pavement should be greater than 250 mm/hr or increased by at least 50% of the pre-maintenance infiltration rate (ASCE, 2018; WDNR, 2021).

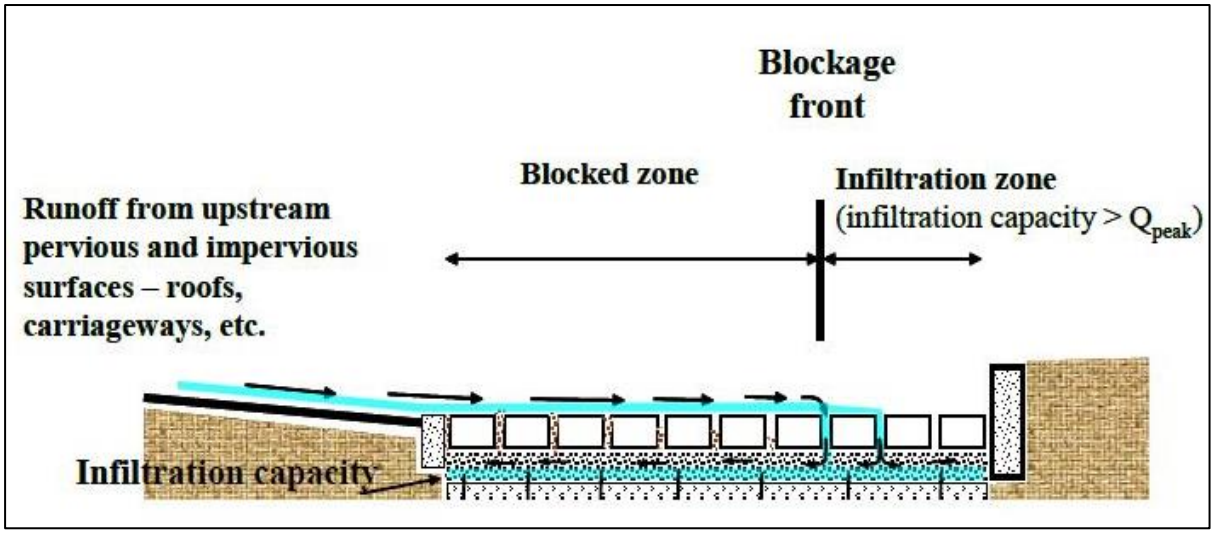

Figure 2-26: Summary of the PICP clogging process (Beecham *et al*., 2010)

PICP mostly traps sediment in the top 25 mm of the paver joints in the early years of their installation (Bean *et al*., 2007). Thus maintenance procedures need to be able to remove sediment at this depth. However, the method of maintenance depends on the level of clogging and the type of particulate that is trapped between the PICP joints. Although maintenance prolongs the service life of PICP, it does not restore the pavement's initial infiltration capacities (Hein, 2018a; Simpson *et al*., 2021). Different kinds of maintenance techniques have been developed to improve the hydraulic performance of PICP, these include: street sweepers, brooms, pressurized air and water jetting.

2.10.1 Street sweeper trucks

Street sweeper trucks are pavement cleaning technologies that pick up sediment from its surfaces. They are classified into three main categories (CIE, 2022) (Figures 2-27 to 2-29), namely: i) mechanical street sweepers, ii) vacuum-based sweepers, and iii) regenerative sweepers.

Figure 2-27: Mechanical street sweeper (NCDEQ, 2020)

(a) Vacuum-based street sweeping mechanism **(b) Rotating windrow broom 'close up'**

Figure 2-28: Vacuum-based street sweeper (Drake *et al*., 2020; NCDEQ, 2020)

(a) Street sweeping mechanism **(b) Street sweeper in action**

Figure 2-29: Regenerative street sweeper (Drake *et al*., 2020; NCDEQ, 2020)

Mechanical sweepers are a conventional technology characterised by rotating brooms that channel the dirt into a conveyor belt and temporarily stored in a hopper. Vacuum-based sweepers are fitted with rotating windrow brooms that guide pavement sediment towards a suction head and into a hopper. A regenerative street sweeper truck consists of rotating brooms that direct detritus into a blower head and suction compartment and into a hopper whilst circulating high-pressure air (Sehgal *et al*., 2018; Drake *et al*., 2020).

Drake & Bradford (2013) and Drake *et al.* (2020) determined that regenerative and vacuum-based street sweeping – individually applied – can improve the pre-maintenance surface infiltration of PICP by removing the superficial 'gunk' in the paver joints by up to 4340% and 1620%. Individual regenerative air sweeper tests, however, provide widely varying performances. The equipment may struggle to lift wet sediment and thus to improve the infiltration rate of the PICP section (Simpson *et al*., 2021).

Vacuum-based sweepers are more efficient than mechanical sweepers. Five mechanical sweeper passes have been reported to significantly increase a young (<two years) surface infiltration rate of a PICP section by up to 350% (Winston *et al*., 2016). Razzaghmanesh & Beecham (2018) suggest that vacuum-based street sweepers should be used to maintain PICP if possible because of their ability to remove loose sediment from the pavement's surface. However, it is unclear how many passes need to be applied on permeable pavement and how often should the pavement be maintained to get satisfactory infiltration improvement as pavement clogging is usually not uniform.

Regenerative air sweepers and vacuum trucks are designed to displace and pull the sediment from paver joints (Sehgal *et al*., 2018), however they may also pull out the pavement bedding as in some instances it is much the same size as the grit material. This would undermine the pavement, hence care must be taken to adjust the sweeper suction to prevent this from happening (Hein, 2018a).

2.10.2 Pressurized air and vacuuming

The Pavetech ® pressurized air and vacuum comprise Typhoon ® and Pavevac ® which forcefully dislodge trapped joint sediment and vacuum it away respectively (Figure 2-30) (Danz *et al*., 2020; Drake *et al*., 2020). Drake *et al*. (2020) found that this maintenance strategy significantly rejuvenated the PICP infiltration rate by around 109%. The vacuuming effect stops any potential for the dislodged detritus from being trapped in the joints again by removing sediment up to a mean of 21 mm (Drake *et al*., 2020). Application of Pavetech ® equipment has seen a substantial (1703%) infiltration capacity improvement on some sites (Danz *et al*., 2020). This method is however labour-intensive and it may require extended periods to clean a large parking area, but it is generally considered worthwhile.

(a) Pavetech Typhoon ® **(b) Pavevac ® suction system**

Figure 2-30: Compressed air and vacuuming (Drake *et al*., 2020)

2.10.3 Rejuvenater

Figure 2-31 presents a Rejuvenater attached to the back of a regenerative sweeper. This design comprises a device fitted with rotating water spray nozzles at 22 MPa that is pushed along by the operator. When applied on a commercial PICP site, the pavement infiltration capacity increased by 1075% (Simpson *et al*., 2021). More testing is necessary to investigate the effectiveness of this method on different sites though.

Figure 2-31: A rejuvenater (Simpson *et al*., 2021)

2.10.4 Hand power brush and vacuuming

Efficient maintenance requires dislodging sediment between pavers and vacuuming it, thus Sehgal *et al*., (2018) investigated a hand-held power brush equipped with a 1.4 kW motor at ~20,685 kPa (3000 psi) (Figure 2-32) followed by vacuuming of the detritus.

Figure 2-32: Application of a power brush (Sehgal *et al*., 2018)

In their study, they found that the maintenance methods can substantially reinstate the PICP infiltration capacity, but there was considerable spatial variation on 3-4 mm paver joints – leaving some sections clogged. The bristles of the power brush may be likened to those of a mechanical street sweeper which do not penetrate deeper into the pavement joints likely resulting in limited improvement of the infiltration rates (NCDEQ, 2020).

2.10.5 Power washer and vacuuming

Power washing consists of a forcing water at high pressure through a nozzle to form a jet directed along the joints of the pavement to loosen the sediment (Drake *et al*., 2020) (Figure 2-33). The sediment is picked up by vacuum suctioning (Seghal *et al*. 2018). When used in combination with either a manual vacuum or regenerative sweeper, it can restore the PICP infiltration capacity between 25% and 505% (Drake *et al*., 2020; Simpson *et al*., 2021). Danz *et al*. (2020) found that power washing can improve the surface infiltration of PICP by 172% when used in conjunction with application of three vacuum sweeper passes. Simpson *et al*. (2021) showed that the power washer alone can restore infiltration rates in wide-jointed pavers (13-14 mm) by up to 149%. Despite its significant surface improvement, the power washer is however likely to push some fine sediments deeper into the pavement structure consequently contributing to the long-term clogging of the pavement (Kia *et al.*, 2017). Moreover, the dislodged sediment may be scattered on the pavement.

Figure 2-33: Water jetting (Sehgal *et al*., 2018)

2.11 Other considerations

A site-specific maintenance plan is essential for the longevity of PICP surface infiltration (Razzaghmanesh & Beecham, 2018). It seems that the best hydraulic maintenance practice for the effective infiltration capacity of the PICP system is to dislodge the fines in the pavement joints which should then be removed – preferably by vacuum suction of the sediment rather than sweeping.

Unfortunately, there comes a point when the PICP infiltration capacity cannot be retrieved (<250 mm/hr) because of severely clogged joints, bedding or geotextile (if any). At this point, a corrective measure is required (Smith, 2019). It may be necessary to remove and replace the pavers and bedding layer with clean one. If a top geotextile is fitted between the bedding layer and the base, it is substituted and new or washed bedding and pavers are laid. Clean gritstone is then swept and vibrated into the joints (Hein, 2018a).

2.12 Summary

PICP has the potential to reduce stormwater volume, flow rate and pollutants content. In the process, it can promote groundwater recharge, water harvesting, biodiversity, and amenity of a development. The pavement's infiltration capacity is sensitive to sediment accumulation within the paver joints. With time the infiltration rate drops and maintenance is required. A well designed, constructed and maintained PICP will slow clogging and prolong the pavement's life.

3. Methods

3.1 Overview

This section outlines the methods used to investigate the clogging behaviour of PICP. They comprised a literature review, fieldwork, laboratory work, and input from a specialist working group comprising representing local authorities, consultants, suppliers and academics – including students – who guided the study. The literature highlighted current knowledge and allowed gaps to be identified. Research into the current performance of PICP installed across SA was carried out. Maintenance trials were carried out to see the effectiveness of the compressed air blower. Where there was evidence of failure, sections of PICP were dismantled to see where the problems lay. Insight into the clogging rates of the different paver and geotextile types were provided through accelerated tests in the laboratory to address these gaps. The method is summarised in Figure 3-1.

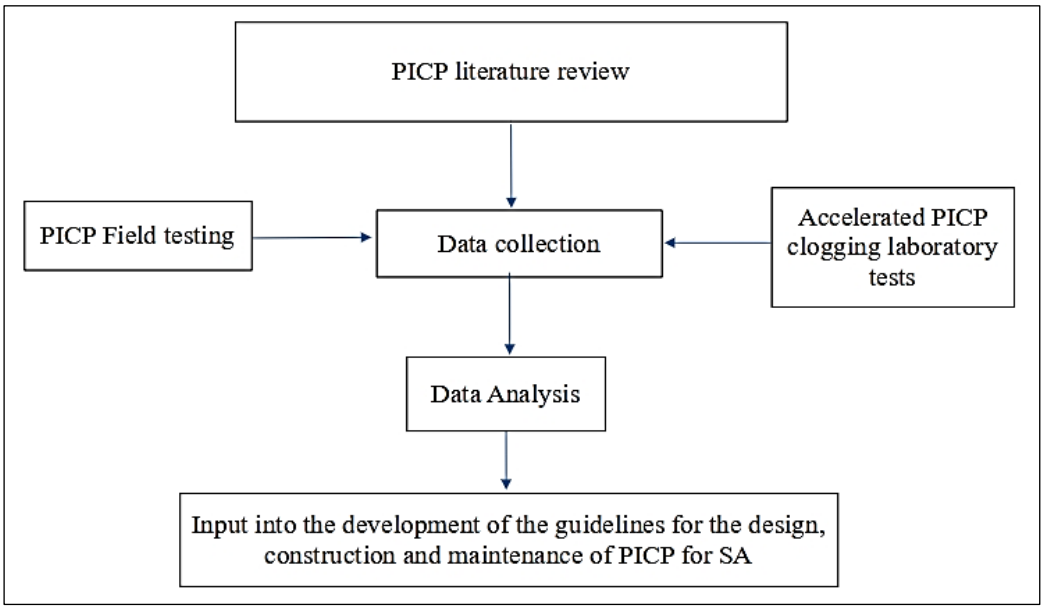

Figure 3-1: The study method summary

3.2 PICP site selection criteria

It was thought that the best way to understand how PICP is performing in South Africa (SA) would be to go out and view a range of installations. To that end, a list of PICP sites was compiled with the assistance of local authority representatives, paving suppliers, and consultants. Most of the sites were situated in and around Cape Town and Gauteng. Representative sites were then selected for possible investigation taking into account their:

- Geographical location,
- Variation in pavement design,

- Variation in environmental factors such as: vegetation and sediment proximity for example,
- Site slopes,
- Run-on factors,
- Traffic loading,
- Method of construction,
- Known state of clogging,
- Age,
- Known maintenance.

Permission to perform infiltration and pavement investigative tests on these sites was then requested. Overall, eleven test sites were identified: nine in and around Cape Town and two in Gauteng. More details of the test sites are presented in Chapter 4.

3.3 Laboratory investigation into the link between the upper geotextile and clogging

Research in Australia (AUS), the United States of America (USA), and South Africa (SA) suggests that fine material can propagate into the permeable pavement system and potentially clog any geotextile present (Fassman & Blackbourn, 2010; Biggs, 2016; Winston *et al*., 2016). The fine material originates from both the PICP surrounds as well as from within the pavement structure owing to the use of dirty aggregates and/or from their crushing under the impact of traffic. Thus, accelerated laboratory experiments were designed and conducted in four HDPE test cells situated in the University of Cape Town (UCT) laboratory to investigate:

1. The link between different geotextiles and clogging (with pavers) (Peyi, 2021; Blackshaw, 2021),
2. The link between the paver opening and clogging (Mqadi, 2022),
3. The link between different geotextiles and clogging (without pavers) (Morritt-Smith, 2022).

The first experiment was performed twice, once with Aquaflow ® and once with Permaflow ® pavers at slightly different loading rates – all with three different geotextiles plus one control without any geotextile to explore the impact of the different geotextiles. The second experiment was performed using four different pavers each laid on a non-woven, non-heat treated geotextile – Kaytech Bidim A1 ® – to explore the impact of different joint openings on clogging. The third experiment was designed similarly to Experiment 1 but with no pavers and relatively higher sediment loading rates.

3.4 PICP infiltration test methods

There is currently no universally accepted PICP infiltration test method. The most commonly adopted method appears to be ASTM C1701/1701M: *Standard Test Method for Infiltration of In Place Pervious Concrete*, sometimes called the Single-Ring Infiltrometer Test (SRIT) because it only uses one ring as opposed to the Double-Ring Infiltrometer Test (ASTM D3385:2009) which is preferred for the measurement of soil infiltration rates. There are, however, problems with the SRIT when used to measure infiltration rates in PICP. These include: leakage, marking of the surface, excessive water use, and the unacceptably long test time for partially blocked PICP. While the ASTM C1701/1701M / SRIT method was used as a benchmark for infiltration testing in this project – albeit in a modified form which will henceforth be termed the Modified ASTM (Mod-ASTM) – alternative methods were also investigated that ended up in the creation of the Modified Stormwater Infiltration Field Test (Mod-SWIFT).

3.4.1 Determining surface infiltration rates using the Modified ASTM

Most PICP testing in this project was carried out using ASTM C1701/1701M / SRIT with some minor modifications – thus it will be termed Modified ASTM (Mod-ASTM) here. The first modification involved the method of creating a watertight sealant between the pavement surface and the testing apparatus. A plumber's putty is normally used, but this increases the cost of the test (for the putty), is tedious, and marks the PICP surface (ASTM C1701/1701M, 2017). It was thus replaced with a 10 mm neoprene foam strip glued to the bottom of a 315 mm outside diameter, 500 mm long unplasticized vinyl chloride (uPVC) pipe weighted down with small concrete blocks when in use (Figures 3-2 and 3-3). The test procedure otherwise followed the method described in ASTM C1701/1701M. The Mod-ASTM was used in both the laboratory and field testing. 10 and 15 mm head marks were lined out as per *ASTM C1781M-14a*.

A further modification to the standard ASTM C1781 procedure entailed the length of the test. After experiencing unacceptably long test periods where it appeared that significant quantities of water leaked out of the system via the gaps between the pavers that could not be completely plugged with small neoprene pieces, the maximum testing time was limited to 15 minutes. After this, no further water was added. The timer was stopped when all the remaining water in the apparatus had infiltrated into the test spot. The total quantity of water infiltrated into the PICP was then determined by subtracting the remaining water determined with the aid of a measuring cylinder from the initial 18 litres prescribed for the full test. *ASTM-C1781-14a* states that 3.6 litres of water should be used for pre-wetting, however, when the Mod-ASTM test was carried out in combination with the Mod-SWIFT test (Section 3.4.2), the latter was performed first which wetted the surface making the pre-wetting stage redundant and thus reducing the total amount of water required for the first test. Equation 2-1 was used to determine the surface infiltration of the PICP for the Mod-ASTM.

(a) Mod-ASTM C1781 test apparatus

(b) ASTM C1781 test apparatus

Figure 3-2: The impact of the plumbers' putty as used in ASTM C1781

(a) Mod-ASTM C1781 test apparatus

(b) Mod-ASTM C1781 test apparatus underside

Figure 3-3: Mod-ASTM infiltration test apparatus

3.4.2 Determining surface infiltration rates using Modified SWIFT

The other test that was used to determine the PICP surface infiltration rate was the Modified Stormwater Field Test (Mod-SWIFT, Figure 3-4). The Stormwater Field Infiltration Test (SWIFT) infiltration capacity is determined by counting the number of wetted bricks and linking this to the possible need for maintenance (Table 2-7) (Lucke *et al*., 2015). Its strength lies in the reduced water requirement its speed and its ease of use. Its weakness is that pavers come in different sizes and shapes and counting fully-wetted bricks as per the method is tedious and may lead to errors owing to different sized paving units.

In a bid to make the SWIFT test both more general as well as more informative, the counting of fully-wetted pavers was replaced with an approximation of the wetted surface area by assuming that it is roughly elliptical (circular if the surface is flat). Noting the constant ratio between an ellipse and a rectangle bounding it, the calculations were then further simplified by relating the wetted area to this rectangle. The infiltration rate could then be related to that derived by the Mod-ASTM through multiple tests carried out by the two test methods on the same spots and using Excel to fit a curve through the resultant scatter diagram (Figure 3-5 and Equation 3-1). The curve fit comprised data points from previous PICP research conducted at UCT.

(a) Modified SWIFT test apparatus **(b) Modified SWIFT test apparatus underside**

Figure 3-4: Mod-SWIFT test apparatus

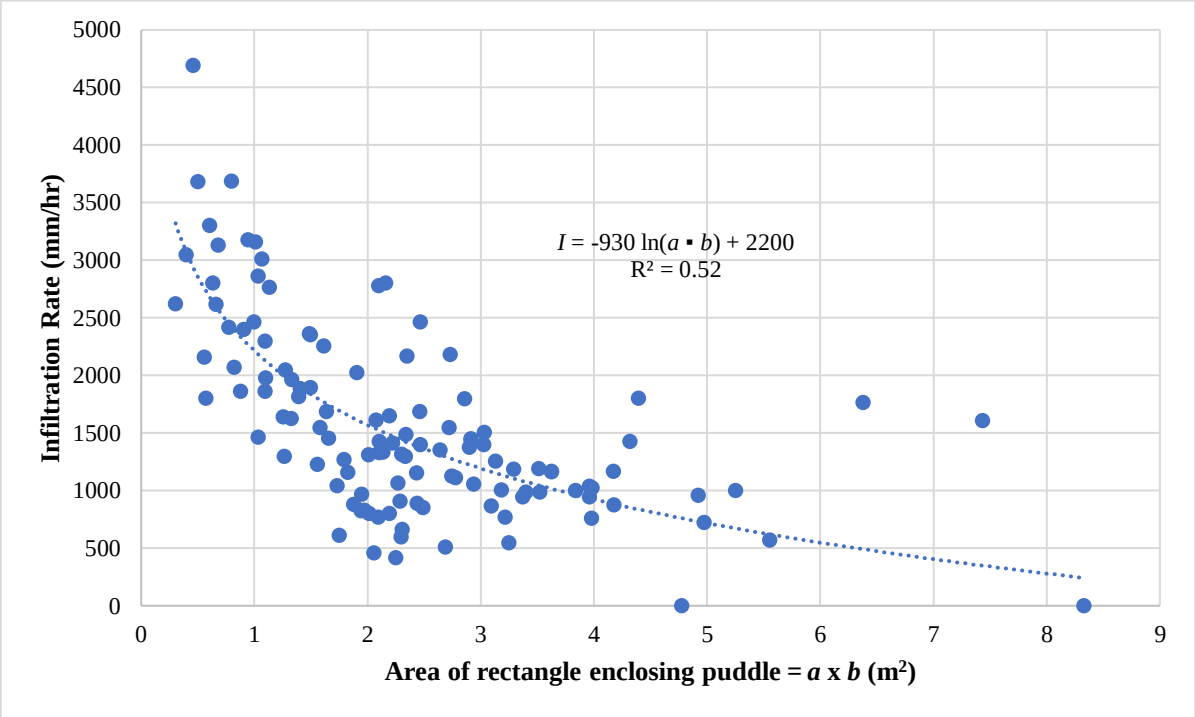

Figure 3-5: Plot of Mod-ASTM infiltration rate to representative wetted area in the Mod-SWIFT (Armitage, 2019)

$$I = 2210 - 930 \ln(a \times b) \qquad (3\text{-}1)$$

Where:

I	=	Infiltration rate (mm/hr)
a	=	Length of longest wetted section (m)
b	=	Length of the longest wetted section perpendicular to a (m)

The test procedure for the Mod-SWIFT is similar to that for the SWIFT described by Lucke *et al*. (2015). The Mod-SWIFT was particularly helpful in the field when there was limited access to test water. The Mod-ASTM test was, however, preferred in the laboratory or where adequate supplies of test water were available to allow comparisons with published data.

3.5 Summary

The experiments – both field and laboratory – shed considerable light on PICP clogging behaviour that was used in the development of the guidelines for the design, construction and maintenance of PICP in South Africa.

4. Field testing of existing PICP installations

4.1 Overview

Research has shown that the hydraulic performance of the PICP decreases with the age of installation (Lucke *et al*., 2015; Barnard, 2019). The oldest recorded installation of PICP in SA was built in 2007. This section details the PICP field tests that were conducted in SA between September 2021 and July 2022 to determine which factors were having the biggest impact on the infiltration performance and indicate how best to mitigate them under a variety of conditions. The field tests included the determination of infiltration rates, experiments with surface maintenance – mainly the blowing of compressed air – and the opening up of selected clogged sites for diagnostic assessments.

4.2 Detailed field test methods

Seeing the overwhelming number of PICP installations were in Cape Town and Gauteng, the field tests were entirely carried out in these two locations which also conveniently covered both a coastal, winter rainfall situation as well as an inland, summer rainfall situation (Table 4-1, Figure 4-1, Table 4-2, and Figure 4-2). According to SANRAL (2013), the Mean Annual Precipitation (MAP) for Cape Town is 400-1200 mm while that of Gauteng is 600-800 mm. The following general approach was followed:

- A detailed list of PICP sites was compiled into a compendium with key design, construction, and maintenance details (where known), and stakeholders' details.
- After securing permission from the owners, eleven PICP test sites were chosen for investigation – nine in Cape Town and two in Gauteng region –and linking the outcome to different designs, construction methods, maintenance approaches (if any), and environmental conditions.

Table 4.1: Research carried out on the Cape Town PICP study sites with codes

Infiltration test sites	Maintenance trials and diagnostic assessment sites
Blue Route Mall (BRM)	Blue Route Mall (BRM)
New Engineering Building (NEB)	New Engineering Building (NEB)
School of Economics (SOE)	School of Economics (SOE)
Irma Stern Museum (ISM)	Grand Parade (GRP)
Grand Parade (GRP)	MyCiti Bus Rapid Transport Depot (BRT)
MyCiti Bus Rapid Transport Depot (BRT)	Hirsch's Appliances Milnerton (HAM)
Stor-Age Facility (SAF)	
Hirsch's Appliances Milnerton (HAM)	
Nirvana Residential Complex (NVC)	

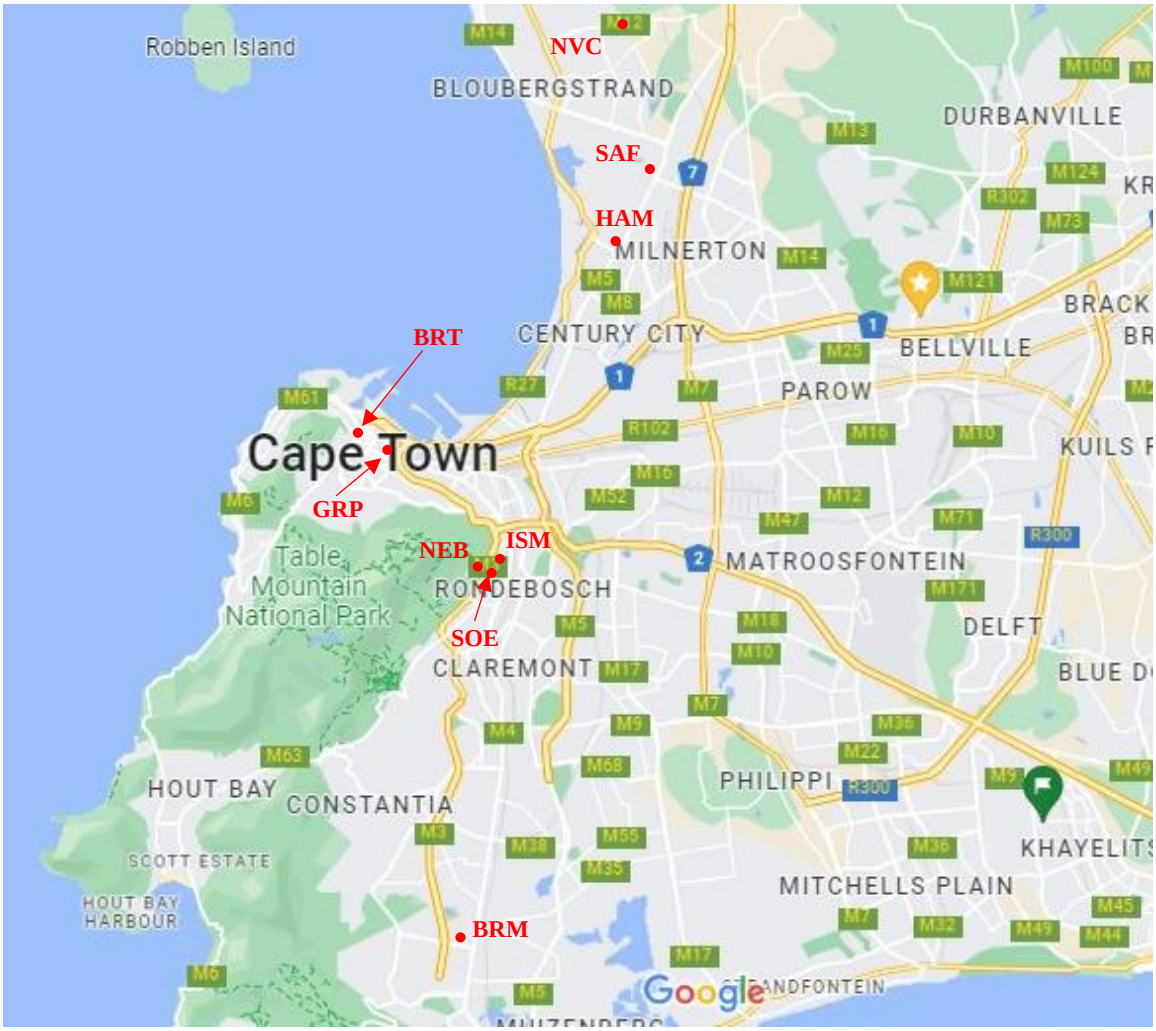

Figure 4-1: Cape Town PICP test sites (Map source: Google Maps, 2022)

Table 4.2: Research carried out on the Gauteng PICP study sites with codes

Infiltration tests sites	Diagnostic assessments sites
Wits First years' parking area (WITS)	Wits First years' parking area (WITS)
Bosun Brick Pavers (BBP)	

- During the first site visit, potential test spots were selected depending on the characteristics of the PICP sections. Typical considerations included: the proximity of vegetation and debris sources, traffic loading, and probable clogging state as determined by visual inspection. The number of test spots was largely governed by the size of the site.
- The test spots were named according to the site code, PICP area number (if any), and test spot – for example; Blue Route Mall-Area 4-Test spot 4 would be called: BRM-4-04. If the PICP was not divided into isolated areas, the naming convention would be simplified, e.g., SOE-01 for School of Economics Test spot 1.

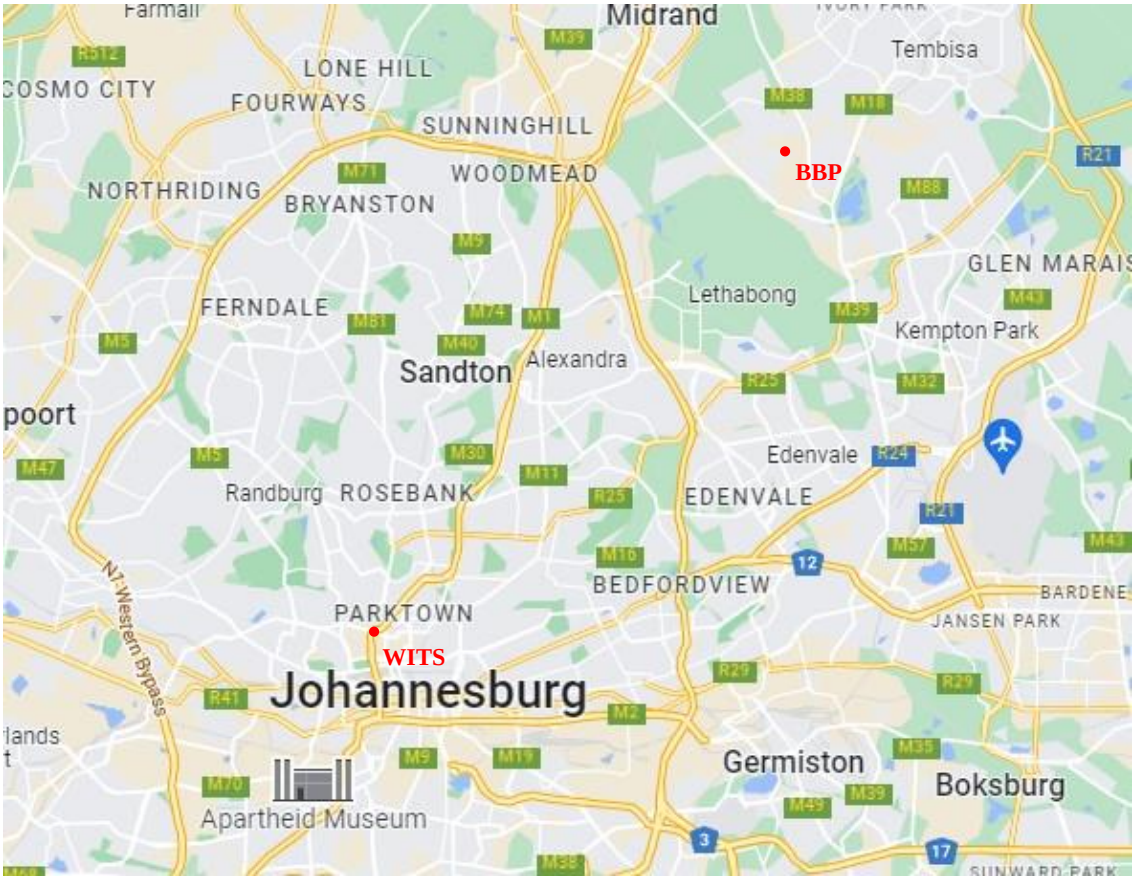

Figure 4-2: PICP test sites in Gauteng (Map source: Google Maps, 2021)

- Surface infiltration tests were then performed using the Modified ASTM single-ring infiltrometer (Mod-ASTM) and/or the Modified Stormwater Infiltration Field Test (Mod-SWIFT). Section 3.4 presents the test procedure for the two surface infiltration tests. The Mod-ASTM was conducted where there was access to sufficient testing water while the Mod-SWIFT test was conducted on sites with limited access to the test water. Occasionally, both tests were undertaken on the same spot to provide additional data points for the correlation plot (Figure 3-5), with the Mod-SWIFT test conducted first to replace the pre-wetting phase of the Mod-ASTM test. In this chapter, infiltration tests refer to Mod-ASTM unless stated otherwise.
- The infiltration results were compared with previous data when available to give an indication as to how the PICP performance was deteriorating over time.
- Maintenance trials were carried out at selected sites.
- Diagnostic assessments were carried out at some of the maintenance sites.

4.3 The PICP maintenance trials

The long-term performance of PICP is determined to a large extent by its maintenance, particularly with respect to reducing the clogging process. There are effectively three types of

maintenance: routine, restorative and reconstruction. Routine maintenance is the regular maintenance designed to identify and slow down the rate of clogging and potential structural failure (Woods Ballard *et al*., 2015). Restorative maintenance attempts to remove the material causing the clogging. Reconstruction is required when the PICP become so clogged that the only sensible remedy is to remove the pavers and the underlying bedding material, clean and reinstate them (Sehgal *et al*., 2018).

At the time the research was carried out, the only maintenance of PICP being carried out in SA was at a limited number of sites in Cape Town where the joints were being regularly blown to remove clogging material. Compressed air was directed along the joints and the dislodged material swept by a hand broom to the edge of the pavement from where it was collected. Any gritstone that may have been blown out with the gross pollutants from the joints was sieved, washed, and re-used for filling the joints where required. Alternatively, new clean gritstone was swept into the paver gaps. Attempts were made to investigate the maintenance performance of:

1. Blowing followed by sweeping (the current practice)
2. A street sweeper truck,
3. A vacuum truck, and
4. An industrial vacuum cleaner

Unfortunately, it was not possible to secure street sweeper or vacuum trucks as they were being fully utilised, however, an effort was made to investigate the maintenance combination of the compressed air blower and a 2000 W wet/dry industrial vacuum cleaner – but this proved ineffective. Some researchers (e.g., Drake & Bradford, 2013; Nichols *et al*., 2014) contend that blowing followed by vacuuming is the most effective method to maintain PICP but it is likely that this requires a much more powerful vacuum machine than that was available for this project. On the other hand, Hein (2018a) notes that if the vacuum is too powerful there is a risk of the bedding and/or pavers being lifted causing failure of the surface. In the end, maintenance trials were carried out at six sites in Cape Town. The general procedure for the trials was as follows:

- Permission to perform maintenance trials was first obtained from the site owners.
- Mod-ASTM surface infiltration rates were conducted on the identified PICP test spots. These results were recorded as base infiltration rates.
- The test spots were surrounded by a shade-cloth fence to protect adjacent property or people from flying debris. The workers wore appropriate Personal Protective Equipment (PPE).
- Maintenance was performed on the test spot using a 700 kPa compressed air blower attached via a flexible hose to a steel ‘wand’ with an 8 mm nozzle. The minimum area of cleaned surface was 2 m x 2 m. The blown-out debris was blown to one side and collected for removal and/or recycling (in the case of the joint gritstone).

- The post-blowing and post-maintenance infiltration rates were then measured to determine the effectiveness of the maintenance.

4.4 PICP diagnostic assessments

Diagnostic assessments were performed on selected pavement test spots that did not show significant signs of surface infiltration improvement in a bid to understand where the clogging was taking place. The general procedure was as follows:

- The pavers were carefully lifted and the joints and bedding inspected for signs of clogging.
- The infiltration rate through the bedding was determined using the Mod-ASTM test.
- The bedding was carefully scooped away to expose the upper geotextile or the base course (no upper geotextile design). All observations were recorded. Another Mod-ASTM was carried out on the geotextile or base course as applicable.
- If the geotextile – if present – was clogged, a piece was carefully cut out and the underlying aggregate inspected – all the way down to the lower geotextile or sub-base as applicable.
- Once the location and type of clogging had been identified, the paving was reinstated taking care to compact each layer and fill the joints between the pavers with washed gritstone.
- The post-maintenance infiltration rates of the pavers were measured upon completion of the re-gritting.

Four types of PICP clogging were identified in the course of the diagnostic assessments:

- Type I clogging – the most common type – is when fine material fills the joints, typically the first 20 to 30 mm depth from the surface.
- Type II clogging takes the form of a sediment ‘wedge’ on the bedding layer immediately under the joints and usually looking like a silhouette of the paving pattern.
- Type III clogging is when the bedding layer and the top of any geotextile have been filled with sediment.
- Type IV clogging sees sediment throughout the full depth of the PICP layers (complete failure).

4.5 Blue Route Mall (BRM) parking area

Blue Route Mall (BRM) is a shopping centre located in Tokai, Cape Town (34° 3'50.65"S, 18°27'15.45"E), at an altitude of 15 m above mean sea level (a.m.s.l.) (Figure 4-3). The current mall was constructed in 2012 when PICP was installed over large portions of the outside

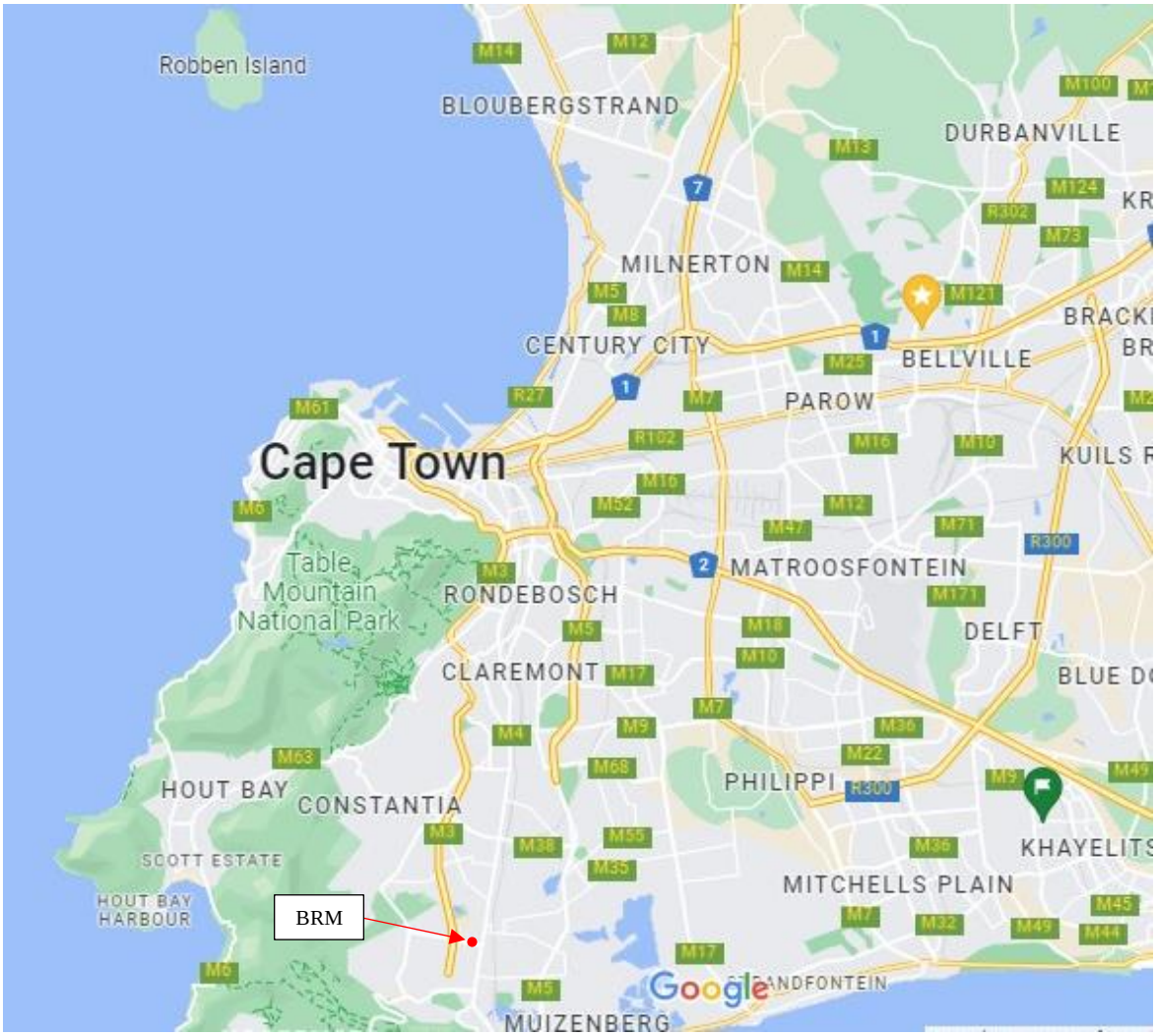

Figure 4-3: Blue Route Mall PICP locality plan (Map source: Google Maps, 2022)

parking area including both parking bay zones and the main vehicle roadways. The traffic is mainly cars with occasional delivery trucks.

The mall is surrounded by the asphalt-surfaced Tokai Road on the southern side, Keyser River Drive on the western side, Vans Road on the western side, and part of the Access Road on the northern side. Some portions of the Access Road are also PICP. The mall site slopes at 2% towards a stream that runs parallel and adjacent to the northern part of Access Road. The stream joins the Keysers River a short distance east of the mall (Figure 4-4).

Trees with needle-shaped leaves overhang the PICP adjacent to Vans Road. Various evergreen trees and shrubs are also located adjacent to the PICP – potentially acting as a source of debris (Figures 4-5 and 4-6). Figure 4-7 shows the roof downpipes that drain directly on the permeable pavement. The pedestrian walkways in the parking area consist of conventional brick pavement that drain onto the PICP.

Figure 4-4: BRM site layout (Map source: Google Earth Pro, 2022)

(a) **(b)**

Figure 4-5: Trees hanging over PICP

The permeable area is 35,500 m^2 and the impermeable area is 13,760 m^2 giving a run-on factor (RoF) of approximately 0.4 (Barnard, 2019; Matolengwe, 2021). Thus, the PICP mainly services direct rainfall. The BRM PICP sections comprised: 80 mm Aquapave ® pavers, 2-3 mm joint material, 80 mm deep x 4-6 mm bedding stone, an upper Inbitex ® geotextile, a 100 mm deep x 19-25 mm stone basecourse, a 250 mm deep x 50-63 mm subbase layer, and a

(a) Evergreen tree **(b) Shallow bush**

Figure 4-6: Vegetation adjacent to the parking area

Figure 4-7: Roof downpipes draining onto the PICP

lower Inbitex ® geotextile to protect the subgrade.

4.5.1 Field infiltration testing

Mod-ASTM infiltration tests were conducted in 2017, 2018, 2019, and 2021 by students at the University of Cape Town (UCT). In 2017 and 2018, nine test spots were carefully identified and infiltration surface tests conducted (Test spots 1 to 9). In 2019 and 2021, 15 test spots were chosen for surface infiltration investigation (Test spots 1 to 15). Test spots 1, 3, 5, 6, 8, 10 to 15 were each located within parking bays. Test spots 2, 4, and 7 were located along the roadway. Test spot 9 was located on a truck off-loading bay. Test spots 10 to 15 were located within a section of the parking that is infrequently used (Figure 4-8). Carrying out multiple infiltration tests over a number of years helps with tracking the performance of the PICP with age.

Figure 4-8: BRM surface infiltration test locations (Map source: Google Maps, 2022)

Figure 4-9 presents the measured infiltration rates. The infiltration capacity of the PICP site had decreased with age from 2017 to 2021 at Test spots 2 to 9. Test spots 10 and 12 to 15 illustrate the same pattern of infiltration capacity drop with the age of PICP from 2019 to 2021. The outliers were test spots 1 and 11 both of which were both located within parking bays. Most of the infiltration capacities were below 2000 mm/hr in 2017 except for Test spots 2, 3, and 4. By 2018, the infiltration rates for Test spots 2 and 3 had also decreased to below 2000 mm/hr. Generally, the test spots located along the vehicle roadways had lower infiltration rates than those located within the parking bays. By 2021, all infiltration rates had dropped although none were less than 250 mm/hr – the benchmark used to indicate total blocking (measured infiltration rates likely to be more leakage than infiltration). The lowest infiltration rate recorded in 2021 was 280 mm/hr for Test spot 15, while the highest was only 1600 mm/hr for Test spot 1. For Test spots 1 to 5, the infiltration capacities had dropped despite the maintenance that was performed in 2021 indicating that maintenance only temporarily improves PICP infiltration rate, it does not fully restore it. Over the period 2017 to 2021, the BRM PICP maintenance was being performed on a three-year cycle.

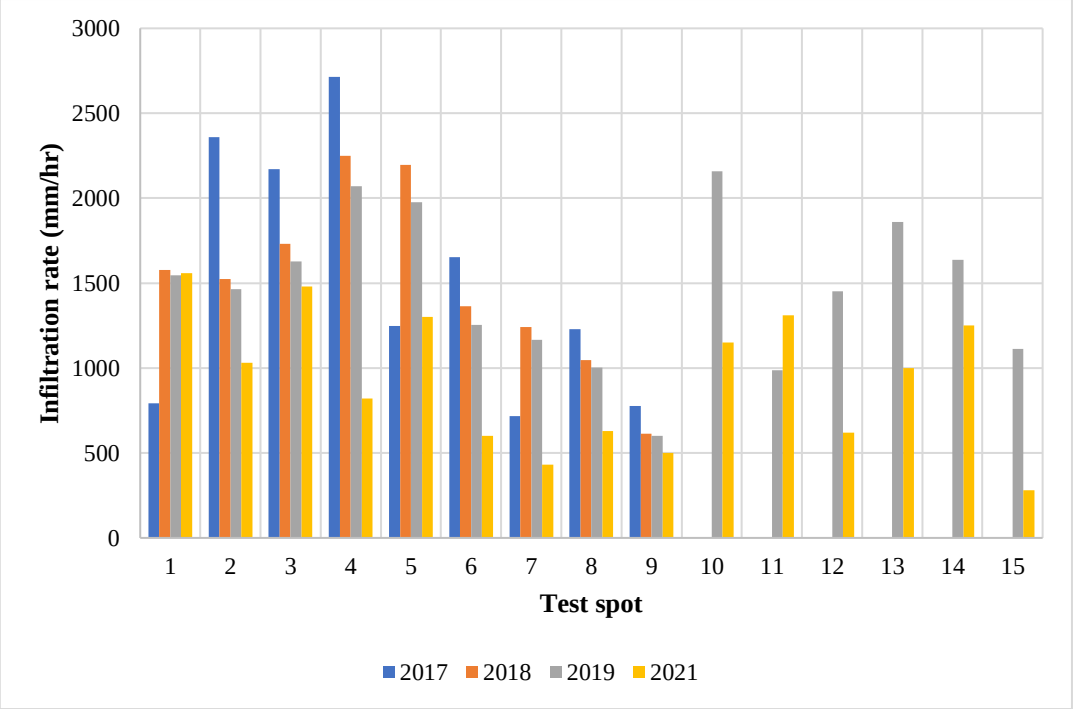

Figure 4-9: 2017-2021 BRM ASTM infiltration rates
(After Artus, 2017; Vella, 2018; Barnard, 2019; Matolengwe, 2021)

4.5.2 Pavement maintenance trials

Compressed air blowing maintenance trials were performed at the BRM PICP site in 2022 to investigate the effectiveness of the compressed air blower as a maintenance method. Test spots in two adjacent PICP sections were chosen for the trials. One was in a vehicle parking bay area (Area 3 / BRM-3), while the other was in a highly-trafficked PICP roadway section (Area 4 / BRM-4) (Figure 4-10). Four test spots were located in Area 3 and 11 in Area 4.

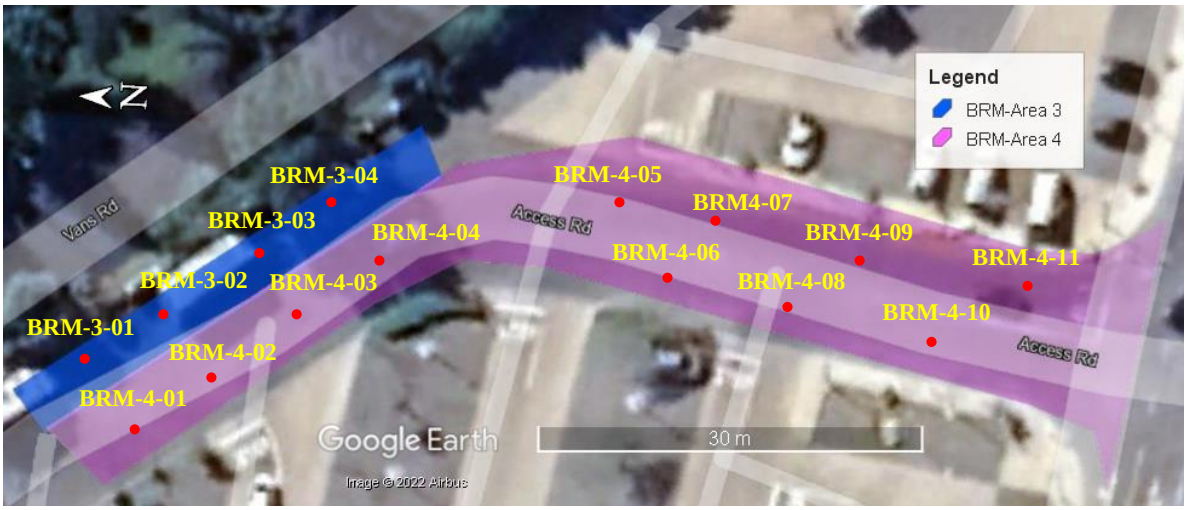

Figure 4-10: BRM PICP Areas 3 and 4 test spots (Map source: Google Earth Pro, 2022)

4.5.2.1 Parking bays

Maintenance trials were carried out in Area 3, a series of parking bays located adjacent to Vans Road on the eastern side of the site. The PICP section was overhung by pine trees that shed needle-shaped leaves onto the surface (Figure 4-5). Three types of infiltration tests: pre-maintenance, post-blowing, and post-maintenance, were performed on all the BRM-3 test spots except for Test spot BRM-3-01 because of its location near where the joint sediment was collected after blowing. The measured infiltration rates for the four Area 3 test spots are presented in Figure 4-11.

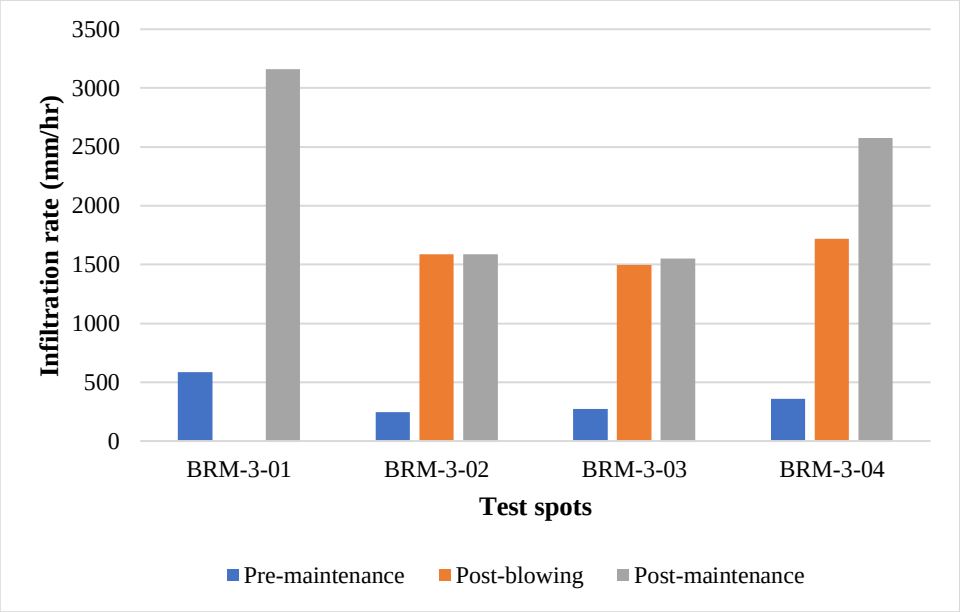

Figure 4-11: BRM Area 3 Mod-ASTM test infiltration rates

The pre-maintenance infiltration rates measured at all four BRM-3 PICP section test spots were equal to or less than 600 mm/hr. BRM-3-02 recorded a 200 mm/hr base infiltration rate, which is just below the nominal PICP blockage failure infiltration rate. BRM-3-01, BRM-3-03, and BRM-3-04 recorded base infiltration rates of 600, 300 and 400 mm/hr respectively. Visually, the main cause of these low infiltration rates appeared to be the combination of organic and inorganic matter clogging the paver joints (Figure 4-12).

The substantial increase from 325% to 700% in post-blowing infiltration rates indicated that compressed air blowing improved the pavement infiltration capacity. There was a small difference between the post-blowing and post-maintenance infiltration rates for BRM-3-02 and BRM-03-03, while the infiltration rate appeared to increase considerably for BRM-3-04 for some unknown reason – possibly lateral flow of the test water.

Compared to the pre-maintenance infiltration rates, the post-maintenance infiltration capacity of the four test spots was increased by 438%, 549%, 464%, and 614% for the four test spots. However, none of them returned to the likely newly laid values which typically range from 7000 to 20,000 mm/hr (ASCE, 2018). This suggests that some residual clogging remains

– probably at the base of the joints (Type II). This is likely to increase with the age of the pavement.

Figure 4-12: Typical PICP section with needle-shaped leaves wedged in the joints

4.5.2.2 Heavily trafficked sections

Figure 4-13 presents the Mod-ASTM pre-maintenance, post-blowing, and post-maintenance infiltration rates for Area 4. The pre-maintenance infiltration rates recorded for Area 4 were relatively high; the lowest was 1700 mm/hr for test spot BRM-4-06, while the highest was 16,700 mm/hr for test spot BRM-4-03. On the other hand, it was apparent that the paver joints in BRM-4 had frequently been widened by up to 14 mm leading to substantial water losses in the infiltration measurements calling into questioning their reliability (Figure 4-14). Typically, the Aquapave ® paver installed on the site is designed to have a joint width of 6 mm.

Somewhat surprisingly, the post-blowing infiltration rates for many test spots were lower than pre-maintenance. This suggested that the fine sediment material was being pushed deeper into the pavement sublayers thus contributing to the blockage of the pavement. On the other hand, BRM-4-06, BRM-4-07, and BRM-4-11 showed increases in the post-blowing infiltration rates of 217%, 42%, and 328% respectively, suggesting that, in these cases at least, sediment material blown out of the joints had a greater impact than any fine material pushed deeper into the layers. For most test spots, filling the joints with gritstone decreased the infiltration rates.

Overall, air blowing had a variable impact – with an improvement of 144% observed in one case, but a drop of 59% in another. On the whole, however, the post-maintenance infiltration rates were mainly above 2000 mm/hr which is considerably above the nominal clogged rate of anything below 250 mm/hr.

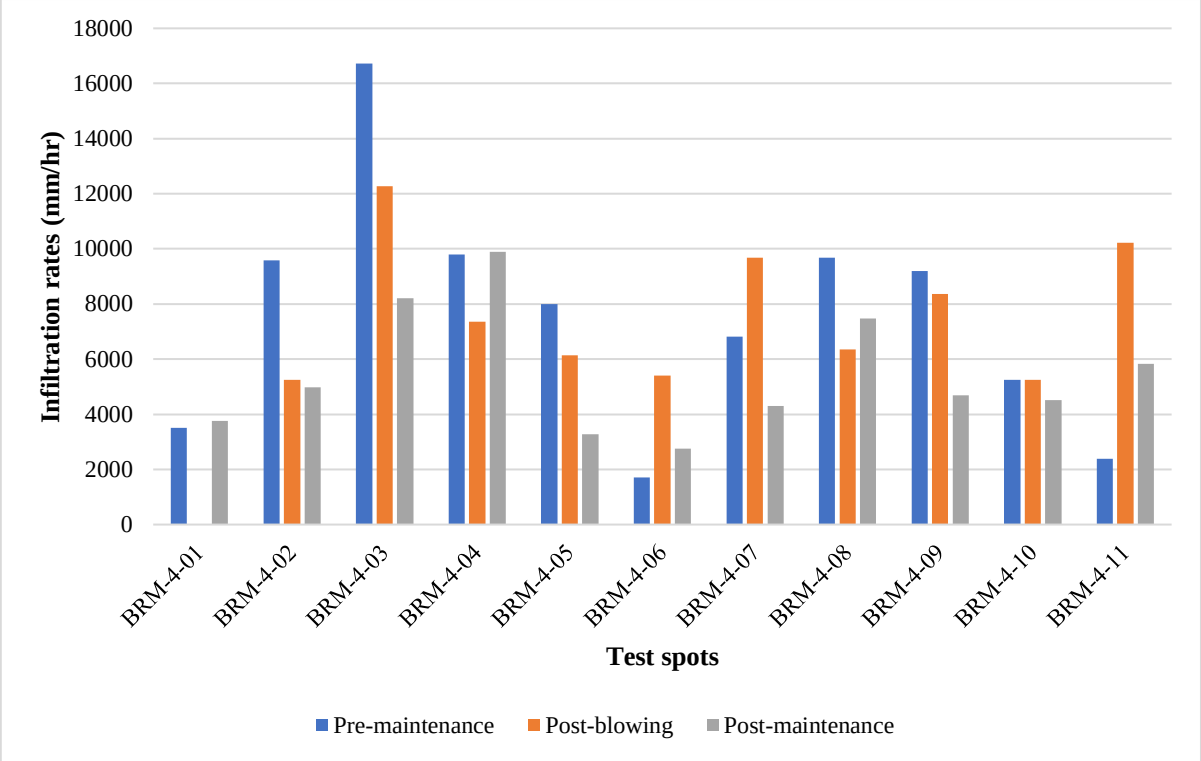

Figure 4-13: BRM Area 4 test infiltration rates

(a) 10 mm wide joint **(b) 20 mm wide joint**

Figure 4-14: PICP section widened joints

The reason for the failure of the compressed air blowing to improve the infiltration rates within the PICP is likely structural in nature. It was noticeable that the PICP pavers at places with high levels of turning traffic were displaced due to damaged and / or insufficient lateral support by the edge restraints. Hein (2018a) ranks the damage caused by inadequate edge restraint as low if the paver joints are widened by 6-10 mm, medium of 11-15 mm or severe if greater than

15 mm. The paver joints on this PICP section were up to 20 mm wide suggesting severe damage. Further, there was an excessive loss of grit (Figure 4-14).

4.5.3 Diagnostic assessments

Diagnostic assessments were performed on the two PICP sections – one in a parking bay (Area 3), and three in a heavily trafficked section (Area 4).

4.5.3.1 Parking bays

A diagnostic assessment was performed on Test spot BRM-3-04 with the measured infiltration rates given in Figure 4-15. The sediment in the joints was intermixed with the joint material (Figure 4-16 (a)) for the top 25 mm (Type I clogging). However, the sediment outlining the paver pattern on the bedding (Figure 4-16 (b)) suggested that Type II clogging was also taking place. On the other hand, the geotextile was intact with only small quantities of trapped sediment. When cut, it was evident that the underlying aggregate layers were clean (Figure 4-16 (c)).

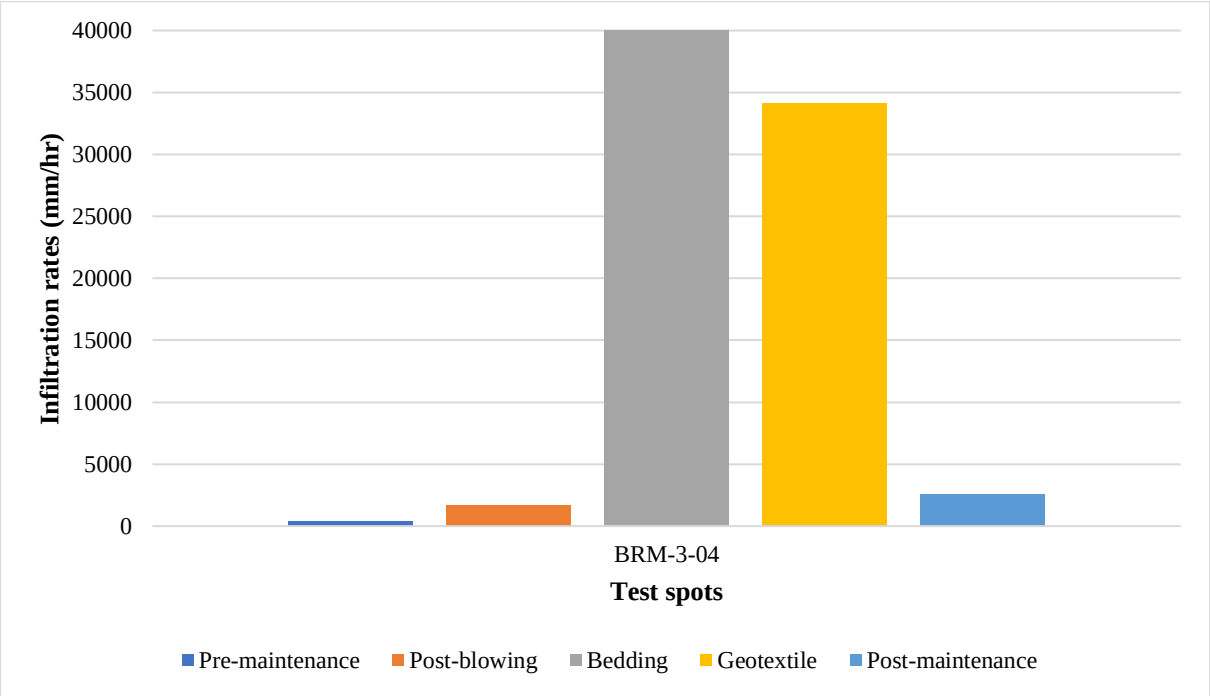

Figure 4-15: BRM Area 3 PICP diagnostic assessment infiltration rates

The bedding and geotextile infiltration rates were both exceptionally high: 40,000 and 34,100 mm/hr respectively. This is suggestive of clean gravel that typically provides an infiltration rate of at least 36,000 mm/hr (Look, 2007) clearly indicating that they are not blocked. Once the organic matter caught between the paver joints (Figure 4-12) had been blown

out by the compressed air blower, the infiltration capacity of the test spot was improved by 550%.

(a) Sediment in joints **(b) Sediment outline** **(c) Intact geotextile**

Figure 4-16: BRM-4 PICP section geotextile state

Overall, it appeared that PICP blockage in parked areas was superficial (mainly Type I – in the top 25 mm, leading to Type II) with few fines propagating to the geotextile.

4.5.3.2 Heavily trafficked sections

Figure 4-17 presents the infiltration rates measured on the three Area 4 test spots selected for diagnostic assessment. BRM-4-04 was chosen because there were widened paver joint openings (Figure 4-14). BRM-4-08 and BRM-4-11 were selected because they were located at intersections that were subjected to considerable turning moments and hence vulnerable to damage. The pre-maintenance, post-blowing, and post-maintenance infiltration capacities for these test spots were discussed in Section 4.5.2.2.

The three test spots' bedding infiltration rates, i.e., upon removal of the overlying pavers, were 600, 300, and 500 mm/hr for BRM-4-04, BRM-4-08 and BRM-4-11 respectively. Figure 4-18 shows that the bedding of the three test spots was substantially intermixed with fine material. Organic matter (leaves) and cigarette buds were also visible.

The bedding layer was then carefully cleared to access the geotextile (Figure 4-18). It was found that the geotextile had been punctured by more than 50% of its surface area in many places allowing sediment to propagate into the lower PICP basecourse layers. This could be a consequence of dynamic vehicle loading as vehicles traverse the paving. Furthermore, the damaged geotextile shown in Figure 4-19 started to de-thread when hand-pulled suggesting that heat-treated unwoven geotextiles are not a good choice of material in highly trafficked sections. This finding is consistent with literature (e.g., Lucke & Beecham, 2011a).

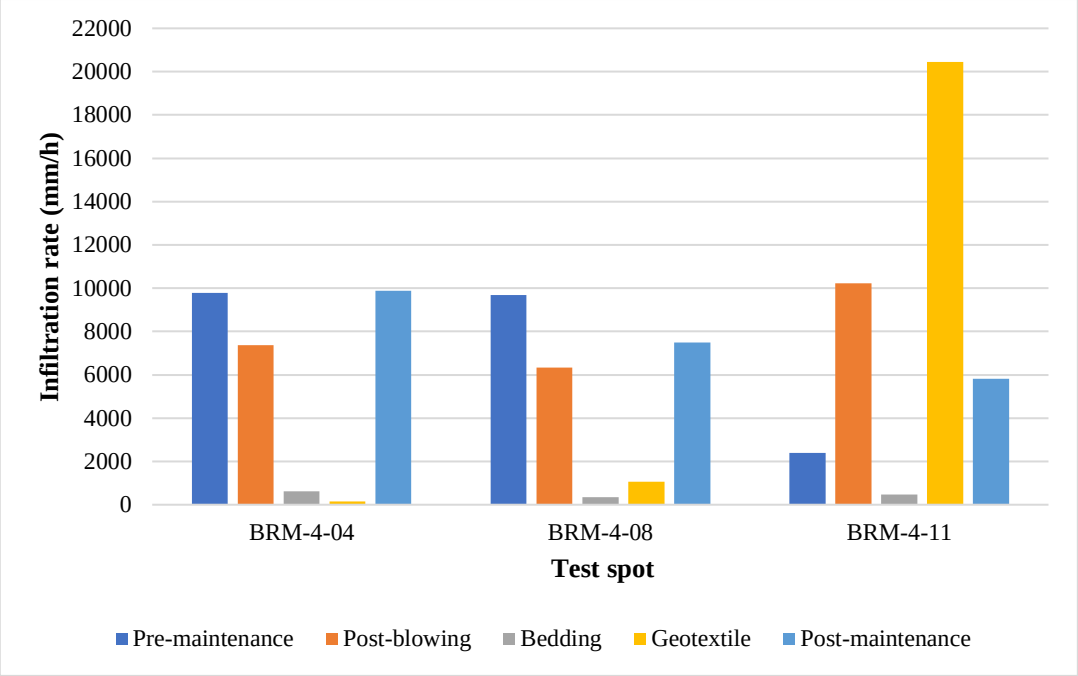

Figure 4-17: BRM Area 4 PICP diagnostic assessment infiltration rates

(a) BRM-4-04 **(b) BRM-4-08** **(c) BRM-4-11**

Figure 4-18: BRM-4 bedding, clogging and sediment outline

(a) BRM-4-04 **(b) BRM-4-08** **(c) BRM-4-11**

Figure 4-19: BRM-4 geotextile state

The measured infiltration rates on the geotextile under the bedding for the test spots were 150, 1100, and 20,400 mm/hr – but naturally these measurements were greatly influenced by the extent of the puncturing. BRM-4-04 and BRM-4-08 were thus subjected to Type IV clogging.

It was not possible to excavate deeper into the pavements because of the lack of suitable equipment at the time of data collection. While the bedding at BRM-4-11 appeared clogged with significant amounts of fine material deposited on the geotextile, once the bedding was removed, a very high infiltration rate was measured through it. The test spot thus demonstrated Type III clogging.

Paradoxically, the post-maintenance infiltration rates of the test spots were all greater than 5000 mm/hr (Figure 4-17). This suggests that the test method is not accurately measuring the true infiltration rate with test water potentially flowing laterally within the surface paver joints. This is of great concern as it suggests that the most common test methods are unreliable indicators of true PICP performance.

Overall, it appears that PICP installed on high-frequency trafficked roadways and parking adjacent to vegetation is more prone to blockage. In addition, the upper geotextiles are subject to damage due to mechanical wear caused by movement of the bedding and base layers.

4.6 UCT Upper Campus New Engineering Building (NEB) parking area

The New Engineering Building (NEB) PICP parking area is located at the University of Cape Town (UCT) Upper Campus on the Madiba Circle Road, Rondebosch, Cape Town (33°57'34.4"S 18°27'32.1"E) within the Table Mountain Nature Reserve. The parking area is at 130 m a.m.s.l. It is mainly used by university staff with the occasional delivery trucks coming to the civil engineering laboratory in the NEB. The parking area is largely comprised of PICP.

Figure 4-20 presents a locality map of the parking area. NEB PICP is lined with broad-leafed trees (Figures 4-21 and 4-22) to the east and west. The northern and western boundaries of the parking area comprise vegetated slopes of 25% and 12% respectively towards the PICP (Figure 4-21). The ground to the east of the PICP drains away from it. There is a 50 m^2 impermeable area between the sloping northern vegetated area and the PICP.

The permeable area is 700 m^2 and associated impermeable area is 560 m^2 giving a RoF of around 0.8 – thus, the PICP services mainly direct rainfall. The PICP slopes towards the entrance at a mean slope of 5%. It is divided into two distinct sections – one with, and the other without an upper geotextile – that are separated by an underground concrete check dam. Both PICP sections consist of: 80 mm Aquapave ® pavers, 2-3 mm joint material, 80 mm deep x 4-6 mm bedding stone, 100 mm deep x 19-25 mm stone basecourse, 250 mm deep x 50-63 mm subbase layer, and a geomembrane to prevent groundwater infiltration. The upper geotextile, where installed, is an Inbitex ®. An impermeable membrane prevents infiltration of rainwater into the subgrade; hence water that drains into the PICP is removed via underdrains that are situated adjacent to the check dams. Two inspection chambers on the eastern side of the PICP allow flow rates to be measured and samples taken for water quality analyses. The underdrains

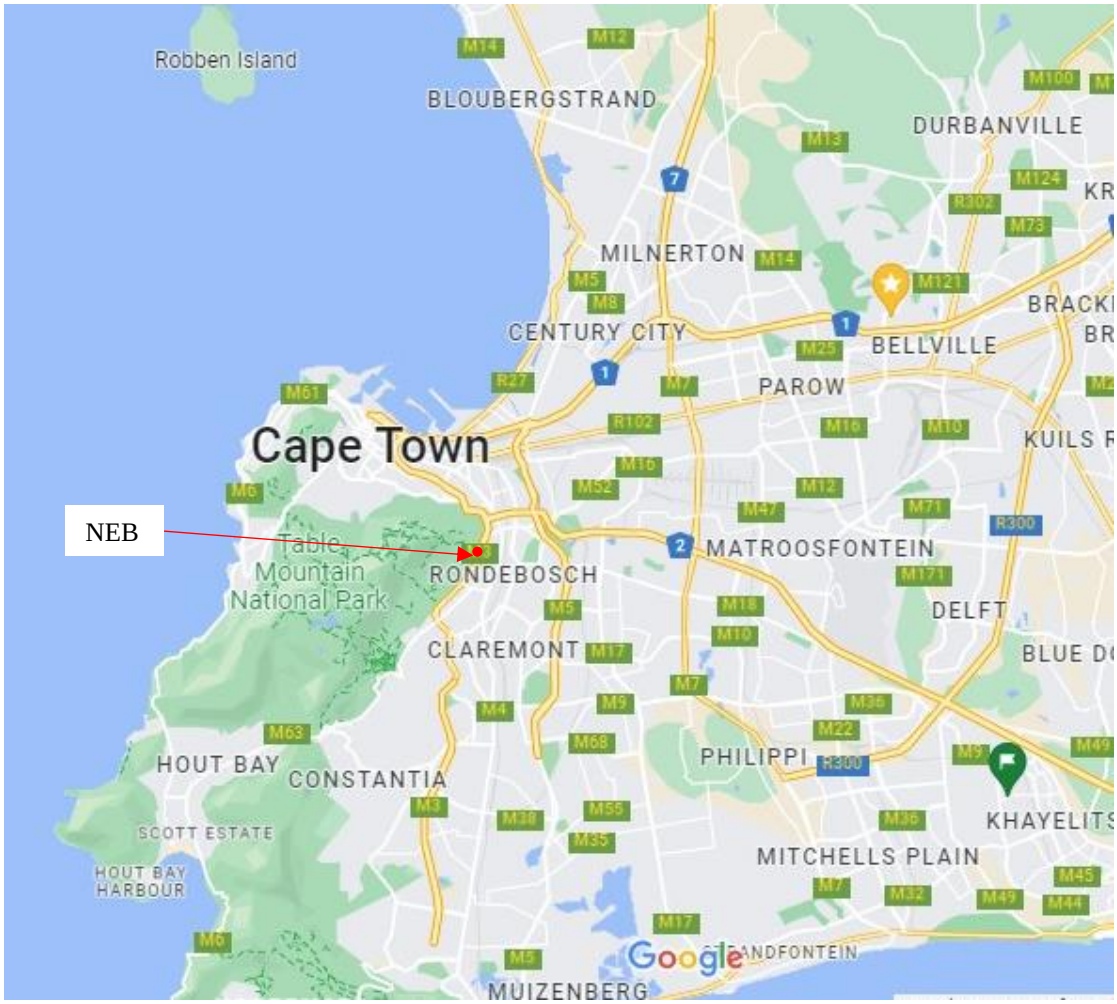

Figure 4-20: NEB PICP parking area locality map (Map source: Google Maps, 2022)

Figure 4-21: The NEB PICP parking area layout (Map source: Google Maps, 2022)

Figure 4-22: Vegetation surrounding the NEB parking area

are connected to a conventional stormwater line on Madiba Circle (Biggs, 2016). The NEB has not been maintained since the construction of the PICP site in 2014.

4.6.1 Field infiltration testing

Figures 4-23 and 4-24 show the location of the nine infiltration test spots on the section fitted with a geotextile and their measured 2016, 2017 and 2021 infiltration rates. It was difficult to determine any particular trend other than the general decrease in infiltration capacity towards the edges of the parking area from a maximum near the centreline. The concept of a clogging front working in from the sides has been described by Pezzaniti *et al*. (2009) and Beecham *et al*. (2010). The potential reason for the discrepancy between the 2016 / 2017 values and those measured in 2021 may have something to do with the way the pavement's joint widths seem to have widened with little grit visible along the vehicle wheel paths (Figure 4-25) resulting in a possible loss of the test water due to lateral flow.

Figure 4-23: NEB parking area test locations (After Biggs, 2016)

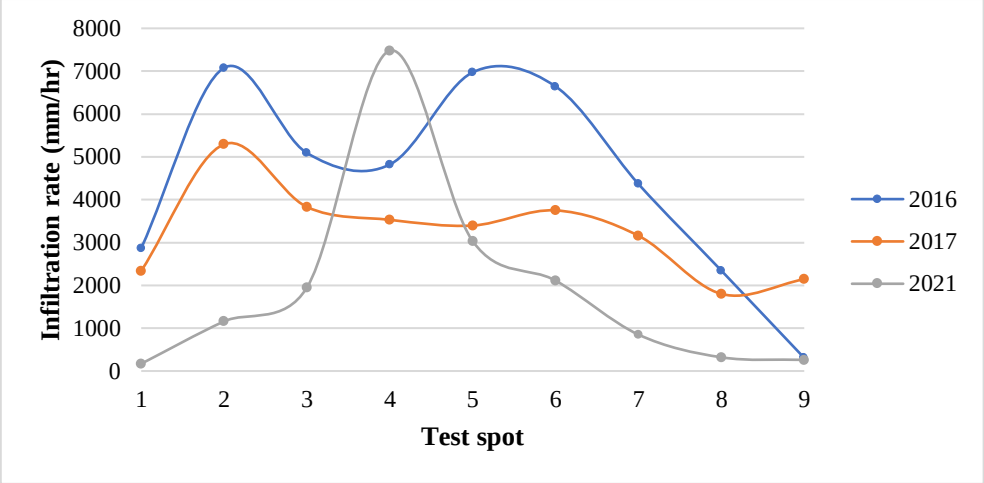

Figure 4-24: 2016, 2017, and 2021 NEB infiltration rates trend
(Adapted from ; Biggs, 2016; Artus, 2017; Matolengwe, 2021)

Figure 4-25: Typical PICP section with missing grit and fine sediment on the pavers

4.6.2 Pavement maintenance trials

Ten test spots were carefully identified on the NEB for maintenance trials (Figure 4-26). Test spots NEB-01 and NEB-02 were located on the section of the PICP that did not have a geotextile installed, while Test spots NEB-03 to NEB-10 were located on the PICP section that had a geotextile installed. Test spots NEB-05 and NEB-10 were chosen because they were close to the western slope and under the broad-leafed trees. Test spots NEB-02, NEB-04, NEB-07 and, NEB-09 were along the vehicle driveway, while the remainder were within the parking bays.

Test spots NEB-01 and NEB-02, and NEB-03, NEB-04, and NEB-05 were adjacent to each other and thus relatively exposed to the same environmental conditions but differed in the use of a geotextile under the bedding layer. Infiltration testing was carried out: pre-maintenance, post-blowing, and post-maintenance (Figure 4-27).

Figure 4-26: NEB PICP maintenance test spots layout (Map source: Google Maps, 2022)

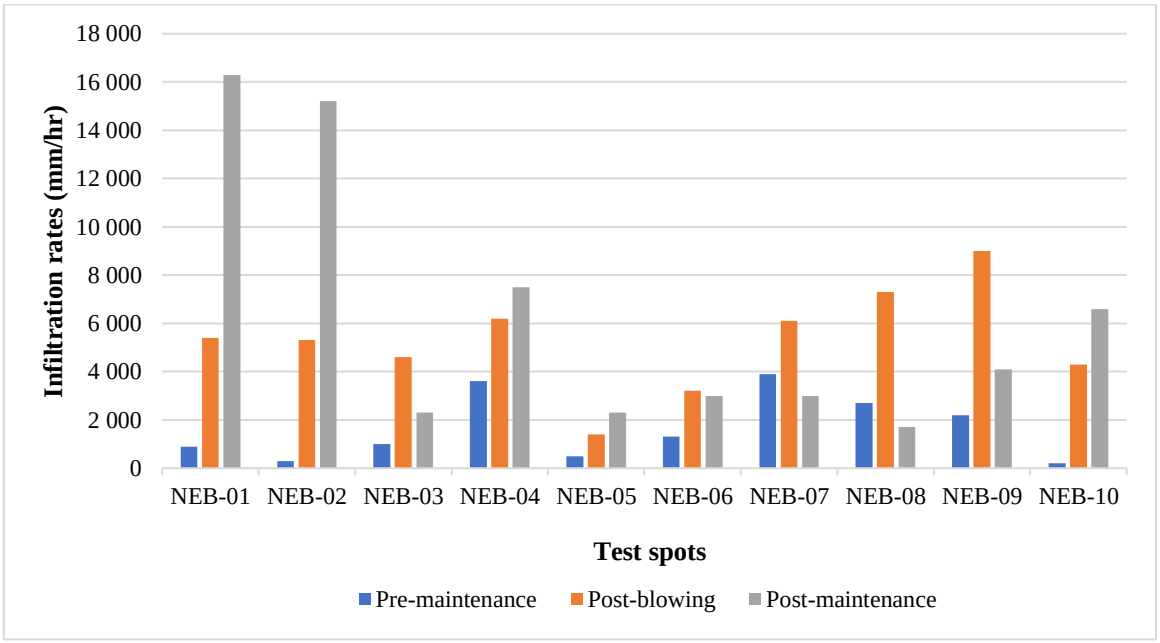

Figure 4-27: NEB Mod-ASTM maintenance infiltration tests

Although no maintenance had been performed on the site since its construction in 2014, the PICP was still functioning effectively – albeit with decreased infiltration capacity and one blocked test spot (NEB-10 at 200 mm/hr).

The increase in the infiltration rates – between 56% and 2050% – post-blowing suggested that most of the clogging was Type I which could be remedied through the blowing of the sediment out of the joints.

The change in the pre-maintenance to post-maintenance infiltration capacities ranged from 23% to 5000%. The wide range was mainly a consequence of conducting diagnostic assessments on Test spots NEB-01 and NEB-02. The outliers were NEB-07 (vehicle driveway) and NEB-08 (parking bay) where the post-maintenance infiltration capacities decreased by 23% and 37% respectively. Potentially this was due to the maintenance method pushing the sediments deeper into the pavement joints. Further, the measured high pre-maintenance infiltration rates for the two test spots might have been partly exaggerated by lateral flow during testing. Generally, the measured infiltration rates at most test spots showed an increase from initial to post-blowing followed by a reduction after the re-gritting, likely due to a decrease in joint void ratio as the washed grit was swept into the joints. NEB-05 was oil stained on the pavement surface and within the joint and recorded a low post-maintenance infiltration rate. It is possible that the oil made it difficult for water to infiltrate into the pavement.

An exception to the norm of a PICP clogging from the outside inwards was observed along the transect NEB-08, NEB-09, and NEB-10. The pre-maintenance infiltration capacities decreased from NEB-08 to NEB-10 – probably because NEB-09 and NEB-10 were closer to vegetation (overhung trees) than NEB-08 and thus more susceptible to clogging by leaves, seed material and pollen.

4.6.3 Diagnostic assessments

Diagnostic assessments were carried out on four test spots to determine the state of the bedding and geotextiles / bedding-layer interface. The spots were: NEB-01, NEB-02, NEB-04 and NEB-05.

Figure 4-28 presents typical test spots at the NEB. The moss in the paver joints likely absorbs runoff, ultimately, slowing the runoff infiltration into the pavement. It was evident that the PICP joints in the roadway sections were missing gritstone. It is unclear whether these had settled into the underlying bedding material or lifted out by passing traffic. In all cases, the test spots joint widths were typically as per the design, i.e., 6 mm suggesting that the pavers were properly ‘locked-up’ with adequate edge restraints.

a) Typical parking bay test spot **b) Typical vehicle driveway test**

Figure 4-28: NEB typical test spots surfaces

4.6.3.1 PICP without a geotextile

Test spots NEB-01 (parking bay) and NEB-02 (roadway) were located in the area of PICP without a geotextile under the bedding layer. The measured infiltration rates presented in Figure 4-29 displayed similar performance. The bedding and base infiltration rates of the two test spots were both recorded as 40,000 mm/hr because the infiltration rates were so high that they could not be measured and thus it was assumed that they were probably in the order of clean coarse-grained aggregates or greater than 36,000 mm/hr. Both test spots showed a good response to maintenance (air-blowing); the measured infiltration rates for NEB-01 increased from 900 to 16,300 mm/hr, while those for NEB-02 increased from 300 to 15,200 mm/hr.

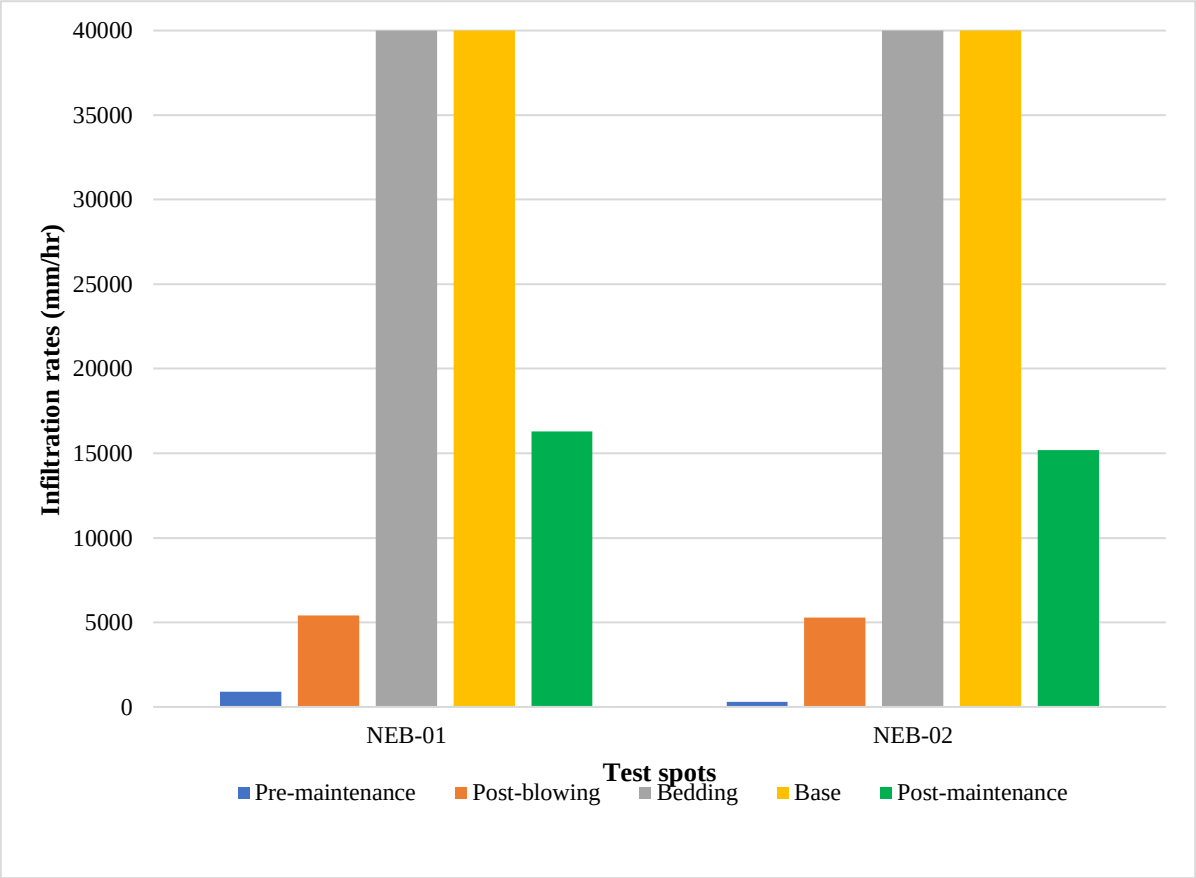

Figure 4-29: NEB no-geotextile design diagnostic assessment infiltration rates

Figure 4-30 shows the state of the bedding and bedding-basecourse interface of the two test spots. Very little sediment was trapped in the top 20-30 mm of the joints (Type I clogging). On the other hand, considerable fine material could be seen on the top of the bedding layer in the form of an outline of the paver pattern – particularly for NEB-02, possibly because of the increased vehicle vibration along the roadway (Burak, 2006). The fact that very little fine material was visible directly underneath the pavers explains the high infiltration rates measured on the bedding material – although the bedding was observed to be covered in a light muddy film at both test spots. Moreover, very little fine material was visible at the interface of the

(a) NEB-01 joint material

(b) NEB-02 joint material

(c) NEB-01 sediment outline

(d) NEB-02 sediment outline

(e) NEB-01 bedding-base interface

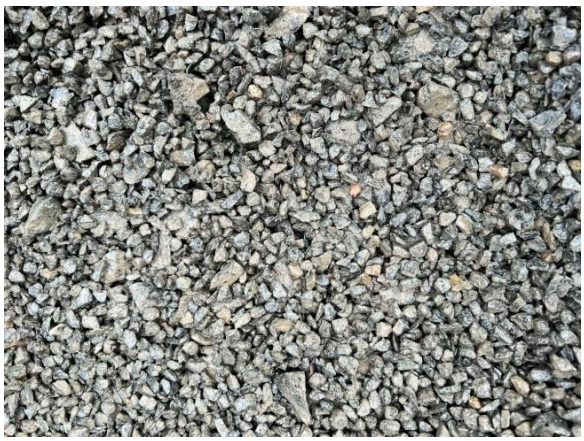

(f) NEB-02 bedding-base interface

Figure 4-30: NEB-01 and NEB-02 diagnostic assessments

bedding and the base. It appeared that the clogging was likely a combination of Type I – which is highly amenable to air blowing – and Type II clogging. The lack of a geotextile under the bedding layer appeared to have no impact on the performance of the PICP at all. However, the interface of the bedding and base aggregate layers showed signs of aggregate sublayer mixing.

4.6.3.2 Assessment of PICP with geotextile

Diagnostic assessments on the PICP area with an underlying geotextile were performed on Test spots NEB-04 (roadway) and NEB-05 (parking bay) (Figure 4-31). There was a significant difference between the test spots infiltration rates. NEB-04 showed a higher pre-maintenance infiltration rate than NEB-05 but this did not extend to the bedding and geotextile infiltration capacities. This could have been because the site chosen happened to be where the geotextiles overlapped (NEB-04) thus reducing the geotextile infiltration capacity (Rowe *et al*., 2009). The infiltration capacities after the maintenance trials of the two test spots improved by 108% and 360% for NEB-04 and NEB-05 respectively.

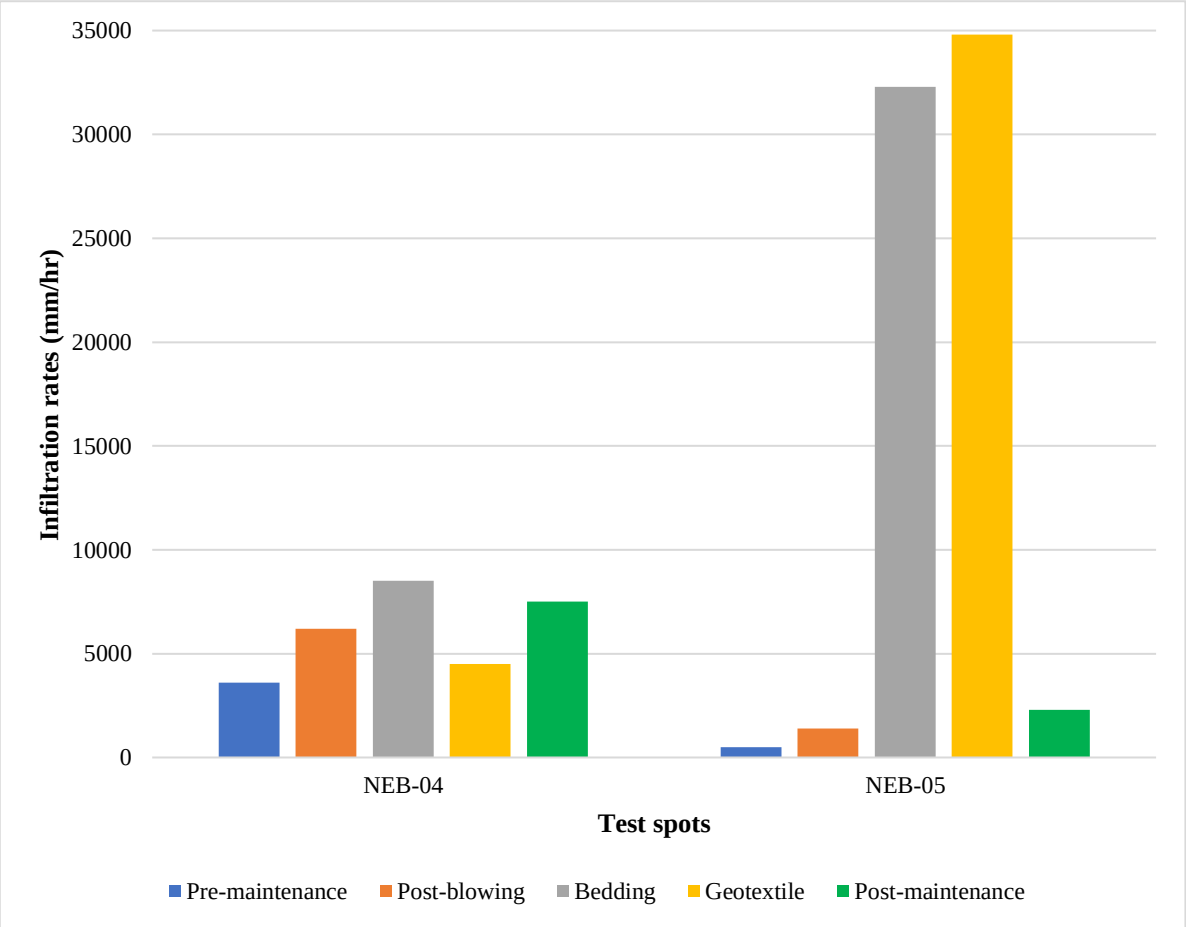

Figure 4-31: NEB geotextile design diagnostic assessment infiltration rates

Figures 4-32 and 4-33 show the state of the bedding, geotextile, and base of NEB-04 and NEB-05. NEB-04 (roadway) had more composite sediment trapped on the various different layers than NEB-05 (parking bay). This may be a consequence of vehicle vibration resulting in material being propagated deeper into the PICP. On the other hand, NEB-05 initially supported a lower infiltration rate but was more responsive to maintenance. It is possible that this was because the nature of the blockage is through leaf and pollen drop from the

overhanging tree and oil stain resistance to infiltration. Both test spots were therefore exposed to Type II clogging.

(a) NEB-04 joint material

(b) NEB-05 joint material

(c) NEB-04 bedding outline

(d) NEB-05 bedding outline

Figure 4-32: NEB-04 and NEB-05 bedding diagnostic assessments

The use of angular aggregates in the PICP layers is crucial in ensuring that the pavement sublayers lock-up (SANRAL, 2014) to avoid any potential for settlement (Hein, 2018a), however, they can be detrimental to the life of a geotextile. The combination of the dynamic vehicle load and the angular aggregates results in the geotextile being punctured. Both the top and bottom NEB-04 overlapping geotextile layers were pierced (Figure 4-33). Furthermore, the base layer was observed to be covered with a light muddy film. This was an indication that some of the fines were propagating into the underlying pavement structure. On the other hand, the NEB-05 geotextile did not illustrate any tearing and the base material appeared cleaner than the NEB-04 base material probably because there is little vehicle vibration in parking bays. If

the geotextile gets torn it ceases to be effective and the behaviour of the PICP will increasingly resemble that of a design without an upper geotextile.

(a) NEB-04 state of the geotextile

(b) NEB-05 state of the geotextile

(c) NEB-04 state of the base

(d) NEB-05 state of the base

Figure 4-33: NEB-04 and NEB-05 geotextile diagnostic assessments

4.7 UCT Middle Campus School of Economics (SOE) parking area

The School of Economics (SOE) PICP parking area is located at the UCT Middle Campus in Rondebosch, Cape Town at 33°57'26.1"S 18°27'59.2"E (Figure 4-34). The site was constructed in 2011 as part of the SOE building development and is situated at 50 m a.m.s.l. It is mainly used for the parking of cars by students staying at the nearby UCT residence and students and staff at the Department of Economics. In 2022, it was used as an access for tipper and delivery trucks for the construction of the UCT Design School situated at the corner of M89 and Cross Campus Road.

The parking area is surrounded by broad-leaved trees. The trees are also planted between the central parking bays (Figures 4-35 and 4-36). The parking area is 100 mm lower than the top of the kerbs marking the central planters. 50 mm diameter unplasticized polyvinyl chloride (uPVC) drainage pipes spaced at approximately two metre intervals are fitted through the kerb

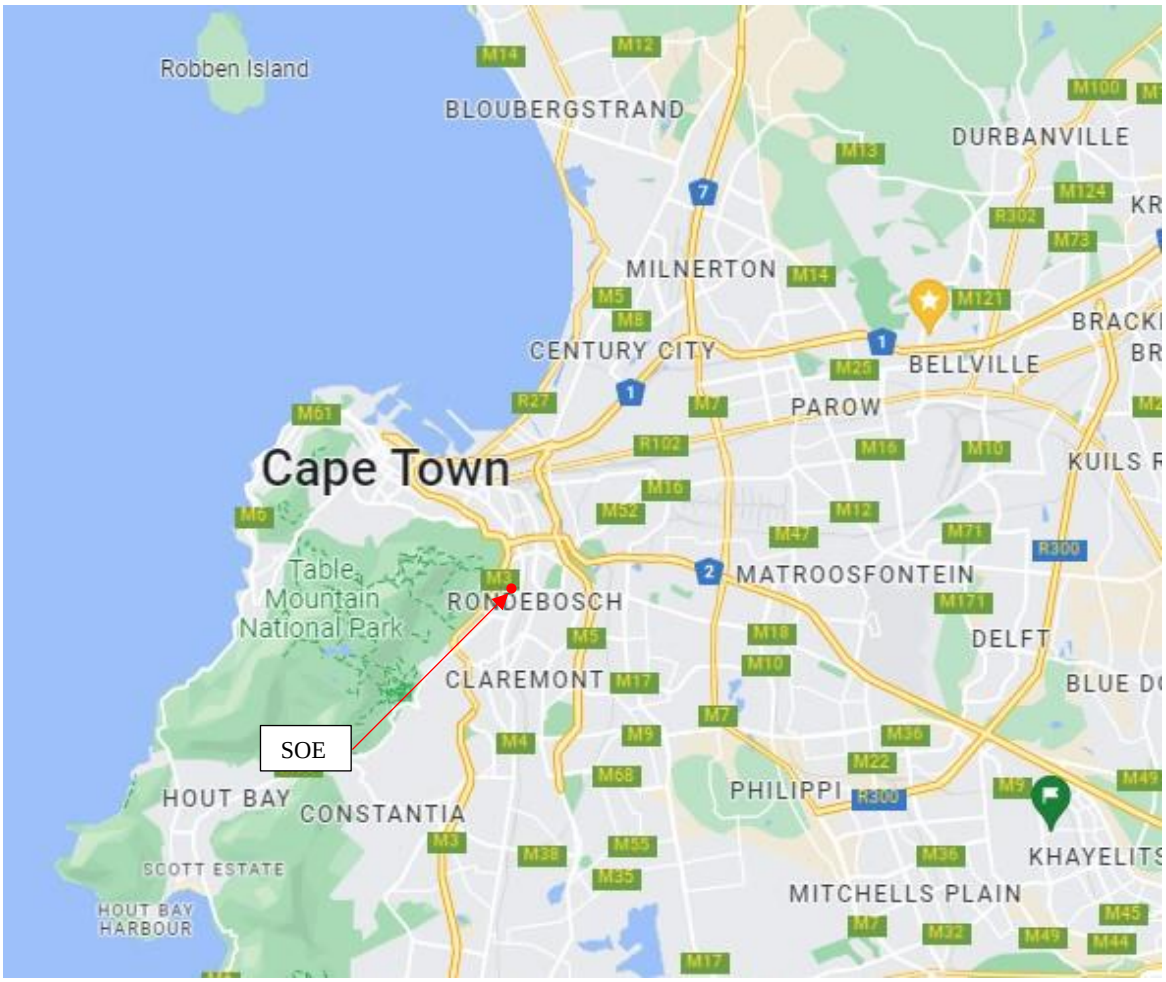

Figure 4-34: School of Economics (SOE) PICP locality map
(Map source: Google Maps, 2022)

stones on the western side of the parking area to drain an adjacent vegetated area (Figure 4-37). The parking area has an average slope of 3%. The PICP area is 2800 m^2 while the impermeable area draining to it is 1100 m^2 to give a RoF of 0.39.

The PICP cross-section design has two components – the vehicle roadway and the parking bays. Both components' designs comprised: 80 mm exposed aggregates pavers infilled with 2-3 mm grit, 80 mm deep x 4-6 mm bedding, and no geotextile. Additionally, the vehicle driveway consisted of a 250 mm deep x 11 mm aggregate base course layer.

Figure 4-35: View of the SOE parking area

Figure 4-36: Typical tree planter at the SOE parking area

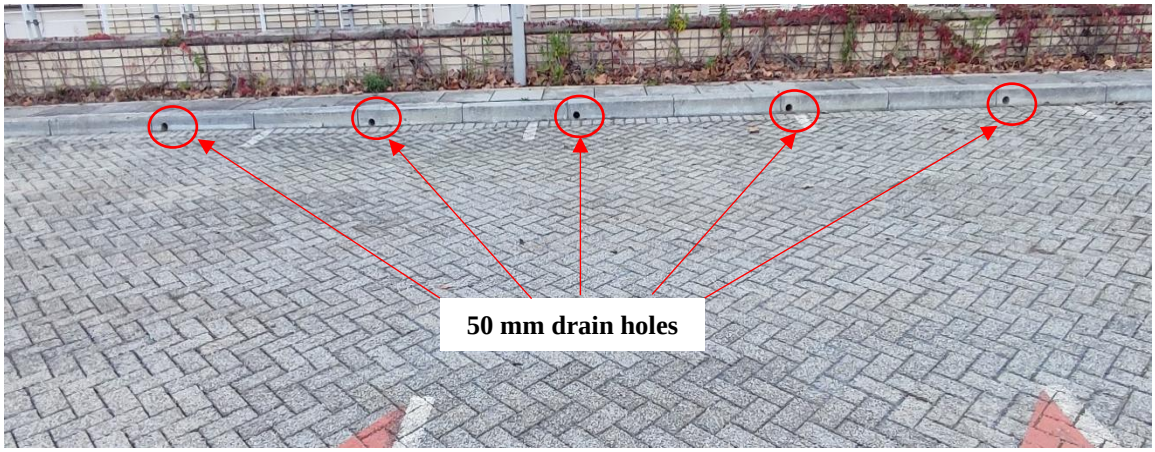

Figure 4-37: View of the 50 mm uPVC drain holes

4.7.1 Field infiltration testing

Figure 4-38 shows the position of the infiltration test spots at the SOE. The choice of the test spots was based on the desire to provide some variation in the proximity to vegetation and include both the parking area and vehicle roadway. The infiltration test results are shown in Figure 4-39.

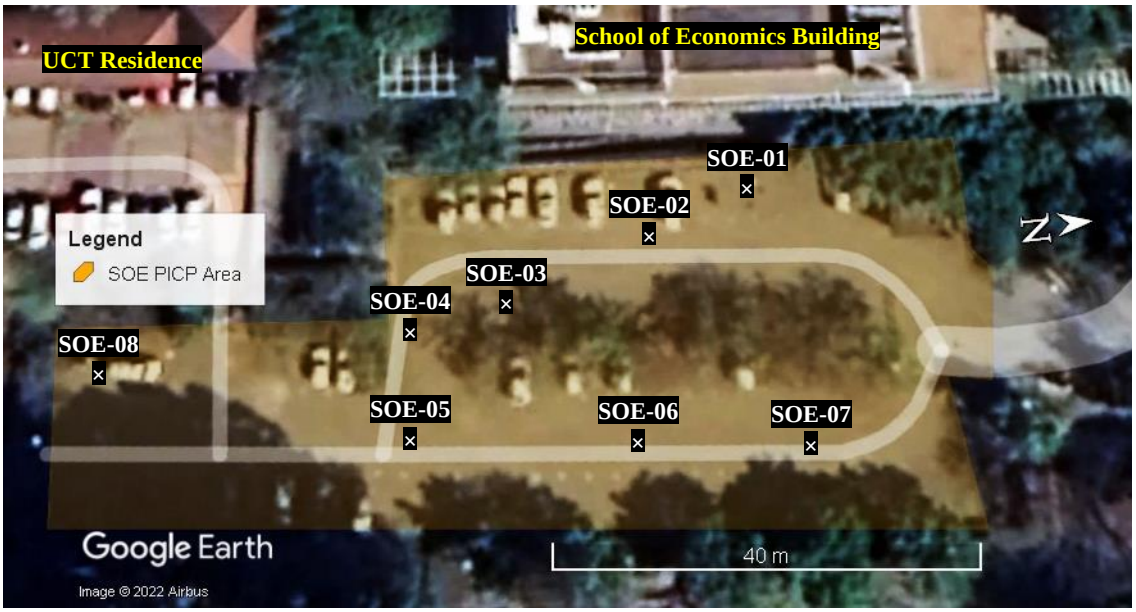

Figure 4-38: Position of SOE PICP test spots (Map source: Google Earth Pro, 2022)

The site has not undergone any maintenance since its installation, however the infiltration rates measured on the site were reasonably high, ranging from 1100 to 2900 mm/hr measured by Mod-ASTM and 1400 to 2400 mm/hr measured by Mod-SWIFT. There was however an outlier (Mod-ASTM) of 6600 mm/hr at SOE-06 which would seem to be an over-estimate as a consequence of the widened joint opening at the test spot. Although some of the surfaces of

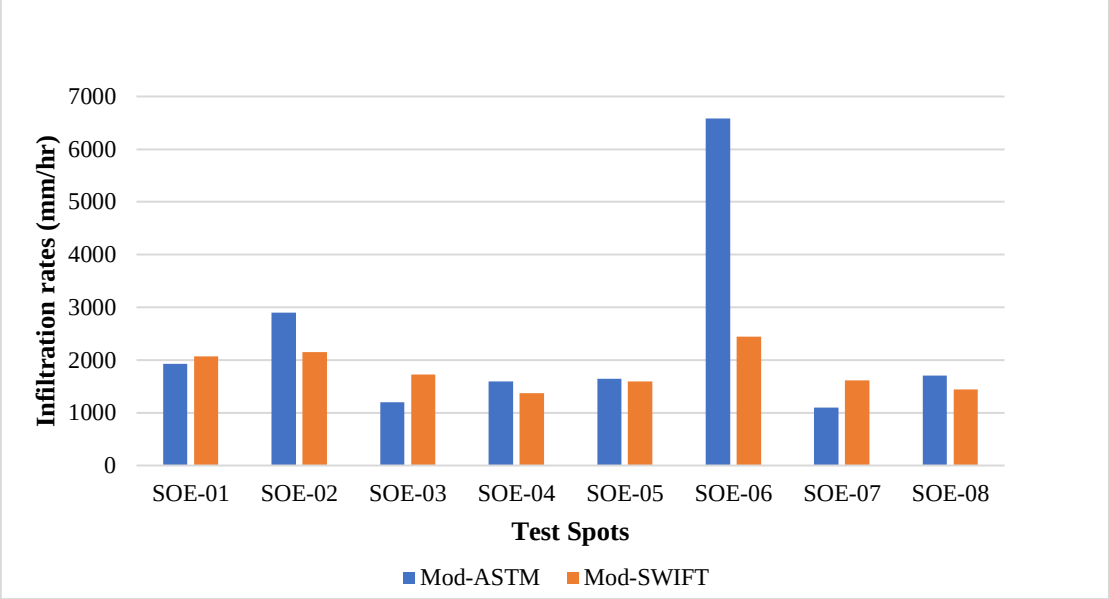

Figure 4-39: SOE surface infiltration rates

the test spots appeared to be clogged by fine material and organic matter, the infiltration rates were all comfortably in excess of the nominal 250 mm/hr used to indicate blocked paving (Interpave, 2020). Figures 4-40 shows the typical states of the SOE PICP surface observed during the site investigation.

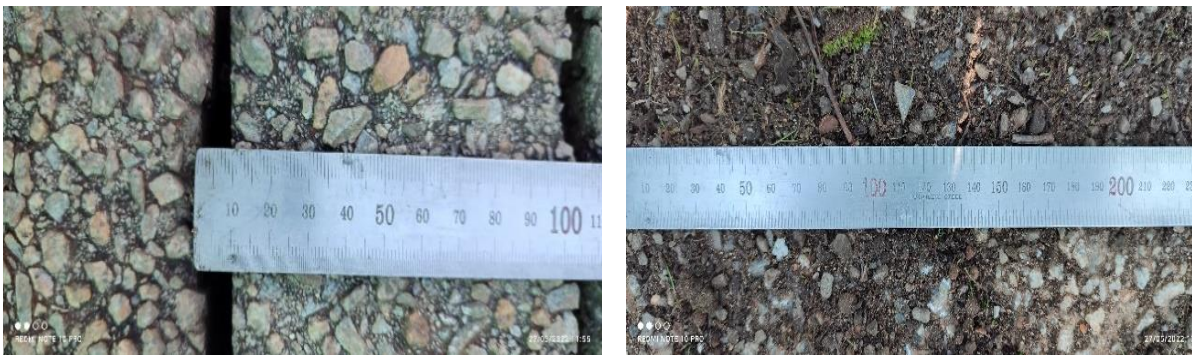

(a) Widened joints with no grit **(b) Sediment trapped in joints**

Figure 4-40: Typical SOE surface condition

4.7.2 Pavement maintenance trials

Figure 4-41 presents the Mod-ASTM pavement maintenance infiltration rates for the test spots shown in Figure 4-38.

The drop in infiltration rates measured between post-blowing to post-maintenance is perhaps due to the joint filler material as it reduces the effective void ratio of the joints. The compressed air blower generally increased the infiltration rate of the test spots although it decreased for

SOE-08 by 59% as a consequence of widened joints with no gritstone, thus overestimating the pre-maintenance infiltration rate.

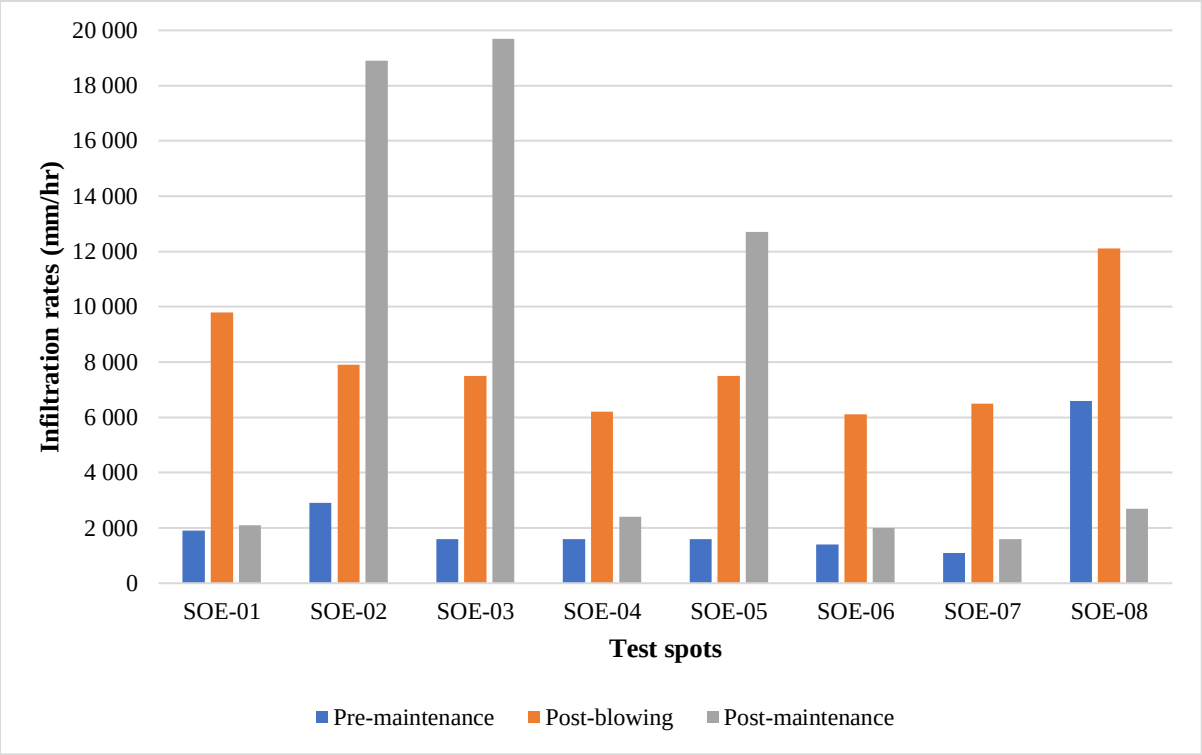

Figure 4-41: SOE infiltration measurements

4.7.3 Diagnostic testing

The diagnostic tests were performed on two test spots on the vehicle roadway (SOE-02 and SOE-05) and one on the parking bay (SOE-03).

4.7.3.1 PICP roadway pavement investigation

The infiltration rates for the bedding for Test spots SOE-02 and SOE-05 were significantly greater than 40,000 mm/hr and 23,700 mm/hr indicating negligible clogging (Figure 4-42). The basecourse infiltration rates were beyond the measuring rate and thus reported as 40,000 mm/hr. Both the bedding and base layer were however covered in a muddy film of the fine material that had worked its way into the structure of the PICP presumably by the vibratory movement of vehicular traffic combined with runoff and the absence of any geofabric to block migration into the base layer (Figure 4-43). Although the sediment pattern on the bedding is similar for the two test spots, the different colours – with SOE-02 lighter than SOE-05 – suggest different sediment sources, however both test spots demonstrated Type II clogging.

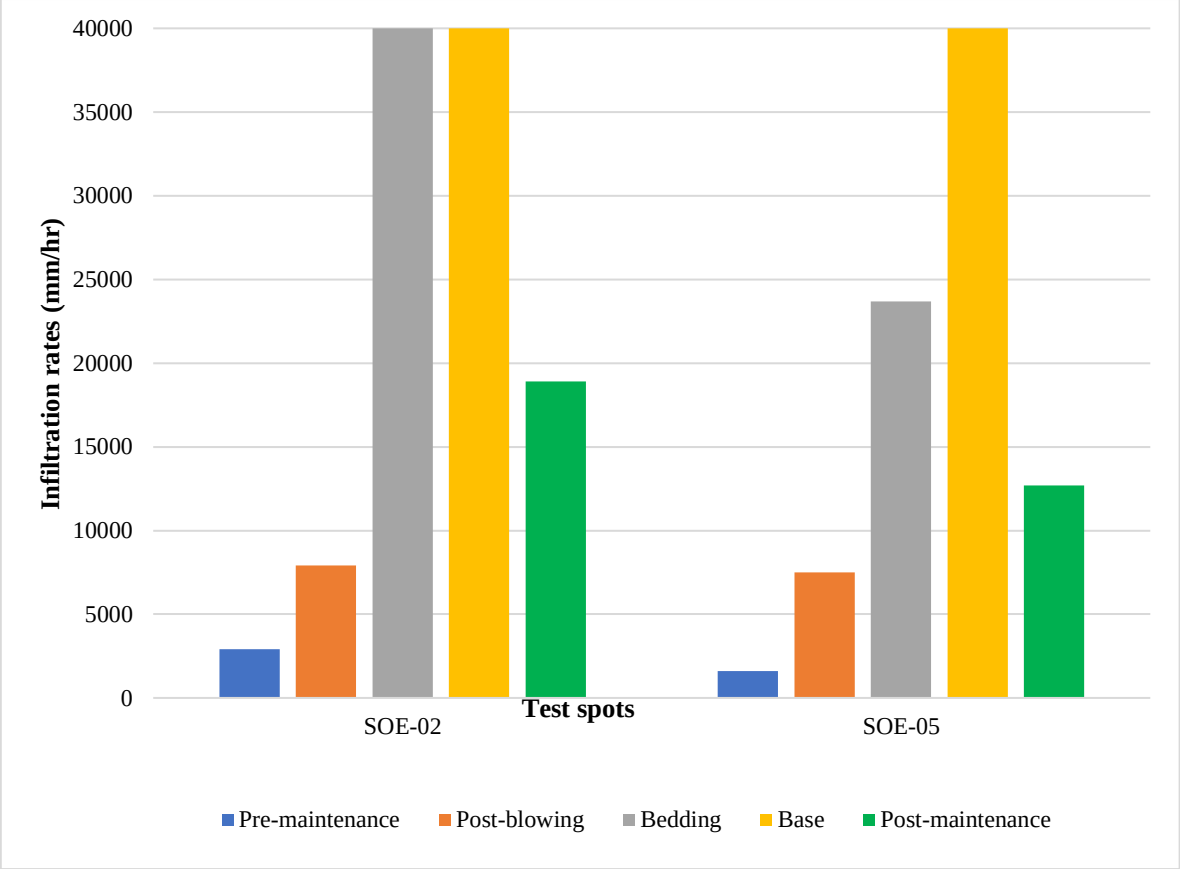

Figure 4-42: SOE diagnostic assessments infiltration rates

(a) SOE-02 bedding outline

(b) SOE-05 bedding outline

(c) SOE-02 muddy base

(d) SOE-05 muddy base

Figure 4-43: SOE-02 and SOE-05 state of the bedding and base

4.7.3.2 PICP parking bay pavement investigation

Test spot SOE-03 was located within a parking bay and overhung by broad-leafed trees. Some of the humus from the tree planter was found within the joints of SOE-03 before the maintenance trial of the test spot was conducted. The measured SOE-03 infiltration rates are shown in Figure 4-44. The 80 mm underlying bedding layer had a measured infiltration rate of 39,000 mm/hr while the measured subgrade infiltration rate was much lower but still adequate at 3200 mm/hr.

Figure 4-45 shows the state of the bedding and subgrade of SOE-03. There was a sediment outline on the bedding layer. The 80 mm deep bedding layer had a sediment outline imprinted on it, but relatively little of this sediment appeared to have found its way through the layer as the subgrade appeared to be in a good condition. SOE-03 thus exhibited a mix of Type I and Type II clogging.

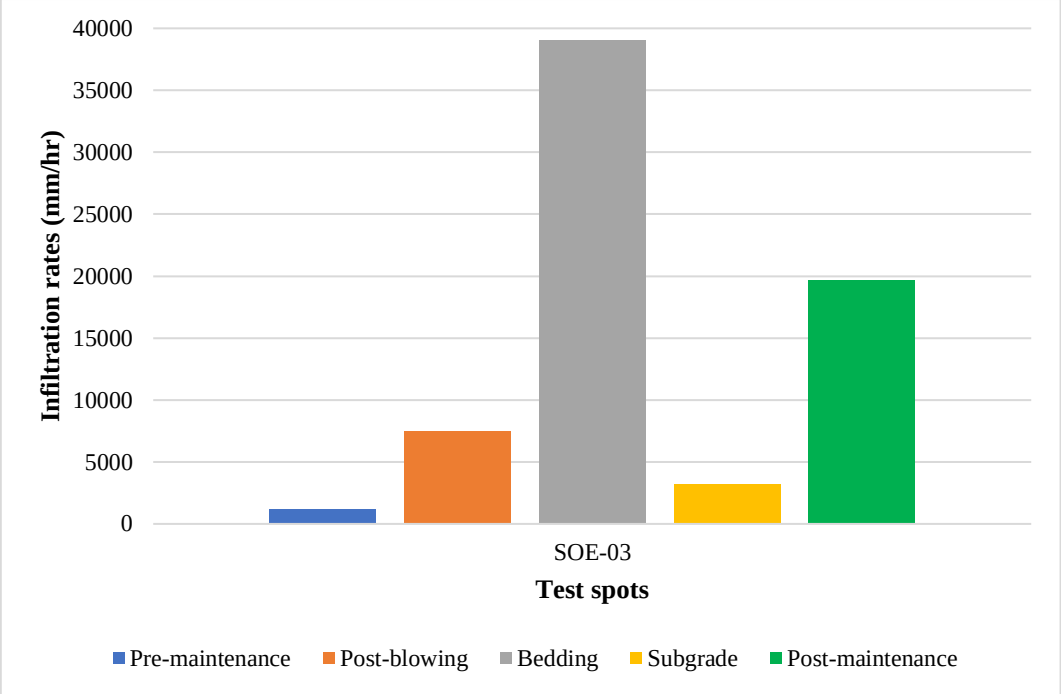

Figure 4-44: SOE-03 measured infiltration rates

(a) Sediment outline **(b) Bedding profile** **(c) Subgrade state**

Figure 4-45: SOE-03 condition

4.8 UCT Lower Campus Irma Stern Museum (ISM) parking area

Irma Stern Museum (ISM) parking area is an enclosed PICP parking area situated in a build-up area at the corner of Cecil and Chapel Roads in Rosebank, Cape Town (33°57'13.5"S 18°28'09.9"E) (Figures 4-46 and 4-47). It is at an altitude of 30 m a.m.s.l and is mainly used by the ISM and UCT staff.

The ISM parking area is surrounded by broad-leaved trees and slopes at about 4% towards the east. Potential overland flow drains to a catchpit at the lowest point of the PICP on the southern corner that is connected to the conventional municipal stormwater drain.

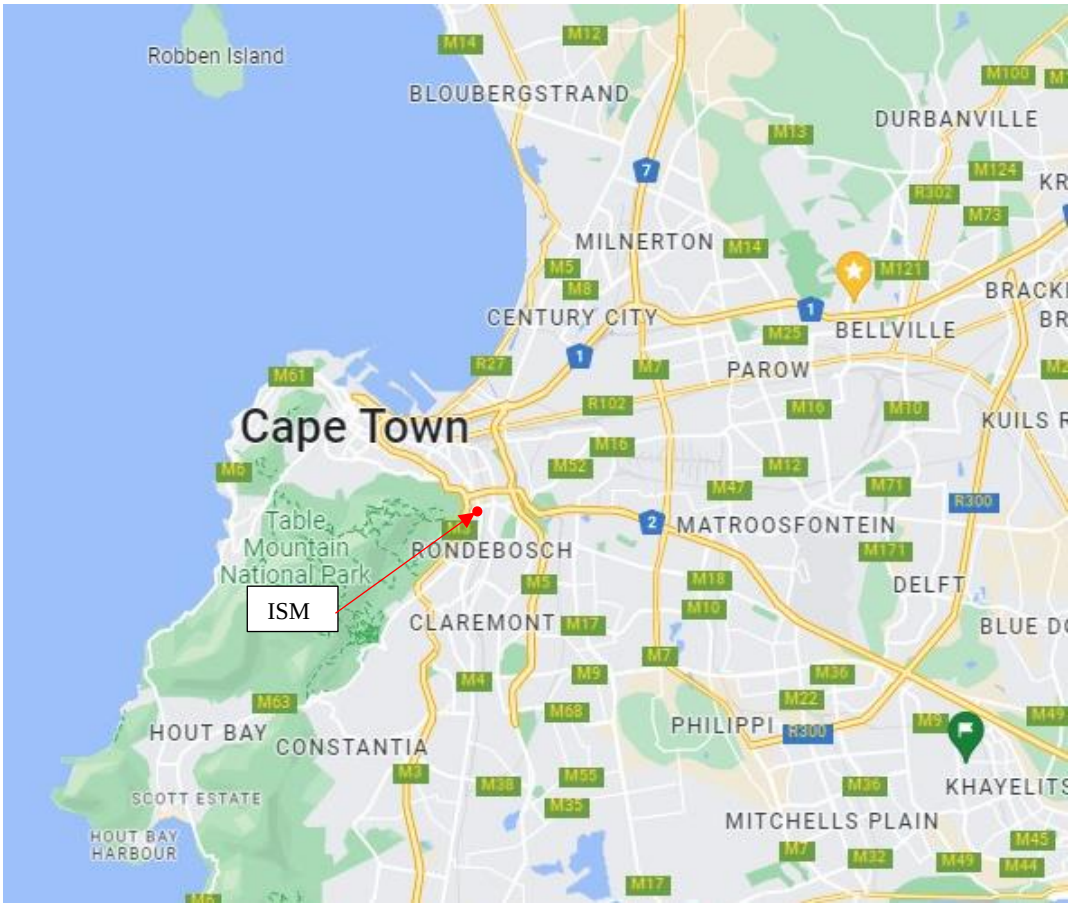

Figure 4-46: ISM PICP parking area locality map (Map source: Google Maps, 2022)

Figure 4-47: ISM PICP parking area (Map source: Google Maps, 2022)

The parking area comprises 295 m^2 and 675 m^2 of permeable and impermeable areas respectively to give a RoF of 2.3. The pavement consists of 70 mm exposed aggregate pavers with a 2-3 mm gritstone infill, a 50 mm deep x 6.75 mm bedding layer, an upper Inbitex ® geotextile, a 100 mm deep x 9.5-19 mm base layer, a 250 mm deep x 19-53 mm subbase layer, a lower Inbitex ® geotextile, and a compacted subgrade. The ISM parking area was constructed in 2013 and has never been subjected to any form of maintenance.

Figure 4-48 shows the ISM 18 test spots. Test spots ISM-01 to ISM-04 and ISM-15 to ISM-18 were located in parking bays, ISM-05 to ISM-14 along the roadway (Figure 4-48).

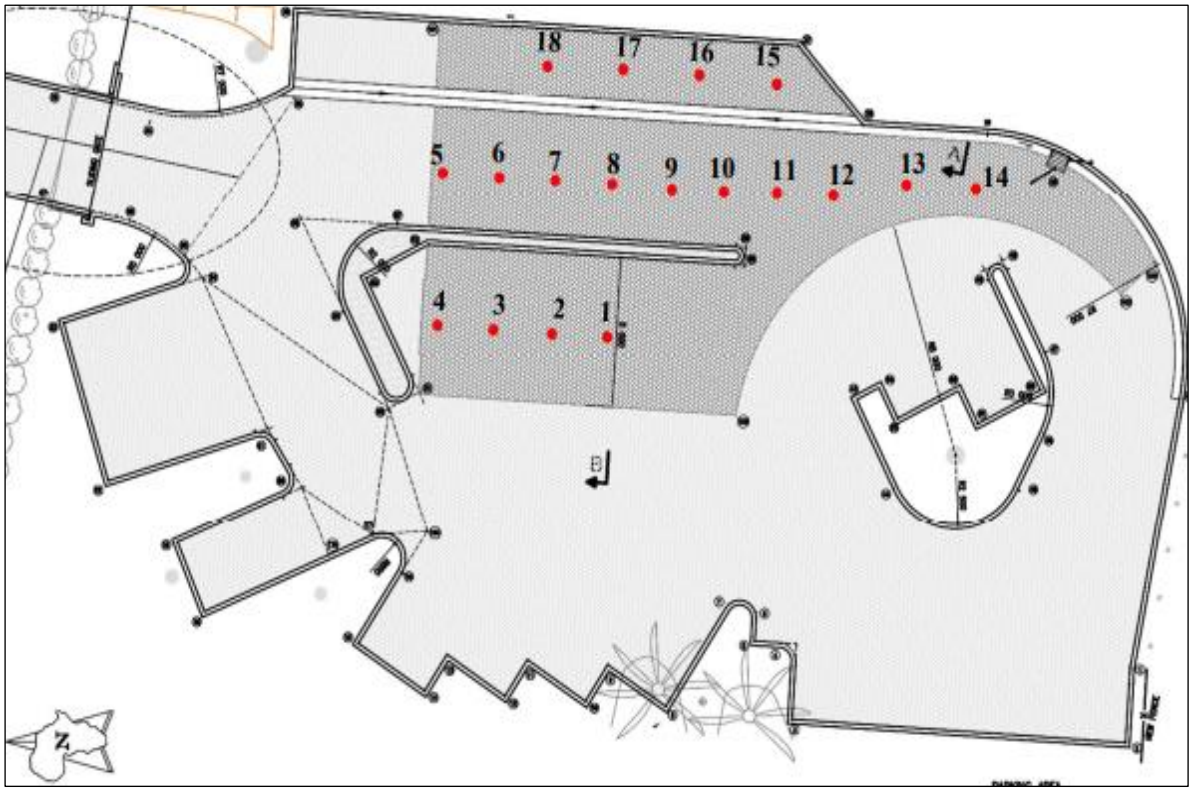

Figure 4-48: Location of ISM infiltration test spots (Matolengwe, 2021)

The Mod-ASTM infiltration rates indicate that the PICP site is still effectively functional as none of the test spots had an infiltration rate of less than 250 mm/hr (Figure 4-49). The lowest infiltration rates were 400 and 500 mm/hr for ISM-08 and ISM-10 respectively – potentially due to sediment and organic matter build-up in the joints (Figure 4-50), while the highest infiltration rate was for ISM-12 which recorded an infiltration rate of 3200 mm/hr. No particular pattern was evident in the measured infiltration rates. Although ISM-12, ISM-13 and ISM-14 were located directly below a tree, their measured infiltration rates were high. ISM-15 to ISM-18 were located adjacent to vegetation, yet, their infiltration rates were substantial too.

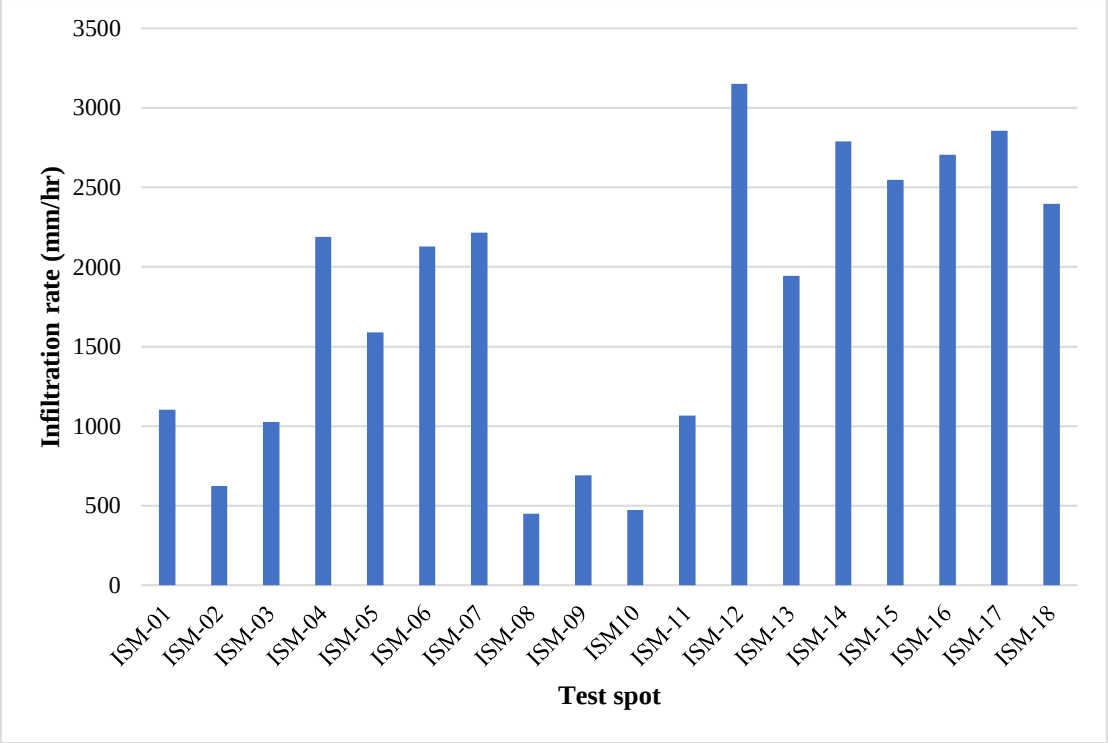

Figure 4-49: ISM surface infiltration rates (After Matolengwe, 2021)

Figure 4-50: Typical ISM-08 and ISM-10 surface assessment

4.9 Grand Parade (GRP)

The Grand Parade (GRP) is a 20,400 m^2 multi-purpose space of a combination of conventional interlocking pavement and PICP situated in the Cape Town CBD at the corner of Darling Street and Castle Street at 33°55'30.04"S; 18°25'30.22"E (Figures 4-51 and 4-52). The site is located at 10 m a.m.s.l. The space is currently used as a public and City of Cape Town (CoCT) car parking area and supports a market with temporary structures. Occasionally, CoCT light trucks are parked in the area. It was constructed in 2009.

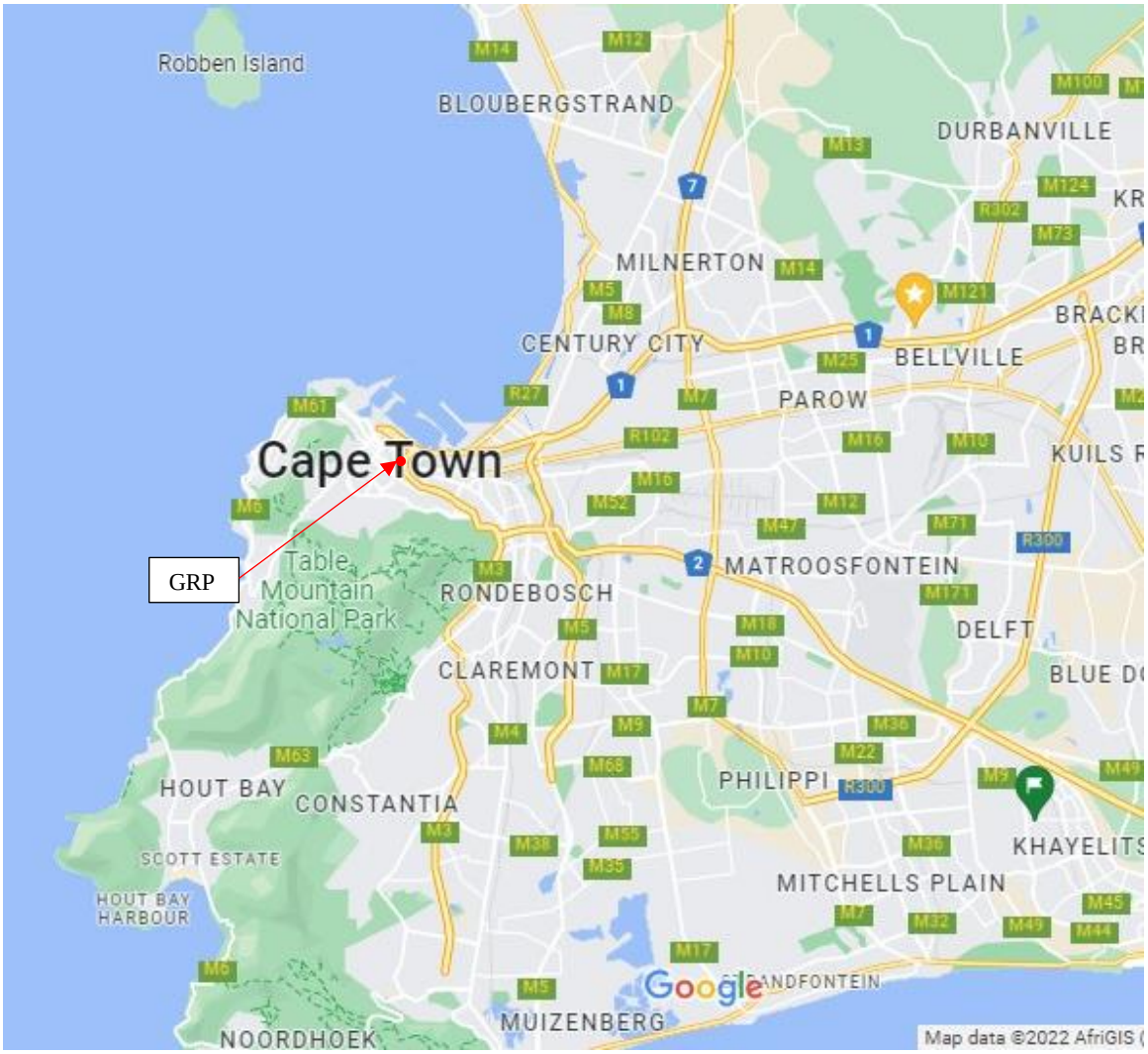

Figure 4-51: GRP locality map (Map source: Google Maps, 2022)

Figure 4-52 and Table 4-3 show the layout of the GRP and the areas dedicated to each activity. There is a 17,400 m^2 impermeable paving area and a 3000 m^2 PICP area to give a RoF of 5.8. The site slopes from the impermeable area towards the permeable area at an average slope of 5.7%.

The north-eastern part of the PICP area is lined with trees with needle-shaped leaves. There is a bus station adjacent to the PICP on the north-eastern side while there are fast food shops and public toilets on the far north-western side. A typical interface between the PICP and impermeable paving areas is shown in Figure 4-53.

The pavement structure comprised 80 mm Aquaflow ® pavers, 50 mm deep x 5 mm bedding, an upper Inbitex ® geotextile, a 100 mm deep x 5-20 mm base layer, a 250 mm deep x 10-63 mm subbase layer, and a lower composite geotextile to protect the subgrade, all placed on a compacted hornfels subgrade.

Figure 4-52: GRP pavement distribution (Map source: Google Earth Pro, 2022)

Table 4-3: GRP parking area use distribution

Use	Pavement type	Area (m^2)	
Multi-purpose parking	Normal pavers	6 000	7 200
	PICP	1 200	
Temporary structures market	Normal pavers	8 200	10 000
	PICP	1 800	
Permanent structures market	Normal pavers	3 200	3 200

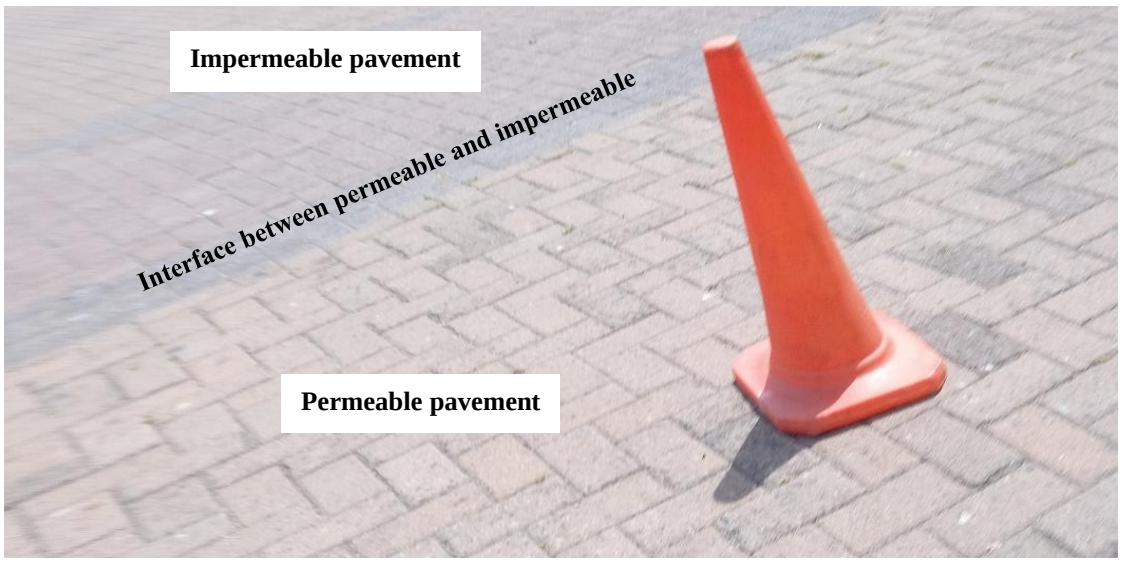

Figure 4-53: Permeable and impermeable perspective at the GRP

4.9.1 Field infiltration testing

Figure 4-54 shows the location of test spots where infiltration tests were conducted. The PICP was divided into three areas: Area 1 (GRP-1), Area 2 (GRP-2), and Area 3 (GRP-3). 15 test spots were chosen with GRP-1 allocated nine test spots, GRP-2 one test spot, and GRP-3 five test spots.

Figure 4-54: GRP infiltration test spots (Map source: Google Earth Pro, 2022)

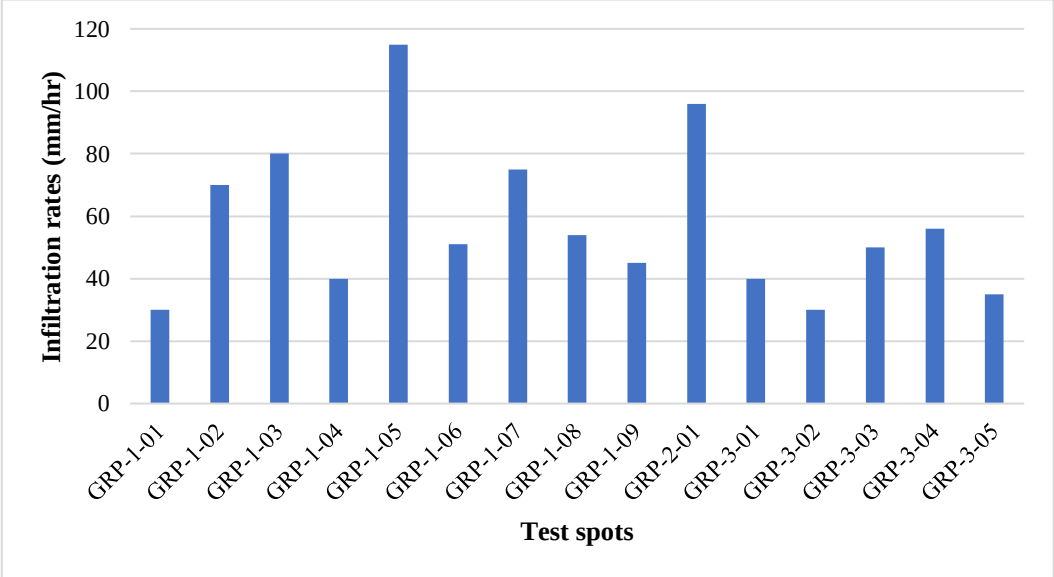

Figure 4-55: Grand Parade surface infiltration rates

The measured infiltration rates ranged from 30 to 115 mm/hr (Figure 4-55) and were all thus effectively fully clogged with Mod-ASTM infiltration rates much lower than 250 mm/hr

(Winston *et al.*, 2016). All results, however, should be regarded with some circumspection as it was difficult to prevent leakage from the side of the test apparatus and this is likely to have constituted a large proportion of the 'infiltration'. The site has never been maintained since its construction.

4.9.2 Maintenance trails

Attempts to improve the performance of the PICP through the blowing of compressed air into the joints on Test spots GRP-1-01 to GRP-1-03 failed.

4.9.3 Diagnostic assessments

The pavers at Test spots GRP-1-01, GRP-1-02, GRP-1-03, GRP-2-01, GRP-3-01, and GRP-3-05 were lifted for the purpose of diagnostic assessment. Figure 4-56 presents the infiltration rates at the six infiltration test spots. Pre-maintenance infiltration tests have been discussed in Section 4.9.1. All the measured bedding layer infiltration tests were high except for GRP-1-01 which recorded an infiltration rate of only a nominal 25 mm/hr. The GRP-1-01 geotextile was clearly completely blocked although the geotextile was still intact (Figure 4-57(b)).

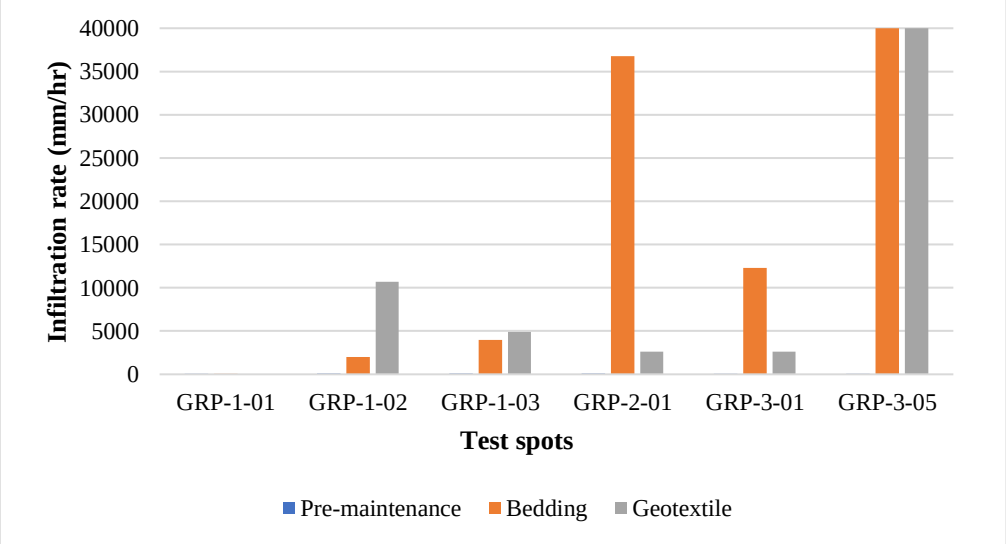

Figure 4-56: Grand Parade diagnostic assessment infiltration rates

Views of the bedding and geotextiles for GRP-1-01 are presented in Figure 4-57. Considerable quantities of sand were intermixed with the stone aggregates. The pavement thus illustrates Type IV clogging i.e., full pavement clogging. Given that the lower layers were completely wrapped in geotextile, this could only have been the result of bad construction practice where the aggregate was installed together with considerable quantities of fine material.

(a) High sediment content **(b) High sediment content** **(c) High sediment content**

Figure 4-57: GRP-1-01 bedding, geotextile, and sublayers' state

The GRP-1-02 geotextile was easily de-threaded by hand (Figure 4-58(b)) – perhaps a consequence of vibration caused by regular traffic movement. The fine sediment outline visible in Figure 4-58(a) suggests that the surface migration of fines was likely only responsible for Type I and possibly Type II clogging. It was highly unlikely to have resulted in the greater clogging that is present.

(a) Sediment outline **(b) Damaged geotextile** **(c) Muddy film aggregates**

Figure 4-58: GRP-1-02 bedding, geotextile, and sublayers' state

The measured infiltration rates for GRP-2-01 and GRP-3-01 bedding and geotextiles suggest Type III clogging. It is likely that this is mainly a result of vehicle dynamic loading. GRP-3-05 substantial bedding and geotextile infiltration rates refer to Type I clogging.

The PICP is an example of poor design (excessive RoF; too close to the needle-shaped trees on the boundary), poor construction (fine material in the underlying aggregate layers), and no maintenance.

4.10 MyCiti Bus Rapid Transit Depot (BRT)

The MyCiti Bus Rapid Transit Depot (BRT) is located at the corner of Prestwich and Napier Streets in De Waterkant, Cape Town near the harbour at 33°54'48.57"S; 18°25'10.03"E (Figure 4-59). The site is situated 15 m a.m.s.l.

Figure 4-59: MyCiti BRT Depot locality map (Map source: Google Maps, 2022)

The site is used as a depot and mechanical maintenance facility for the MyCiti buses. Some of the pavement sections on the site are fitted with PICP (Figure 4-60 and Table 4-4). The PICP was designed to capture stormwater to be pumped into roof tanks and used within the site to reduce the municipal water footprint. However, the mechanical system has not been maintained and was not functional at the time of testing.

The total permeable area on the site is 6390 m^2 while the impermeable area is 10,100 m^2. The impermeable area is comprised of roofs and concrete pavements. 3960 m^2 of the impermeable area drains to a vegetated bioretention filter at the entrance of the facility on Napier Street (Figure 4-60). The PICP services the remaining 6140 m^2 of impermeable surfaces to give a RoF of 0.97. It is installed on the bus parking bays and the areas adjacent to the maintenance workshops. There are four areas of PICP on this site indicated as Areas 2, 3, 6, and 7 in Figure 4-60. Areas 2 and 3 form part of the access to the maintenance workshops while Areas 6 and 7 are bus parking bays.

Figure 4-60: BRT PICP layout (Map source: Google Earth Pro, 2022)

Table 4-4: BRT PICP area distribution

PICP section	PICP area (m^2)
BRT-Area 2	460
BRT-Area 3	1680
BRT-Area 6	2000
BRT-Area 7	2250
Total	**6390**

Area 2 is adjacent to broad-leafed trees (Figure 4-61). An impermeable concrete pavement and the bus mechanical / wash bays workshops line the northern and western sites of Area 2 respectively. Area 2 PICP slopes by 5% towards the eastern side of the PICP to a catchpit that connects to the municipal stormwater line.

Area 3 lies across the exit to the bus workshops and wash bays and is lined with needle-shaped leaves trees on the western and southern sides respectively. The pavement is adjacent to the bus workshops and wash bays, and an impermeable concrete pavement on the eastern and northern sides respectively. The surface is relatively flat. The wash bays were connected to a reusable water facility that consisted of a sediment trap to avoid clogging the PICP.

Areas 6 and 7 are bus parking bays surrounded by impermeable concrete pavement roadways. Area 6 is the inner bus bay area. There is a bus filling station that drains away from the PICP and it is located 10 m away from Area 6 on the southern side. Area 7 is adjacent to an area lined with vegetation located 10 m from the PICP on the northern side. The ground slopes for Areas 6 and 7 are around 3%.

Figure 4-61: Area 2 corner showing overhanging trees

The BRT PICP layer design comprised 80 mm Permealock ® filled with 2-4 mm gritstone, a 50 mm deep x 6.75 mm bedding layer, an upper Inbitex ® geotextile, a 100 mm deep x 19-25 mm base layer, a 100 mm deep x 25-53 mm upper subbase layer, a TriAx ® geogrid layer, and a 250 mm deep x 50-63 mm lower subbase layer. The PICP was installed in 2011.

4.10.1 Field infiltration testing

Figures 4-62 and 4-63 show the location of the test spots and their measured infiltration rates. The test spots in Areas 3 and 7 – a bus parking bay and a roadway –all had measured Mod-ASTM infiltration rates somewhat greater than 1000 mm/hr – a moderately high infiltration rate. BRT-2-01 and BRT-2-03, on the other hand, had infiltration rates of 1000 and 800 mm/hr respectively. These test spots are closer to the edge of the site and situated under trees. By way of comparison, BRT-2-02 and BRT-2-04, which were clear of the trees, supported higher infiltration rates – 2400 and 1600 mm/hr respectively. This illustrates the negative impact of vegetation on the surface infiltration of PICP. A lack of joint gritstone was also apparent. Figure 4-64 shows a typical surface of the PICP in BRT Area 2 under trees. Exposure to traffic appeared to have an insignificant impact on the measured infiltration rates.

BRT Mod-SWIFT infiltration rates ranged from 100 to 1800 mm/hr. The BRT-2-04 measured infiltration capacity was likely affected by a long wet strip generated by the test water thus reducing the infiltration rate.

The site managers indicated that water jetting maintenance was conducted in 2016, however no documentation indicating the impact of this maintenance was available.

Figure 4-62: BRT PICP test spot location (Map source: Google Earth Pro, 2022)

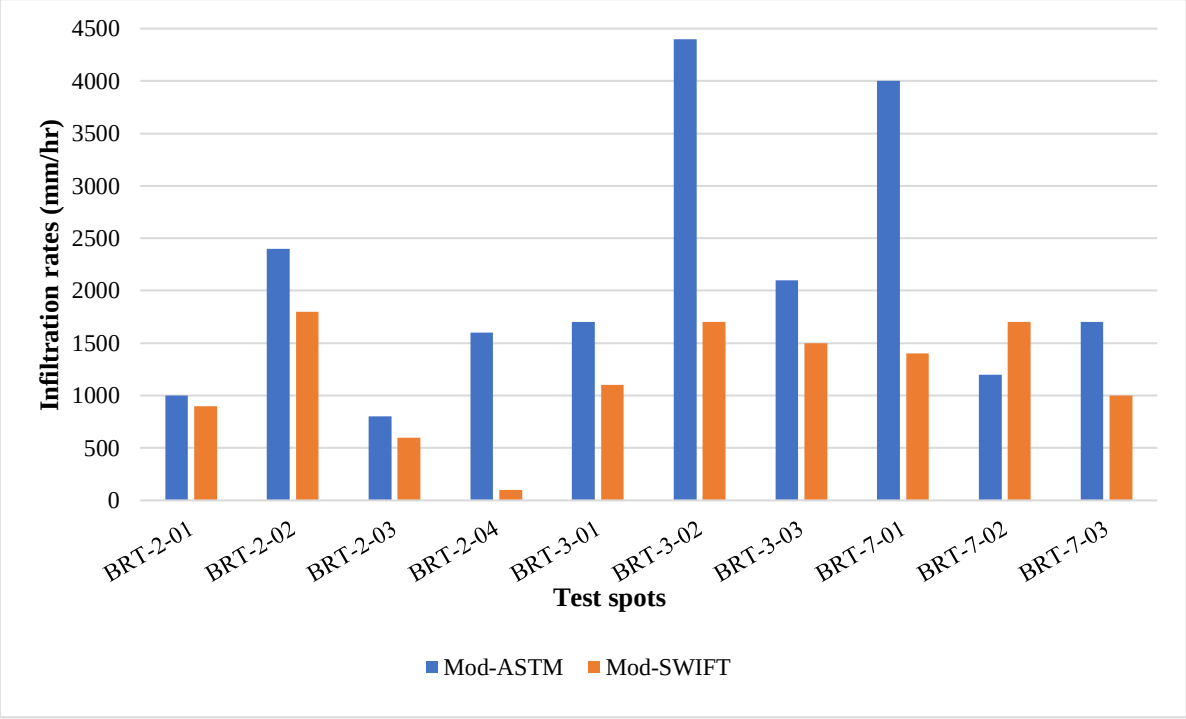

Figure 4-63: BRT surface infiltration rates

Figure 4-64: Typical Area 2 sediment and organic filled joints

4.10.2 Pavement maintenance trials

Figure 4-65 presents the maintenance trials infiltration rates: pre-maintenance, post-blowing, and post-maintenance tests, of the test spots (Figure 4-62). The pre-maintenance tests are discussed in Section 4.10.1. The compressed air blower increased the test spots' post-blowing infiltration rates by 253% to 2563%.

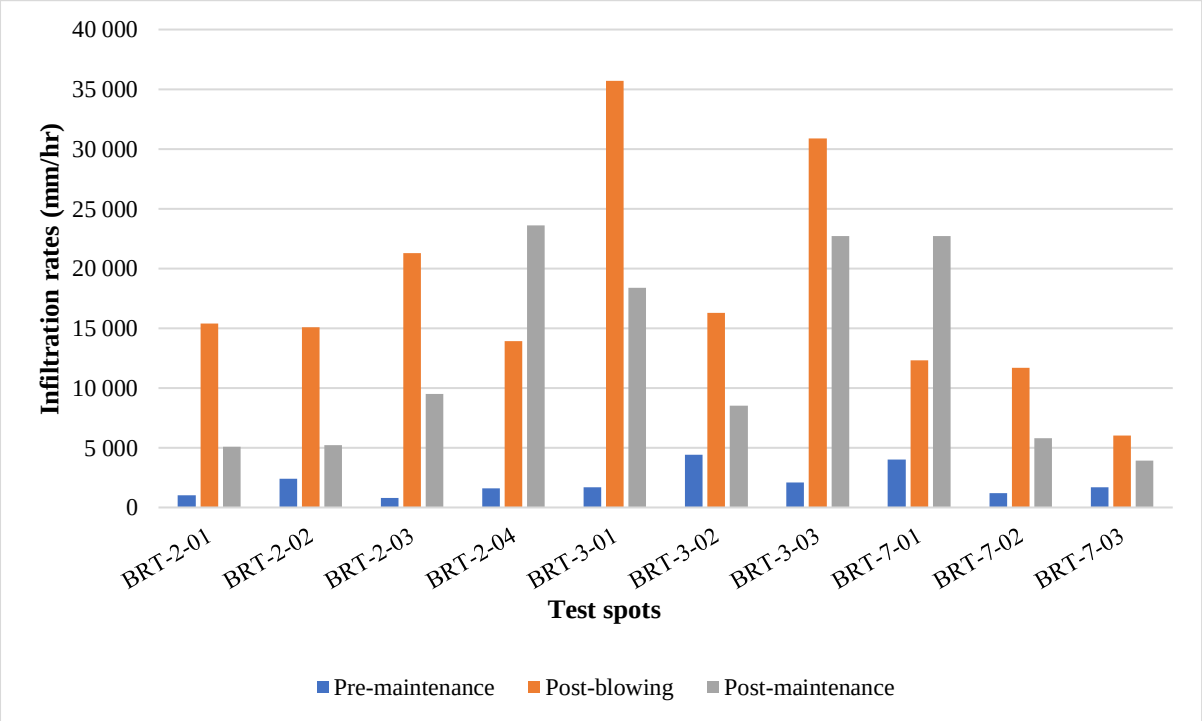

Figure 4-65: BRT maintenance trials infiltration rates

The percentage increase in infiltration rate between the pre-maintenance and post-maintenance infiltration rates was 93% and 1088%. The compressed air blowing significantly improved the hydraulic performance of the test spots as sediment was removed from the paver joints. There was a drop in infiltration between the post-blowing and post-maintenance when the clean gritstone was swept into the joints. Relative to other test spots, BRT-7-03 recorded the lowest post-maintenance infiltration rate − 3900 mm/hr. It is likely that the fine material in the joints were pushed deeper into the joints since BRT-7-03 was missing gritstone (Figure 4- 66).

Figure 4-66: BRT-7-03 missing gritstone (up to 30 mm)

4.10.3 Diagnostic assessments

Figure 4-67 shows the measured infiltration rates for the diagnostic assessments of BRT-2-04 and BRT-7-01. The measured bedding and geotextile infiltration rates for BRT-2-04 were extremely high – 33,800 mm/hr and 40,000mm/hr – while equivalent rates for BRT-7-01 were 19,200 mm/hr and 16,600 mm/hr respectively. The likely difference for the performance of BRT-7-01 was its proximity to a run-on area and vegetation.

Figure 4-68 shows the state of the bedding, geotextile, and base layer of the test spots. The two test spots had a wedge-like outline of sediment intermixed with joint material on the bedding. BRT-2-04 geotextile was lightly punctured while BRT-7-01 was still intact (Figure 4-69). Bus vibration and turning may be responsible for damaging the geotextile at BRT-2-04. Figure 4-70 shows a geogrid that was installed to increase the pavement structural stability at BRT-7-01. Both two test spots predominantly demonstrate Type I clogging but BRT-7-01 is starting to show Type II clogging as sediment is being washed deeper into the joints.

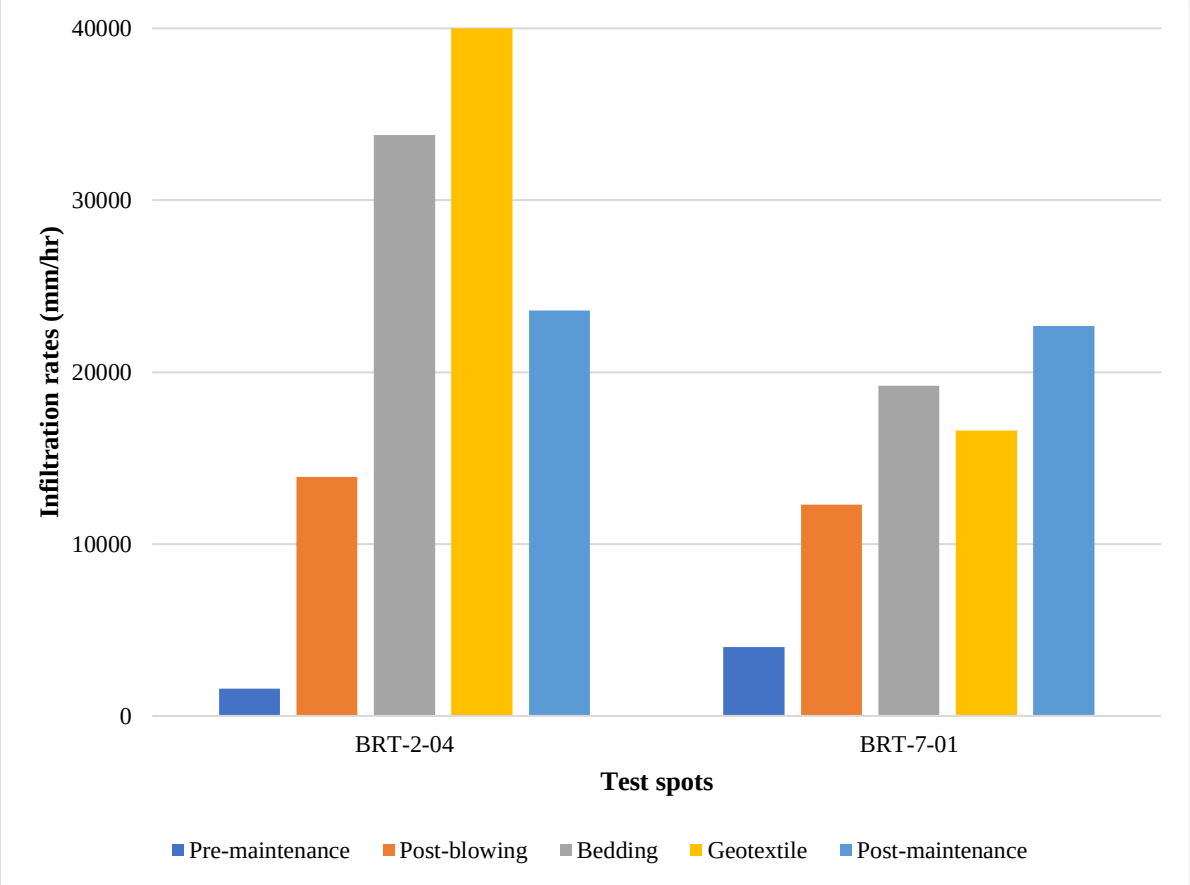

Figure 4-67: BRT diagnostic assessment infiltration rates

(a) Sediment outline **(b) Sediment in joints** **(c) Lightly punctured geotextile**

Figure 4-68: BRT-2-04 bedding, geotextile, and pavement sublayers views

(a) Sediment outline **(b) Sediment in joints** **(c) Intact geotextile**

Figure 4-69: BRT-7-01 bedding and geotextile views

Figure 4-70: Geogrid installation

4.11 Stor-Age Tableview Facility

Stor-Age Facility (SAF) in Tableview, Cape Town is a self-storage facility located in Milnerton on Koeberg Road (M14) at 33°50'8.24"S; 18°31'29.78"E (Figure 4-71). The site is situated in a flat built-up area that is 11 m a.m.s.l. The SAF PICP parking area was constructed in 2011. The permeable pavement area is used for staff cars and light delivery trucks parking.

The parking area is paved with 2670 m^2 PICP. The impermeable area draining onto the PICP consists of the facility roof and various conventional pavements around the site with a total area of 5830 m^2 to give a RoF of 2.2.

The north, west, and south boundaries of the facility are fenced with precast concrete walls with a vegetated area adjacent to the PICP. There are trees on the eastern side of the site (Figures 4-72 and 4-73). In some portions of the PICP there was evidence of accumulated sediment in the joints – particularly those adjacent to the vegetated areas (Figure 4-74). The SAF layer design is shown in Figure 4-75.

Figure 4-71: SAF locality map (Map source: Google Maps, 2022)

Figure 4-72: SAF site layout (Map source: Google Earth Pro, 2022)

(a) **(b)**

Figure 4-73: Vegetation adjacent the PICP

Figure 4-74: Typical sediment accumulation in joints adjacent to vegetated areas

It was not possible to perform maintenance and diagnostic tests on the site because it was impossible to find a convenient time that would not disrupt business. The PICP in SAF did undergo maintenance in 2019 using compressed air blowing (Matolengwe, 2021), however no records were kept.

Ten test spots were selected for infiltration testing (Figure 4-76). Figure 4-77 shows the Mod-ASTM and Mod-SWIFT infiltration rates for the test spots. The Mod-ASTM infiltration capacities ranged from 200 to 1200 mm/hr. STF-04 measured infiltration rate was 200 mm/hr and was thus considered blocked. Test spots that were closer to the vegetated area recorded lower infiltration rates compared with those that were further from the vegetation while infiltration rates increased from the outside of the PICP system to the centre (e.g. STF-03 and STF-04). This confirms the proposition that sediment and vegetation contribute to the surface clogging of the PICP. Test spots on the roadway recorded higher infiltration rates relative to those in the parking bays. The Mod-SWIFT measured infiltration rates ranged from

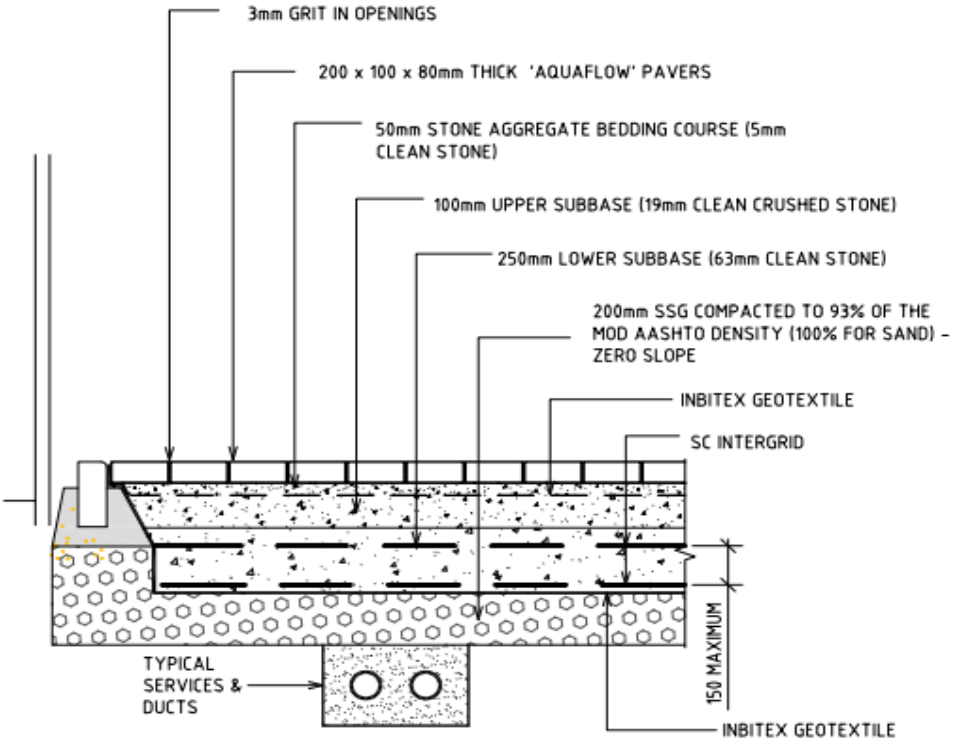

Figure 4-75: SAF PICP design layers (Matolengwe, 2021)

Figure 4-76: Stor-Age Tableview facility test spot locations (Matolengwe, 2021)

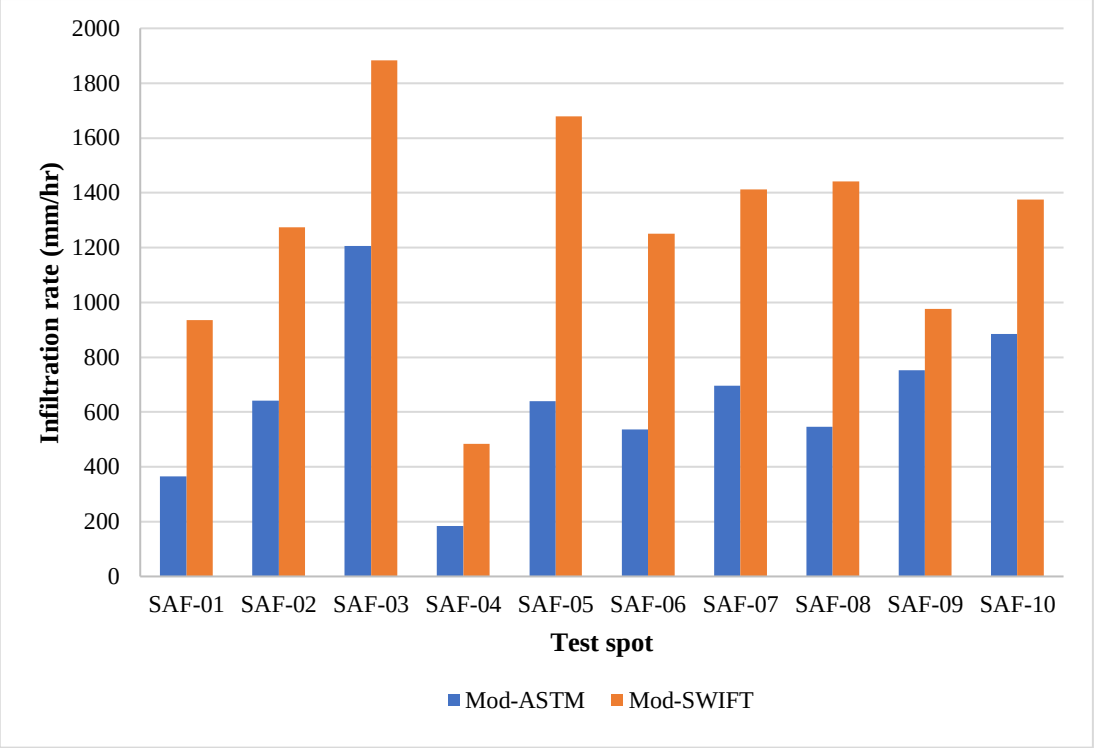

Figure 4-77: Mod-ASTM and Mod-SWIFT infiltration rates (After Matolengwe, 2021)

500 to 1900 mm/hr and showed the same pattern as the Mod-ASTM rates, although their corresponding test spots' values were different.

4.12 Hirsch's Appliances Milnerton (HAM)

Hirsch's Appliances in Milnerton (HAM) is a household electric appliances store located at the corner of Racecourse Road and the M5 (Koeberg Road) in Milnerton at 33°51'53.49"S; 18°30'27.88"E, at an elevation of 9 m a.m.s.l (Figure 4-78).

The site is divided into a permeable pavement area (PICP), an impermeable conventional interlocking concrete pavement, a car wash, and impermeable roof warehouse structures. The PICP section is in the middle of the site. The roofs drain onto the adjacent impermeable pavement sections which consequently drain directly onto the PICP (Figure 4-79), thus having a bigger blockage impact. The area distribution of the site is summarised in Table 4-5. The RoF is 3.

The car wash and the concrete-lined channel drain away from the PICP. There is a short grass-vegetated area that slopes towards the concrete lined channel on the Bridle Way side. There are broad-leaved trees along the parking bays (Figure 4-80). The PICP was installed in 2012 and carries considerable car traffic plus occasional delivery trucks.

The pavement layer design comprises: 80 mm Aquaflow ® pavers, 2-3 mm gritstone, 50 mm deep x 6.75 mm bedding, an upper Inbitex ® geotextile, a 100 mm deep x 9.5-19 mm base layer, a 250 mm deep x 19-53 mm subbase layer, and a lower Inbitex ® geotextile.

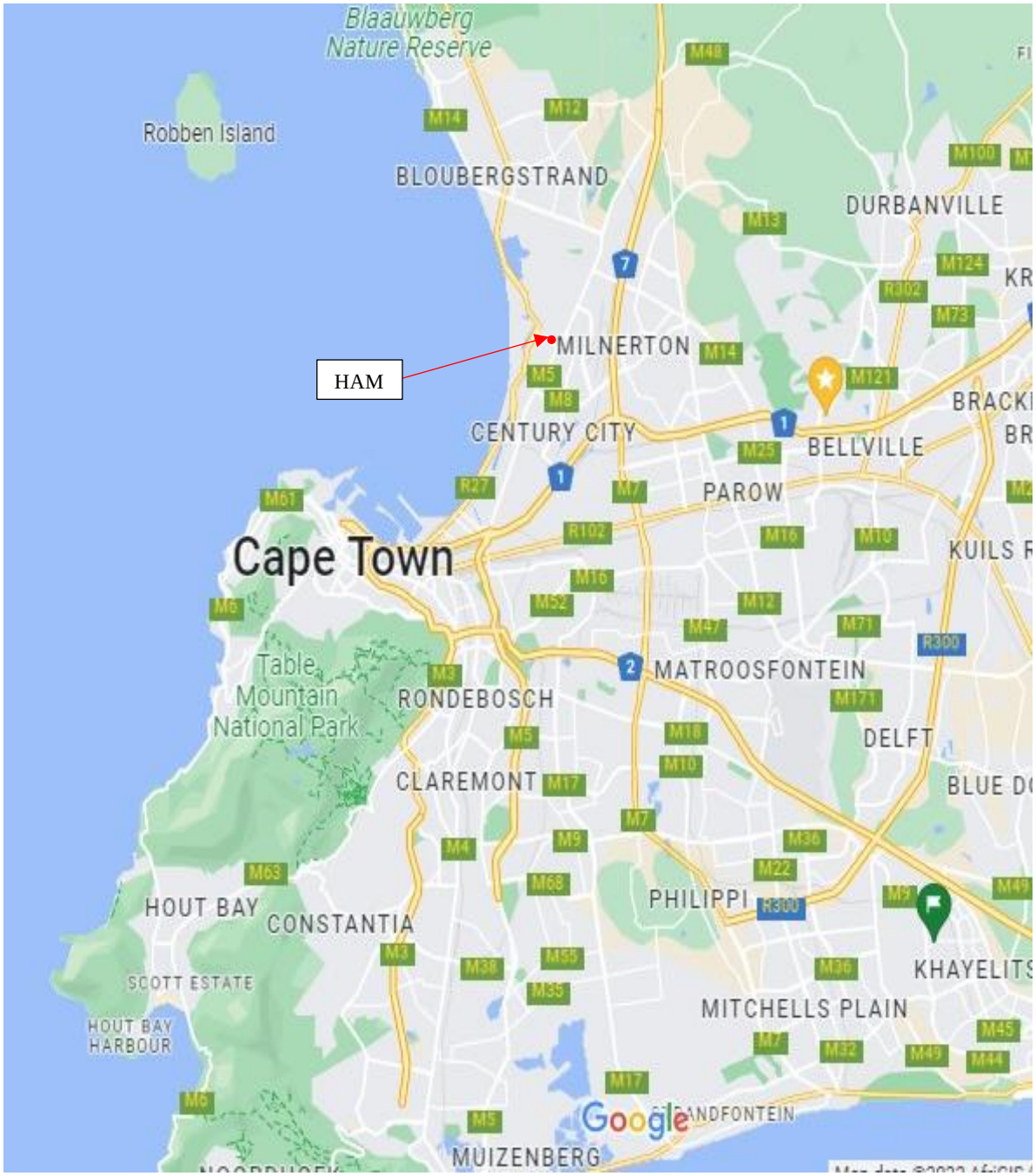

Figure 4-78: HAM locality map (Map source: Google Maps, 2022)

Table 4-5: HAM PICP area distribution

PICP section	Pavement area (m^2)	Sub-total (m^2)	Total area (m^2)
PICP	2760	2760	11,020
Impermeable pavement	3350	8260	
Impermeable roofing	4910		

Figure 4-79: HAM PICP area distribution (Map source: Google Earth Pro, 2022)

Figure 4-80: HAM PICP permeable and impermeable pavements, and tree distribution

4.12.1 Field infiltration testing

20 test spots were identified and infiltration tests were measured on the HAM PICP site in 2021. 15 of the test spots were chosen because of previous research conducted by UCT students investigating the performance of the PICP with time. Five test spots were added to the investigation to provide additional information on what was happening in the vehicle pathways, intersections, close to vegetation, and parking bays (Figure 4-81). Figure 4-82 presents the measured 2017, 2018, 2019 and 2021 infiltration rates of the test spots.

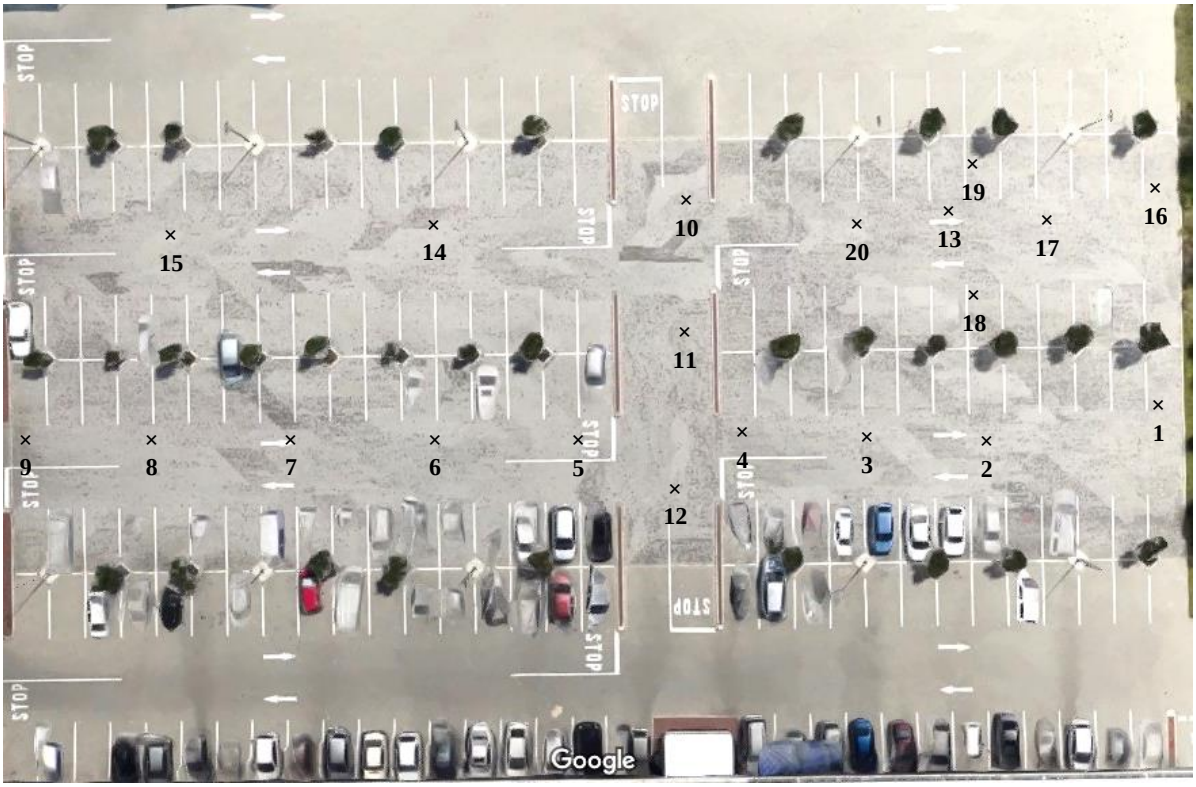

Figure 4-81: HAM infiltration rates test spots (After Matalongwe, 2021)

The measured infiltration rates at Test spots 2 to 9, 14, and 15 have decreased annually from 2017 to 2021. The infiltration rates were generally higher farther away from the pavement edges, e.g., Test spots 2 to 9. Strangely, the infiltration rates appear to have increased between 2019 and 2021 at Test spots 1, 10, 11, 12, and 13. These might be explained by an overestimation of the infiltration rates owing to the loss of gritstone in the joints and the associated seepage out of the sides of the measuring ring as the site has not been maintained since its installation. Proximity to vegetation did not appear to have a significant impact on the infiltration rate c.f., Test spots: 1, 16, 18 and 19 – although it should be said that the vegetation was not particularly prolific. Indeed, overall test spot location had minimal impact on the measured infiltration rate at HAM.

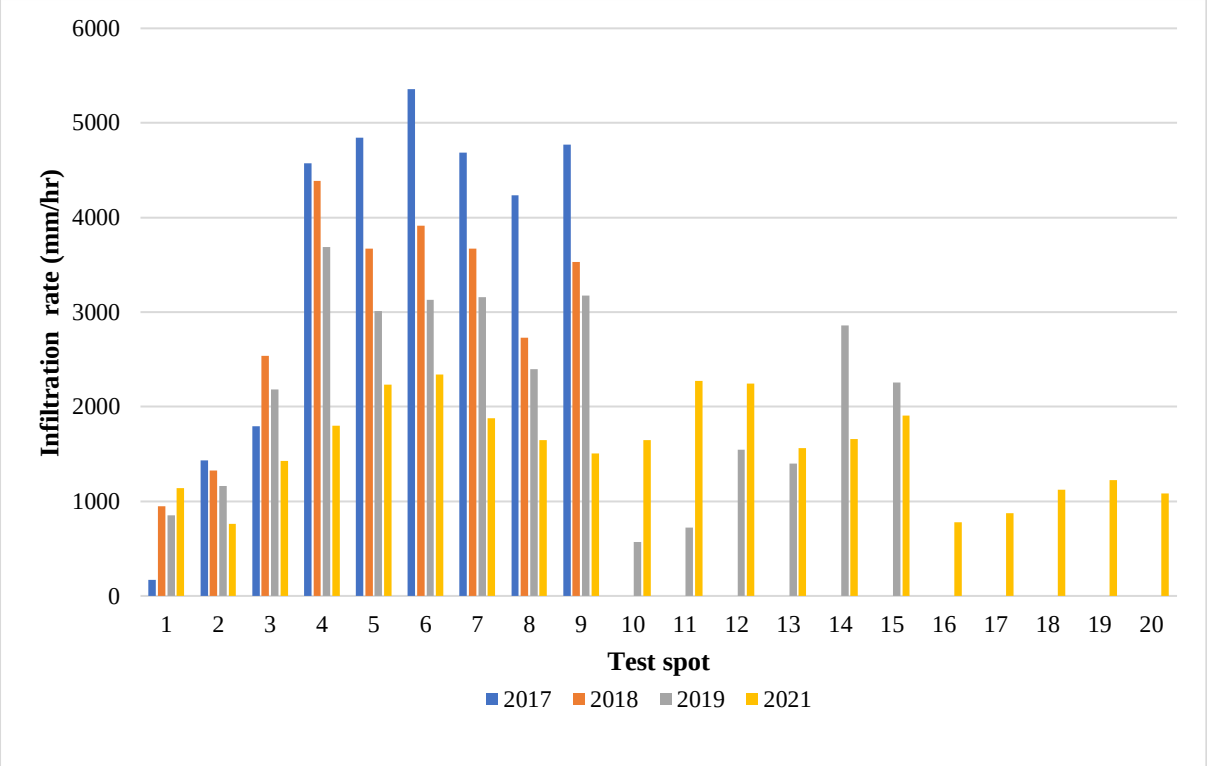

Figure 4-82: 2017-2021 HAM infiltration rates
(Adapted from Artus, 2017; Vella, 2018; Barnard, 2019; Matolengwe, 2021;)

4.12.2 Pavement maintenance trials

Pavement maintenance trials were conducted on eight test spots at the HAM PICP site (Figure 4-83). Access to the site was only possible during operating hours, thus some sections of the PICP were inaccessible for maintenance. These included Test spots HAM-06, HAM-07 and HAM-08. HAM-07-A replaced HAM-07 to better represent an interior intersection performance.

The measured infiltration rates of HAM-04, HAM-05 and HAM-06 were 700 mm/hr, 700 mm/hr, and 1300 mm/hr respectively (Figure 4-84). These PICP sections were seldom used relative to the other test spot sections. HAM-04 and HAM-05 were adjacent to each other and their measured pre-maintenance infiltration rates were similar, despite the former being in a parking bay and the latter on the roadway. The frequently used PICP sections had measured infiltration rates that ranged from 900 mm/hr and 6000 mm/h with little obvious difference between the intersections (900-6000 mm/hr) and the roadway (3600-4800 mm/hr). Some of the infiltration rates were likely overestimated as a result of missing grit in the joints (Figure 4-85). Blowing the muck out of the joints significantly increased the infiltration capacities (post-blowing) by 92% to 829%, however, they generally decreased upon addition of clean grit in the joints.

Figure 4-83: HAM PICP test spot locations (Map source: Google Earth Pro, 2022)

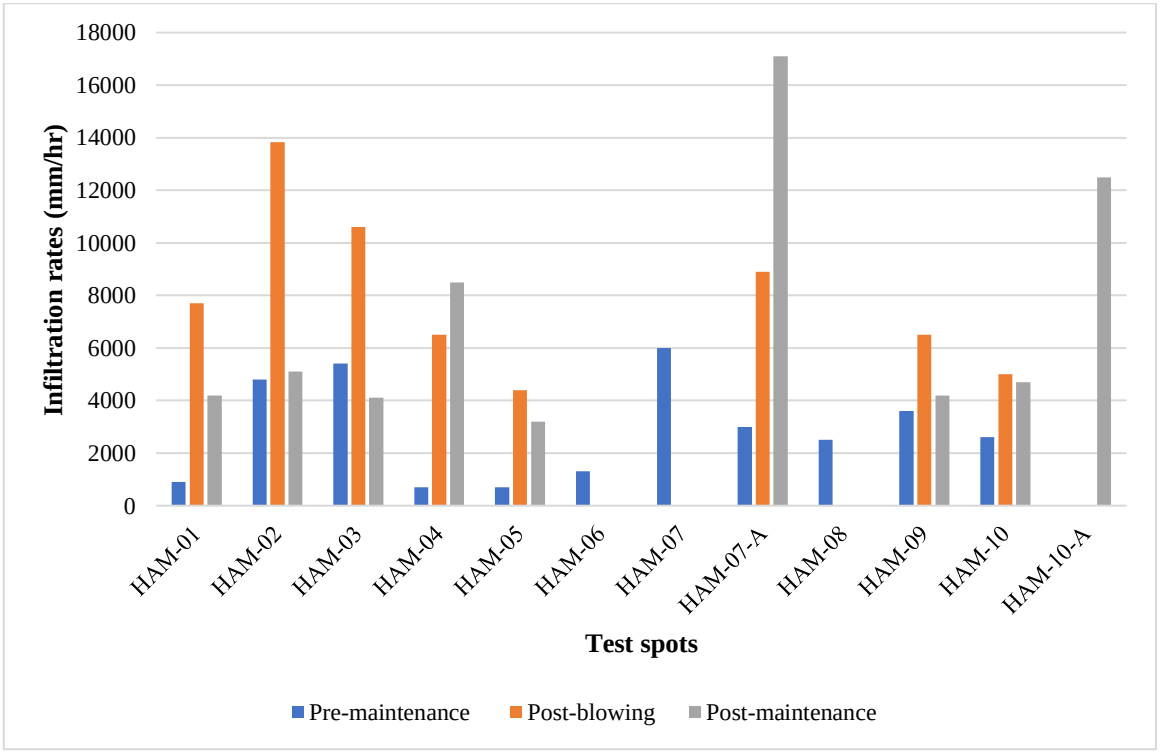

Figure 4-84: HAM maintenance trials infiltration rates

Figure 4-85: Typical PICP section with missing grit

4.12.3 Diagnostic assessments

Diagnostic assessments were conducted on HAM-04 (parking area), HAM-07-A (intersection), and HAM-10-A (intersection approach) (Figure 4-86). Test spot HAM-10-A replaced HAM-10 because, during the maintenance trials, the pavers were forcefully uplifted by the compressed air blower. The bedding and geotextile infiltration rates of the test spots were high – ranging between 6700 and 21,200 mm/hr for the former and 7100 and 40,000 mm/hr for the latter.

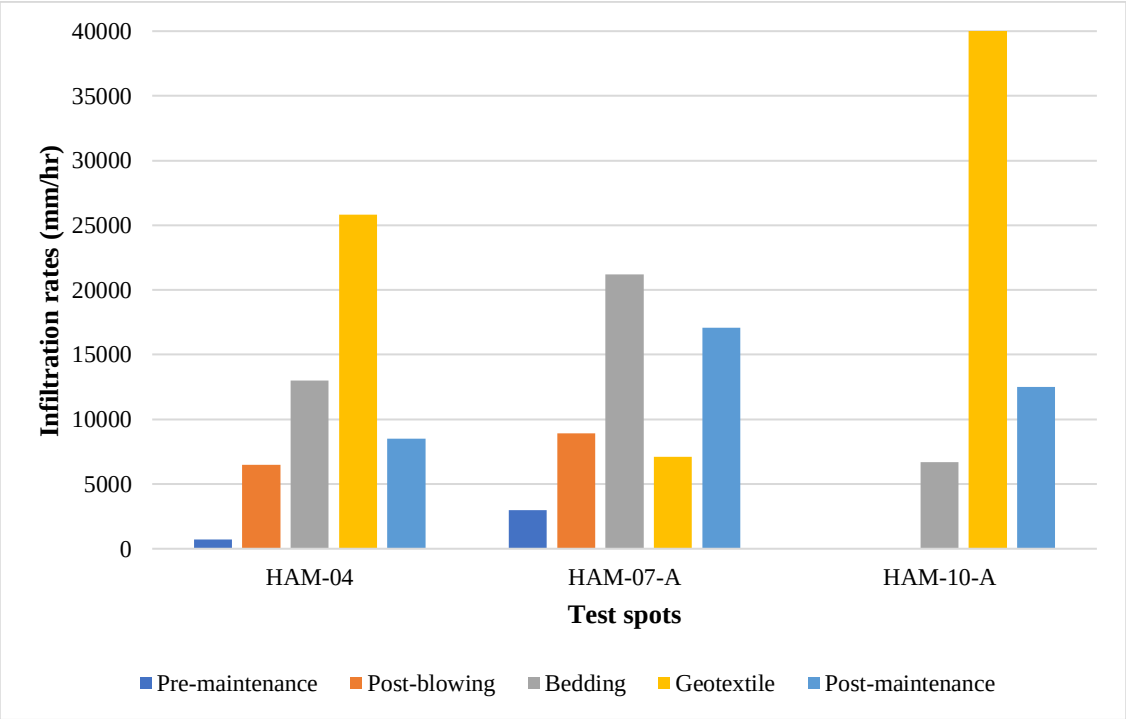

Figure 4-86: HAM diagnostic assessment infiltration test results

A sediment outline was observed under the pavers on HAM-02 and HAM-07-A but the sediment was more uniformly spread over the bedding of HAM-10-A – likely due to the braking and turning effects of vehicles at the intersection (Figure 4-87). The geotextile appeared to be intact for HAM-04, lightly punctured for HAM-07-A, but completely shattered for HAM-10-A. There were few fines visible on the geotextile in HAM-04 and HAM-07-A. HAM-10-A bedding and basecourse interface had no fines trapped likely because they were washed into the pavement base layer since the geotextile had disintegrated (Figure 4-88). HAM-04 and HAM-07-A were subjected to Type II clogging, whilst HAM-10-A was exposed to Type III – likely soon to be Type IV clogging with the sediment starting to be distributed throughout all layers with the geotextile badly damaged by vehicle dynamic loading.

(a) HAM-04 **(b) HAM-07-A** **(c) HAM-10-A**

Figure 4-87: HAM diagnostic bedding assessment observations

(a) HAM-04 **(b) HAM-07-A** **(c) HAM-10-A**

Figure 4-88: HAM diagnostic geotextile assessment observations

4.13 The Nirvana Residential Complex

The Nirvana Residential Complex (NVC) is a residential complex located in Parklands at 33°48'4.72"S; 18°30'43.00"E along the Chelsea Crescent Road at 21 m a.m.s.l. (Figure 4-89). The PICP on the site was constructed in 2019.

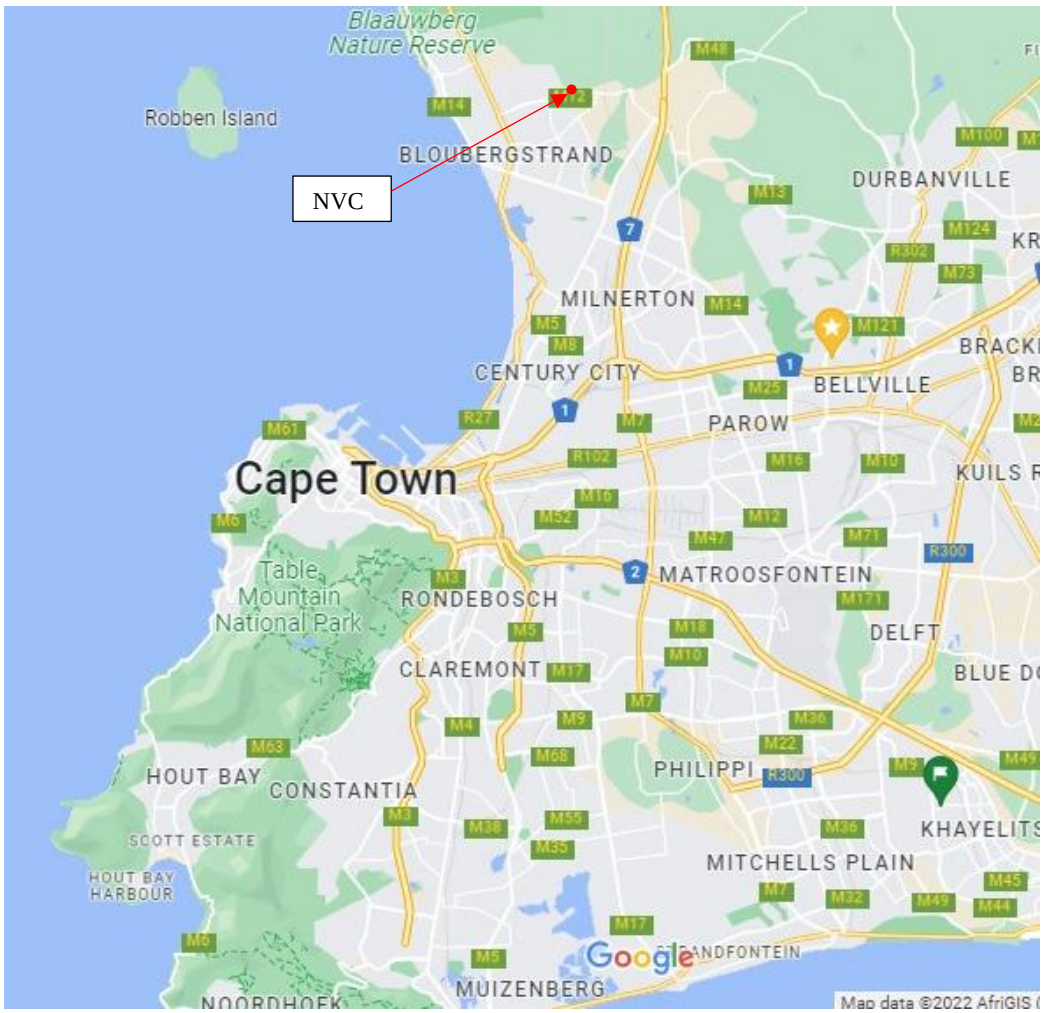

Figure 4-89: NVC locality map (Map source: Google Maps, 2022)

The PICP carries considerable light-vehicle traffic together with occasional delivery trucks on a two-lane single-carriageway driveway in a relatively flat area. It mainly services direct rainfall and roof runoff from nearby residential apartments. Figure 4-90 and Table 4-6 show the area distribution. The RoF is 4.8. The permeable surfaces of the site comprise the PICP (NVC-PICP) and a vegetated lawn area (NVC-PA). The impermeable areas are made up of roof surfaces (NVC-IS) and impermeable pavement (NVC-IP). The vegetation area within the site consisted of strips adjacent the permeable pavement corridor, trees, and low grass within a mini park. A small park is located between the residential apartment blocks and the PICP. There are two overflow surface outlets on the perimeter wall of the complex.

Figure 4-90: NVC Area distribution (Map source: Google Earth Pro, 2022)

Table 4-6: NVC area distribution

Area section	Area distribution (m^2)	Sub-total (m^2)	Total area (m^2)
PICP (NVC-PICP)	1880	1880	11,450
Impermeable pavement (NVC-IP)	160	9030	
Impermeable surface (roofing: NVC-IS)	8870		
Permeable area (vegetated: NVC-PA)	540	540	

Some of the strip areas that were supposed to be vegetated were barren of vegetation exposing fine material adjacent to and potentially draining onto the PICP (Figures 4-91).

The NVC PICP consisted of two pavement layer designs: NVC-PICP (01) and NVC-PICP (02), which had 80 mm pavers with the corners cut off them (Figure 4-92), 2-3 mm gritstone, a 50 mm deep x 6.75 mm bedding, an upper Inbitex ® geotextile, and a 100 mm deep x 9.5-19 mm base layer. NVC-PICP (01) had a 250 mm deep x 19-53 mm subbase layer, whilst NVC-PICP (02) was provided with a deeper subbase – 350 mm, to increase the open-aggregate storage reservoir volume. A lower Inbitex ® geotextile was fitted between the subgrade and the lower part of the NVC PICP in both cases.

Ten test spots were identified and both Mod-ASTM and Mod-SWIFT infiltration tests were carried out. The test spots were targeted at intersections, along the roadway adjacent to the vegetated areas, and at points where the pavement appeared structurally sound (Figure 4-93).

(a) Downpipe and vegetated strip **(b) Mini-park adjacent the PICP**

Figure 4-91: NVC typical vegetated areas

Figure 4-92: Typical 'cut-off' pavers

Figure 4-94 presents the measured infiltration rates of the test spots. Mod-ASTM infiltration rates ranged from 400 mm/hr to 7800 mm/hr. NVC-04, NVC-06 and NVC-07 recording 400 mm/hr, 400 mm/hr and 800 mm/hr respectively, were all located on the roadway and close to the impacts of vegetation, loose sediment and discharge from roof downpipes. NVC-09 was not adjacent to obvious sources of sediment, nevertheless its joints were filled with sediment and its measured infiltration was only 600 mm/hr. On the other hand, NVC-10, exposed to seemingly similar conditions as NVC-09 recorded a substantial infiltration rate of 7800 mm/hr – but this might have been a measurement error because of missing grit in the joints (Figure 4-95(b)). All the other test spots that were clear of vegetation and sediment exposure recorded infiltration rates greater than 1000 mm/hr. The Mod-SWIFT infiltration capacity

Figure 4-93: NVC infiltration test spots layout (Map source: Google Earth Pro, 2022)

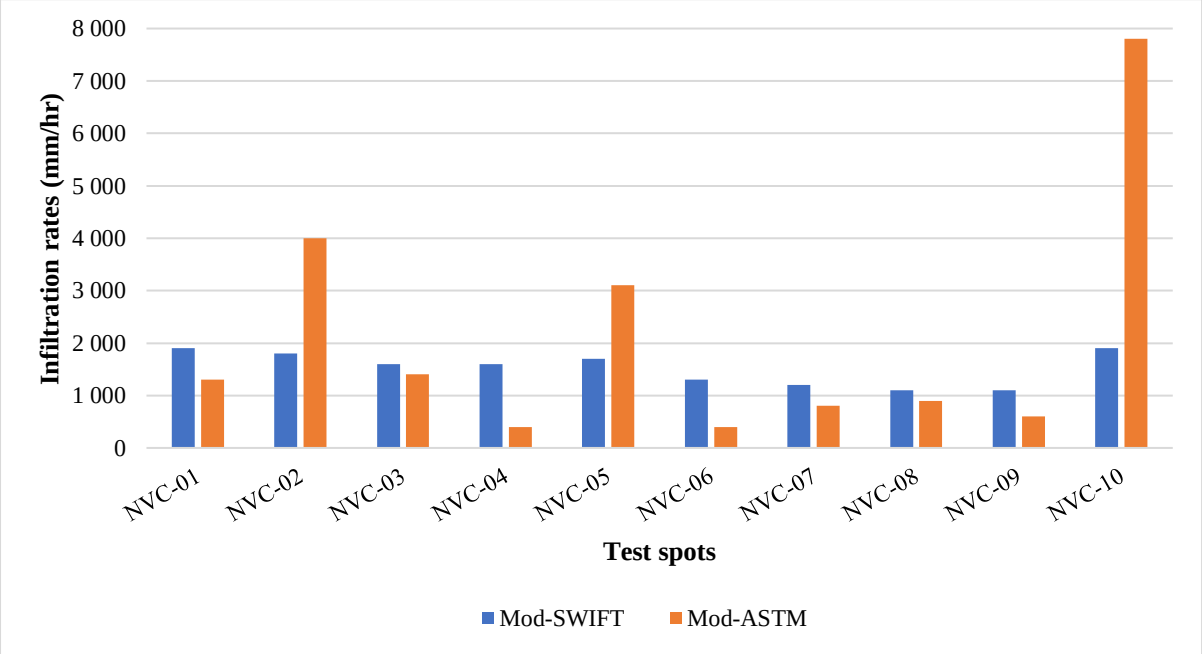

Figure 4-94: The NVC infiltration rates

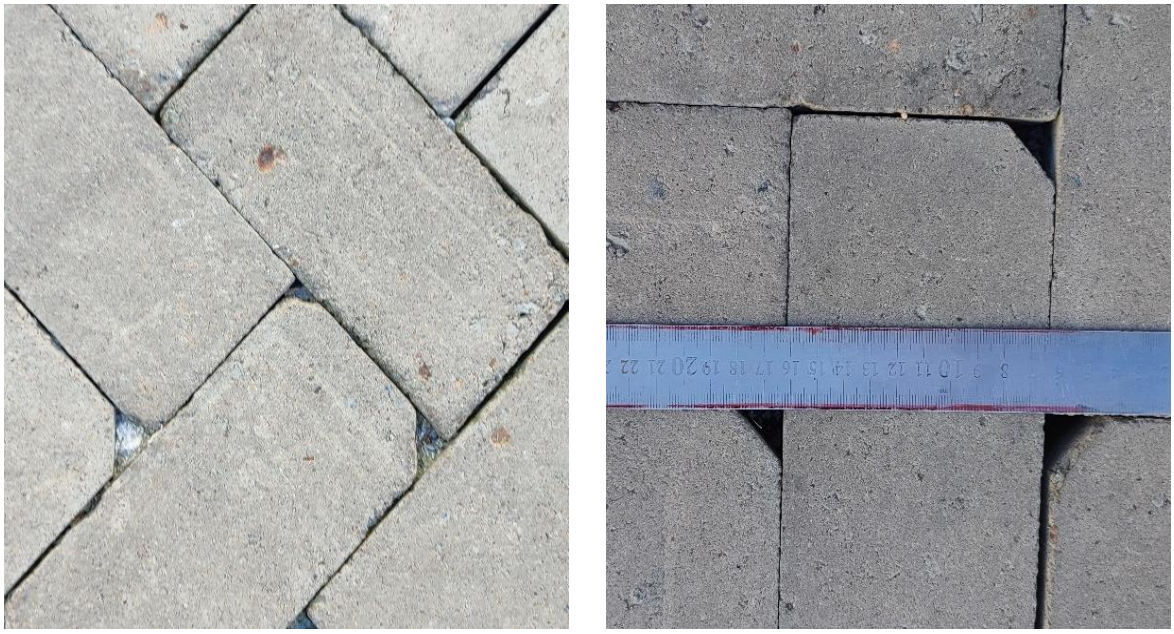

(a) NVC-09 clogged surface **(b) NVC-10 missing grit**

Figure 4-95: The NVC joints state

ranged from 1100 to 1900 mm/hr, with little variation. Overall, it appeared that the PICP location did not have a significant effect on the infiltration capacity of the test spots. Lack of gritstone in the paver joints and dislocated pavers permitted fine sediment to accumulate within the joints (Figures 4-95 and 4-96).

Figure 4-96: Compromised paver 'lock-up'

4.14 University of Witwatersrand First-year parking area

The University of Witwatersrand (WITS) First-year parking area is a permeable parking area located on Alumni lane in the Wits Braamfontein West Campus in Johannesburg at 26°11'9.44"S; 28° 1'35.67"E (Figure 4-97). It is one of the oldest PICP sites – constructed in 2008, and is used mainly by staff, students and occasional trucks. The parking area consists of two levels: the upper (WITS-U) and lower parking (WITS-L), at an altitude of 1704 m a.m.s.l. and 1699 m a.m.sl. respectively.

Figure 4-97: WITS First-year parking locality map (Map source: Google Maps, 2022)

WITS-L is 5400 m^2 and WITS-U is 7250 m^2 and both largely receive direct rainfall although small vegetated areas are connected to them, thus the RoF is ~0. Overflow from the WITS-U is directed to the WITS-L through concrete-lined chutes. The two parking levels are surrounded by grass and needle-shaped leaf trees. The trees overhang the PICP in some parts of the parking area (Figures 4-98 to 4-101). The PICP parking area has not been maintained since it was installed.

The PICP layer design comprised of 70 mm Aqua Trojan Slab ® pavers, a 50 mm deep x 2-6 mm bedding layer, an upper Inbitex ® geotextile, a 100 mm deep x 4-20 mm basecourse layer, a 250 mm deep x 10-63 mm subbase layer, and a lower Inbitex ® geotextile.

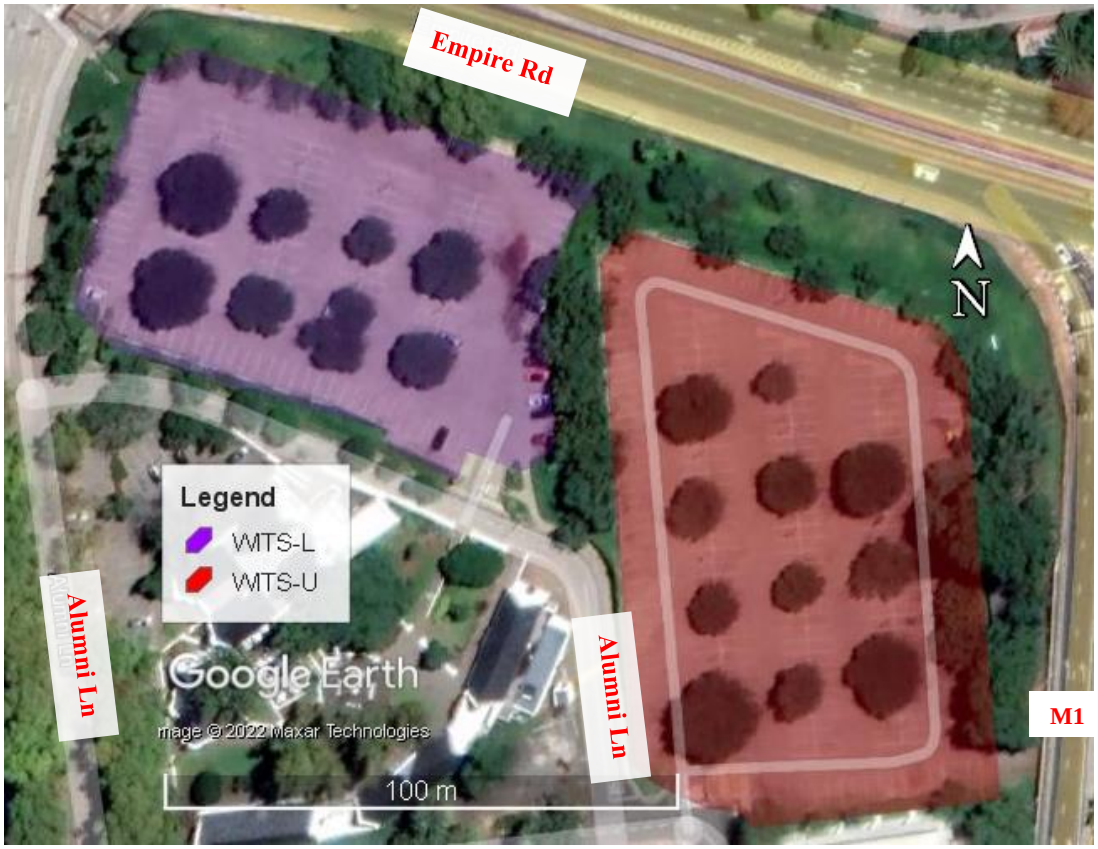

Figure 4-98: Wits First-year parking layout (Map source: Google Earth Pro, 2022)

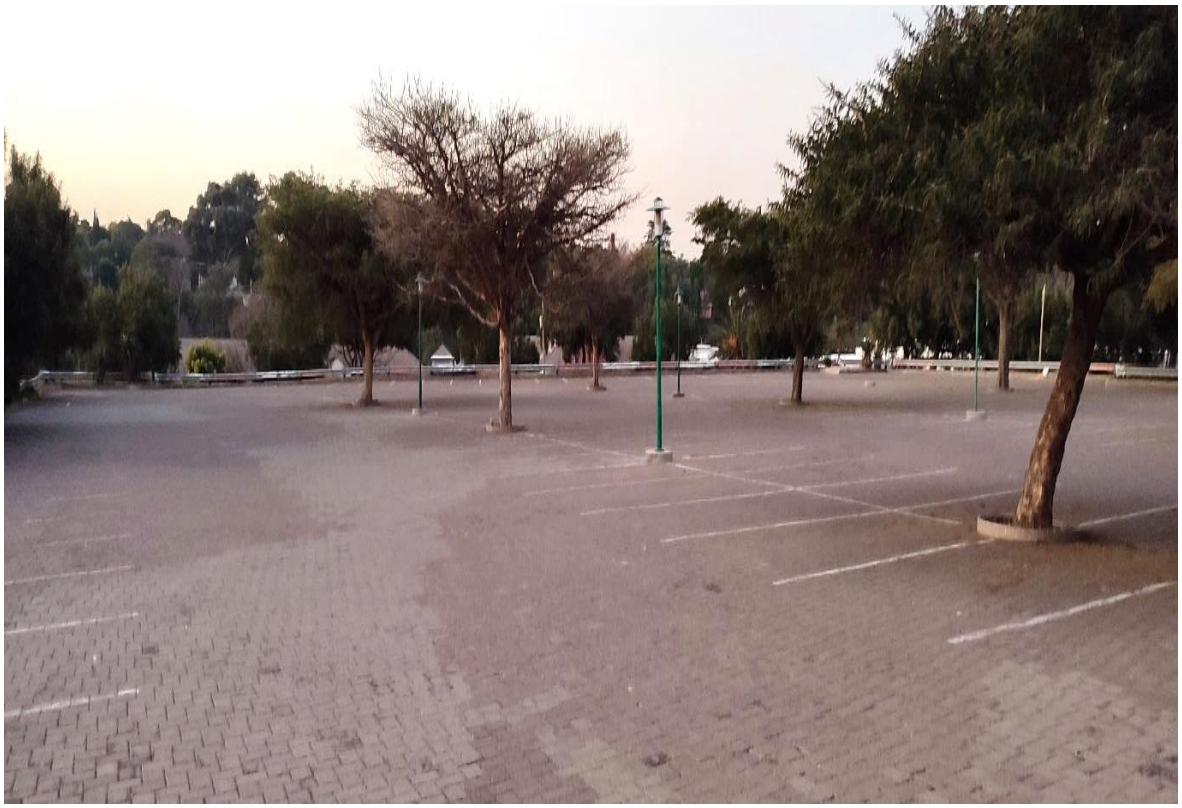

Figure 4-99: Overhanging trees at WITS-U

Figure 4-100: Grass and overhanging trees at WITS-L

Figure 4-101: Typical concrete-lined chute between WITS-U and WITS-L

4.14.1 Field infiltration testing

Ten infiltration test spots were chosen at critical points in the PICP parking areas (Figure 4-102) – five Mod-ASTM and Mod-SWIFT tests on each level.

Figure 4-102: WITS parking area test spots (Map source: Google Earth Pro, 2022)

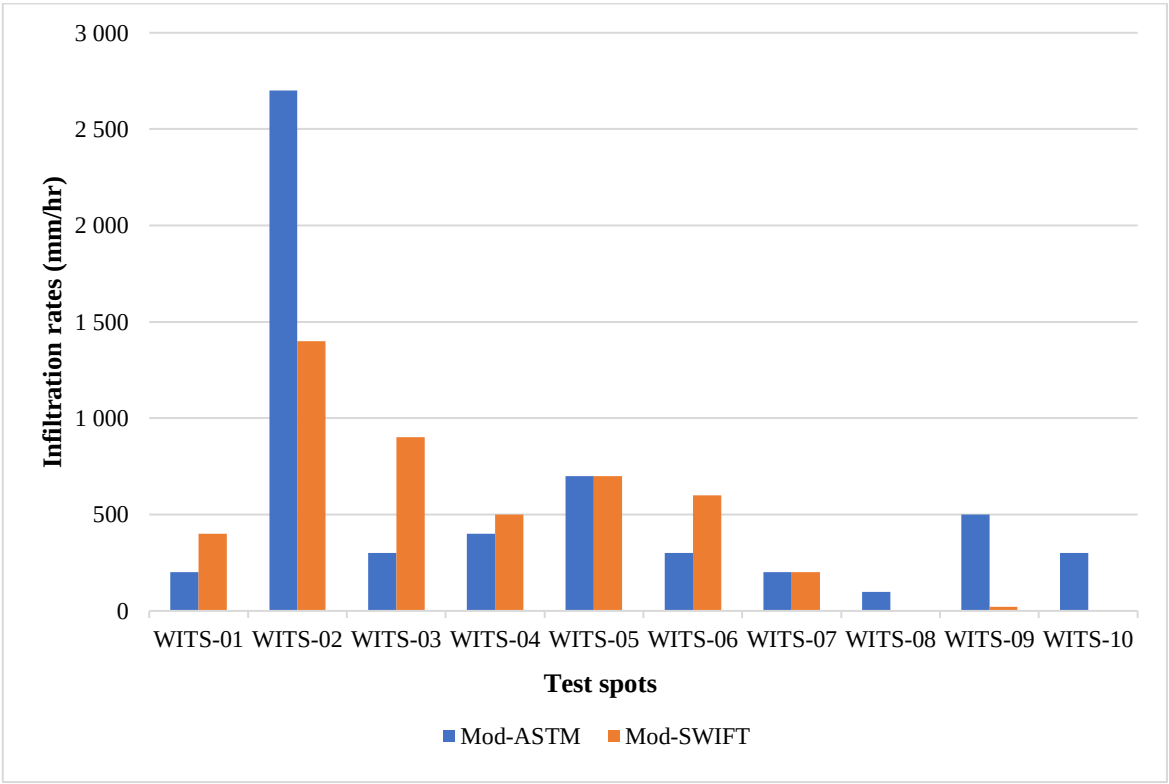

Figure 4-103: WITS infiltration rates

Figure 4-103 presents the infiltration rates of the test spots. The measured Mod-ASTM and Mod-SWIFT infiltration rates ranged from 100 mm/hr to 2700 mm/hr and fully clogged (WITS-08 and WITS-10) to 1400 mm/hr respectively. WITS-02, which recorded 2700 mm/hr for Mod-ASTM and 1400 mm/hr for Mod-SWIFT was clear of vegetation and sediment exposure, and it was located on a bend in the roadway. The Mod-ASTM infiltration rate may have been over-estimated because there was no grit in the joints and there was considerable lateral flow. WITS-01, WITS-07 and WITS-08 all appeared to be blocked. It is apparent that vegetation, lack of grit and sediment exposure significantly impacted the infiltration rate of a PICP section.

4.14.2 Diagnostic assessments

Two test spots were selected for diagnostic assessments: WITS-05 was selected because it was along the vehicle wheel path and nearby pavers were damaged, while WITS-07 was chosen because it was clogged (Figure 4-104). Figure 4-105 shows the diagnostic assessments' infiltration rates. The measured bedding infiltration rates of both test spots were high: 10,200 (WITS-05) and 15,300 mm/hr (WITS-07). However, when the bedding was removed, the measured infiltration rates on the geotextile were 14,800 mm/hr for WITS-05 and 4800mm/hr for WITS-07. This suggests that the bedding measurement on WITS-07 was an overestimate – probably because of the difficulty in preventing lateral flow during the test.

(a) Dislocated pavers adjacent to WITS-05 **(b) Blocked WITS-07**

Figure 4-104: The state of WITS-05 and WITS-07 PICP surfaces

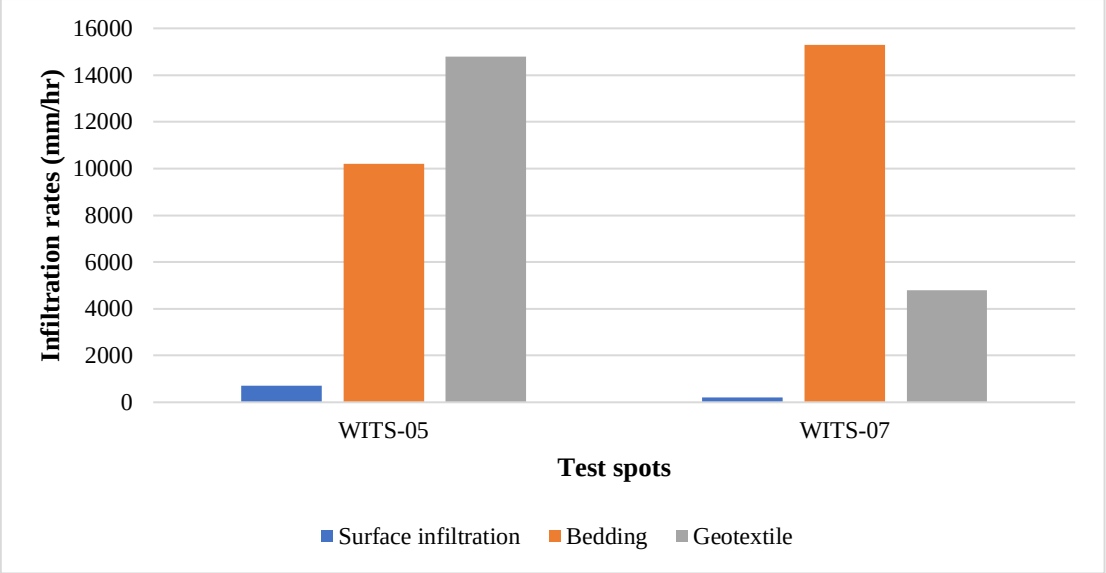

Figure 4-105: Mod-ASTM infiltration diagnostic tests

(a) WITS-05 sediment outline **(b) WITS-05 organic matter** **(c) WITS-05 geotextile**

(d) WITS-07 sediment outline **(e) WITS-07 joint material** **(f) WITS-07 geotextile**

Figure 4-106: WITS diagnostic testing observations

Figure 4-106 show different colours for the sediment outlines on the bedding indicating that they come from different sources – dark for WITS-05 and a different colour but similar to the one on the adjacent slope for WITS-07 suggesting that material was transported from the slope. The paver joints at WITS-05 were filled with organic matter while at WITS-07 were filled with a mix of sediment and grit. The WITS-05 geotextile was damaged – likely caused by vehicle braking as it was located near the entrance to WITS-U. On the other hand, the geotextile for WITS-07 – situated in a parking bay – appeared intact. In both sites, the sediment deposited on the bedding layer showed the pattern of the pavers which is typical of Type II clogging. The relatively high infiltration rates measured through the bedding and geotextile infiltration suggest that little sediment has been transported further into the PICP layers.

4.15 Bosun Brick Pavers (BBP) permeable pavement section

Bosun Brick Pavers (BBP) is a paving brick manufacturer situated in Midrand at the corner of Musket and Cresset Roads at an altitude of 1580 m a.m.s.l. (26° 2'24.09"S, 28° 9'40.71"E). (Figure 4-107). The PICP was installed in 2019 and is on a roadway that carries heavy-duty loading trucks and special construction plant such as front-end loaders.

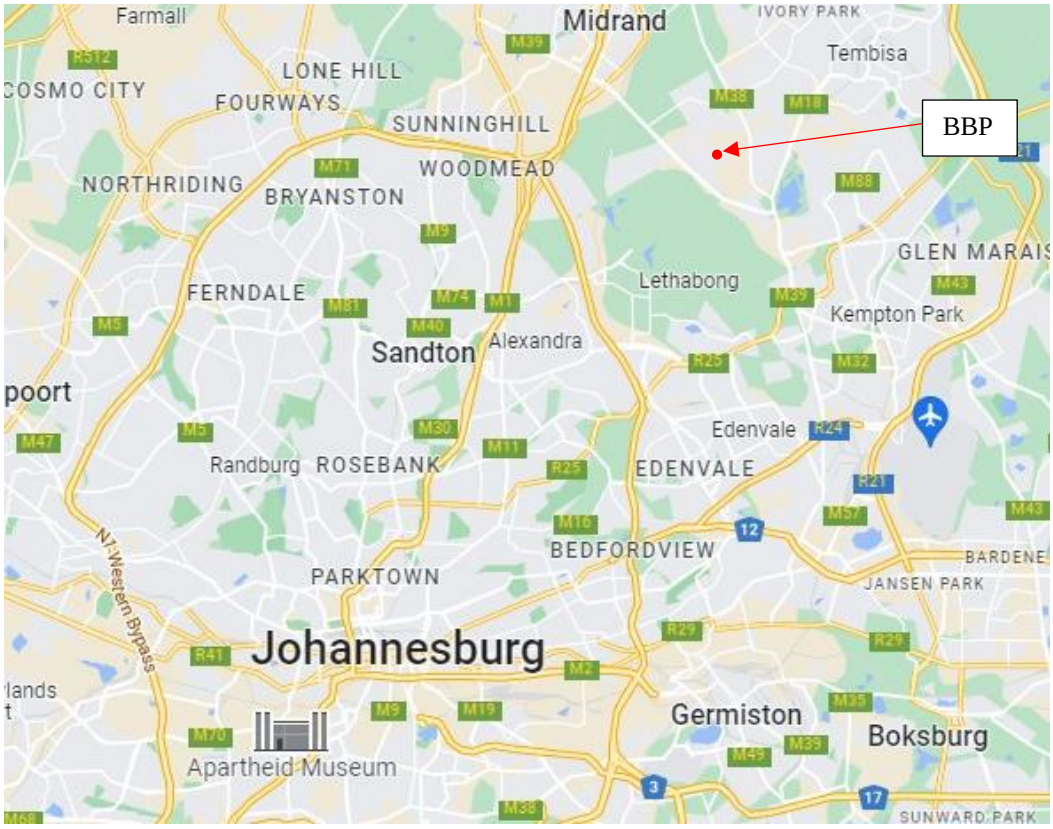

Figure 4-107: BBP locality map (Map source: Google Maps, 2022)

Stockpiles of small aggregates and crusher dust lie on the western side of the PICP and pose a threat from dust generated, blown, and/or drained onto the PICP. A ‘V’-drain concrete channel

directs surplus runoff through the site (Figure 4-108). An emergency overflow has also been installed within the pavement. Stacks of pavers are laid on impermeable concrete platforms in the north and south of the PICP section.

Figure 4-108: Bosun PICP site layout (Map source: Google Earth Pro, 2022)

As the permeable pavement area is 40 m^2 and the concrete impermeable draining to it is 120 m^2, the RoF is 3. The pavement cross-section consists of 100 mm thick Buffalo ® pavers (Figure 4-109), 6 mm joint gritstone, a 100 mm deep x 6 mm clean stone bedding, and a geomembrane between the bedding and subgrade. Figure 4-110 shows that the PICP was covered in a thick layer of fine material at the time of inspection.

Figure 4-109: The Buffalo ® permeable paver

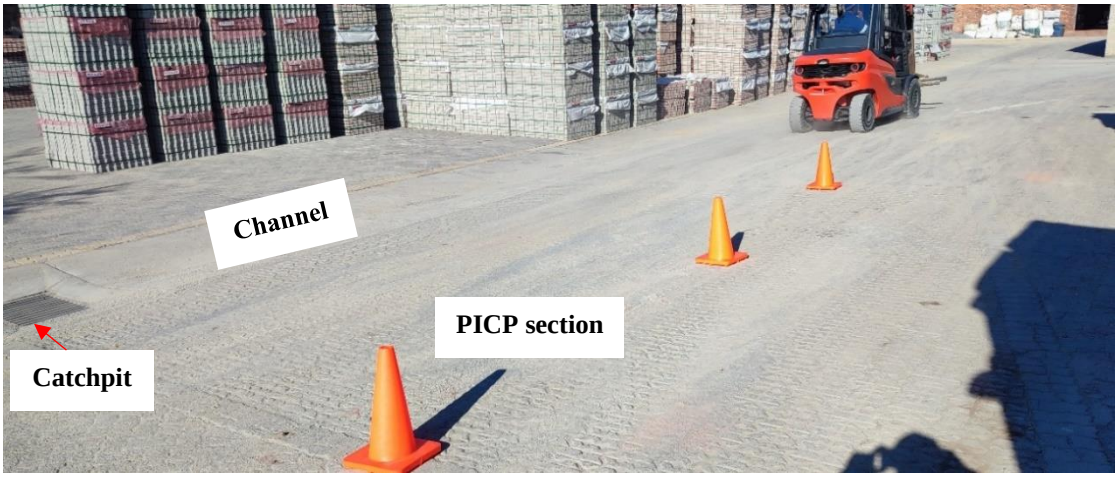

Figure 4-110: BBP PICP section

Since it was impossible to conduct reliable Mod-ASTM tests due to excessive lateral flow, the Mod-SWIFT test was used on four test spots selected for investigation (Figure 4-111). The measured infiltration rates ranged from 800 to 1400 mm/hr (Figure 4-112.). Despite the thick layer of sediment covering the PICP, the measured infiltration rates suggested that it was still working to some extent. However, it is likely that the surface of the PICP would be quickly blocked.

Figure 4-111: BBP PICP test spots locations

The PICP has not been maintained since its installation. An attempt to perform diagnostic tests was abandoned when the equipment at the disposal was inadequate to lift pavers.

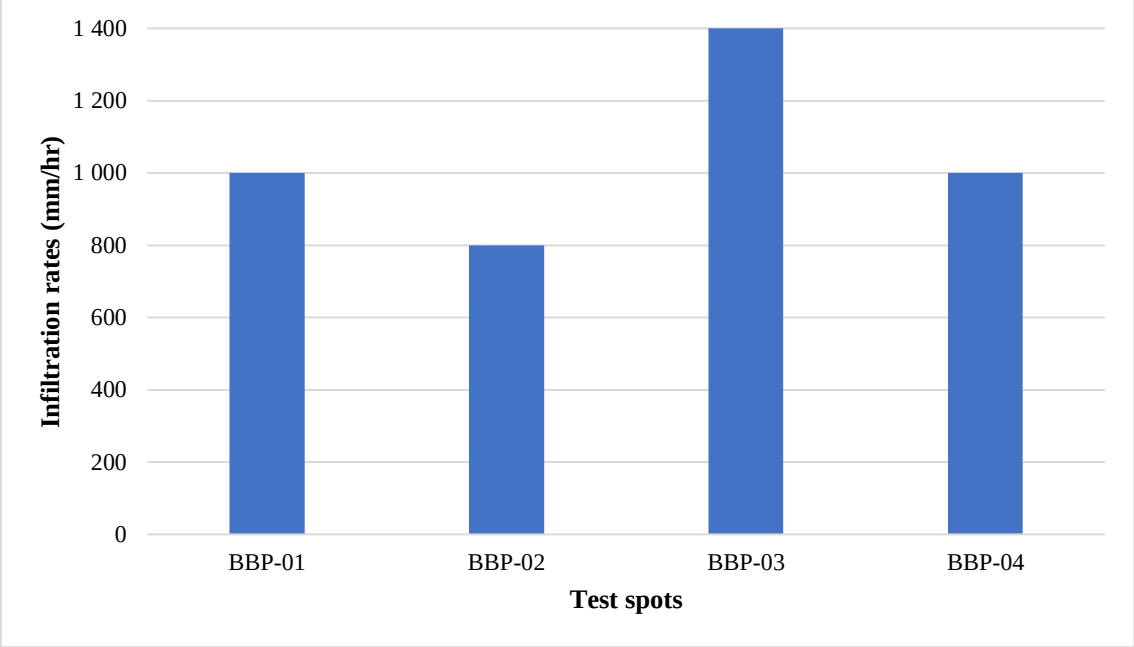

Figure 4-112: BBP Mod-SWIFT infiltration tests

4.16 Summary

This section investigated eleven PICP sites in Cape Town and Johannesburg. Maintenance trials were carried out on six of the sites and diagnostic assessments on seven. There was evidence of poor site design conditions; *inter alia* exposure to loose sediment and excessive pollen and leaf drop from nearby vegetation, as well as a lack of maintenance in many of the installations which likely lead to premature failure of the pavements. However, some sites are performing reasonably well even without maintenance. While air-blowing proved reasonably successful in rejuvenating many of the PICP surface infiltration rates, an attempt to use an industrial vacuum cleaner to improve the surface infiltration rate of PICP by sucking out the material caught in the paver joints was unsuccessful. Areas of PICP subject to continual vehicle braking and turning appeared to be deteriorating much faster than elsewhere with the puncturing of the upper geotextiles a particular problem.

5. Accelerated laboratory tests

5.1 Overview

Clogging is a common failure mechanism in PICP. All sorts of particles including cigarette butts, twigs, leaves, sand etc., collect in the joints between the pavers. Fine particles, typically passing an ASTM No. 16 (1.180 mm openings) sieve, may travel further into the underlying layers to accumulate on or in the bedding, on any geotextile that may be present, and ultimately into the base layers if they happen to pass the geotextiles. Ultimately, this will cause clogging of the PICP and its eventual hydraulic failure (Pezzaniti *et al*., 2009; Biggs, 2016). This outlines the findings of accelerated laboratory experiments carried out under controlled conditions to investigate: (i) Clogging in the upper geotextile (with pavers), (ii) The relationship between paver joint opening and clogging, and (iii) Clogging in the upper geotextile (without pavers). Table 5-1 presents the summary of the accelerated laboratory tests.

Table 5-1: Summary of the accelerated laboratory tests materials

Experiment run	Cell	Pavement type	Geotextile type	Name of geotextile
Experiment (1), first run	A	Aquaflow ®	No geotextile	Control
	B		Non-woven heat treated	Fibretex F25 ®
	C		Non-woven non-heat treated	Kaytech Bidim A1 ®
	D		Non-heat treated woven	Kaytech Kaytape S120 ®
Experiment (1), second run	A	Permaflow ®	No geotextile	Control
	B		Non-woven heat treated	Fibretex F25 ®
	C		Non-woven non-heat treated	Kaytech Bidim A1 ®
	D		Non-heat treated woven	Kaytech Kaytape S120 ®
Experiment (2)	A	Aquapave ®	Non-woven non-heat treated	Kaytech Bidim A1 ®
	B	Aquaflow ®		
	C	Permaflow ®		
	D	Permealock ®		
Experiment (3)	A	Not applicable	No geotextile	Control
	B		Non-woven heat treated	Fibretex F25 ®
	C		Non-woven non-heat treated	Kaytech Bidim A1 ®
	D		Non-heat treated woven	Kaytech Kaytape S120 ®

5.2 Clogging in the upper geotextile (with pavers)

This section covers the results of the two series of experiments that were conducted to investigate clogging in different geotextiles. In the first experimental run, Blackshaw (2021) used Permaflow ® pavers, while in the second experimental run, Peyi (2021) used Aquaflow

® pavers. The main difference between the pavers was the paver joint openings as shown in Figure 5-1.

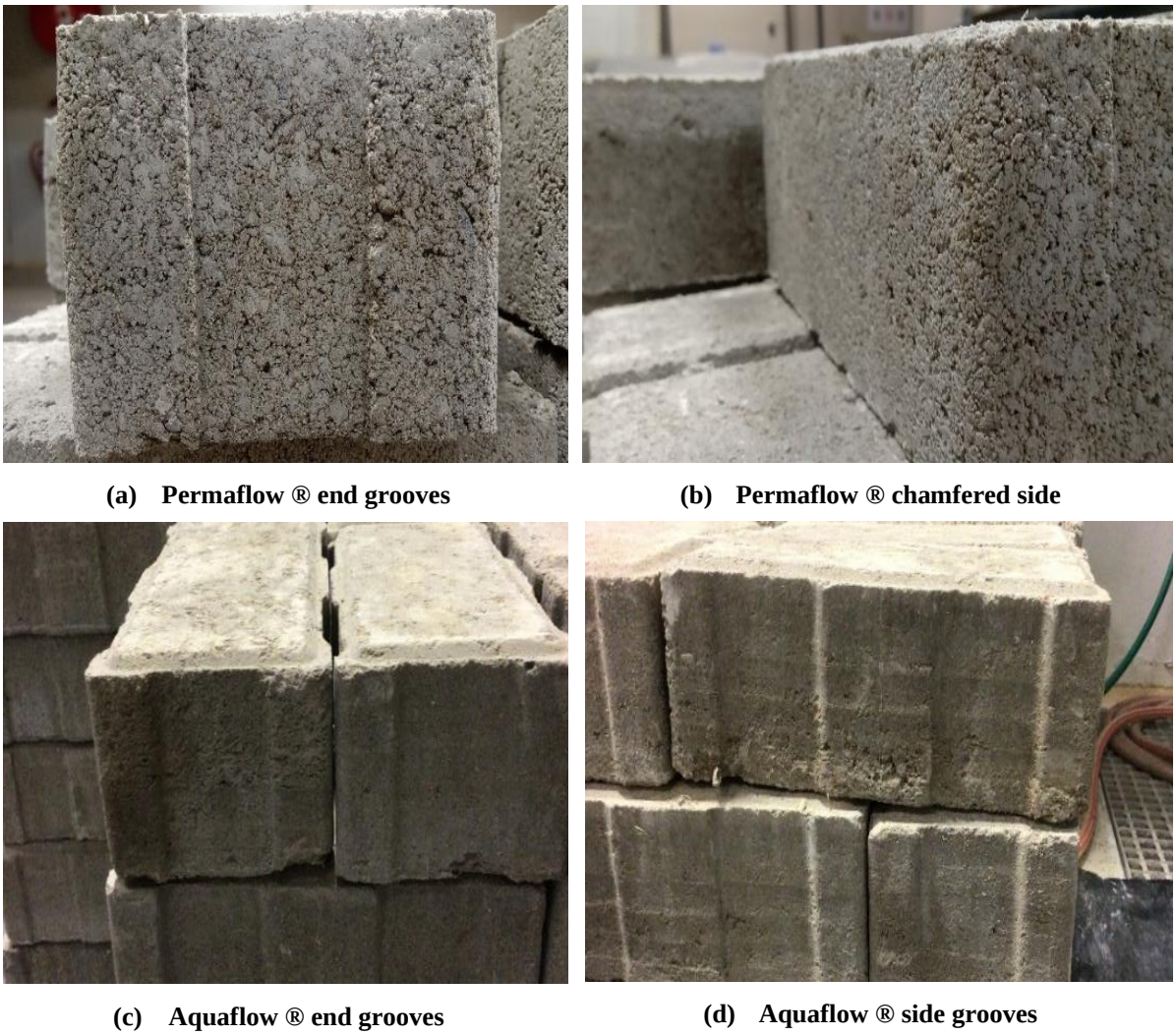

(a) Permaflow ® end grooves **(b) Permaflow ® chamfered side**

(c) Aquaflow ® end grooves **(d) Aquaflow ® side grooves**

Figure 5-1: Pavers used for the accelerated geotextile clogging tests

5.2.1 Experimental setup

The experiments were carried out in four 1.1 m wide, 1.2 m long, and 0.8 m deep HDPE rectangular PICP test bins set up in the Civil Engineering Laboratory at UCT (Figure 5-2).

A typical PICP system (Figure 5-3) was constructed in each bin comprising – from bottom to top (Figure 5-4) i.e., the order of construction:

Figure 5-2: Experimental cells used for the accelerated tests

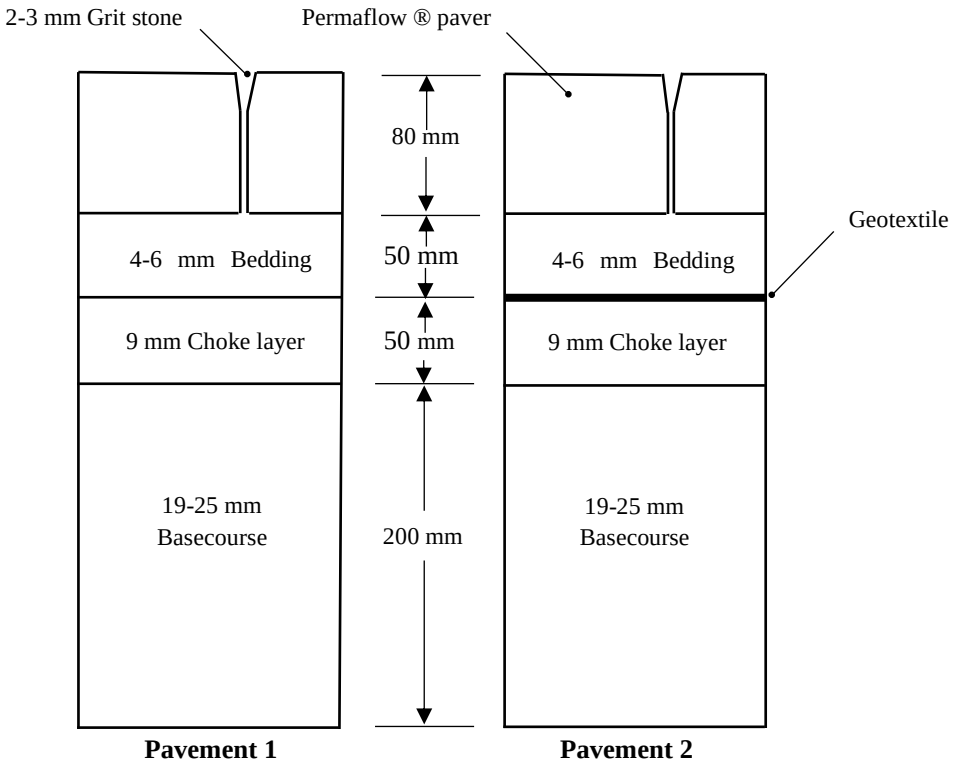

Figure 5-3: PICP cross-section used for accelerated tests (After Blackshaw, 2021)

- A 200 mm deep basecourse layer of 19-25 mm crushed stone aggregate placed on the floor of each cell. The aggregate was constructed in 100 mm layers which were compacted by hand.

(a) Laying the basecourse

(b) Hand compacting the basecourse

(c) 100 mm deep compacted layer

(d) 200 mm deep compacted layer

Figure 5-4: Construction of the basecourse layers in the experimental cells

- A 50 mm deep ‘choke’ layer of 9 mm Standard Hornfels aggregate (to prevent migration of the bedding into the basecourse in the event of there not being any geotextile separator in place) was placed by hand on top of the basecourse and hand compacted in 25 mm layers.
- The geotextile – as required – was then carefully laid on the choke layer.
- A 50 mm thick bedding layer of washed 4.75-6 mm aggregate was placed on the choke layer or geotextile as appropriate. It was hand-compacted in 25 mm deep layers. A spirit level was used to ensure a flat surface.
- The 80 mm pavers were then laid in a herringbone pattern on the bedding layer. Edge pavers were cut to fit snugly into the gaps between the whole pavers and the cell walls. The pavers were then bedded down using a wooden plank and mallet (Figure 5-5).
- Washed dry 2-3 mm gritstone was brushed and vibrated into the joints.

Figure 5-5: Pavers being installed in the experimental cells

All aggregates were washed using laboratory water in a hose prior to installation such that no discoloured water was evident. The bases of the cells were perforated to allow immediate drainage of the PICP systems. All water and sediment were trapped and recovered for re-use. The cells were fitted out as follows (Figure 5-6):

- Cell A – No geotextile installed (Control)
- Cell B – Fibertex F25 ® (Nonwoven, needle-punched, heat-treated)
- Cell C – Kaytech Bidim A1 ® (Nonwoven, needle-punched)
- Cell D – Kaytech Kaytape S120 ® (Woven)

(a) Fibertex F25 ® **(b) Kaytech Bidim A1 ®** **(c) Kaytech Kaytape S120 ®**

Figure 5-6: Geotextiles used for the accelerated clogging tests

5.2.2 The Permaflow ® paver experiment

This experiment was run over five weeks. Infiltration tests were carried out first thing every Monday morning. The cells were then loaded with sediment and 'washed' with synthetic rain each weekday. They were allowed to dry out over each weekend. It was hoped that this combination of wetting and drying cycles approximated what might be expected in the field. A schematic of the experimental method is presented in Figure 5-7. A more detailed description of the experiment follows:

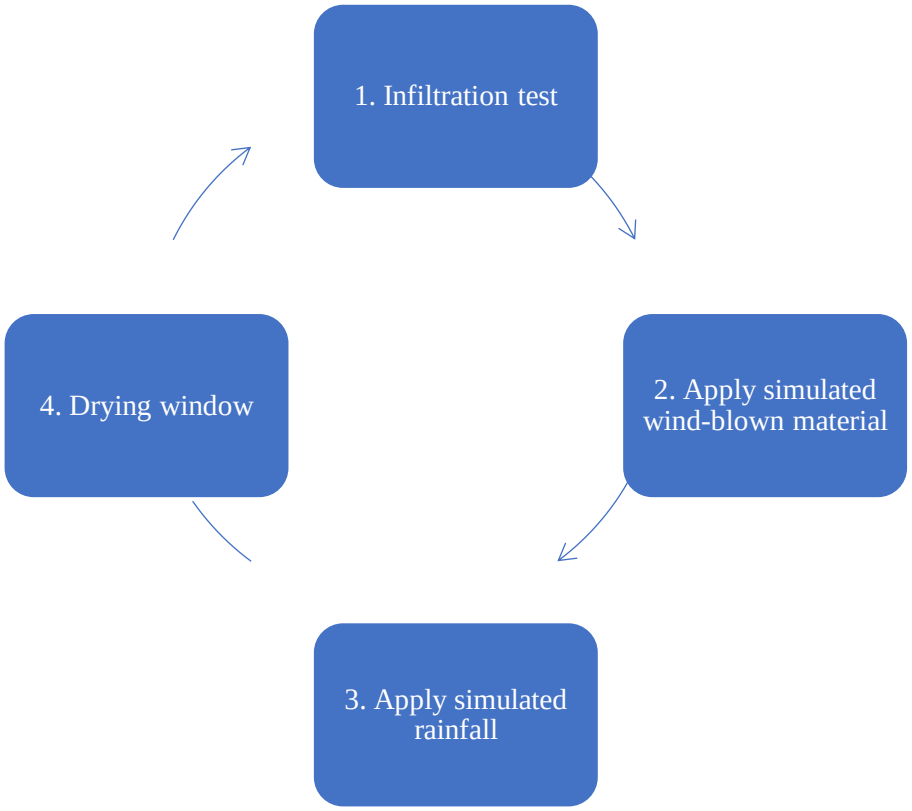

Figure 5-7: Schematic of the experimental method for the Permaflow ® paver test

1. Initial infiltration tests were carried out on Day 1 using the Mod-ASTM procedure to establish the base surface infiltration rates for the PICP cells prior to sediment loading.
2. For the first three weeks, each test cell was loaded with 100 g/m^2/week of dry granular material passing through an ASTM No. 16 (1.180 mm openings) sieve. The material was largely sourced from field fines (BRM and Steenvilla) supplemented by material having a similar grading (Unwashed aggregates sediment) (Figure 5-8). The sediment was spread by hand with the aid of the 1.180 mm sieve taking care to ensure a reasonably even distribution across the surface of each cell (Figure 5-9).

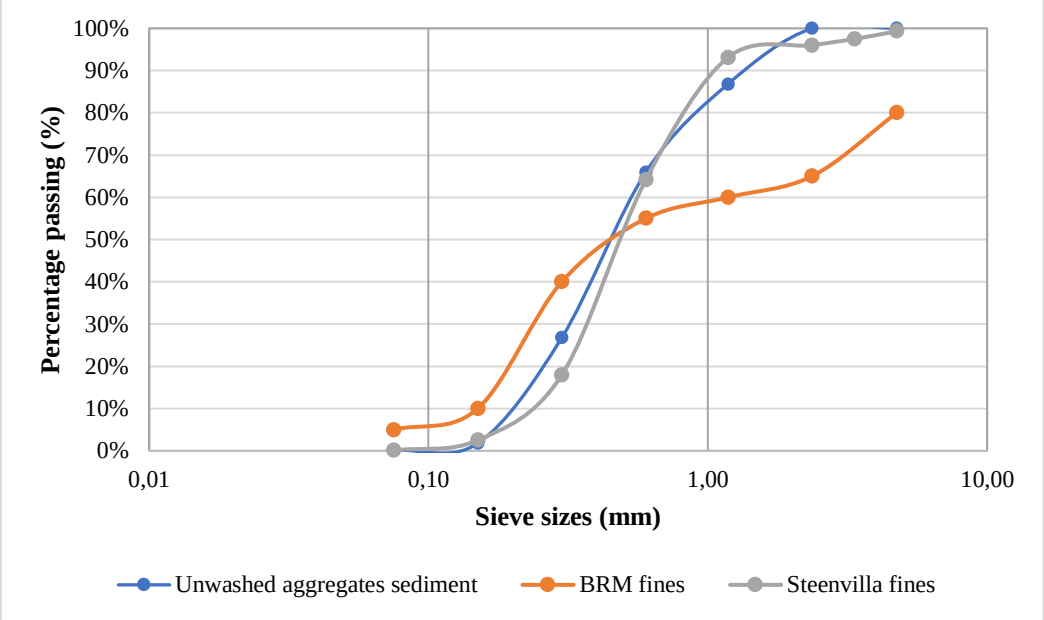

Figure 5-8: Test fines grading curves

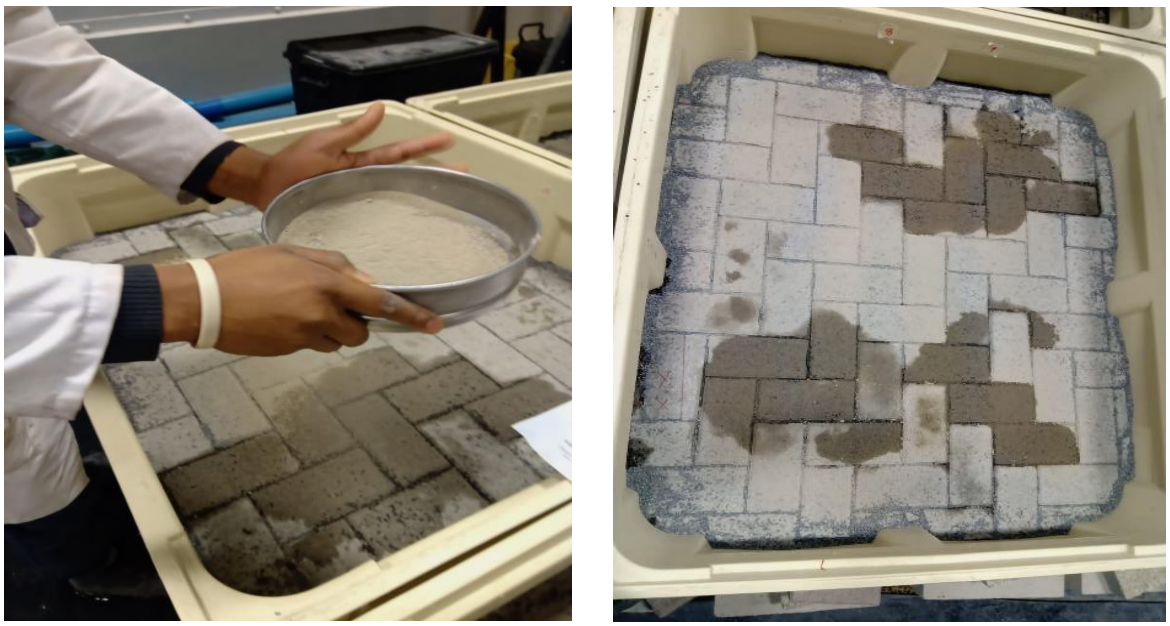

(a) Applying the sediment load **(b) Evenly distributed sediment load on cell**

Figure 5-9: Loading simulated sediment on the PICP test cells

3. Rainfall was simulated by sprinkling tap water at a rate of 100 mm/m^2/day for five days – Monday to Friday – onto the cell surfaces using a 12 litre watering can (Figure 5-10). As the plan area of each PICP cell was 1.32 m^2, the daily weekday 'rainfall' volume per cell was 132 L or eleven full watering cans. The total weekly 'rainfall' was 500 mm/m^2 – or approximately the MAP at Cape Town International Airport. The weekly 'rainfall' volume was thus 660 L per cell per week.

Figure 5-10: Application of the synthetic rainfall on the PICP test cells

4. The test cells were allowed to dry out over the two days on the weekend i.e., Saturday and Sunday.
5. Infiltration tests were performed first thing each Monday morning using the Mod-ASTM procedure apparatus before loading the fine material. The results were compared to the base infiltration rates.
6. The goal of the experiments was to have at least one cell 'fail' after five weeks (the time limit given to the undergraduate researcher as a condition of their course). Failure was defined as an infiltration rate measuring less than 250 mm/hr at which point PICP is generally regarded as fully clogged (Sehgal *et al*., 2018). As it became apparent that this was not going to be achieved at the rate infiltration rates had been dropping over the first three weeks, the sediment loading was increased to 200 g/m^2 at the beginning of Week 4.
7. As the measured infiltration rates were still relatively high at the beginning of Week 5, the sediment loading was increased to 500 g/m^2 for this last week. This brought the total sediment loading to 1000 g/m^2.
8. At the end of Week 5, the experiment was stopped with none of the test cells fully clogged.
9. The cells were then stripped layer by layer down to the top of the choke layer with each component visually examined for evidence of clogging.

Table 5-2 and Figure 5-11 show the drop in infiltration rates of the four PICP test cells after five weeks of fine sediment loading. The base infiltration rates of the test cells ranged from

Table 5-2: Drop in infiltration rates for the Permaflow ® paver experiment
(After Blackshaw, 2021)

Test cell	Geotextile	Geotextile type	Infiltration drop	R^2
Cell A	Control	No geotextile	84%	0.95
Cell B	Fibertex F25 ®	Unwoven heat-treated	94%	0.98
Cell C	Kaytech Bidim A1 ®	Unwoven non-heat-treated	85%	0.90
Cell D	Kaytech Kaytape S125 ®	Woven	92%	0.98

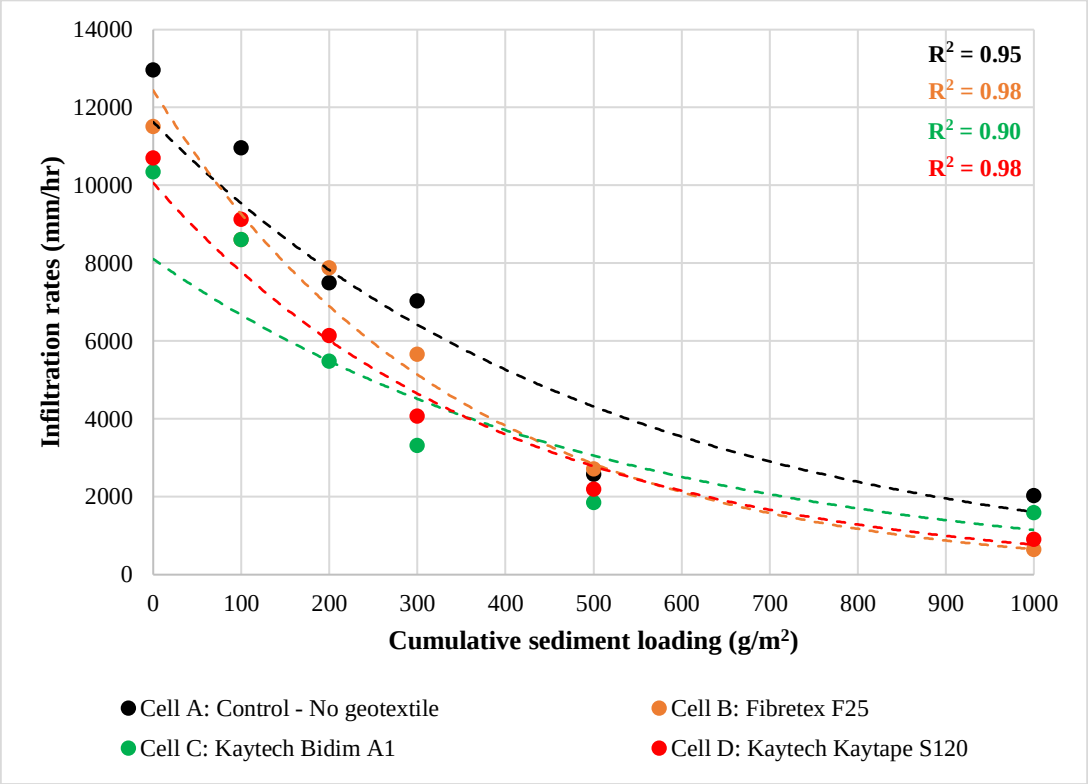

Figure 5-11: Permaflow ® sediment cumulative loading versus infiltration rates
(After Blackshaw, 2021)

13,000 and 10,300 mm/hr for Cell A (Control) and Cell C (Kaytech Bidim A1 ®) respectively. Upon commencement of the experiment, Cell A (Control) generally demonstrated the highest infiltration rates, followed by Cell B (Fibertex F25 ®), Cell C (Kaytech Bidim A1 ®), and Cell D (Kaytech Kaytape S120 ®). An exception was in Week 5, where the lowest recorded infiltration rate was for Cell B, followed by Cells D, C, and A. The drop in infiltration rates is described by exponential trend curves with high R^2 values.

None of the test cells failed in the sense of a recorded infiltration rate of less than 250 mm/hr. The lowest infiltration rate measured was in Cell B (Fibertex F25 ®) at 600 mm/hr.

Figure 5-12 (a), (b) and (c) show typical test cells sediment accumulation on the surface, between the paver joints, and on the bedding layer respectively after five weeks of experimentation. A large wedge-like sediment outline of the paver pattern was clearly visible

on the bedding. Figure 5-12 (d), (e) and (f) show the state of the three geotextiles – insignificant quantities of sediment was observed on each of them. Infiltration measurements were attempted on the geotextiles, but no definite values could be obtained as the water ran freely through all of them. It was apparent that the slowdown in infiltration rates was mainly as a consequence of Type II clogging with a small contribution from Type I clogging.

(a) Sediment accumulation in joints

(b) Sediment in joints

(c) Sediment outline on the bedding

(d) Fibertex F25 ®

(e) Kaytech Bidim A1 ®

(f) Kaytech Kaytape S120 ®

Figure 5-12: Typical sediment accumulation in the Permaflow ® pavers experiment
(After Blackshaw, 2021)

5.2.3 The Aquaflow ® paver experiment

The inconclusive outcome of the Permaflow ® paver experiment led to slight revisions in the test method:

1. The Permaflow ® pavers were replaced with Aquaflow ® pavers that had larger joint openings (Figure 5-1).
2. Vehicle loading was simulated by applying a concrete poker vibrator to a 10 mm metal base plate arbitrarily on five spots distributed over the pavers' surface for 150 s each. A rubber sheet was placed between the pavers and the base plate to prevent any damage to the pavers from the vibration of the base plate (Figure 5-13).

(a) Vibration points **(b) Vehicle simulation application**

Figure 5-13: Simulated vehicle loading application (After Peyi, 2021)

3. The sediment loading rate was increased to 100 g/m^2 per weekday (500 g/m^2 per week) from the outset.
4. The experiment was stopped when all four cells became effectively blocked (measured infiltration rate of 250 mm/hr or less) after three weeks.

As with the Permaflow ® paver tests, the base infiltration rates were all high – ranging between 15,600 and 10,200 mm/hr for Cells B (Fibretex ®) and D (Kaytape ®) respectively. Figure 5-14 presents the measured infiltration rates for the three-week accelerated tests. At this point, the values were relatively similar at 250, 200, 210, and 240 mm/hr for Cells A, B, C, and D respectively. They can all be considered as having hydraulic failure as the values were equal to or less than 250 mm/hr with losses of infiltration capacity of 98-99% (Table 5-3).

Table 5-3: Drop in infiltration rates for the Aquaflow ® paver experiment

Test cell	Geotextile	Geotextile type	Infiltration drop	R^2
Cell A	Control	No geotextile	98%	0.94
Cell B	Fibertex F25 ®	Unwoven heat-treated	99%	0.97
Cell C	Kaytech Bidim A1 ®	Unwoven non-heat-treated	98%	0.95
Cell D	Kaytech Kaytape S125 ®	Woven	98%	0.91

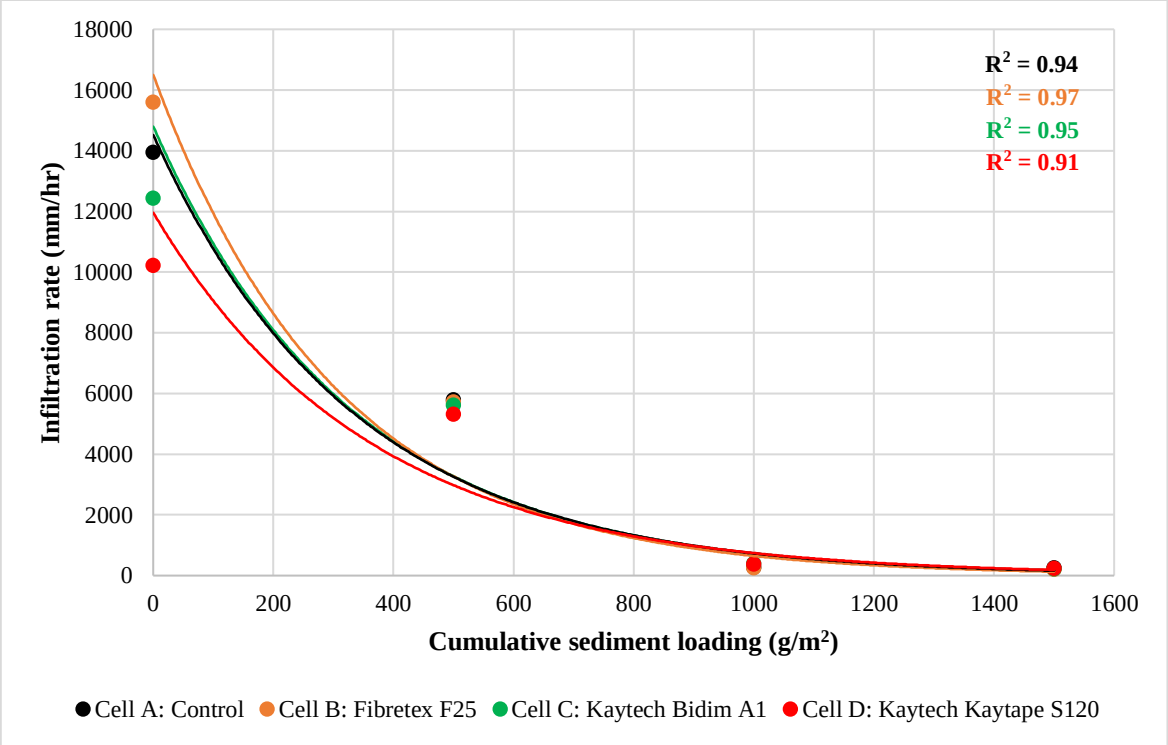

Figure 5-14: Drop in infiltration rate for the Aquaflow ® paver experiment
(After Peyi, 2021)

Figure 5-15 shows a typical view of the sediment accumulation between the Aquaflow ® paver joints after the three-week experimentation regime. Although the openings between the pavers were wider than for the Permaflow ® pavers, the sediment loading was much higher – thus, leading to clogging of the cells.

The formation of the sediment deposition in the shape of the pavers on the bedding was observed in all cases (Figure 5-16(a)). Once the bedding had been carefully removed it was immediately apparent that very little sediment had found its way down to the geotextiles (Figures 5-16(b) to (d)). The extremely high infiltration rates measured on the geotextiles confirmed that they are not blocked. The underside of the geotextiles and the top of the choke layer showed little evidence of fine sediment deposits. The drop in infiltration rates seemed largely attributable to Type I and Type II clogging caused by sediment trapped in the paver joints and the sediment wedge on the bedding.

Figure 5-15: Typical sediment accumulation between the Aquaflow ® pavers

(a) Grit & sediment outline on the bedding

(b) Fibertex F25 ®

(c) Kaytech Bidim A1 ®

(d) Kaytech Kaytape S120 ®

Figure 5-16: Aquaflow ® pavers experimental test sediment assessment
(After Peyi, 2021)

5.2.4 Comparison of the two tests

The clogging rates of the Permaflow ® and Aquaflow ® pavers are compared in Figure 5-17. The main differences between the two experiments were: the joint openings, the loading rate of the sediment, and the application of the vehicle vibration simulation for the Permaflow ® experiment. The Aquaflow ® pavers' base infiltration rates were noticeably higher than those of the Permaflow ® pavers except for Cell D. Conversely, the final infiltration for the Aquaflow ® pavers was lower than that of the Permaflow ® pavers probably owing to a high sediment loading and vehicle vibration simulations. However, as sediment was loaded onto the cells, the measured infiltration rates of the different cells converged. It appears – after correcting for the different geotextiles – the behaviour of the different cells can be most easily explained by the greater joint storage with the Permaflow ® pavers (Figures 5-17 and 5-18).

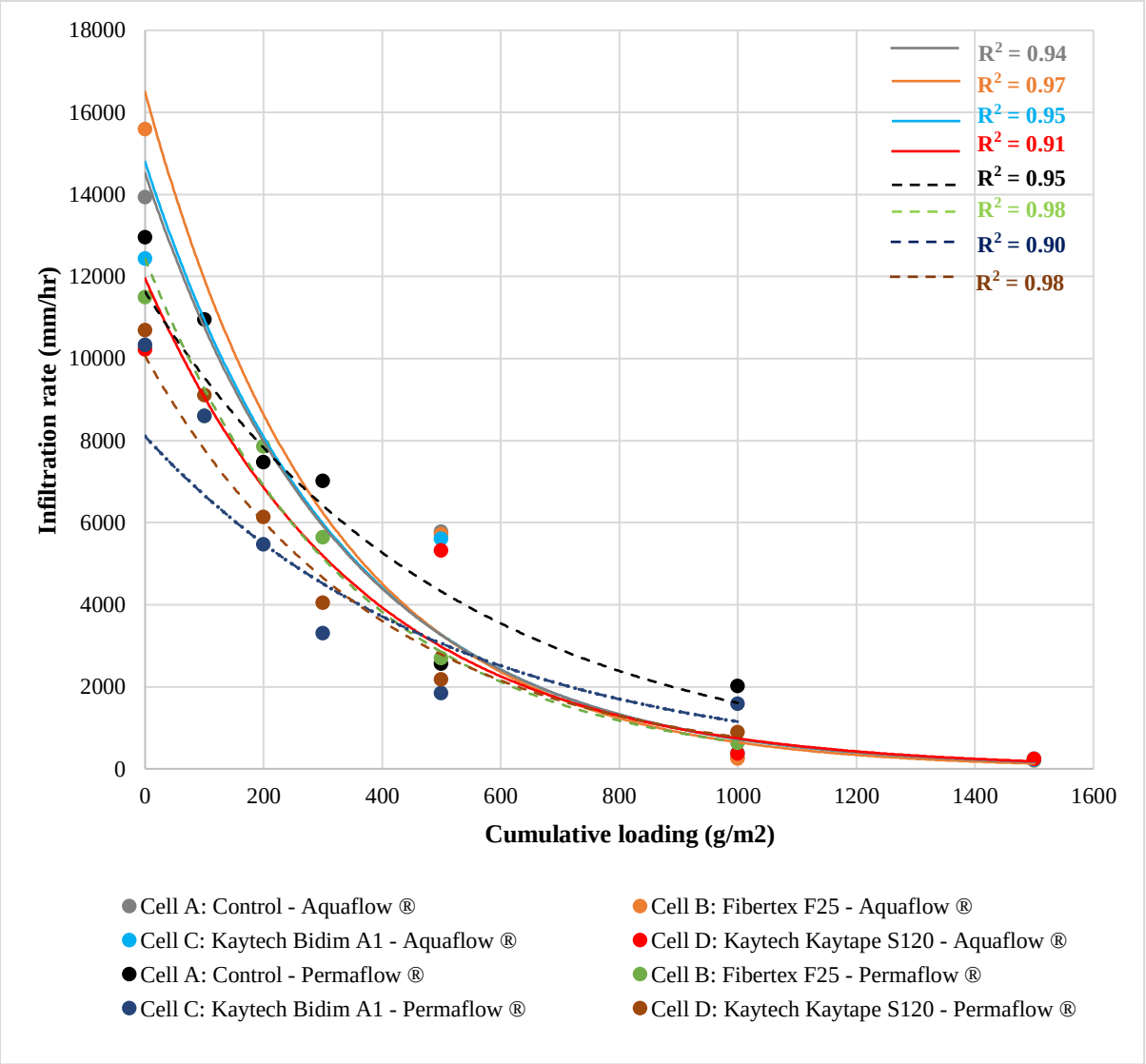

Figure 5-17: Infiltration rate versus Cumulative sediment loading for Permaflow ® and Aquaflow ® pavers (Blackshaw, 2021; Peyi, 2021)

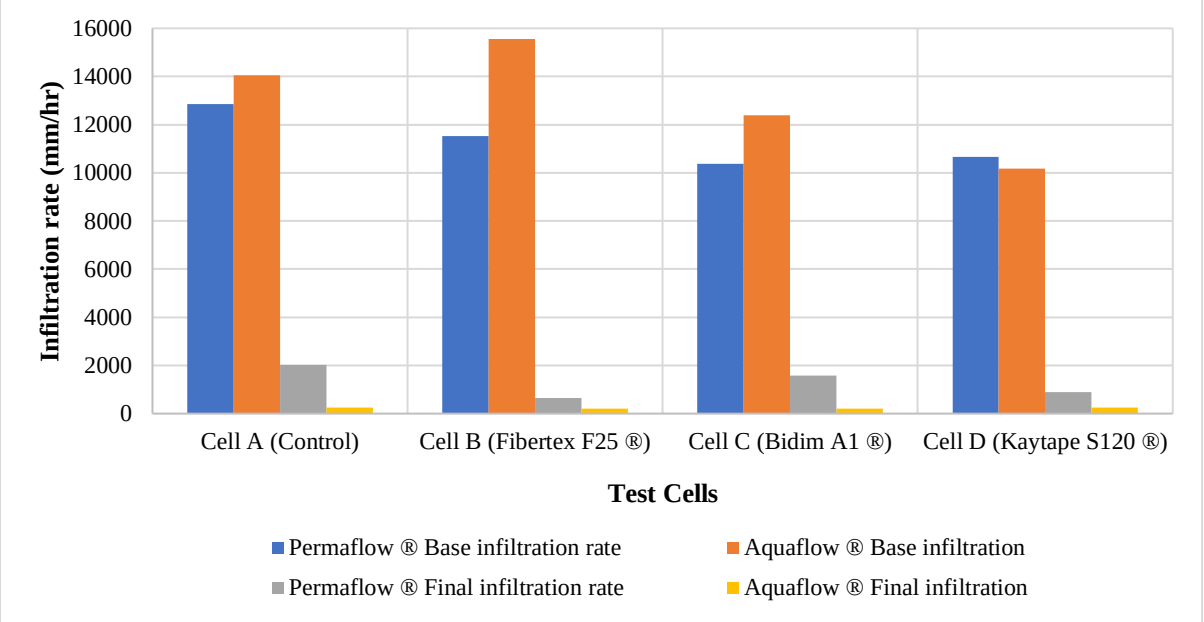

Figure 5-18: Comparison of Permaflow ® and Aquaflow ® base and final infiltration rates (Blackshaw, 2021; Peyi, 2021)

Some limitations of the two experiments include:

- The cell walls tended to bulge due to the weight of the PICP layers and the added water. This made the cutting and laying of the edge pavers challenging.
- Compaction was limited to hand methods.
- Only non-cohesive fine material was used for the sediment. There may have been a different outcome had cohesive material been used.
- Only three geotextiles were evaluated. Inbitex ® – the geotextile that was most commonly used with the older field installations was not tested owing to its lack of availability at the time of the experiments. On the other hand, Fibertex ® was identified to have similar specifications.
- The vehicle simulation may not adequately reflect what happens in the field.
- Hand watering can never accurately represent what happens in the field with variable rainfall intensities and the potential for run-on from adjacent catchments.

5.3 The relationship between joint opening and clogging

The laboratory investigations described in Section 5.2 suggested that the joint opening of the pavers play a significant role in the rate of clogging in PICP. Two mechanisms were suggested: i) a larger storage volume that potentially delays Type I clogging, and ii) greater exposure of the bedding material that potentially delays Type II but potentially promotes Type III clogging. Mqadi (2022) thus reconfigured the four test rigs to have the same aggregate layers as before (Section 5.2.1), but this time each cell was equipped with a non-woven, non-heat-treated

Kaytech Bidim A1 ® geotextile between the bedding layer and the choke layer, and – most significantly – each cell had a different paver (Figure 5-19):

- Cell A: Aquaflow ®
- Cell B: Aquapave ®
- Cell C: Permaflow ®
- Cell D: Permealock ®

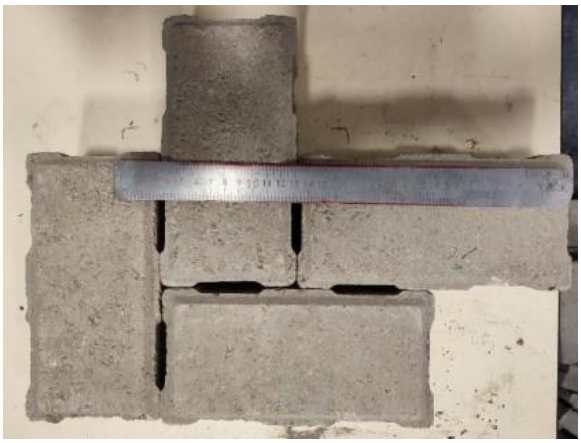

Cell A: Aquaflow ®

Cell B: Aquapave ®

Cell C: Permaflow ®

Cell D: Permealock ®

Figure 5-19: Accelerated laboratory tests different paver types

The modified experimental method involved:

1. Determining the void ratio of each paver using various methods: i) Method 1 (shading), ii) Method 2 (AutoCAD outline), and iii) Method 3 (1m × 1m AutoCAD outline). Method 1 used a blank white sheet of paper to trace the paver pattern. The pavers were laid in a herringbone pattern, the paver outlines traced and then carefully cut out with scissors. Both the paper paver outlines and the remaining joint areas were then weighed to the nearest 0.1 mg (Figure 5-20). Equation 5-1 was used to determine the paver void

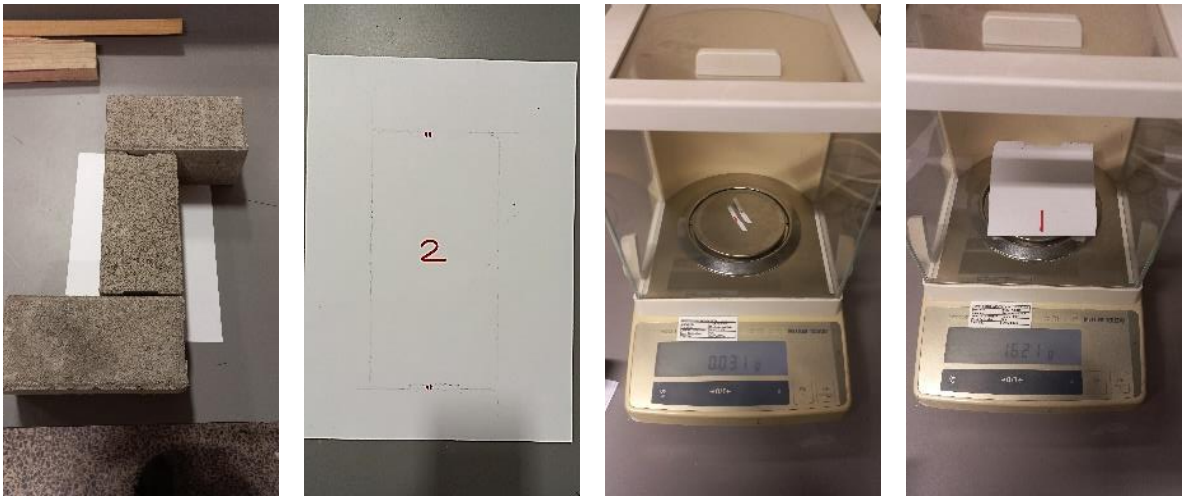

(a) Laid pavers **(b) Tracing paver** **(c) Joint pieces** **(d) Paver pieces**

Figure 5-20: Test procedure for Method 1 (Mnqadi, 2022)

ratio. The Permealock ® void ratio was not determined using Method 1 because of the difficulty of tracing its irregular shape.

$$\text{Void ratio (\%)} = \frac{\text{mass of voids cut out}}{(\text{mass of voids cut out} + \text{paver cut out})} \times 100 \qquad (5\text{-}1)$$

Method 2 involved using AutoCAD to draw an outline of a single paver captured on a photographic image (Figure 5-21). The void ratio was then determined using the area function on AutoCAD (Equation 5-2).

$$\text{Void ratio (\%)} = \frac{\text{Overall area - single paver area}}{\text{Overall area}} \times 100 \qquad (5\text{-}2)$$

Method 3 used a 1 m × 1 m wooden frame to clearly outline a portion of the paver pattern when they were laid on a flat floor surface in the laboratory. The images of the pavers were then captured at a height of approximately 2 m using a ladder with a flood light to illuminate the pavers. This helped to reduce image distortion (Figure 5-22). As with Method 2, the images were then imported into AutoCAD and the outline of the pavers marked out. Equation 5-3 was then used to determine the void ratio of the pavers.

$$\text{Void ratio (\%)} = \frac{1\ \text{m}^2 - (\text{No. of pavers} \times \text{single paver area})}{1\ \text{m}^2} \times 100 \qquad (5\text{-}3)$$

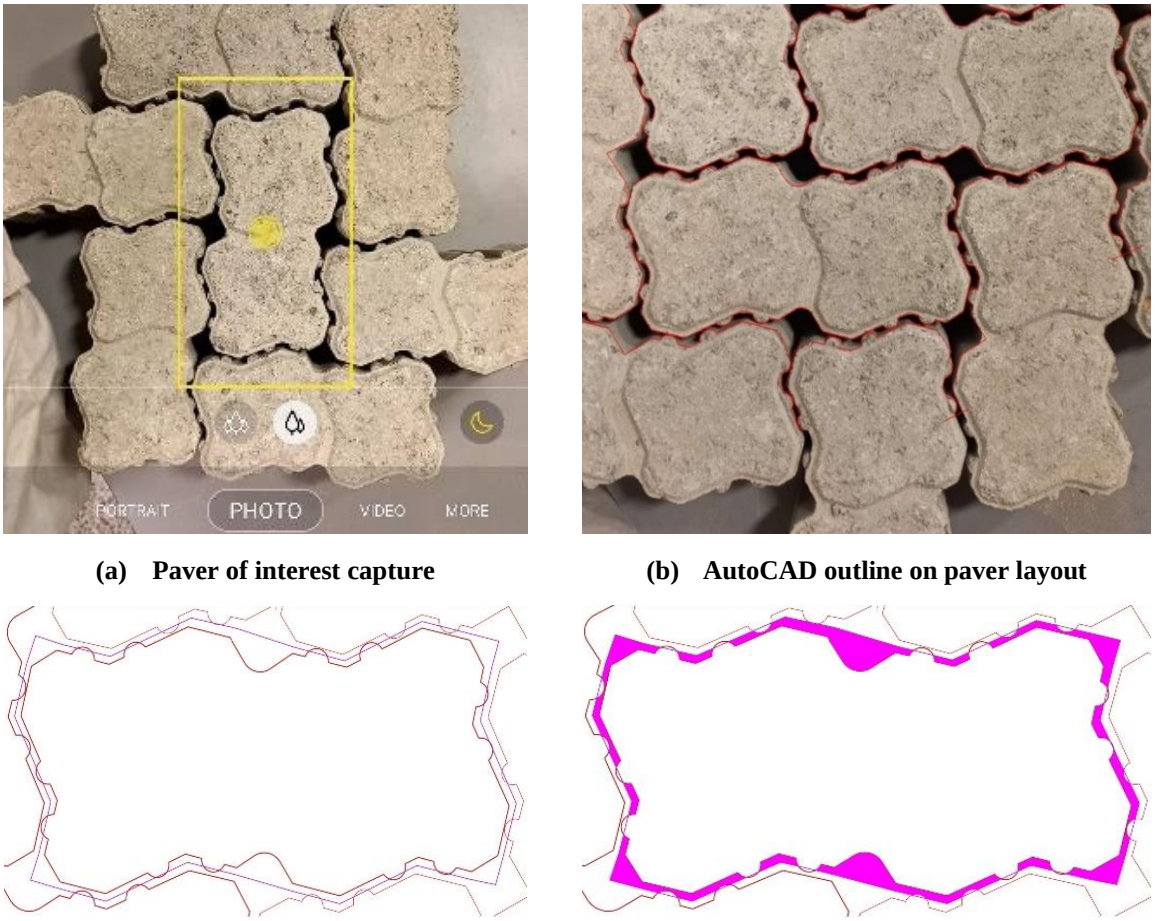

(a) Paver of interest capture **(b) AutoCAD outline on paver layout**

(c) Paver of interest outline **(d) Paver of interest hatched void area**

Figure 5-21: Test procedure for Method 2 (Mnqadi, 2022)

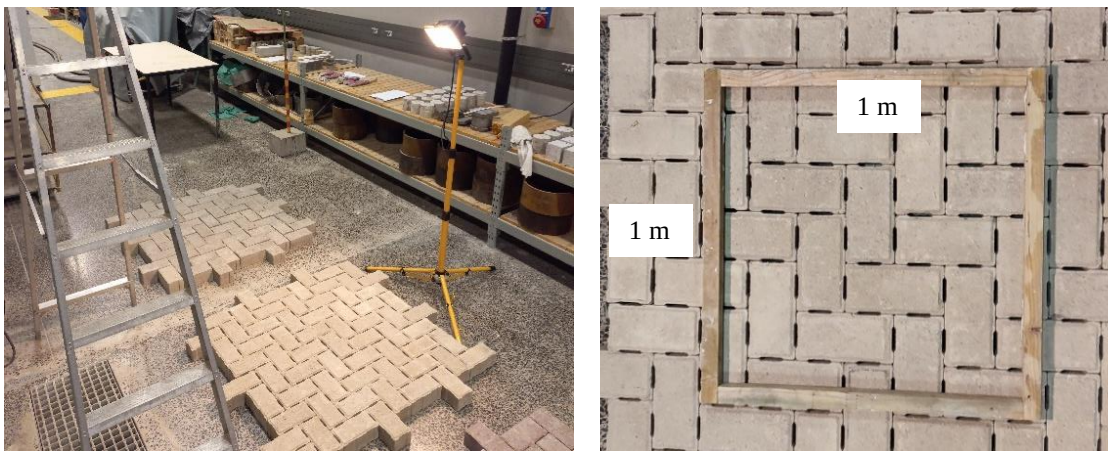

(a) Set-up **(b) 1 m x 1 m outline**

Figure 5-22: Test procedure for Method 3 (Mnqadi, 2022)

The means of the different void ratios were then determined (Table 5-4).

Table 5-4: Mean void ratio associated with different paver types (After Mqadi, 2021)

Test cell	Paver type	Method 1: Shading (%)	Method 2: AutoCAD (%)	Method 3: Square frame (%)	Mean void ratio (%)
Cell A	Aquaflow ®	4.64	4.37	5.68	4.90
Cell B	Aquapave ®	3.54	2.79	2.79	3.04
Cell C	Permaflow ®	1.76	1.16	1.23	1.39
Cell D	Permealock ®	-	8.54	8.70	8.62

2. Mod-ASTM base infiltration rates for each cell were determined on Day 1 of the experiment. In Week 1, the sediment loading was 120 g/m^2/weekday per cell. As the infiltration rates were already showing signs of surface clogging by the end of the second week, the sediment loading was decreased to 60 g/m^2/weekday per cell in Week 3.
3. The vehicle and rainfall simulations were applied in the same way as in Section 5.2.
4. After Week 3, the pavers were lifted to visually assess the clogging of the cells.
5. The measured infiltration rates versus cumulative loading with and without taking the void ratio into account are presented in Figures 5-23 and 5-24.

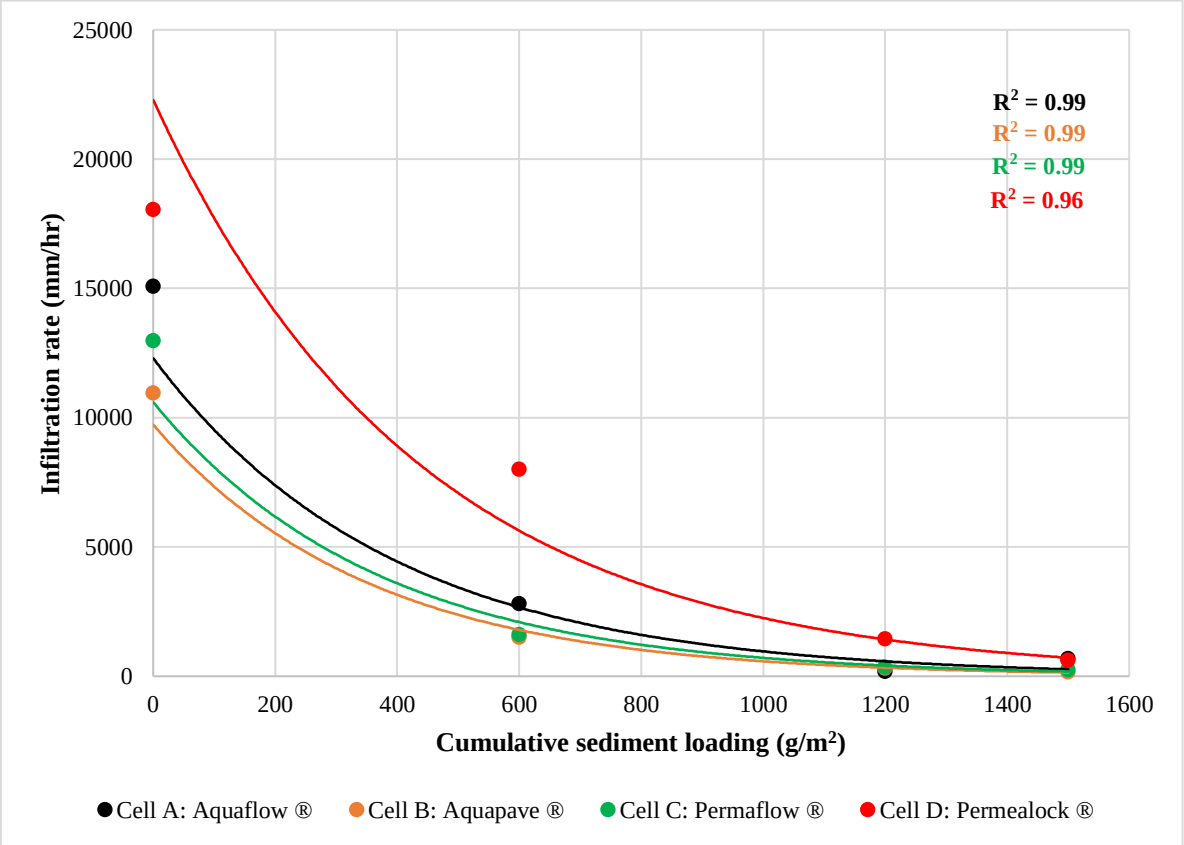

Figure 5-23: Infiltration rate versus Cumulative sediment loading for the different pavers (After Mqadi, 2022)

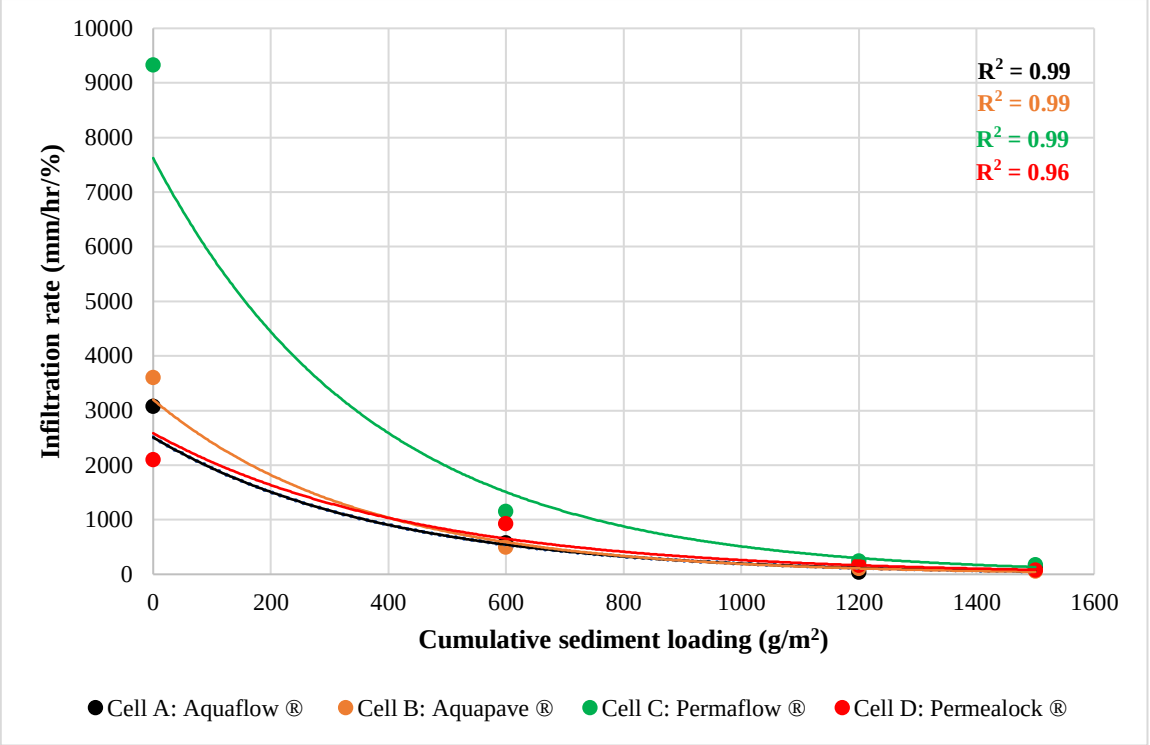

Figure 5-24: Cumulative sediment loading versus infiltration rates expressed in percentage void ratio (After Mqadi, 2022)

As with the previous experiments (Section 5.2), the surface infiltration rates of the PICP decreased with the cumulative sediment loading. As expected, the Permealock ® pavers, with the highest void ratio (8.62%), consistently supported the highest infiltration rates while Permaflow ® pavers with the lowest void ratio (1.39%) tested amongst the lowest infiltration rates. On the whole, the experiment confirmed that the rate of clogging is related to the void ratio, however, by the time 1.5 kg/m^2 of sediment had been added, all pavers seemed to be either clogged or close to it (Figure 5-23). The measured infiltration rates for Cells A and D were relatively comparable: 670 mm/hr for the former and 620 mm/hr for the latter. Similarly, Cells B and D infiltration rates were not significantly different – 160 mm/hr and 240 mm/hr respectively, and they were both practically clogged.

To highlight the importance of void ratio in the rate of clogging, the measured infiltration rates were divided by the void ratio in percent (Figure 5-24). However, this unexpectedly showed the Permaflow ® pavers, with the lowest void ratio, outperforming the others that more or less followed the same trend. It is likely that this was because the small void ratio prevented large sediment content into the joints.

Figure 5-25 shows the sediment pattern on the bedding once the pavers had been removed – clearly indicating Type II clogging. When the bedding was removed there was little evidence of sediment on any of the four geotextiles and the measured infiltration rates suggested that they were all unblocked.

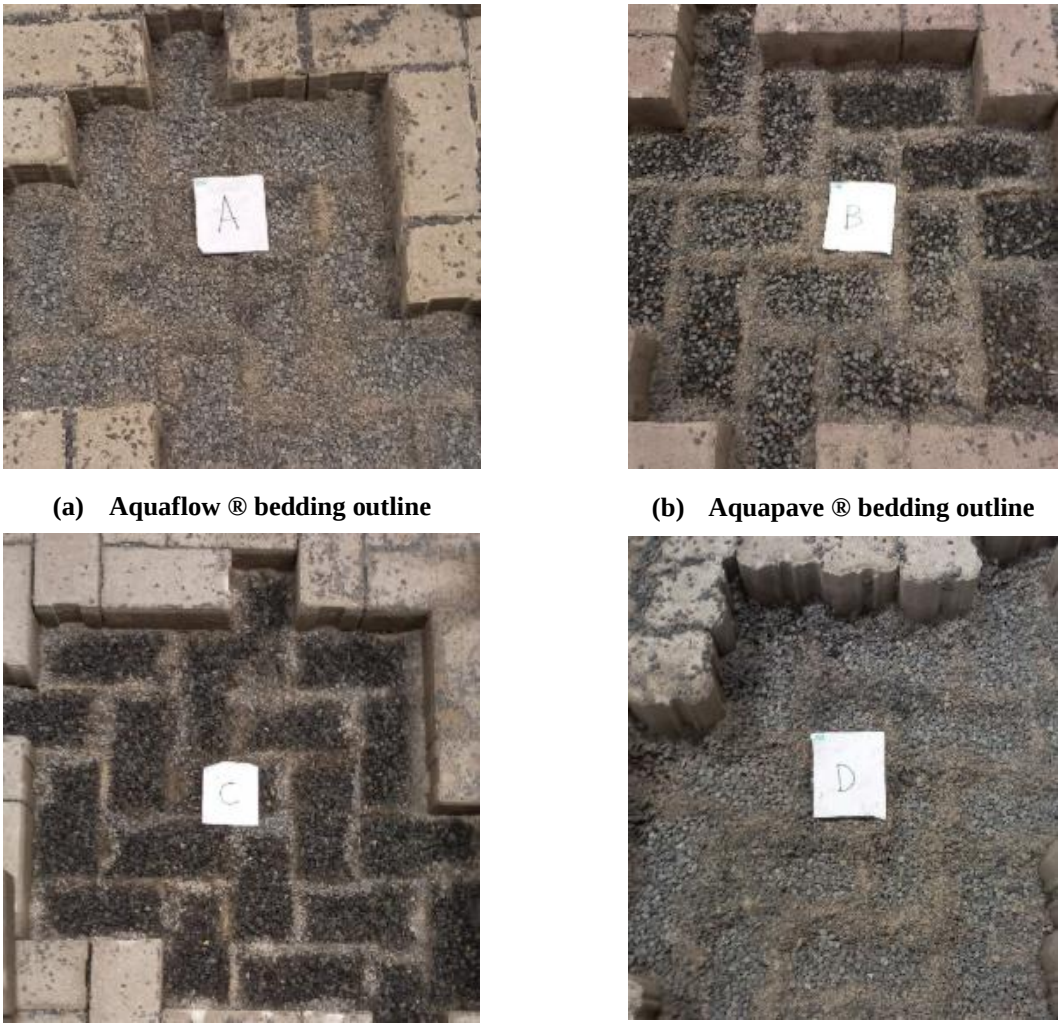

(a) Aquaflow ® bedding outline

(b) Aquapave ® bedding outline

(c) Permaflow ® bedding outline

(d) Permealock ® bedding outline

Figure 5-25: The sediment outline on the bedding of the different pavers
(Mqadi, 2022)

5.4 Clogging in the upper geotextile (without pavers)

None of the three previous accelerated laboratory tests resulted in clogging of the upper geotextile. In an attempt to identify which geotextile might be most susceptible to clogging in the field, Morritt-Smith (2022) designed an experiment without pavers to investigate upper geotextile clogging in PICP. The experimental method was as follows:

1. The experimental set-up described in Section 5.3 were dismantled to the top of the choke layer and the visible dust washed with tap water.
2. A hand compactor and spirit level were used to level the surface of the choke layer.
3. Three geotextiles were identified, cut, and fitted in three of the test cells. One test cell was left for a control set-up. The cell allocation was as follows:
    - Cell A – No geotextile (Control)
    - Cell B – Fibertex F25 ®

- Cell C – Kaytech Bidim A1 ®
- Cell D – Kaytech Kaytape S120 ®

4. A 50 mm thick x 4.75 mm washed bedding aggregate was laid and compacted to level in all the cells.
5. The sediment material that was used in the previous three tests (Sections 5.2 and 5.3) was depleted thus more material had to be sourced (Figure 5-26). Four potential sediment samples were identified, oven tried at 105 ˚C and sieved to determine their particle size distribution. These were BRM sample, Sample 1, Sample 2 and Sample 3 which comprised BRM post-maintenance joint sediment, UCT Middle Campus stockpile Batches 1 (Sample 1) and 2 (Sample 2), and laboratory crusher dust (Sample 3) respectively. Based on Figure 5-26 grading curve and material availability, Sample 3 was selected as the experiment's simulated sediment material.

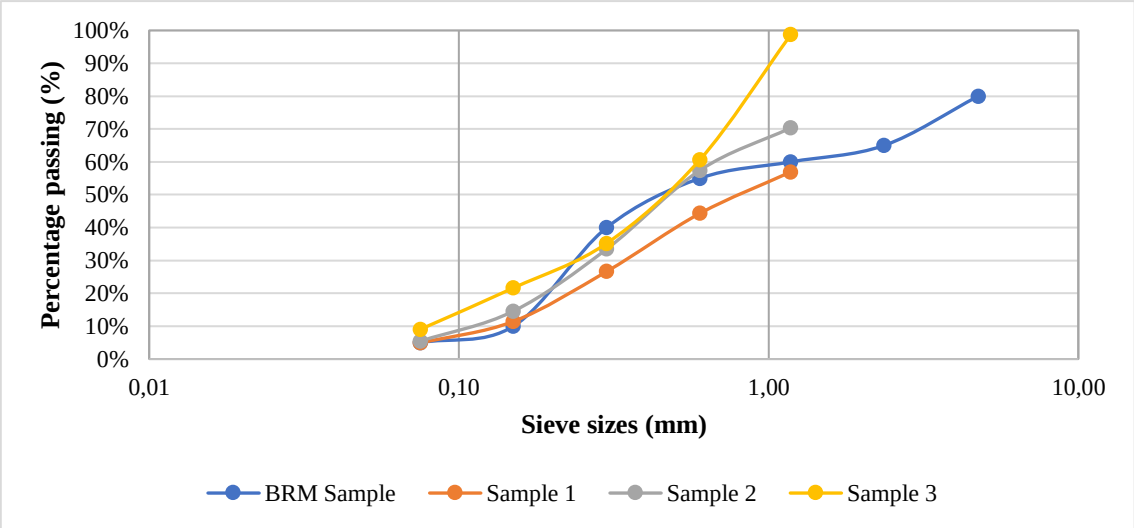

Figure 5-26: Sediment grading curve (Morritt-Smith, 2022)

6. Base infiltration tests were then conducted to establish the hydraulic performance of the cells before loading any fine sediment.
7. In the first week, each cell was evenly loaded with 200 g/m^2/weekday followed by the application of the vehicle dynamic and rainfall simulations similar to those described in Section 5.2. The drop in infiltration rate after the first two weeks was negligible therefore the sediment loading was increased to 350 g/m^2/weekday in Week 2 and 1000 g/m^2/weekday in Week 3 for each cell.
8. After three weeks, the experimental cells were carefully stripped down to the geotextile (the choke layer for Cell A) and the distribution of the sediment within the bedding layer and on the geotextile visually inspected.

9. Because none of the test cells' bedding clogged, that is, recorded an infiltration rate of or less than 250 mm/hr, it was necessary to measure the infiltration capacities of the respective geotextiles using the Mod-ASTM test apparatus. Table 5-5 illustrates permeability of the geotextiles according to their respective manufacturers.

Table 5-5: Geotextiles hydraulic properties(Kaytech, 2020; Fibertex, 2021)

Geotextile type	Pore size (µm)	50 mm head Permeability	
		m/sec	mm/hr
Fibertex F25	70 ($O_{90\%}$)	0.07	252,000
Kaytech Bidim A1	200 (O_{95W})	0.0048	172,280
Kaytech Kaytape S120	670 (O_{95W})	0.0028	10,080

10. A further inspection of the sediment trapping behaviour of the geotextiles was performed on a Scanning Electron Microscope (SEM) located on the NEB in the Electron Microscope Unit. 50 mm x 50 mm geotextile pieces were cut and placed in the SEM for analysis (Figure 5-27).

(a) Scanning Electron Microscope **(b) Geotextile pieces in the SEM**

Figure 5-27: SEM geotextile samples (Morritt-Smith, 2022)

The three-week Mod-ASTM infiltration rates of the four test cells are presented in Figure 5-28. The respective trend lines have moderate to very high correlation coefficients (R^2). The measured base infiltration rates of all the test cells were extremely high – over 40,0000mm/hr. After Week 1 loading, only the Cell D infiltration rate had decreased – and then only slightly being still above 40,000 mm/hr. This was a sign that some sediment was likely being trapped on the surface of the geotextile. Cells with geotextiles retained moisture longer.

In Week 2, Cell D recorded an infiltration rate of 29,0000 mm/hr while the other test cells' infiltration capacities were still all beyond 40,000 mm/hr although they had dropped. The control cell recorded an unexpected rise in infiltration rate which might have been a test error e.g., leakage of the test water.

By the end of the experiment, the high 1000 g/m^2/weekday sediment content had resulted in major decreases in the measured infiltration rate of all four test cells although none of the cells came close to clogging. The final infiltration of Cell D was the lowest with 9000 mm/hr, followed by Cells C and B at 12,000 mm/hr and 26,000 mm/hr respectively. The infiltration rate for Cell A – the control without a geotextile – was still above 40,000 mm/hr showing that the geotextiles were largely responsible for the decreased infiltration rates. It had been expected

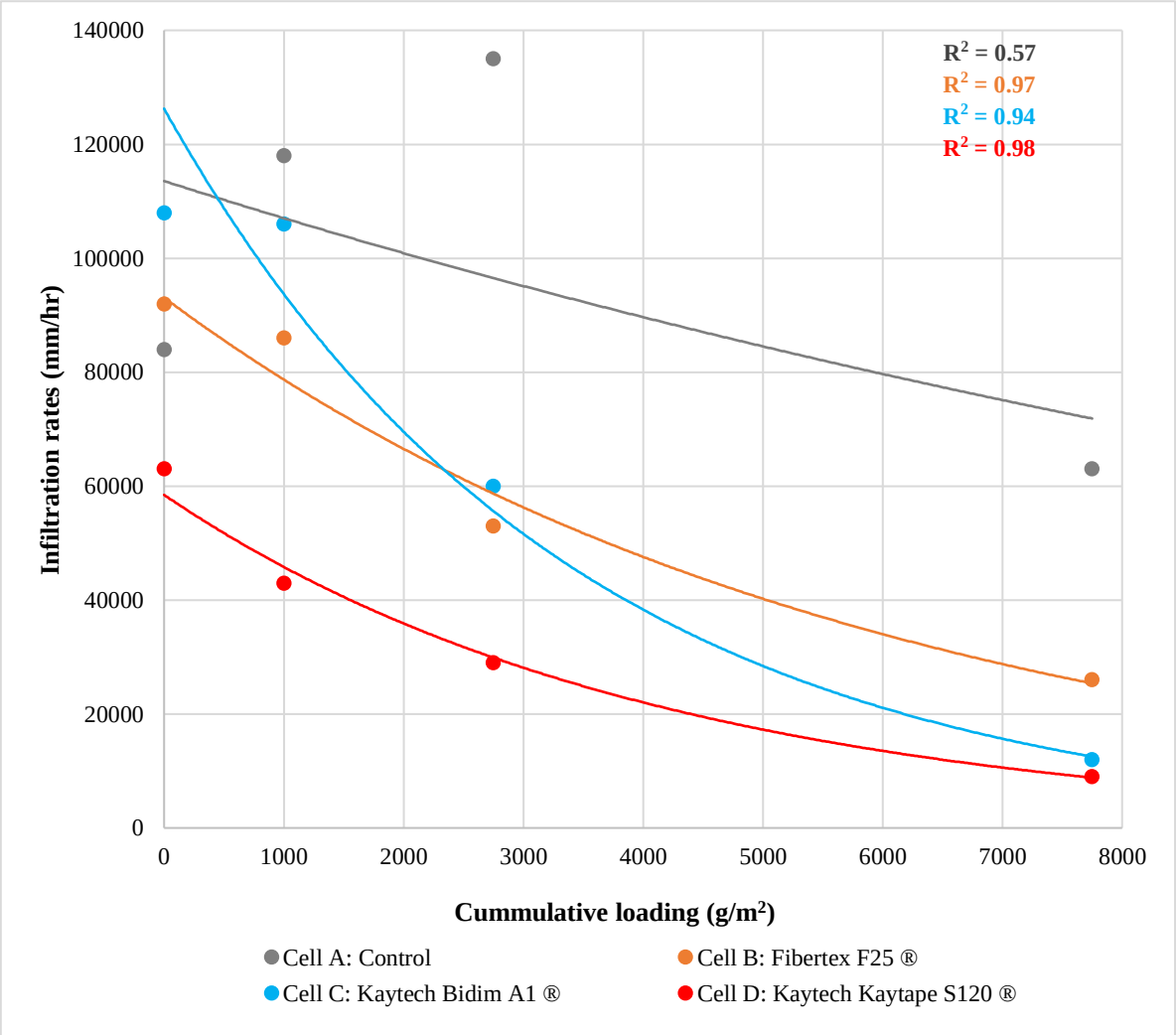

Figure 5-28: Infiltration rate versus Cumulative sediment loading for the different geotextiles (Morritt-Smith, 2022)

that the infiltration rates would correlate with aperture size, i.e., Cell D (Kaytech Kaytape S120 ®) would be lowest followed by Cells B (Fibertex F25 ®) and C (Kaytech Bidim A1 ®) however the rates for Cell C dropped much faster than the others.

The cells were stripped down to determine the distribution of sediment within the pavement layers. Cell A was investigated to the bottom of the cell while Cells B, C, and D were explored to the surface of the upper geotextile (Figures 5-29 to 5-32). The bedding in all the cells contained a substantial proportion of the simulated sediment material. Considerable fine material in Cell A – the control without a geotextile – had migrated to and accumulated on the bottom of the test cell. Conversely, the geotextiles in the other three cells appeared to help retain the sediment and the choke layer underneath them was clear of any fines. Fine material retained on the Kaytape S120 ® was in the form of a slurry. The control cell demonstrates that, in the absence of a geotextile, sediment may accumulate on the bottom of the base layers likely inhibiting infiltration with time.

(a) Bedding **(b) Bottom of the cell**

Figure 5-29: Cell A (Control) sediment distribution (Morritt-Smith, 2022)

(a) Bedding **(b) Geotextile and choke layer**

Figure 5-30: Cell B (Fibertex F25 ®) sediment distribution (Morritt-Smith, 2022)

(a) Bedding **(b) Geotextile and choke layer**

Figure 5-31: Cell C (Kaytech Bidim A1 ®) sediment distribution (Morritt-Smith, 2022)

(a) Bedding **(b) Geotextile and choke layer**

Figure 5-32: Cell D (Kaytech Kaytape S120 ®) sediment distribution
(Morritt-Smith, 2022)

There were signs that the exceptionally high Mod-ASTM bedding infiltration rates were not representative of the geotextiles' clogging, therefore the bedding was carefully removed to test directly on the geotextiles and basecourse for Cell A. Two infiltration tests were performed for each cell, one at the centre and one at the corner (Figure 5-33). This was due to concerns of a poker vibrator vehicle simulation compaction at the centre. The infiltration rates of Cell A were all high, as anticipated. The infiltration rates measured on Cell B were 13,000 mm/hr at the centre and 22,000 mm/hr at a corner. The infiltration rates on Cell C were 37,000 mm/hr (centre) and 26,000 mm/hr (corner). The lowest measured infiltration rates were for Cell D,

with 450 mm/hr at the centre (the closest to failure) and 2000 mm/hr at a corner. This confirms that the bedding layer infiltration rates were distorted by leakage, hence, they are not representative of the geotextiles' hydraulic performance.

A Scanning Electron Microscope (SEM) was further used to generate an understanding of the particle distribution on the three geotextiles (Figures 5-34 to 5-36). The images on the left represent clean geotextiles while those on the right show the situation post-experiment. Both Fibertex F25 ® and Kaytech Bidim A1 ® trapped significant quantities of sediment, however their large opening ratios accounted for the high infiltration rates presented in Figure 5-33. The smaller openings of Fibertex F25 ® (Figure 5-34) compared with the Kaytech Bidim A1 ® (Figure 5-35) on the other hand, seemed to promote the 'clumping' of sediment into larger particles. Kaytech Kaytape S120 ® (Figure 5-36) had the lowest open area of the three which explains the reason for the lowest infiltration rates in Figure 5-33.

None of the cells and/or geotextiles clogged over the limited duration of the experiment.

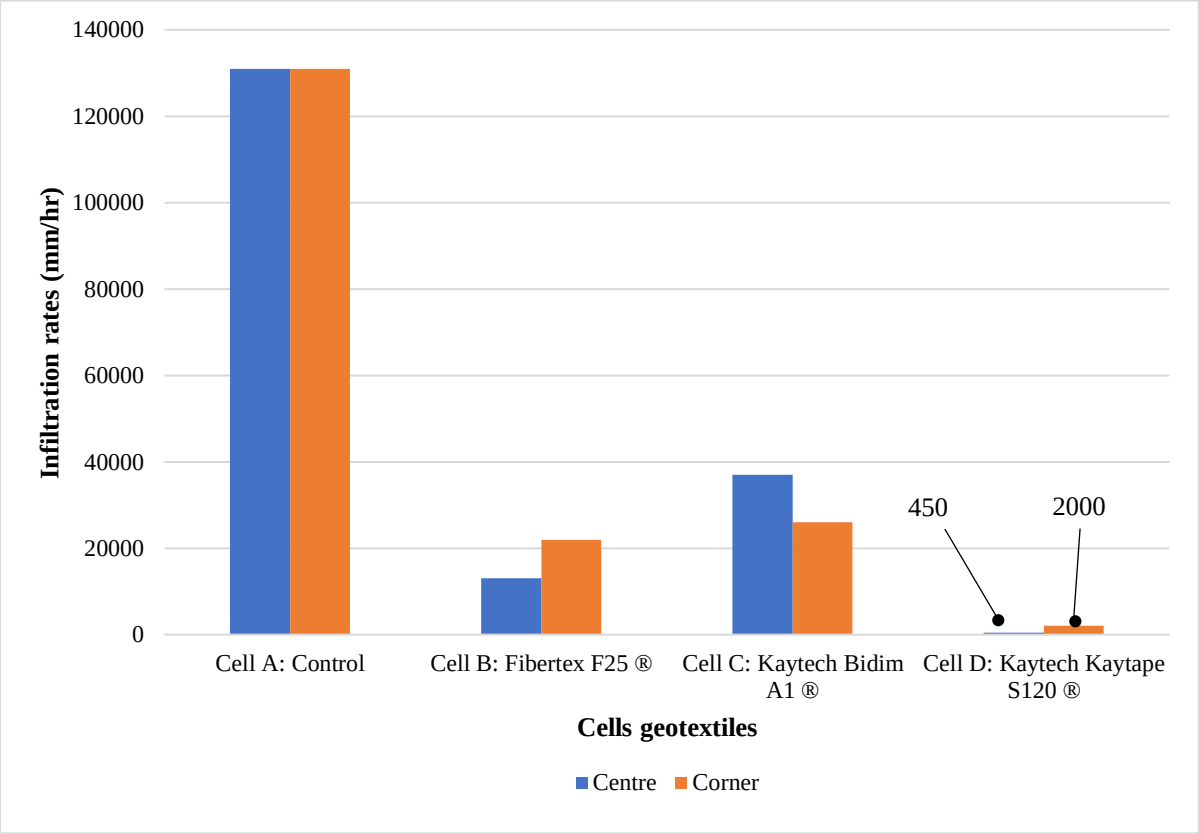

Figure 5-33: Different geotextiles infiltration rates (Morritt-Smith, 2022)

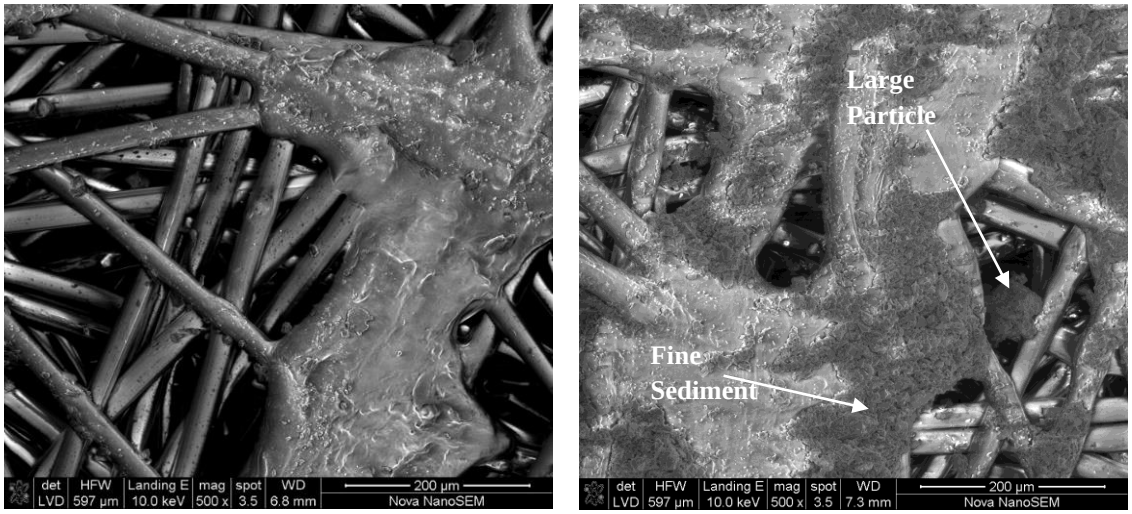

Figure 5-34: Fibertex F25 ® SEM view magnified to 500x (Morritt-Smith, 2022)

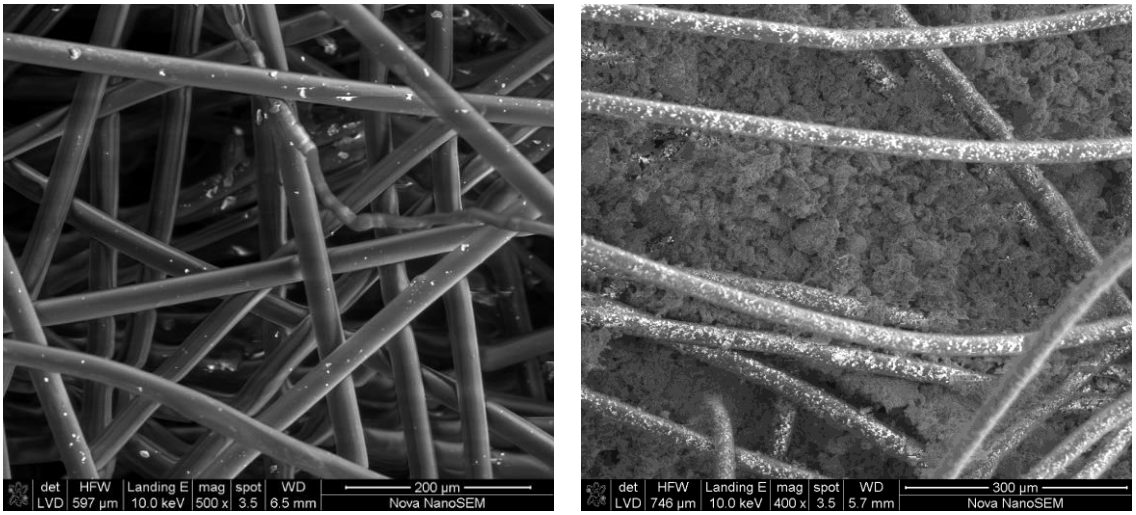

Figure 5-35: Kaytech Bidim A1 ® SEM view magnified to 500x (left) and 400x (right) (Morritt-Smith, 2022)

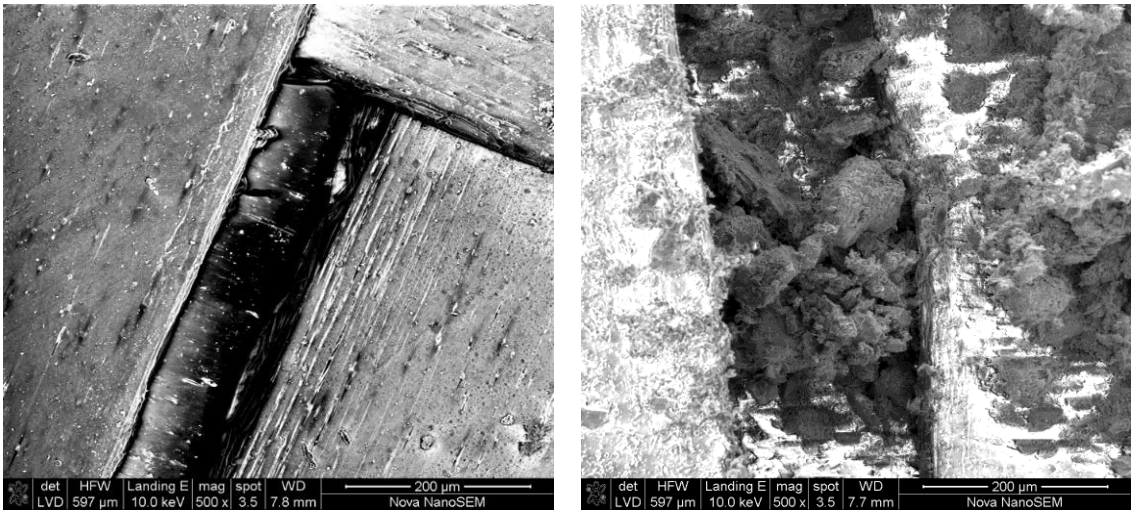

Figure 5-36: Kaytech Kaytape S120 ® SEM view magnified to 500x
(Morritt-Smith, 2022)

5.5 Summary

The base infiltration rates of the PICP cells were all high irrespective of the PICP design. The PICP surface infiltration capacity decreased with the sediment loading in all instances but the larger the joint void ratio, the longer it took for the sediment to block the surface of the PICP. The accelerated laboratory results were thus consistent with what has been reported in published research (Norderstedt *et al*., 2015; Hein & Smith, 2016) and most of the field observations in South Africa. However, it was observed that it is relatively difficult to clog PICP in the laboratory and when it does, it is almost wholly in the joint spaces of the pavers i.e., a combination of Type I and Type II clogging. On the other hand, different results may have been obtained if the sediment had a higher clay content and/or the simulated traffic loading had been more vigorous.

6. Conclusions and recommendations

6.1 Overview

The adequate design, construction, and maintenance of Permeable Interlocking Concrete Pavement (PICP) are vital in assuring its purpose viz. controlling runoff and its quality, is achieved. A key concern is clogging which is a major cause of failure. This project reviewed research carried out into clogging in eleven locations across South Africa (SA) subject to different conditions, as well as supplementary accelerated laboratory experiments used to provide additional insight into clogging mechanisms. The key finding was that the hydraulic performance of PICP is affected by various parameters. This chapter thus reviews what has been found about clogging mechanisms and how best to ameliorate clogging in PICP.

6.2 Clogging typology

As mentioned in Section 4.4, four types of PICP clogging were identified in the course of the research:

- Type I clogging – the most common type – is when fine material fills the joints, typically the first 20 to 30 mm depth from the surface.
- Type II clogging takes the form of a sediment 'wedge' on the bedding layer immediately under the joints and usually looking like a silhouette of the paving pattern.
- Type III clogging is when the bedding layer and the top of any geotextile have been filled with sediment
- Type IV clogging sees sediment throughout the full depth of the PICP layers (complete failure)

These are also in the rough order of occurrence – with Type I clogging being not only the first to take place but is also the most common by far, while Type IV clogging is the least common although it can be 'built in' during construction.

6.3 Clogging and age

All PICP surface infiltration rates start off extremely high – typically between 7000 to 20,000 mm/hr ASCE (2018), but they rapidly decrease with the age of the installation. Some sites' surface infiltration rates however drop at a faster rate than others (Borgwardt, 2015). For example, Nguyen *et al*., (2022) reported PICP still recording significant infiltration capacity (800 mm/hr) after 20 years in operation, while other sites may fail within days as a consequence of poor design, construction and/or (lack of) maintenance. The gritstone placed in the gaps between the pavers acts like a filter trapping fine particles. While this is of considerable benefit for downstream water quality, these fine particles ultimately clog the pavement (Type I

clogging), unless removed. The particles can only go in one of two directions: i) through physical removal onto the surface e.g., through air blowing and subsequent sweeping and/or vacuum removal, or ii) by being driven further into the layers where they tend to collect at the base of the openings between the pavers where they form a 'wedge-shaped' mass that inhibits infiltration (Type II clogging). Traffic movement – particularly on poorly restrained pavers that can move laterally – combined with runoff can redistribute some of the fines into the bedding layer and clog any geotextile present (Type III clogging). Ultimately, fine particles may find their way into the base layers where they fill the openings and reduce the overall porosity and permeability (Type IV clogging). All of this takes time.

Given the clear link between the clogging mechanisms and time, it would be expected that the field research would show a clear trend linking age with lower infiltration rates. Unexpectedly, this was not the case. Figure 6-1 shows very little correlation between age and measured infiltration rates for the eleven sites that date back to the Wits parking area which had been in operation for 14 years at the time of testing. This suggests that other factors are far more significant than mere age in accounting for the deterioration of PICP infiltration performance.

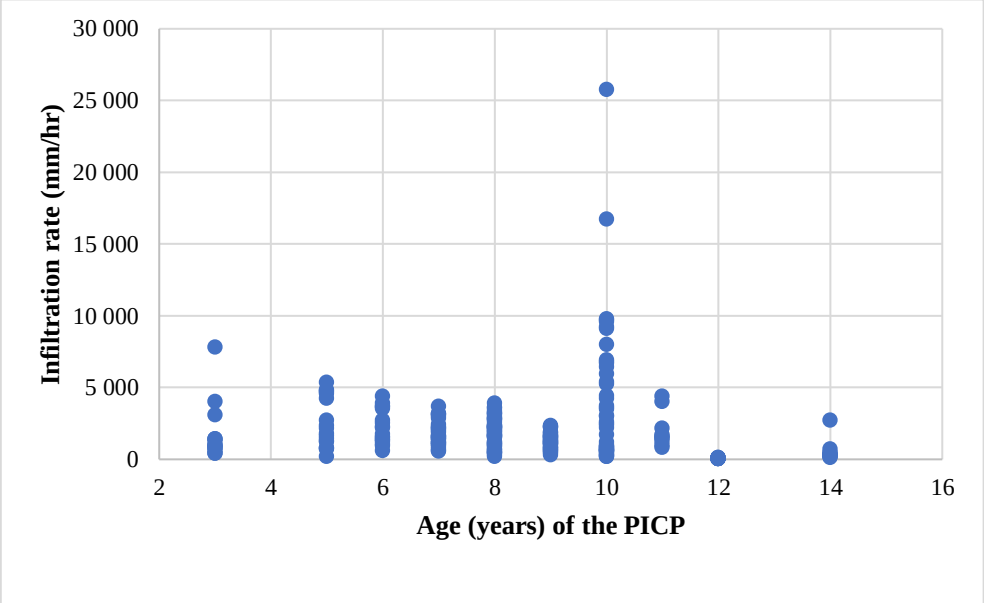

Figure 6-1: Infiltration rate versus age (years) of the PICP

6.4 Clogging and Run-on Factor (RoF)

The Run-on Factor (RoF) is the ratio of the impermeable area that drains to the PICP to the area of the PICP itself. The higher the RoF, the more the runoff volume is generated and the greater the quantity of sediment deposited on the PICP per storm. For this reason, many authorities recommend limiting the RoF – for example, a RoF of 2 (ASCE, 2018; Interpave, 2018), or 3 (Lucke & Beecham, 2011), however, much higher RoFs have been reported, e.g., 27.6 (Tirpak *et al*., 2021). Clearly, a RoF = 0 (no contribution from impermeable surfaces) is

likely to result in the best performance. Figure 6-2 presents the RoF recorded from the 11 PICP sites investigated in the course of this project – the time factor was eliminated by dividing the measured infiltration rate by the relevant pavement age. The RoF ranged from 0 to 5.8.

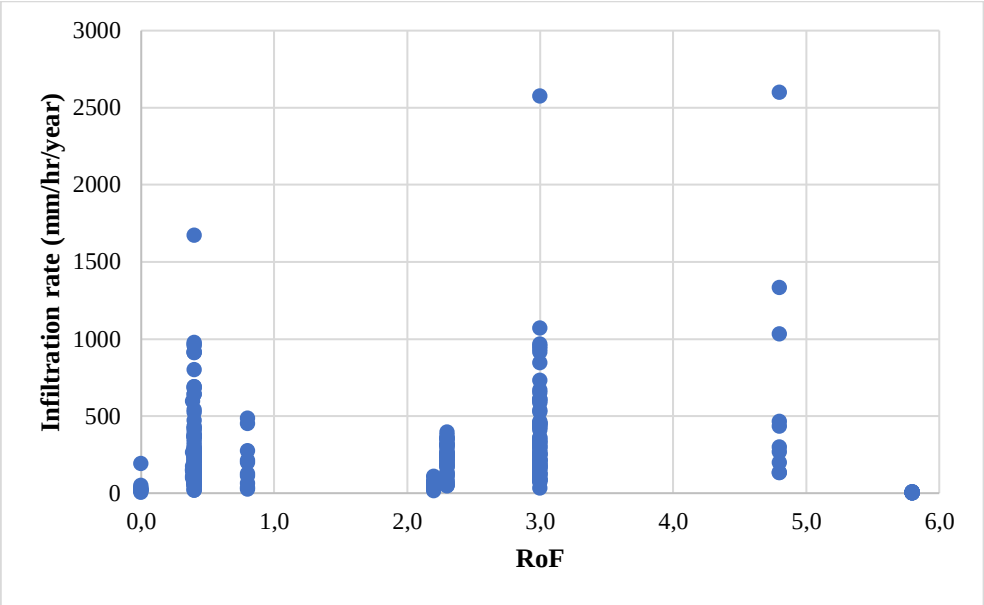

Figure 6-2: Infiltration rate versus Run-on Factor (RoF)

There is no particular pattern that was evident in the relationship between the RoF and the infiltration rates in Figure 6-2 – possibly because PICP infiltration capacity not only relies on RoF and pavement age. It was expected that the higher the RoF, the low the infiltration rates will be due to surface clogging. The lowest infiltration rate measured was 3 mm/hr/year for an RoF of 5.8 and the highest is 2600 mm/hr/year for RoFs 3 and 4.8. RoF = 0 infiltration rates ranged from 7 to 193 mm/hr/year – but the pavement was old. Thus, it can be concluded that RoF alone does not fully explain the clogging rate.

6.5 Clogging and paver type

Various paver types are available on the market. Tests carried out in the UCT laboratory (Section 5.3) showed that the rate of clogging correlates inversely with the void ratio i.e., the larger the joint openings, the slower the clogging rate.

6.6 Clogging and the upper geotextile

Geotextiles are geosynthetic fabrics that are used in pavements to separate, filter, drain, and protect the subgrade. The most commonly used upper geotextile seen in the field investigations is Inbitex ® – a heat-bonded non-woven geotextile – installed between the bedding layer and the base layer. In most instances, there was no sign of clogging. Where there was evidence of

clogging, this was associated with heavy traffic loading and movement of the pavers. Furthermore, the geotextiles that are installed in high-traffic situations, even when unblocked, were frequently found to be severely damaged even after only a relatively short period (e.g., eight years) of the PICP in operation, and thus unlikely to be fulfilling any function in the system. On the other hand, geotextiles installed in parking bays were generally intact even after more than 14 years of service.

Research carried out in the laboratory showed no evidence whatsoever of geotextiles clogging, but this may be simply because of the experimental method and/or material used.

Some instances of both clogged and punctured upper geotextiles have been reported in the literature (Pezzaniti *et al*., 2009; Lucke & Beecham, 2011a). Currently, the trend in the USA is to leave it to the discretion of the design engineer as to whether to use an upper geotextile in the design of PICP (NCDEQ, 2020). On the other hand, the practice in the UK is to install non-woven heat-treated geotextiles to improve the stormwater effluent quality (Charlesworth *et al*., 2017). This research suggests that geotextiles can be used in many instances but should be avoided in high-trafficked sections.

6.7 Clogging and environmental factors

Since clogging in PICP is largely due to the trapping of sediment it is unsurprising that there is a strong correlation between the position of the PICP and clogging. Typical ‘danger’ areas are proximity to unstable slopes (Figure 6-3), overhanging trees (Figures 6-4 and 6-5), planters of various shapes and sizes (Figure 6-6), or sources of wind-blown sand (Figure 6-7).

(a) Exposed sediment on a slope **(b) Sediment clogging the PICP surface**

Figure 6-3: Impact of unstable sloped surface on PICP

Figure 6-4: Trees can significantly increase clogging in PICP

Figure 6-5: PICP surfaces clogged by leaves or pollen from overhanging trees

The PICP clogging rate and extent is likely governed by the size of the site, that is, the smaller the site with extreme exposure to sediment, the faster it will clog *viz*. However, if the site is clear off sediment, then it will take longer to clog.

(a) Tree planter on bend

(b) Tree planter adjacent parking bay

Figure 6-6: Damaged tree planters

(a) Sediment source adjacent PICP

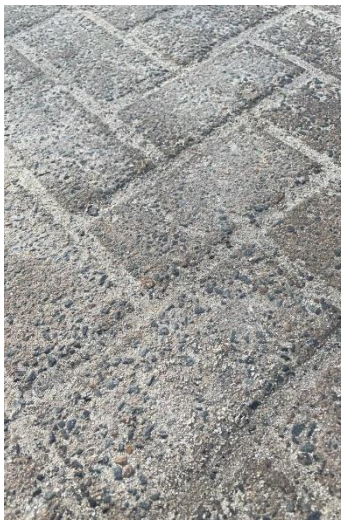

(b) Clogged joints

(c) Type II to Type III clogging

Figure 6-7: Typical wind-blown sediment PICP clogging scenarios

6.8 Clogging and poor paver installation

If pavers are not properly installed with adequate edge restraint, they will move – particularly if subject to high turning movements near busy intersections (Figure 6-8). This allows sediment to easily enter the widened gaps (Figure 6-9) between the pavers from where it is 'worked' under the pavers layer and into the bedding layer. If a geotextile is present, Type III clogging is likely. If not, the PICP will eventually fail with Type IV clogging. The long-term performance of PICP can be improved through: i) sturdy edge restraints and well-spaced trees (Figure 6-10), and ii) low RoF and away from vegetation (Figure 6-11).

Figure 6-8: A failed PICP edge restraint at a bend in the road

(a) Widened joints with no grid

(b) Organic matter filled joints

Figure 6-9: Examples of widened joints

Figure 6-10: Example of well-spaced trees and appropriate edge restraints

Figure 6-11: Example of low RoF and clear of vegetation PICP

6.9 Clogging and maintenance

Like any pavement, PICP must be maintained if it is to provide the desired level of serviceability over a long period of time. It was apparent from the site investigations that this – at a minimum – requires:

- Immediate attention to any structural issues such as widening openings between pavers, rutting, broken pavers etc.
- Keeping the surface as clean as reasonably possible.
- Ensuring that the gritstone is regularly 'topped-up' to trap sediment before it gets into the underlying layers.
- Periodically blowing out the contaminated gritstone (Type I clogging) and replacing it with clean gritstone.
- Since some material will inevitably find its way to the bedding, it will eventually become necessary to temporarily remove the pavers and bedding, clean them, and replace them – taking care to add new (clean) gritstone in the voids between the pavers.

6.10 Recommendations for future research

The following should be considered for future research:

- Accelerated laboratory experiments with cohesive sediments to see if this changes the failure modes.
- Continue to test existing PICP installations to determine their performance with time.
- Develop more reliable infiltration test methods.

- Evaluate a wider range of maintenance approaches e.g., municipal vacuum or sweeper trucks, in a bid to find the most appropriate for SA.
- Perform diagnostic assessments on a wider range of failed PICP designs in a bid to increase understanding of the causes.
- Generally, there was limited evidence on the link between the PICP site sizes and their blockage patterns. Further investigation may be required.

References

Armitage, N., Vice, M., Fisher-jeffes, L., Winter, K., Spiegel, A., Spiegel, A. & Dunstan, J. (2013). *Alternative Technology for Stormwater Management: The South African Guidelines for Sustainable Drainage Systems*. WRC Report no. TT 558/13. Pretoria: Water Research Commission. https://www.researchgate.net/publication/274076390_South_African_Guidelines_for_Sustainable_Drainage_Systems.

Armitage, N., Fisher-jeffes, L., Carden, K., Winter, K., Naidoo, V., Spiegel, A., Mauck, B. & Coulson, D. (2014). *Water Sensitive Urban Design (WSUD) for South Africa: Framework and Guidelines*. WRC Report no. TT 588/14. Pretoria: Water Research Commission. https://www.researchgate.net/publication/270792720_Water_Sensitive_Urban_Design_WSUD_for_South_Africa_Framework_and_Guidelines.

Armitage, N., (2019). *Plot of Mod-ASTM infiltration rate to representative wetted area in the Mod-SWIFT*. Unpublished.

Artus, J. (2017). Testing the infiltration capacities of Permeable Pavements (PICPs). BSc(Eng) Research Report, University of Cape Town: Unpublished.

ASCE. (2018) ASCE/T&DI/ICPI Standard 68-18, *Permeable Interlocking Concrete Pavement*. American Society of Civil Engineers, Reston: USA, 2010. http://doi.org/10.1061/9780784415009.

Azawi, H.K.S. & Sachit, D.E. (2018). Investigation of Permeable Pavement Implementation in Baghdad Using PCSWMM Model. *Environment and Natural Resources Research*. 8(3): 117-125. http://doi.org/10.5539/enrr.v8n3p117.

Barnard, C. (2019). Testing Permeable Pavement Systems to determine capacity and correlation. BSc(Eng) Research Report, University of Cape Town. Unpublished.

Bean, E.Z., Hunt, W.F. & Bidelspach, D.A. (2007). Field Survey of Permeable Pavement Surface Infiltration Rates. *Journal of Irrigation and Drainage Engineering*. 133(3): 249–255. http://doi.org/10.1061/(asce)0733-9437(2007)133:3(249).

Beecham, S., Pezzaniti, D., Myers, B., Shackel, B. & Pearson, A. (2009). Experience in the Application of Permeable Interlocking Concrete Paving in Australia. In: *Proceedings of the 9th. International Conference on Concrete Block Paving. Buenos Aires, Argentina, 2009/10/18-21 Argentinean Concrete Block Association (AABH) - Argentinean Portland Cement Institute (ICPA) Small Element Paving Technologists (SEPT)*. (October 2014):3. https://www.researchgate.net/publication/228495602.

Beecham, S., Lucke, T., Myers, B. & Lakes, M. (2010). Designing Porous and Permeable Pavements for Stormwater Harvesting and Reuse. In: *Proceedings of the 1st European International Association for Hydro-Environment Engineering and Research (IAHR) Conference*. April 2010, Edingburgh.

Bezuijen, A. & Izadi, E. (2022). Damage of geotextile due to impact of stones. *Geosynthetics*

International. 29(2): 151–162. https://doi.org/10.1680/jgein.21.00036.

Biggs, B. (2016). The Impact of Unwashed Aggregate on Water Quality Emanating From Permeable Pavements. MSc(Eng) Dissertation, University of Cape Town. https://open.uct.ac.za/bitstream/handle/11427/23016/thesis_ebe_2016_biggs_benjamin%20%281%29.pdf?sequence=1&isAllowed=y. (Accessed 14 April 2021)

Blackshaw, J. (2021). The impact of geotextiles on Permeable Interlocking Concrete Pavements (PICP) performance. BSc(Eng) Research Report, University of Cape Town. Unpublished

BoDean. (2022). BoDean Washed Aggregates. URL: https://bodeancompany.com/washed-aggregates/. (Accessed 06 November 2022)

Boogaard, F. & Lucke, T. (2019). Long-term infiltration performance evaluation of Dutch permeable pavements using the full-scale infiltration method. *Water (Switzerland)*. 11(2): 1–13. http://doi.org/10.3390/w11020320.

Borgwardt, S. (2015). In-Situ Infiltration Performance of Permeable Concrete Block Pavement – New Results. In: *Proceedings of the 11th International Conference on Concrete Block Pavement (ICCBP)*. 1–16. September 2015, Dresden. http://www.bwb-norderstedt.de/iccbp_2015_21_eng_final_borgwardt.pdf.

British Standards Institution (BSI). (2009). *BSI Standards Publication Pavements constructed with clay , natural stone or concrete pavers Part 13 : Guide for the design of permeable pavements constructed with concrete paving blocks and flags , natural stone slabs*. London: BSI.

Bruinsma, J., Smith, K., Peshkin, D., Ballou, L., Eisenberg, B., Lurie, C., Costa, M., Ung, C., et al. (2017). *Guidance for Usage of Permeable Pavement at Airports*. ACRP Research Report 178. Washington, D.C.: Transportation Research Board. http://doi.org/10.17226/24852.

Burak, R. (2006). The Engineer ' s View Bedding Sand Selection for Interlocking Concrete Pavements in Vehicular Applications. (200). https://www.uni-groupusa.org/PDF/06_Nov_Engineers_View_Bedding_Sand_Selection.pdf. (Accessed 01 November 2022)

Bureau of Environmental Services (BES). (2020). *City of Portland Stormwater Management Manual*. Portland: City of Portland. https://www.portland.gov/bes/stormwater/swmm.

Carolina Industrial Equipment (CIE). (2022). Carolina Industrial Equipment Different types of street sweepers. https://ciequipment.com/different-types-of-street-sweepers/#:~:text=There%20are%20currently%20three%20different%20types%20of%20street,mechanical%20sweepers%2C%20vacuum%20sweepers%2C%20and%20regenerative%20air%20sweepers. (Accessed 16 November 2022)

Catchment, Stormwater and River Management Branch (CSRMB). (2009). *Management of Urban Stormwater Impacts Policy*. Catchment, Stormwater and River Management Branch, Roads and Stormwater Department: City of Cape Town.

Charlesworth, S.M., Beddow, J. & Nnadi, E.O. (2017). The fate of pollutants in porous asphalt pavements, laboratory experiments to investigate their potential to impact environmental health. *International Journal of Environmental Research and Public Health*. 14(6). http://doi.org/10.3390/ijerph14060666.

Charleworth, S.M.. & Booth, C.A. (2017). *Sustainable Surafce Water Management: A Handbook for SuDS*. 1st ed. S.M.. Charleworth & C.A. Booth, Eds. Chichester: John Wiley & Sons, Ltd. https://books.google.co.za/books?id=fTQWDQAAQBAJ.

Cheng, Y.Y., Lo, S.L., Ho, C.C., Lin, J.Y. & Yu, S.L. (2019) Field testing of porous pavement performance on runoff and temperature control in Taipei City. *Water (Switzerland)*. 11(12). http://doi.org/10.3390/W11122635.

Concrete Manufacturers Association (CMA) (2020). PICP – A case fpr regular performance: Testing and maintenance. *Precast.* 1. Available at: https://issuu.com/isikhovapublishing/docs/precast_issue1_2020_issuu (Accessed: 22 August 2023).

Concrete Masonry Association of Australia (CMAA) (2010) Permeable interlocking concrete pavements – Design and Construction (PE01*)*. https://www.cmaa.com.au/Technical/Manuals/paving.

Concrete Masonry Association of Australia (CMAA). (2014) Concrete Segmental Pavements – Detailing Guide (PA01). https://www.cmaa.com.au/Technical/Manuals/paving.

Concrete Masonry Association of Australia (CMAA). (2022). DesignPave Info Booklet. https://www.cmaa.com.au/DesignPave/registration. (Accessed 03 November 2022)

Council for Scientific and Industrial Research (CSIR). (2019). *Stormwater*: 1st ed. Pretoria: CSIR.

Danz, M.E., Selbig, W.R. & Buer, N.H. (2020). Assessment of restorative maintenance practices on the infiltration capacity of permeable pavement. *Water (Switzerland)*. 12(6):1–16. http://doi.org/10.3390/W12061563.

Department of Planning and Local Government (DPLG). (2010). *Water Sensitive Urban Design Technical Manual for the Greater Adelaide Region*. Adelaide: Government of South Australia.

Drake, J. & Bradford, A. (2013). Assessing the Potential For Rehabilitation of Surface Permeability Using Regenerative Air and Vacuum Sweeping Trucks. *Journal of Water Management Modeling*. (June). 303-317. http://doi.org/10.14796/jwmm.r246-16.

Drake, J., Bradford, A. & Van Seters, T. (2010). Performance of permeable pavements in cold climate environments. In: *Proceedings of the Low Impact Development 2010: Redefining Water in the City - Proceedings of the 2010 International Low Impact Development Conference*. 41099(April 2014):1369–1378. http://doi.org/10.1061/41099(367)117.

Drake, J., Sarabian, T. & Jody, S. (2020). *Maintenance Equipment Testing on Accelerated Clogged Permeable Interlocking Concrete Pavements*. Toronto: University of Toronto.

Fassman, E.A. & Blackbourn, S. (2010). Urban Runoff Mitigation by a Permeable Pavement System over Impermeable Soils. *Journal of Hydrologic Engineering*. 15(6):475–485. http://doi.org/10.1061/(asce)he.1943-5584.0000238.

Fibertex (2021). Product data sheet Fibertex geotextiles. Available at: Product overview_EN_01-2021.pdf (fibertex.com) (Accessed: 21 September 2023)

García-Casuso, C., Lapeña-Mañero, P., Blanco-Fernández, E., Vega-Zamanillo, Á. & Montenegro-Cooper, J.M. (2020). Laboratory assessment ofwater permeability loss of geotextiles due to their installation in pervious pavements. *Water (Switzerland)*. 12(5): 1-16. http://doi.org/10.3390/w12051473.

Giroud, J.P. (2010). Development of criteria for geotextile and granular filters. In: *Proceedings of the 9th International Conference on Geosynthetics, ICG 2010*. 45–64, Guaruja.

Hein, D.K. (2018a). Maintenance Guidelines For Permeable Interlocking Concrete Pavement Systems. In: *Proceedings of the Environmental & Water Resources Institute Conference,* September 2018, Sacramento.

Hein, D.K. (2018b). Off Road Benefits of Permeable Interlocking Concrete Pavements. In: *Proceedings of the 12th International Conference of Concrete Block* Pavement, 16-19 October 2018, Seoul.

Hein, D.K. & Schaus, L. (2013). Permeable pavement design and construction: What have we learned recently? In: *Proceedings of the 2nd Green Streets, Highways, and Development Conference*. 3-6 November 2013, Austin. http://doi.org/10.1061/9780784413197.003.

Hein, D.K. & Smith, D.R. (2015). Development of an ASCE Standard for Permeable Pavement. In: *Proceedings of the International Conference on Concrete Block Pavements*, October 2015, Dresden.

Imteaz, M.A., Ahsan, A., Rahman, A. & Mekanik, F. (2013). Modelling stormwater treatment systems using MUSIC: Accuracy. *Resources, Conservation and Recycling*. 71:15–21. http://doi.org/10.1016/j.resconrec.2012.11.007.

Industrial Fabrics. (2022). Industrial Fabrics Sediment Control. https://ind-fab.com/silt-fence/. (Accessed 08 November 2022)

Innovyze. (2022). Sustainable Drainage Design. URL: https://www.innovyze.com/en-us/products/microdrainage/microdrainage-mdsuds. (Accessed 05 November 2022)

Interlocking Concrete Pavement Institute (ICPI) Tech Spec No. 23. (2013). Maintenance Guide for Permeable Interlocking Concrete Pavements. Chantilly, VA: ICPI

Interpave. (2018). Design & Construction Of Concrete Block Permeable Pavements: 7th ed. Hodsons, C. ed. https://www.bosun.co.za/wp-content/uploads/2022/03/Interpave-Design-Construction-of-Permeable-Pavements.pdf.

Interpave. (2020). Understading Permeable Paving & SuDS. https://www.paving.org.uk/home/downloads/ (Accessed 30 October 2022)

Kaytech (2020). Technical Data Sheet – *Light Grades* – *SANPAC*. Available: Data-sheet-A1-A15-Bidim.pdf (sanpac.com). (Accessed: 23 September 2023)

Kia, A., Wong, S. H. and Cheeseman, R. C. (2017). Clogging in permeable concrete: A review. *Journal of Environmental Management*. 193 (221-223). http://dx.doi.org/10.1016/j.jenvman.2017.02.018

Knapton, J., Morrell, D. & Simeunovich, M. (2012). Structural Design Solutions for Permeable Pavements. In: *Proceedings of the 10th International Conference on Concrete Block Paving*, 24-26 November 2012, Shanghai. Available: http://www.sept.org/techpapers/Knapton-on-Heavy-Duty-PICP-Structural-Design.pdf.

Lashford, C., Charlesworth, S., Warwick, S., & Blackett, M. (2017). Modelling the flood risk reduction potential of different SuDS devices using MicroDrainage. In: *Proceedings of the 14th International Conference on Urbn Drainage (ICUD)*, September 2017, Prague.

Liu, B.K. & Armitage, N.P. (2020). The Link between Permeable Interlocking Concrete Pavement (PICP) Design and Nutrient Removal. *Water*, 12(6) 1714. http://doi.org/10.3390/w12061714.

Look, B. (2007). *Handbook of Geotechnical Investigation and Design Tools*. London: Taylor & Francis.

Lucke, T. & Beecham, S. (2011). Field investigation of clogging in a permeable pavement system. *Building Research and Information*. 39(6): 603–615. https://doi.org/10.1080/09613218.2011.602182.

Lucke, T. & Dierkes, C. (2015). Addressing the demands of the new german permeable pavement design guidelines and the hydraulic behaviour of a new paving design. *Journal of Engineering Science and Technology*. 10(Spec. Issue on Advances in Civil and Environmental Engineering ACEE 2015, August 2015):14–28.

Lucke, T., White, R., Nichols, P. & Borgwardt, S. (2015). A simple field test to evaluate the maintenance requirements of permeable interlocking concrete pavements. *Water (Switzerland)*. 7(6):2542–2554. https://doi.org/10.3390/w7062542.

Manteghi, G. & Mostofa, T. (2020). Evaporative pavements as an urban heat island (UHI) mitigation strategy : a review. *International Transaction Journal of Engineering , Management , & Applied Sciences & Technologies* 11(1):1–15. http://doi.org/10.14456/ITJEMAST.2020.17.

Marchioni, M. & Becciu, G. (2015). Experimental results on permeable pavements in urban areas: A synthetic review. *International Journal of Sustainable Development and Planning*. 10(6):806–817. http://doi.org/10.2495/SDP-V10-N6-806-817.

Marshalls. (2022). Permeable paving design guide. URL: https://media.marshalls.co.uk/image/upload/v1583135778/Marshalls_permeable_paving_design_guide.pdf?_its=jtdcjtiydmlkjtiyjtnbjtiyntllmjliyjqtymi3nc00odmyltkzmzetnjhlndyxywy3ogy4jtiyjtjdjtiyc3rhdgulmjilm0elmjjybhr%2bmty3mtayndcxmx5syw5kfjjfnjq1mdhfc2vvx2m0yja1nmqzogyymwyxndi1zti3ndexnzi0zjhmmjnkjtiyjtjdjtiyc2l0zulkjtiyjtnbmtuzmt

eln0q%3d. (Accessed 02 November 2022)

Matolengwe, Q. (2021). Investigation on the long-term performance of Permeable Interlocking Concrete Pavements. BSc(Eng) Research Report, University of Cape Town. Unpublished

McQueen, R. D., J. Knapton, J. Emery, and D. R. Smith. (2003) (updated 2012). *Airfield Pavement Design with Concrete Pavers*. 4th ed. Chantilly, VA: Interlocking Concrete Pavement Institute.

Miszkowska, A., Koda, E., Sieczka, A. & Osiński, P. (2019). Proceedings of the 8th International Congress on Environmental Geotechnics (2). In: Zhan, L., Chen, Y., Bouazza, A. (eds)., *Laboratory tests of the influence of clogging on the hydraulic properties of nonwoven geotextiles*. Singapore: Springer.

Morritt-Smith, J. (2022). The link between geotextiles and clogging in PICP. BSc(Eng) Research Report, University of Cape Town. Unpublished.

Mqadi, T. (2022). The Link Between Pavers and Blockage in Permeable Interlocking Concrete Pavements (PICP)' s. BSc(Eng) Research Report, University of Cape Town. Unpublished.

Mullaney, J. & Lucke, T. (2014). Practical review of pervious pavement designs : a review. *Clean – Soil, Air, Water* 42(2) 111-124. http://doi.org/10.1002/clen.201300118.

National Research Council. (2009). *Urban stormwater management in the United States*. Washington, D.C.: The National Academies Press.

Newman, A.P., Coupe, S.J. & Cresswell, N. (2002). Oil Bio-Degradation in Permeable Pavements by Microbial Communities Oil bio-degradation in permeable pavements by microbial communities. *Water Science & Technology* 45(7) 51-56. http://doi.org/10.2166/wst.2002.0116.

Nguyen, N.P.T., Sultana, A., Areerachakul, N., & Kandasamy, J., (2022). Evaluating the Field Performance of Permeable Concrete Pavers. *Water* 14(2143):1–16. https://doi.org/10.3390/w14142143.

Nichols, P.W.B., Lucke, T. & Dierkes, C. (2014). Comparing two methods of determining infiltration rates of permeable interlocking concrete pavers. *Water (Switzerland)*. 6(8):2353–2366. http://doi.org/10.3390/w6082353.

Nichols, P.W.B., White, R. & Lucke, T. (2015). Do sediment type and test durations affect results of laboratory-based, accelerated testing studies of permeable pavement clogging? *Science of the Total Environment*. 511:786–791. http://doi.org/10.1016/j.scitotenv.2014.12.040.

North Carolina Department of Environmental Quality (NCDEQ). (2020). NCDEQ Stormwater Design Manual. *C-5 . Permeable Pavement*. https://docslib.org/doc/10111985/c-5-permeable-pavement.

Peyi, T. (2021), The link between geotextiles and the long-term performance of Permeable Interlocking Concrete Pavements (PICPs). BSc(Eng) Research Report, University of Cape Town. Unpublished

Pezzaniti, D., Beecham, S. & Kandasamy, J. (2009). Influence of clogging on the effective life of permeable pavements. *Proceedings of the Institution of Civil Engineers: Water Management*. 162(3):1–10. http://doi.og/10.1680/wama.2009.00034.

Poon, L. (2018). Urban flooding is worrying widespread in the U.S., but under-studied. *Bloomberg*. https://www.bloomberg.com/news/articles/2018-12-12/u-s-urban-flooding-study-it-s-bad-and-getting-worse (Accessed: 23 August 2023).

Razzaghmanesh, M. & Beecham, S. (2018). A review of permeable pavement clogging investigations and recommended maintenance regimes. *Water (Switzerland)*. 10(3). http://doi.org/10.3390/w10030337.

Roesner, B.L.A., Bledsoe, B.P. & Brashear, R.W. (2001). Are best -management -practice criteria really environmentally friendly?. *Journal of Water Resources Planning and Management* 127(3) 150–154.

Rosa, D.J., Clausen, J.C. & Dietz, M.E. (2015). Calibration and Verification of SWMM for Low Impact Development. *Journal of the American Water Resources Association*. 51(3):746–757. http://doi.org/10.1111/jawr.12272.

Rowe, A. A., Borst, M., O'Connor, T.P. & Stander, E., (2009). Pervious Pavement System Evaluation. In: *Proceedings of the International Low Impact Development Conference*. Seattle: American Society of Civil Engineers. 1–9. http://doi.org/10.1061/41036(342)141.

Sanicola, O., Lucke, T. & Devine, J. (2018). Using permeable pavements to reduce the environmental impacts of urbanisation. *International Journal of* GEOMATE, 14(41):159–166. http://doi.org/10.21660/2018.41.Key3.

SANRAL. (2013). *Drainage Manual*. 6th ed. E. Kruger, N. Gomes, F. van Vuuren, & M. van Dijk, eds. Pretoria: SANRAL.

SANRAL. (2014). South Africa Pavement Engineering Manual. In: *Chapter 9: Materials Utilisation and Design*. 2nd ed. Pretoria: SANRAL. https://www.nra.co.za/uploads/27/SAPEM-Chapter-9-2nd-edition-2014.pdf.

Sehgal, K., Drake, J., Van Seters, T. & Linden, W.K. Vander. Linden. (2018). Improving restorative maintenance practices for mature permeable interlocking concrete pavements. *Water (Switzerland)*. 10(11):9–13. http://doi.org/10.3390/w10111588.

Simpson, I.M., Winston, R.J. & Tirpak, R.A. (2021). Assessing maintenance techniques and in-situ pavement conditions to restore hydraulic function of permeable interlocking concrete pavements. *Journal of Environmental Management*. 294(8). http://doi.org/10.1016/j.jenvman.2021.112990.

Smith, D.R. (2012). Industry Guidelines for Permeable Interlocking Concrete Pavement in the United States and Canada. In: *Proceedings of the 10th International Conference on Concrete Block Paving*. 24-26 November 2012, Shanghai.

Smith, D.R. (2017). *Permeable interlocking interlocking concrete pavements Design, Specifications, Construction & Maintenance*. 5th ed. Chantilly. Interlocking Concrete Pavement Institute. ISBN 978-0-9886795-3-5

Smith, D.R. (2019). *Tech Brief. Permeable interlocking concrete pavement.* U.S. Department of Transportation. https://www.fhwa.dot.gov/pavement/concrete/pubs/hif19021.pdf.

St John Source. (2017). Improper Silt Fence on Hull Bay Road construction. https://stjohnsource.com/2017/06/26/improper-silt-fence-on-hull-bay-road-construction/. (Accessed 17 November 2022)

Swan, D.J. & Smith, D.R. (2009). Development of the Permeable Design Pro Permeable Interlocking Concrete Pavement Design System. In: *Proceedings of the 9th. International Conference on Concrete Block Paving*. 18–21 October 2009, Buenos Aires.

Støvring, J., Dam, T. & Bergen Jensen, M. (2018). Surface sedimentation at permeable pavement systems: implications for planning and design. *Urban Water Journal*. 15(2):124–131. http://doi.org/10.1080/1573062X.2017.1414273.

The Brick Industry Association (BIA). (2012). *Technical Notes 14E - Accessible Clay Brick Pavements*. Virginia: The Brick Industry Association.

Tirpak, R.A., Winston, R.J., Simpson, I.M., Dorsey, J.D., Grimm, A.G., Pieschek, R.L., Petrovskis, E.A. & Carpenter, D.D. (2021). Hydrologic impacts of retrofitted low impact development in a commercial parking lot. *Journal of Hydrology*. 592. http://doi.org/10.1016/j.jhydrol.2020.125773.

UNI-GROUP. (2008). Permeable Interlocking Concrete Pavement Design Guide & Research Summary. Palm Beach Gardens: UNI-GROUP U.S.A.

United States Environmental Agency (US-EPA). (1999). *Storm Water Technology Fact Sheet: Bioretention*. Washington, D.C.: U.S. EPA.

Urban Water Management (UWM). (2021). Urban Water Management WSUD SA Modelling Tools. URL: www.uwm.uct.ac.za/uwm/modelling-tools (Accessed 05 June 2021)

van Vuuren, J.H., Dippenaar, M.A., van Biljon, R. & van Rooy, L. (2022). Seepage Through Permeable Interlocking Concrete Pavements and Their Subgrades Using a Large Infiltration Table Apparatus. *International Journal of Pavement Research and Technology*. 15(1):44–62. http://doi.org/10.1007/s42947-021-00010-8.

Vela, W. (2018). Testing the infiltration capacity of Permeable Pavements in and around Cape Town. BSc(Eng) Research Report, University of Cape Town. Unpublished

Veldkamp, T.I. & Boogaard, F.C. (2022). Unlocking the Potential of Permeable Pavements in Practice : A Large-Scale Field Study of Performance Factors of Permeable Pavements in The Netherlands. *Water* 14(13) 2080. https://doi.org/10.3390/w14132080.

Wisconsin Department of Natural Resources (WDNR). (2021). Permeable Pavement (1008) Technical Standard. Madison: Wisconsin Department of Natural Resources.

Winston, R.J., Al-Rubaei, A.M., Blecken, G.T. & Hunt, W.F. (2016). A Simple Infiltration

Test for Determination of Permeable Pavement Maintenance Needs. *Journal of Environmental Engineering*. 142(10):06016005. http://doi.org/10.1061/(asce)ee.1943-7870.0001121.

Winston, R.J., Al-rubaei, A.M., Blecken, G.T., Viklander, M. & Hunt, W.F. (2016). Maintenance measures for preservation and recovery of permeable pavement surface in fi ltration rate e The effects of street sweeping , vacuum cleaning , high pressure washing , and milling. *Journal of Environmental Management*. 169:132–144. http://doi.org/10.1016/j.jenvman.2015.12.026.

Wong, T.H.F., Fletcher, T.D., Duncan, H.P., Coleman, J.R. & Jenkins, G.A. (2002). A model for urban stormwater improvement conceptualisation. *Global Solutions for Urban Drainage*. 40644(May 2014):48–53. http://doi.org/10.1061/40644(2002)115.

Woods Ballard, B., Wilson, S., Udale-Clarke, H., Illman, S., Scott, T., Ashley, R. & Kellagher, R. (2015). *The SUDS manual (CIRIA C753)*. London: CIRIA. ISBN: 978-0-86017-760-9.

Xian, B.C.C., Kang, C.W., Wahab, M.A., Zainol, M.R.R.M.A. & Baharudin, F. (2021) Evaluation of low impact development and best management practices on peak flow reduction using SWMM. In: *Proceedings of the IOP Conference Series: Earth and Environmental Science*. 646(1) 1-9. http://doi.org/10.1088/1755-1315/646/1/012045.

Appendices

Appendix A: Modified ASTM single ring infiltrometer test (Mod-ASTM)

A1 Generally regarded as the standard test method for PICP (modified from ASTM C1781).

A2 The test apparatus consists of an approximately 500 mm high, 315 mm outside diameter unplasticized vinyl chloride (uPVC) Class 6 pipe (300 mm inside diameter) that has a 10 mm neoprene strip glued to the lower end to provide a seal against the PICP (Figure A-1). The inside of the pipe is marked with two lines 10 mm and 15 mm respectively above the neoprene strips. A metal rod is inserted through two holes drilled near the top of the pipe and weights hung from it to help load the pipe and thus reduce the leakage under the neoprene strips.

A3 Place the apparatus on the test spot. Small neoprene pieces may also be inserted into the joints between the pavers for the same purpose (Figure A-2).

A4 If the surface of the PICP is not already wet, the inside the apparatus may need to be pre-wetted with 3.6 litres (= 3.6 kg) of water.

A5 The water is steadily poured from a bucket into the ASTM apparatus while trying to maintaining a 10 to 15 mm water head over the PICP for as long as possible. The time taken (*T* to the nearest second) for 18 litres (= 18 kg) of water to infiltrate through the PICP is measured.

(a) Upright **(b) Underside**

Figure A-1: Mod-ASTM apparatus

A6 If the test time is longer than 15 minutes, the PICP can be considered partly or fully clogged and the test stopped. The quantity of water remaining in the bucket is then determined by

weighing the bucket with and without the water in it. This is then deducted from the initial 18 litres to give the approximate quantity of water used in the test (*M* in litres). Note that much of the flow rate measured under these circumstances will be leakage under the apparatus rather than through the PICP surface (Figure A-3).

Figure A-2: Neoprene pieces plugging the joints in Mod-ASTM

Figure A-3: Mod-ASTM leakage

A7 Use Equation 6 to estimate the PICP infiltration capacity (nearest 100 mm/hr).

$$I = 51{,}000\ M / T \qquad \text{Equation 6}$$

Where:	I	=	Infiltration rate (mm/hr)
	M	=	Mass of infiltrated water (kg)
	T	=	Time (s)

A8 If $250 < I < 1000$ mm/hr, the PICP is partially clogged; if $I \leq 250$ mm/hr then it can be considered completely clogged (it is likely that the flow is largely leakage).

Appendix B: Modified SWIFT (Mod-SWIFT)

B1 Used to give a rapid indication of the state of the PICP.

B2 Modified from the Stormwater Infiltration Field Test (SWIFT) (Lucke *et al*., 2015).

B3 The test apparatus consists of a bucket resting on 60 mm high legs (Figure B-1). The bottom of the bucket has a 40 mm hole drilled through its centre that is temporarily sealed with a bathroom plug to prevent water from escaping the bucket prior to the test. A string is tied to the plug to allow it to be rapidly removed.

(a) Inside of bucket **(b) Legs**

Figure B-1: Mod-SWIFT apparatus

B4 The bucket is placed on the spot to be tested. The surface must be dry.

B5 The bucket is filled with six litres of water. It is helpful to have the height attained by the six litres of water pre-marked on the inside to obviate the need to measure the water separately for each test.

B6 Once the water is at rest in the bucket, rapidly pull the plug with the string to allow the water to flow out of the bottom of the bucket.

B7 Immediately remove the bucket once it is empty – remembering to replace the plug for the next test.

B8 Measure the longest wetted length, *a*, to the nearest 0.1 m with a tape measure. Then measure the greatest extent of the wet patch, *b*, perpendicular to *a*, to the nearest 0.1 m (Figure B-2).

B9 Use Equation 7 to estimate the Mod-SWIFT infiltration capacity of the test spot (nearest 100 mm/hr). Anything less than 1000 mm/hr can be considered as clogged. Check using the Mod-ASTM (Appendix A). Both methods are increasingly inaccurate as the infiltration rate decreases.

$$I = -930 \ln(a \times b) + 2200 \qquad \text{Equation 7}$$

Where: I = Infiltration rate (mm/hr)
a = longest wetted length (m)
b = widest wetted perpendicular to a (m)

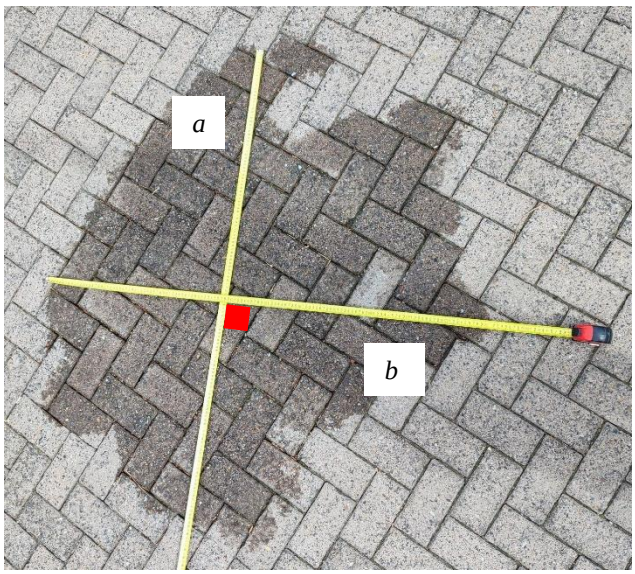

Figure B-2: Mod-SWIFT measurements

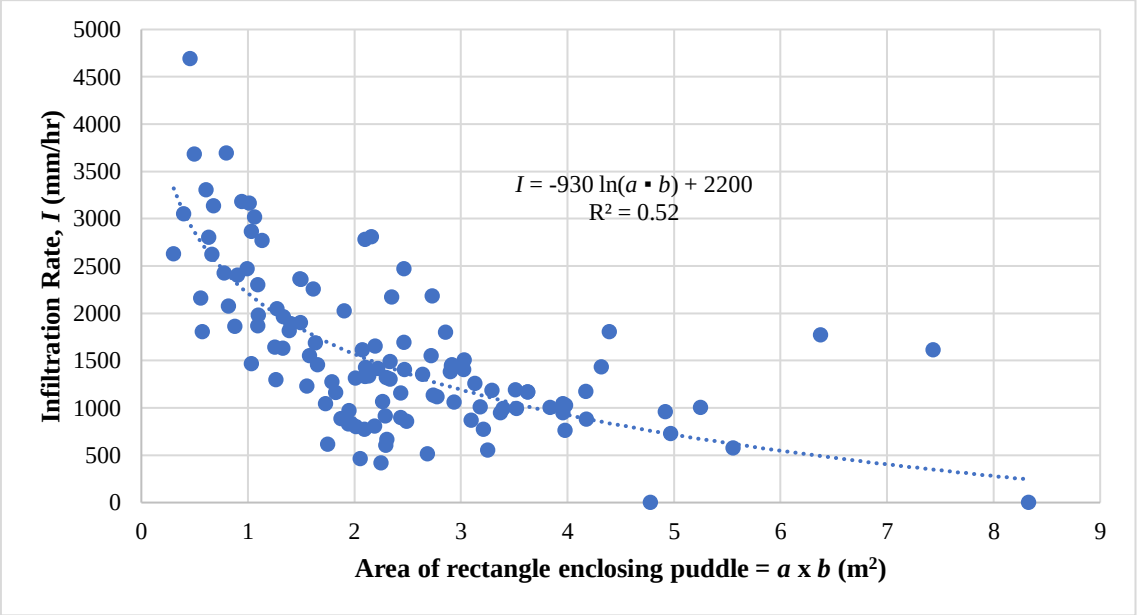

Figure B-3: Mod-SWIFT to Mod-ASTM conversion

Appendix C: Template for Details of PICP installation

Name of development				
Street address				
Town / City				
Province				
Google Map pin				
Property manager		**Contact details**		
Consultant				
Contractor				
Year of construction				
Maintenance	**Contractor**		**Contact Detail**	
	Recurrence			
	Method			
PICP area	**Permeable area**			
	Run-on factor			
	Google Earth plan			
Traffic characteristics				
Pavers	**Type**			
	Depth			
	Joint width			
	Paver dimensions			
	Paver opening ratio			
	Photos			
Geofabric	**Type**			
	Location			
	Function			
	If none; choke layer?			
Layerworks	**Gritstone**		**Thickness (mm)**	
	Bedding			
	Base course			
	Subbase			
Subgrade				

Appendix D: Template for PICP testing

General

D1 Locate site.

D2 Request access to the site to perform the infiltration tests.

D3 Take photos of any features that may be important in understanding the performance of the PICP site such as vegetation around the site, loose sediment, spacing between the pavers filled with dirt, broken pavers, rutting, etc,

D4 Choose the test spots for the infiltration tests and mark these up on a Google Earth clip to help give the physical context.

D5 Label the test spots using the following code: [PICP site code]-[PICP section]-[Test spot]-[Test year]. For example, Test spot A carried out in Section 1 of the Grand Parade in 2021 might be reported as GRP-1-A-2021.

D6 Barricade the working space around the designated test spots providing traffic control if necessary. Ensure all personnel are wearing appropriate PPE. Keep the public at a safe distance.

D7 Determine and record the infiltration capacity of the PICP at the identified test spots using either Mod-ASTM (standard) or Mod-SWIFT as appropriate using the following template or similar.

Location:

Provide maps showing the location of the site and position of the test spots

Date of test:

Carried out by: Contact No.:

Surface infiltration rates for each test spot

Test spot ID	Condition and comments	Test Type	Mod-ASTM		Mod-SWIFT		
			Time (s)	Infiltration rate (mm/hr)	*a* (m)	*b* (m)	Infiltration rate (mm/hr)
		Pre-maintenance:					
		Post-maintenance:					
		After regritting:					
Add blocks as necessary		Pre-maintenance:					
		Post-maintenance:					
		After regritting:					

Appendix E: Instructions for diagnostic assessments

E1 Carry out baseline Mod-ASTM (Appendix A) infiltration tests to locate areas of concern – typically areas with infiltration rates less than 1000 mm/hr.

E2 Select one or more of the areas of concern and isolate areas no smaller than 3 m x 3 m with suitable barriers to protect the public from flying debris.

E3 Attempt to blow out the dirt from the joints using a high-velocity air blower through a suitably-sized nozzle. Ensure that the ejected dirt is carefully removed e.g., with dustpan and brush, so as not to fall back into the joints.

E4 Carry out Mod-ASTM infiltration tests on the selected test spots. If there is a substantial improvement to greater than 1000 mm/hr, then the PICP was likely exhibiting Type I clogging (in the top 25 mm of the joints – Figure E-1).

Figure E-1: Type I clogging (in the joints)

E5 If dissatisfied with the improvement in the infiltration rate, e.g., infiltration rate still less than 1000 mm/hr, carefully lift the pavers for further investigation. It is likely that there will be 'wedges' of dirt below the joints (Figure E-2). If this is the case, it is indicative of Type II clogging (on the top of the bedding layer immediately underneath the joints).

E6 Record and take pictures of the state of the bedding. at each test spot, perform a Mod-ASTM infiltration test on the bedding. There are usually only two clear results from this test owing to the stony nature of the bedding *viz.*: not clogged or completely clogged. The latter will usually be accompanied by high proportions of fines mixed in with the bedding aggregate clearly indicating Type III clogging (clogging of the bedding layer and the underlying geotextile – Figure E-3).

Figure E-2: Type II clogging (below the joints)

Figure E-3: Type III clogging (of the bedding)

E7 If the bedding layer does not appear completely clogged (remember that water can usually easily flow laterally which must be taken into account in this assessment) and a geotextile was provided under the bedding, gently remove the bedding to access it taking care not to damage it.

E8 Record and take pictures of the state of the geotextile. Perform a Mod-ASTM infiltration test on the geotextile. If the geotextile is clogged, this likely means Type III clogging (clogging of the bedding layer and the underlying geotextile) (Figure E-3). If not, then the clogging is likely Type II (on the top of the bedding layer immediately underneath the

openings between the pavers – Figure E-2). Alternatively, the geotextile may be damaged to the point where it serves no function (or is absent) (Figure E-4).

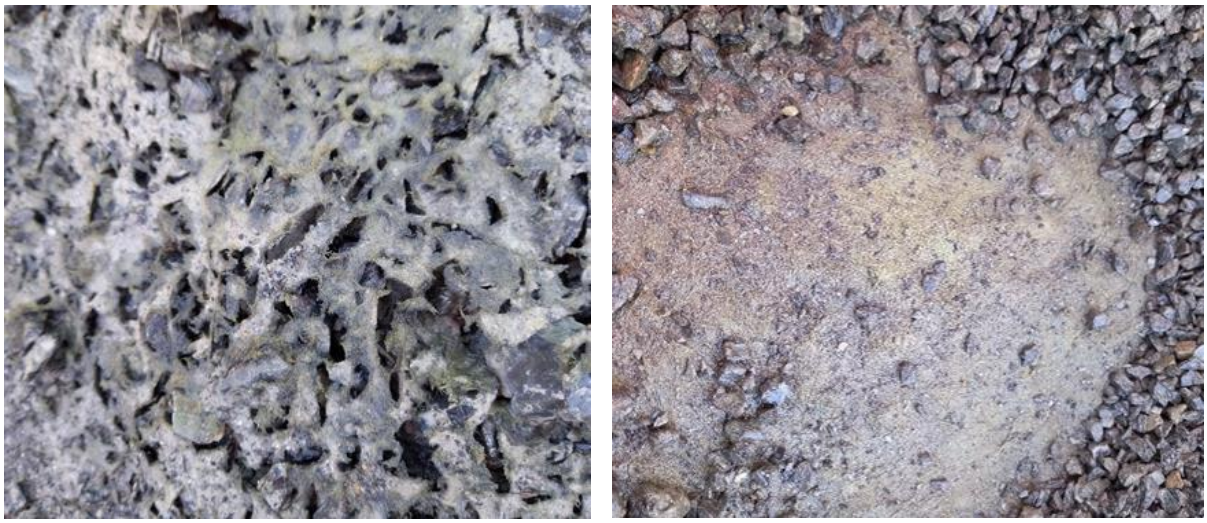

Figure E-4: Top geotextile failure

E9 If the geotextile appears clogged, carefully cut out a section so that the state of the underlying base course can be assessed (Figure E-5). Perform a Mod-ASTM infiltration test if there is concern that it may be clogged. If the base course is unclogged, then the clogging must be Type III (clogging of the bedding layer and the underlying geotextile). If the base course is clogged, then the clogging is Type IV (in the base courses) which should prompt a review of the design and construction methods as this type of failure is rare (Figure E-6).

Figure E-5: Type IV clogging (in the base courses)

E10 If the base course is clogged, carefully excavate a hole down through the layers down as far as the lower geotextile – if present – to see its condition (Figure E-6). Pay attention to the particle size distribution of each layer – each layer should be single-sized. If the layers have mixed particle sizes it is likely that there was a construction error, i.e., the contractor didn't use single-sized aggregate.

Figure E-6: Damaged bottom geotextile

E11 Once the investigation has been completed, carefully reconstruct the aggregate layers ensuring that they are well compacted. Replace the pavers and fill the joints with washed gritstone (Figure E-7).

Figure E-7: Repaired PICP test spot

E12 Record all results.

Appendix F: Template for PICP inspection report

(adjust as appropriate)

Inspector's name		**Contact No.**	
Date of inspection		**Date of last inspection**	
Name of development			
Street address			
Town / City			
Province			
Google Map pin			
Property manager			
Consultant			
Contractor			
Year of construction			
Structural	**Horizontal creep?**		
	Grit pumping?		
	Rutting?		
	Broken / missing pavers?		
	Excessive joint widths?		
	Damaged / displaced edge restraints?		
Hydraulic	**Changes to stormwater design (including RoF)?**		
	Ponding?		
	Visually clogged joints?		
	Sediment / debris etc coming onto the surface?		
	Test results?		
	Diagnostic assessments?		
Other observations			
Action taken			

Inspector:..... Signature:..... Place:..... Date:.....

Original to be kept in the offices of the Property Owner, copy to be made available to the local authority on request.